HYDROFOILS -

DESIGN OF A WIND PROPELLED FLYING TRIMARAN

by

Neil Bose B.Sc.

Submitted as a Thesis for the Degree of

Doctor of Philosophy

Department of Naval Architecture and Ocean Engineering

University of Glasgow

April 1982


KAA

CONTENTS

Acknowledgements

This thesis is based on research carried out from 1978-1981 in the Department of Naval Architecture and Ocean Engineering at the University of Glasgow. The author wishes to record his thanks for the help and encouragement given by Professor D. Faulkner and Acting Head of Department, Mr. N.S. Miller and his supervisor Dr. R.C. McGregor. Thanks are also extended to the staff and technicians of the Hydrodynamics Laboratory at Acre Road for their help with the model testing and computer facilities.

The author is very grateful and would like to thank all those people, far too numerous to mention, for their help with the construction and the full scale testing of the prototype boat, 'Kaa', and especially those who provided material support or finance towards the construction (Appendix C). In particular thanks are conveyed to Mr. S. Penoyre, Dr. C. Edmonds, Mr. R. McMath, Mr. R. Renilson and all of the Bose family.

The project was financed by a Science Research Council Collaborative Training Award and later Studentship.

Finally the author is very grateful for the help received from Miss P. McKay, Miss M. Shields , Mrs. M. Frieze and Mrs H. Taylor for their help in the preparation of this manuscript.

Declaration

Except where reference is made to the work of others, this thesis is believed to be original.

Summary

This study covers the design, construction and testing of a wind propelled hydrofoil trimaran. The work was split into four main parts which when integrated as a whole formed the basis of the information required for a design to be formulated. Much of the work and the computer programs which were written are applicable to hydrofoil craft in general (both motor powered and wind propelled) and because of the type of hydrofoil design considered, they are mainly orientated towards surface piercing hydrofoil systems.

A prototype boat of 5 metres overall length was designed and built in order that full scale tests could be carried out on the open water. Most of the results from these tests were either qualitative or photographic. Even so the results from these trials were a most useful indication of the performance of the design. Structural problems were encountered with the construction of the hydrofoils.

Computer programs were written to predict the calm water steady state lift and drag, and flight orientation of the hydrofoil boat. These calculations included predictions at angles of heel and yaw. The results from these predictions were compared with a series of model tests undertaken on a one quarter scale model of the 5 metre prototype. Agreement was found to be good.

Analysis methods were formulated and predictions obtained for two different wind propulsion systems, a soft sail rig and a horizontal axis wind turbine rig. The soft sail rig was used on the prototype boat, but the turbine was shown to offer scope for a more versatile propulsion system if exceptionally high speeds were not aimed for. High boat speeds in low wind speeds, unfortunately only over a limited range of courses relative to the wind direction, were best obtained by resort to a soft sail or solid aerofoil rig. Consideration was given to the operation of the wind turbine both in the windmill mode and the autogyro mode.

A theoretical study was made of the seakeeping of surface piercing hydrofoil systems in regular head and following seas. This incorporated a linearised solution in the frequency domain and a non-linear step-by-step simulation in the time domain which was executed on a digital computer. From a comparison of the results, of these simulations with a series of model experiments, it was found that the latter method gave the best solution in head seas and offered the best possibilities for an accurate solution in following seas.

NOMENCLATURE

A	Aspect ratio
A_A	Actual area of hydrofoil element
A_H, A_P	Quantities in the linear solution of the heave and pitch motions
B	No. of blades (windmill rotor)
B_H, B_P	Quantities in the linear solution of the heave and pitch motions
B_{PK}	Pankhurst's constant
C_{DO}	Section drag coefficient
C_{DOMIN}	Minimum section drag coefficient
C_f	Friction coefficient (ITTC line)
C_H	Heeling force coefficient
C_L	Lift coefficient
C_{L_i}	Ideal lift coefficient
C_{L2D}	Lift coefficient based on the 2-D lift curve slope of the section
C_M	Pitching moment coefficient
$C_{M}c/4$	Pitching moment coefficient about the ¼ chord point
CONST	Value of the parabolic constant in the empirical formula for the section drag coefficient
C_R	Driving force coefficient
C_{TA}	Total sail force coefficient
C_x	Component of the aerodynamic force normal to the windmill axis
C_y	Component of the aerodynamic force parallel to the windmill axis
C_4	Coefficient of D^4 in the stability equation
D	Drag
D_W	Diameter of windmill rotor

F	Froude chord no. $F = V/\sqrt{gc}$
F_D	Drag force from windmill
F_H	Heeling force from sails or windmill
F_{lat}	Horizontal component of the heeling force
F_T	Overall driving force from the windmill operating in the windmill mode
F_V	Vertical component of the heeling force
F_W	Losses due to a finite number of windmill blades
G_1, G_2, G_3, G_4	Constants of the transient motion in the linear seakeeping solution
I_y	Moment of inertia in pitch (model or boat)
K	Radius of gyration of the compound pendulum
$\bar{K}$	Correction due to loss of lift near the free surface (mean value)
L	Lift
L_c	Lower ordinate of the foil section in functions of chord length
L_f	Luff length of sail (measured vertically)
LOA	Length overall
M	Pitching moment
M_a	Acceleration force due to added virtual mass term in pitch
$M_{c/4}$	Pitching moment about the ¼ chord point
M_P	Pitch response
M_1	Amplitude of the pitch forcing function
P	Power output (windmill)
P_f	Performance factor
P_{MAX}	Maximum power output of an ideal windmill
P_n	Windmill pitch

Q	Windmill torque
Q_c	Windmill torque coefficient
R	Driving force from sails
R_n	Reynold's No.
R_w	Radius of windmill rotor
S	Projected area of hydrofoil element
S_A	Sail area
SF	Side force
T	Thickness of hydrofoil section
T_A	Total sail force
TDR	Total instantaneous drag
T_h	Thrust force
TL	Total instantaneous lift
TPM	Total instantaneous pitching moment
T_w	Windmill thrust
T_{wc}	Windmill thrust coefficient
U_c	Upper ordinate of the foil section in fractions of chord length
U_o	Steady state surge velocity (velocity of boat) - used in linear theory
V	Velocity of hydrofoil, element or boat
V_A	Velocity of the apparent wind
V_c	Critical speed for cavitation
V_{CORR}	Velocity corrected for craft motions
V_{mg}	Speed made good to windward
V_w	Forward velocity of a foil element in a wave
V_{WD}	True wind velocity
V'	Axial inflow velocity (windmill)
W	All up weight
W_w	Effective velocity of the windmill element
$\bar{W}$	Hydrofoil correction due to the formation of waves - mean value

X	X direction, earth axis system
X_a	Acceleration force due to the added virtual mass term in surge
X_{bow}	X co-ordinate of the bow foil
X_F	Surge force
X_G	X co-ordinate of the centre of gravity
X_w	Windmill speed ratio
Y	Y direction, earth axis system
Z	Z direction, earth axis system
Z_a	Acceleration force due to the added virtual mass term in heave
Z_F	Heave force
Z_G	Z co-ordinate of the centre of gravity
Z_H	Heave response
Z_1	Amplitude of the heave forcing function
a	Term in aspect ratio calculations
a'	Term in equation for $\bar{K}$
a_{hw}	Horizontal acceleration of the water particle in waves
a_{vw}	Vertical " " " " " " "
a_w	Wave amplitude
a_{11}, a_{12}, a_{21}, a_{22}	Coefficients of the stability equation (linear theory)
b	Span
b'	Term in equation for $\bar{K}$
c	Chord length
c_A	Chord length at end A of hydrofoil element
c_B	" " " " B " " "
c'	Term in equation for $\bar{K}$
c_r	Root chord length
c_w	Wave celerity

d_i Drag on a hydrofoil element

d' Term in equation for $\bar{K}$

e Product of the transmission and water propeller efficiencies (windmill propulsion theory)

f Prandtl's correction term

g Gravitational acceleration

h Depth

h_A Depth of end A of hydrofoil element

h_B " " " B " " "

h_w Depth in a wave from the undisturbed water surface

i $\sqrt{-1}$

k Wave number

$k_1(S)$ Indicial lift function for a sudden change in sinking speed or angle of attack

$k_2(S)$ Indicial lift function, penetration of a sharp edged normal gust

l Distance from the centre of rotation to the centre of gravity - compound pendulum

l_b Lift on the bow foil unit

l_i Lift on a hydrofoil element

l_s Lift on the side foil unit

l_{st} " " " stern " "

m Mass of boat

n Number of foil elements

n_b Number of bow foil elements

n_s " " side " "

n_{st} " " stern " "

p	Roll velocity
q	Pitch velocity
r	Yaw velocity
r_o	Amplitude of response
r_w	Radius of windmill rotor element
s	Distance travelled in half chords
s_{fi}	Side force on a hydrofoil element
t	Time
u	Surge velocity
u_w	Horizontal wave particle velocity
v	Sway velocity
v_w	Vertical wave particle velocity
w	Heave velocity
x	x direction, body axis system
x_i	x co-ordinate of the foil element from the craft centre of gravity
y	y direction, body axis system
y_1	
y_2	Dependent variables (non-linear motion
y_3	solution)
y_4	
z	z direction, body axis system
z_{ce}	z co-ordinate of the centre of effort of the sails from the centre of gravity
z_{clr}	z co-ordinate of the centre of lateral resistance from the centre of gravity

z_i	z co-ordinate of the foil element from the craft centre of gravity
z_o	Height of flight
z_T	z co-ordinate from the line of the thrust force to the centre of gravity
Γ	Angle of dihedral
Ω	Angular velocity of the windmill
α	Value in the solution of the heave and pitch response (linear theory)
α_i	Angle of incidence
α_T	Angle of incidence in the vertical plane
α_W	Angle of the true wind to the boat's course
β	Value in the solution of the heave and pitch response (linear theory)
β_A	Heading angle to the apparent wind
γ	Angle of sweepback
δ	Axial interference factor (windmill)
δ'	Rotational interference factor (windmill)
ϵ	Phase difference
ϵ_A	Aerodynamic drag angle
ϵ_M	Phase lag of forcing function (pitch)
ϵ_Z	" " " " " (heave)
η	Wave height at any point
η_W	Windmill efficiency
θ	Pitch displacement
θ_h	Angle of heel
θ_W	Face pitch angle (windmill)
λ	Angle of yaw
ρ	Density of fluid (water)
ρ_A	Density of air, 1.293 kg/m^3
σ	Windmill solidity
σ_c	Critical cavitation number
σ_1, σ_2, σ_3, σ_4	Roots of the stability equation (linear motion theory)

$\bar{\sigma}$	Finite span correction (mean value)
τ	Angle of trim
ϕ	Angle of inflow velocity (windmill)
ω	Wave frequency
ω_e	Wave encounter frequency
ω_n	Natural frequency
ω_w	Induced velocity at the windmill blade element
∇	Volumetric displacement

CHAPTER 1

Introduction

This story begins at Christmas, 1974, with a small hydrofoil model which consisted of a wooden frame, two one metre lengths of 40mm diameter PVC pipe as floats, and four hydrofoils and a rudder made from slivers of pine. This model was 'tow tested' on Loch Croispol in North West Sutherland one frosty morning and successfully demonstrated the realities of flight for a hydrofoil craft. From this introduction and from reference to the various hydrofoil boats that were already in existence (3, 4, 8, 33, 38, 49, 95, 135 and 154) a first prototype was built which went through several variations in design, finally ending up with the configuration which was tested in 1978 as a final year project (23).

Postgraduate work started with the award of a 15 month duration Collaborative Training Award from the Science Research Council. The two collaborating bodies were the Department of Naval Architecture and Ocean Engineering at the University of Glasgow and the Cape Wrath Boatyard, which at that time was based at Durness, Sutherland. This situation meant that there were a wide range of facilities available for the design, testing and construction of a

working prototype. The project was entitled, "Design and Development of an Oceangoing Sailing Hydrofoil", and the project description which was sent to the Science Research Council read as follows:

"During the past year preliminary work has been done on the design and testing, both in a towing tank and in open water, of a small sailing hydrofoil. Further analysis and design effort is required to develop an improved foil system suitable for the larger, more advanced craft envisaged. The sailing hydrofoils which exist today are essentially calm water vessels which have been designed to sail at high speeds in a favoured direction relative to the wind. The present project is aimed towards the development of a boat which can manoeuvre adequately on and off the foils in a seaway and still achieve high speeds. To achieve this it is necessary to tackle problems in all the principal areas of naval architecture, i.e. design, construction, structures and hydrodynamics, as well as develop a sailing rig capable of high speeds (low angle of attack, low sail twist and high lift coefficient) and balance this with the foil system. The design will require theoretical and computational problems to be tackled.

The anticipated conclusion of this research is a manoeuvrable multi-hull sailing vessel about 10m long capable of in excess of 30 knots and operations up to sea state 4."

This proposal was ambitious, especially with regard to the time scale and the anticipated conclusion of a 10m multihulled sailing trimaran, and even after a full three year studentship (the original 15 month studentship was extended as a normal S.R.C. studentship) this 10m craft still does not exist. On the other hand much of the ground work has been done and the computer programs have been written and tested to design such a craft with enough confidence that it will perform as is is intended to do in the specification. All that is required to achieve this end is a budget of a sufficient size to be able to overcome the constructional problems that will be encountered in achieving a structure in this category of strength and weight.

In 1978 the two most successful sailing hydrofoil craft were the British boats, 'Mayfly' amd 'Icarus' and at that time they had achieved speeds of 22.6 knots and 21.6 knots respectively. Previous to the campaigns of these two boats the most notable boats had been American. 'Flying Fish' was a canard configuration hydrofoil, that is most of her weight was supported on stern foils with the bow foil serving as a trim control device (4,135,142). Apollonio's boat (4) had a tandem configuration of hydrofoils, with equal foil areas fore and aft, and was based on a purpose built catamaran. Baker's 'Monitor' was a monohull with an aeroplane configuration of ladder foils, that is with most of her weight supported on the forward foils, and she was built with the support of the U.S. Navy during the

fifties. She was paced at over 30 knots (4).

On the ocean going scene the only successful flying hydrofoil was the 31ft. 'Williwaw', which completed many miles at sea mainly in the Pacific. In recent years there have been a number of hydrofoil stabilised trimarans entering the transatlantic races. Most notable of these is the 16.5m trimaran 'Paul Ricard' which in 1980 broke the long standing record for the fastest West-East Atlantic crossing (New York - Lizard Point) in 10 days 5 hours and 14 minutes. This boat is extremely sophisticated and was built from aluminium alloy using aircraft styled technology in Cherbourg.

In 1981 the most successful craft were still 'Mayfly' and 'Icarus' with record speeds of 23.0 knots and 24.5 knots in A and B classes respectively, with the American boat 'NF^2 ' holding the record in C class at 24.4 knots. The overall sailing speed record in the open sail area category (over 27.88m^2) was held by 'Crossbow' at 36.0 knots. 'Crossbow' is not a hydrofoil, but an asymmetrical catamaran with the hulls having a very high length/breadth ratio. A,B and C classes are restricted sail area classes of 10.0 - 13.94 m^2 , 13.94 - 21.84 m^2 and 21.84 - 27.88 m^2 respectively. 'NF^2' has a canard configuration of hydrofoils whereas the foil systems of 'Mayfly' and 'Icarus' are both very similar and they are of the aeroplane type. The record in the sail area division of under 10m^2 was held by the sail board, 'Windsurfer

Prototype' at 24.6 knots.

One of the less successful (in terms of speed), but more interesting boats is the trimaran 'Force 8' (90) which has a fully submerged foil system with a partly automatic (mechanical) and a partly manual incidence control system. She is sailed by a helmsman who sits in a cockpit which is fitted with aeroplane type controls and she is driven by a self adjusting solid wing sail rig.

Going back to 1978, it was decided from the experience gained from the previous tests (23, 118) and from the comments on the motion response of a hydrofoil craft in waves by Eames (59, 62, 63 and 65), to design a craft with a four point suspension system, that is with hydrofoil units at the bow, two sides and at the stern. The bow foil was designed to sense the surface and prevent any nose diving tendencies that might have existed. The bow and the stern foils, together, provided the trim control, whereas the two side foils were designed to carry most of the weight of the craft and provide for stability against heeling moments. In practice a perfectly adequate system for the prototype boat which only operated in sheltered waters was an aeroplane system similar to 'Mayfly' and 'Icarus' and this was eventually tried by moving the side foils forward and dispensing with the bowfoil. This latter system was found to be more efficient for the prototype, but a return to the original system may be required for an ocean going craft where the long bow overhangs create a

strong possibility of the forward ends of the hulls ploughing into waves.

To produce an efficient design it is necessary to do calculations on many variations of the foil system design before a satisfactory solution is reached. In order to do this, it was decided to write a set of computer programs which carried out calculations on a series of hydrofoil elements which made up a system, and gave the results of drag, flight orientation and the lift/drag ratios. These programs are described in chapter 3. A series of towed model tests were undertaken in order to judge the accuracy of the results from these programs. These tests also went a long way in forming an understanding of the operation of the prototype boat and some interesting results were found where ventilated cavities formed on the model foils (chapter 4).

It was also necessary to carry out some work on the wind propulsion of the prototype boat. The performance of the actual cloth sail rig used on the prototype was estimated and compared with an alternative wind propulsion system, that of a horizontal axis wind turbine rig. This latter rig has the advantage that it provides a propulsive force in any direction relative to the direction of the wind and as such is unique in the history of wind propulsion. This rig was chosen for study because of its expected versatility although it was realised that if pure speed in one direction only relative to the wind was

required, the choice of a solid wing sail or aerofoil rig would have been more appropriate. These considerations are discussed in chapter 5.

After the extension of the project to a full three year term was made, it was decided to extend the theoretical work to include the calculation of the motions of the craft in waves. The results of this work are described in chapters 6,7 and 8. Two major studies were undertaken and compared because from the literature it was not clear how adequate the results of a purely linear approach would be. Chapter 6 describes a solution in the frequency domain of the linearised equations of motion while chapter 7 describes a digital time step analysis of the non-linear equations of motion. The results are compared with each other, with a single degree of freedom solution and with a series of model tests (chapter 8) which were carried out in head and following seas.

Finally, this study may have appeared to have been of rather limited use because it has been involved with a sailing hydrofoil vehicle which on face value does not offer any hope of commercial exploitation apart from the possible construction of a class of racing dinghies or ocean racing yachts for the recreational market. This is not quite true for several reasons.

The first and main reason is that many of the studies here are relevant not only to the sailing hydrofoil but to

hydrofoil craft in general. In particular this includes the seakeeping studies, but the search for a hydrofoil system with the minimum possible drag which is especially relevant to a sailing vehicle with a limited power input has been taken further than is done in many cases for a conventional powered craft.

Secondly, the work on wind turbines for propulsion could lead to a wind propulsion system for ships which is attractive enough in terms of efficiency, ease of handling and range of operation, that it becomes a leading contender in the search for alternative power systems for ships in these days of increasing fuel prices. It must be remembered here that weather prediction techniques have also been improved over the last century (Paper No.6, 176, 87) and a high speed wind propelled ship should be able to be routed in such a manner that it avoided the worst areas of low wind speeds. If a wind propelled craft could compete in terms of speed and manning requirements with its motor powered equivalent which seems likely with a wind turbine vessel, then the largest remaining problem is the intermittent nature of the wind which if soluble by some method such as weather routing could make such a ship economically attractive. The feasibility of a commercial wind propelled hydrofoil ship as suggested by Wynne (195) does not yet seem to be a likely proposition.

The last reason, which is relevant in this case, is that the choice of a wind propelled hydrofoil meant that a

prototype boat could be built and tested on the full scale and tried against other similar craft. The cost of building even a small motor powered hydrofoil would have been prohibitive and the study would have been confined to model tests only. There would have been few possibilities for breaking new ground because although hydrofoil craft are still not all that common many small motor hydrofoil craft have been built and extensively tested as a prelude to their larger scale counterparts.

CHAPTER 2

The Prototype

The overall aim of this project was to design a versatile and stable hydrofoil system for a wind propelled surface craft in order to produce a vehicle which was capable of higher speeds over a larger range of courses relative to the wind direction than are normally possible for a sailing craft. The restrictions which affect the maximum speed attainable come about mainly from the limiting effects of the wave making drag from the hulls and the limited propulsive force available from a wind propulsion system. The aim with a hydrofoil craft is to take advantage of the favourable characteristics of the path of the drag curve as the speed increases of a boat fitted with a hydrofoil system in comparison to a displacement or even a planing craft. An example of such a curve is shown in figure 4.9a, chapter 4 for the hydrofoil model which was tested in the towing tank. In the formation of this design considerable use was made of previous work carried out on high speed marine craft (4, 8, 33, 38, 45, 61, 65, 81, 82, 99, 100, 106, 107, 115, 127, 144, 150, 162, 163, 170, 181 and 191).

A project such as this would have been incomplete

without some form of full scale trials carried out on the open water. It would have been ideal to have made these experiments on a craft which was capable of operating in a full scale seaway and at the end to have been in a position to assess the potential of a wind propelled hydrofoil craft as an ocean going vehicle. However, the realities of a Science Research Council Studentship and the lack of any substantial sponsorship made such a course of action clearly impossible. It was decided because of this difficulty to make the full scale tests on a vessel which would have been approximately a half sized model of an actual ocean going vehicle. Even with a craft of this size, severe financial difficulties were encountered and although these were resolved (Appendix C), many of the constructional problems and structural failures of the hydrofoils in particular came about as a direct consequence of this lack of financial resources. The general dimensions and sail areas of this boat are given in Table 2.I.

The Hulls and Deck Structure

The main requirements for the design of the hulls and deck structure of the hydrofoil boat, were a high initial hull-borne speed, light weight and a high initial stability. Coupled with these points was the need to provide adequate support to the hydrofoil system and to keep in mind the overall objective for a versatile craft, a craft that in the final scaled up design would be capable

TABLE 2.I

General Dimensions	
L.O.A.	5.00 m
LWL	4.46 m
Draught - foils extended	1.00 m
Beam - to outside of floats	4.00 m
Beam - centre-line of floats	3.70 m
Sail Areas:	
Main (fully battened)	13.94 m^2
Jib	5.10 m^2
Total	19.04 m^2 (205 sq.ft.)
Main sail A = L_f^2/S_A	5.00
Jib A	5.88
Approx. Displacement - ex crew	220 kg
Performance Factor = $\frac{\sqrt{S_A}}{\sqrt[3]{\nabla}}$	6.7 approx. with one crew

A - aspect ratio
S_A - sail area
L_f - sail Luff height (measured vertically)
∇ - volumetric displacement

of making long distance ocean passages. High speed, light weight and high stability are all factors which pointed towards a multihull, either a catamaran or a trimaran. The initial hydrofoil system design which included a central bow foil was more easily supported by a system of three hulls. In addition for the same length of boat, the beam and hence the stability can be greater for a trimaran than for a catamaran, and these points together with the fact that there had been more favourable experience gained from trimarans than from catamarans in offshore racing (121) were the main reasons behind the choice of a trimaran system of hulls for the prototype boat.

The Hulls

The hull lines were scaled down and adapted from the 'Val' class trimaran which was designed by Newick (141) who is well known for his successful trimarans (for example, 'The Third Turtle' a 'Val' class, 'Three Cheers', 'Rogue Wave','Moxie' and the atlantic proa 'Cheers' which is now exhibited in the Exeter Maritime museum, to mention just a few). The lines of the centre hull were altered from a rounded vee section to almost a U-section and they are shown in figure 2.1, along with the table of offsets in Table 2.II. The design was of the double outrigger type where all of the displacement is in the centre hull and the outriggers are designed to just touch the surface of the water when the craft is at rest.

TABLE 2.II Table of Offsets for Hydrofoil

station / waterline	Transom	0	1	2	3	4	5	6	7	8	9	10	Bow
Sheer	0.125	0.133	0.184	0.228	0.267	0.287	0.300	0.300	0.291	0.255	0.194	0.108	0.000
WLD	0.113	0.123	0.178	0.224	0.263	0.283	0.295	0.289	0.277	0.237	0.167	0.077	
WLC	0.088	0.098	0.160	0.211	0.250	0.270	0.279	0.273	0.262	0.222	0.155	0.056	
WLB		0.000	0.130	0.188	0.228	0.248	0.257	0.252	0.241	0.206	0.129	0.000	
WLA			0.000	0.149	0.193	0.213	0.224	0.219	0.209	0.171	0.062		
Sheer cf WLB	0.300	0.297	0.264	0.239	0.224	0.222	0.237	0.268	0.306	0.352	0.398	0.449	0.500
Keel	0.018	0.000	-0.100	-0.178	-0.221	-0.238	-0.242	-0.240	-0.228	-0.199	-0.133	0.000	0.500
	CENTRAL HULL												
Sheer				0.051	0.094	0.127	0.144	0.150	0.138	0.113	0.077	0.037	
WLE				0.049	0.092	0.123	0.139	0.148	0.128	0.101	0.059	0.012	
WLD				0.031	0.074	0.107	0.123	0.131	0.110	0.080	0.038		
WLC						0.059	0.088	0.098	0.078	0.041			
WLB			Stern										
Sheer cf WLB			0.385	0.363	0.342	0.332	0.338	0.358	0.388	0.432	0.479	0.529	0.560
Profile			0.223	0.170	0.106	0.052	0.017	0.000	0.009	0.044	0.113	0.277	0.560
	OUTRIGGER												

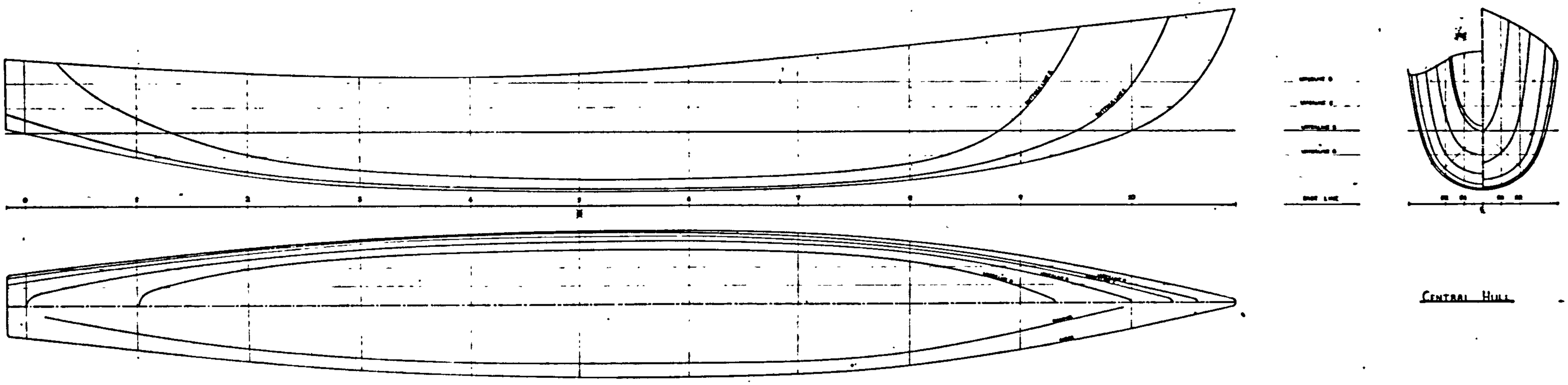

Fig. 2.1 Hull and Outrigger Lines

Each of the two outriggers or floats was split into three compartments by means of watertight transverse bulkheads. Access to these compartments was made through circular deck hatches. The central hull was also split into three sections in a similar manner, but in the initial design the central section was left open forming a long cockpit. This turned out to be a bad design feature for two reasons. The lack of a deck structure caused a deficiency in the torsional rigidity of the central hull which affected the rigidity of the whole boat and secondly large quantities of water were shipped into this cockpit during operation which it was impossible to clear rapidly and which added considerably to the overall flying weight. This area was decked over after the initial trials.

A survey of the available materials that these hulls could be constructed from indicated a choice between aluminium, glass reinforced plastic (G.R.P.), glass reinforced plastic foam sandwich construction and wood (6, 80, 151, 153, 169, 168, 152, 171 and 194). Alternative fibre reinforcements such as 'Kevlar' and carbon fibres were also considered for inclusion into a reinforced plastic construction. Out of the above the two most suitable appeared to be either a wood or a reinforced plastic construction. A single skin reinforced plastic construction would have lacked rigidity unless an adequate thickness was built up and this would have led to an excessive weight. Some form of sandwich construction was therefore necessary and after a study of the various

sandwich materials available (P.V.C. foam, balsa wood, polyurethane foam, honeycomb type materials, 168) polyurethane foam was judged to be the best choice.

Alternative fibre reinforcements were looked at and it was considered that a greater strength/weight ratio could be achieved by using 'Kevlar' instead of glass woven rovings (168), but that the overall weight saving would be minimal because of the need, as with glass woven rovings to provide a layer of glass fibre chopped strand mat in between adjoining layers of woven roving and between the woven rovings and the foam core. These layers of chopped strand matting lower the strength/weight of the lay-up ratio but are necessary to provide good adhesion between the laminations. In some cases they can be omitted by adding short glass fibre millings (approximately 1.5mm in length) to the resin system used in the lay-up (157). 'Kevlar' fibre reinforcements are of course more expensive than glass and in the event, although a donation of the basic fibre from Dupont was eventually offered conditional to the supply free of charge of the cloth from the weavers (Fothergill and Harvey), this offer was not taken up because it had already been decided by this stage to go ahead with a glass reinforced system. Owing to their expense and because the strength requirements of the hulls were not excessively high carbon reinforcements were not considered for addition to the lay-up of the hulls.

The eventual decision between a wood and a G.R.P.

construction was made all the more simple by the donation to the project of resin, fibreglass and polyurethane foam from the suppliers, Scott Bader and Co. Ltd., Fibreglass Ltd. and Unitex Marine. The lay-up of the hulls is given in Table 2.III. These lay-ups give weights of 4.6 kg/$m^2$and 3.8 kg/$m^2$for the shells of the centre hull and the floats respectively whereas a 6mm thick cold moulded plywood hull would vary between 2.9 and 4.2 kg/m^2depending on the choice of veneer, the figures are for gaboon and utile veneers respectively (155). It can be seen that cold moulded plywood would give a marginally lighter construction.

The hulls were made on batten moulds. These were jigs which consisted of moulds (transverse sections) mounted upside down on a backbone which in turn was fastened to the floor. Stringers were laid over the moulds longitudinally at a spacing of approximately 10 centimetres. The resulting jigs were the shape of the hull, minus the thickness of the skin. Foam sheets were laid over these jigs and the outer fibreglass skin was laid up over these sheets. When this lay-up had cured, the foam and outer skin were lifted off the jig and the inner skin laid up inside. The decks were made up out of flat sheets of foam, the outer G.R.P. skin of which was laid up in situ after the sheets complete with their inner skin had been fastened to the shell. Bulkheads of a similar lay-up to the deck were fitted before the deck was fastened down. The outer surfaces of the hulls were then ground off fair and any undulations were filled with a light filler.

TABLE 2.III

G.R.P. Lay-up of Hulls		External → Internal
Centre hull -	shell	Surface Tissue - 600g/m^2 W.R. - 300g/m^2 C.S.M. - 6 mm A65 foam - 300g/m^2 C.S.M. - 280g/m^2 W.R.
	decks	300g/m^2 C.S.M. - 6 mm A65 foam - 300g/m^2 C.S.M.
Floats -	shell	Surface Tissue - 280g/m^2 W.R. - 300g/m^2 C.S.M. - 6 mm A65 foam - 300g/m^2 C.S.M. - 280g/m^2 W.R.
	decks	300g/m^2 C.S.M. - 6 mm A65 foam - 300g/m^2 C.S.M.

C.S.M. - Chopped Strand Mat
W.R. - Woven Rovings
A65 - Polyurethane Foam 104 kg/m^3 (0.624 kg/m^2 @ 6 mm thick)

The Cross Beams and Decking

The three hulls were joined together by means of two aluminium alloy cross beams. These were made from the high strength, heat treatable alloy HE30 of yield strength 294 $N/mm^2$and density 2700kg/m^3, (6). Each beam was a tube, 4m long with an outside diameter of 89mm and a wall thickness of 3mm. The joints between the hulls and the beams were made by G.R.P. clamps which fitted snugly round the tube and were bolted to the hulls. These can be seen in figure 2.2 which shows 'KAA' on Loch Lomond in September 1981. The foil configuration consists of side and stern foils only. The side foils are retracted.

The size of these beams was estimated from a simplified model of the loads incident from the mast, rigging and foil system. The assumptions in this model of the loading which were all expected to be conservative, were as follows. All the loads from the rigging and hydrofoils were assumed to be transmitted across the boat through the fore cross beam only. The most severe loading came when the boat was sailing with a large value of the ratio of the heeling force to driving force, and the mast was assumed to be balanced by the windward shroud only in this case. This produced a large couple acting on the windward side of the fore crossbeam, resulting from the upwards force from the shroud and the compression load in the mast. The windward hydrofoil was assumed to be lightly loaded and the main lift force came from the leeward foil,

Fig. 2.2 *Kaa* on Loch Lomond

but the couple due to this load was considerably less than that produced from the loads from the rigging. The windward portion of the crossbeam was the most highly loaded portion and the calculations were carried out on this part.

Bracing wires were fitted below both crossbeams from the outboard end of the crossbeam to a postion below the beam on the central hull. The fixing eyes on the centre hull where these four wires were fastened were connected across inside the hull by a tie in order that the loads were transmitted adequately and that the fastening eyes did not pull out of the hull. These wires ensured that the dominant load in the cross beams was a compressive one and not a bending moment.

The two spaces formed between the hulls and the cross beams were decked over to enable the crew free movement across the boat. This decking was initially a net, but later a terylene sail cloth 'trampoline' was fitted. A sketch of this arrangement is shown in figure 2.3.

The Sails and Rigging

The original design for a sail plan is shown in figure 2.4 and shows three sails, a mainsail, jib and a genoa for light wind conditions. These sail areas were influenced by the class divisions for the Royal Yachting Association world sailing speed trials which give maximum sail areas

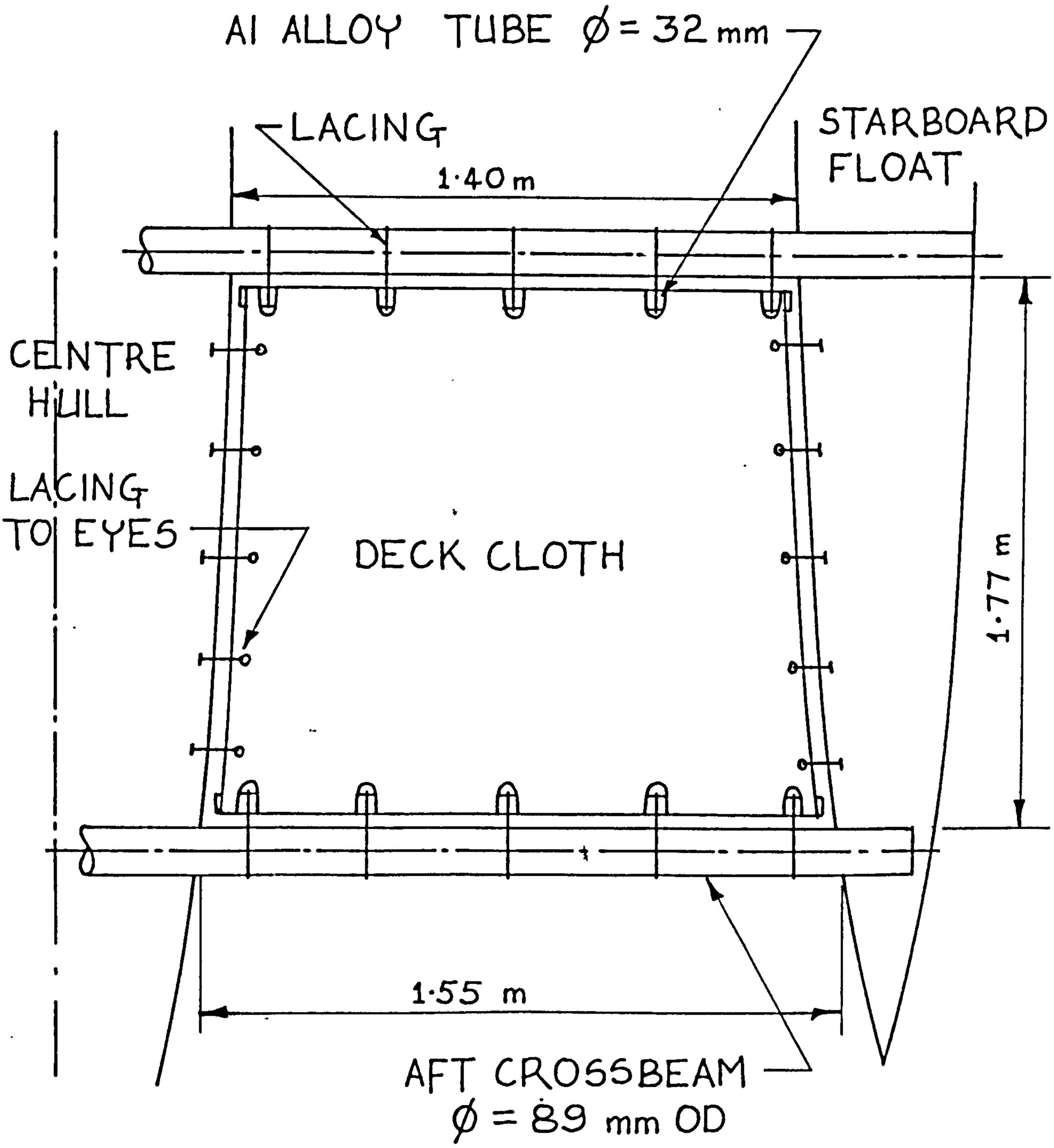

Fig. 2.3 Sketch of Deck Cloths

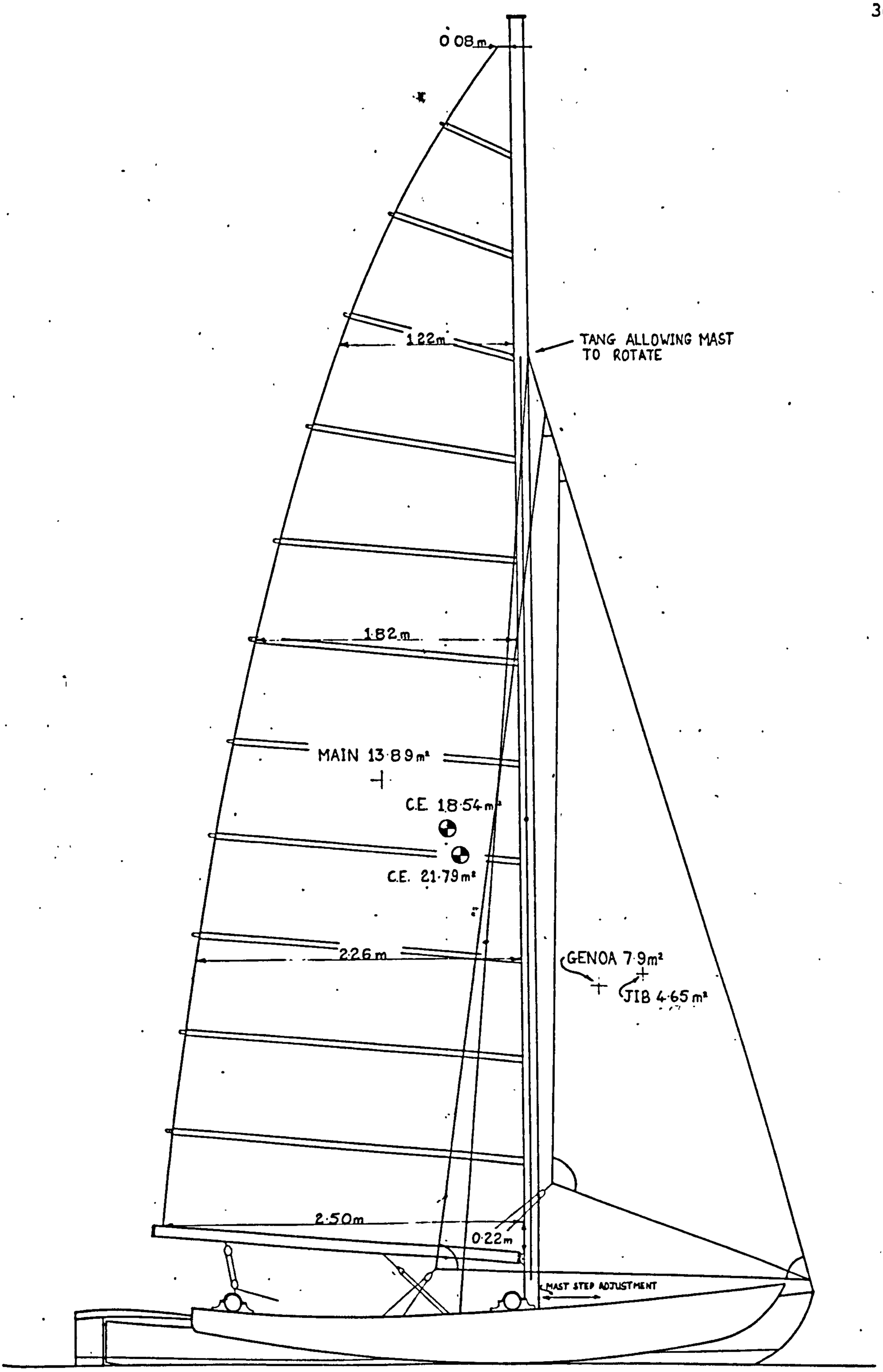

Fig. 2.4 Sail Plan

for A and B classes as 13.94 sq.metres and 21.84 sq.metres respectively. The mainsail alone was designed at the maximum limit for A class, having a sail area of 13.89 sq.metres, leaving the possibility open for trials under mainsail only, although it was found later during the trials that the boat did not perform well under main alone and this option was never used. The combination of jib and mainsail was designed for maximum efficiency, and the genoa was added as an alternative to the jib for light wind use bringing the total sail area under main and genoa to the maximum allowed under B class.

It was realised at this stage that the rig of a Tornado B class catamaran was exactly similar to the mainsail and jib sail plan which had been designed, except that the jib of the Tornado is lower cut with its foot tending to follow the course of the foot of the genoa plan shown. The total sail area of the Tornado rig is 19.04 sq. metres. It was possible because of this to obtain second hand equipment and a suit of sails was obtained from the Scottish sailmakers, Saturn Sails, while an aluminium alloy mast was obtained from the Secretary of the Tornado Association. This was all fairly new equipment, the mainsail in particular had only seen one week of use, and it was ideally suited to the purpose of these trials. The fittings, standing and running rigging were all adapted to suit the application to a trimaran configuration.

The Tornado mainsail is a fully battened high aspect

ratio sail, the battens enable it to be set at low angles of attack without instability and with controlled camber. The mast which is a streamlined section (length/breadth ratio of 2.5) is allowed to rotate in order that the airflow over the low pressure region of the sail just behind the mast is improved. Diamond stays and spreaders are fitted to improve the lateral rigidity of this mast which is low because of the fine section. As with the Tornado, wires were fitted to enable the crew to use a trapeze, thus placing his ballast weight well up to windward and enhancing the lateral stability.

This design was compared with various other boats by calculating values of the non-dimensional performance factor (P_f), the ratio of the square root of the sail area to the cube root of the volumetric displacement, the sail area/displacement ratio and the non-dimensional volumetric displacement /length ratio:

$$P_f = \frac{\sqrt[2]{S_A}}{\sqrt[3]{\nabla}}$$

$$\text{Non-Dimensional displacement/length ratio} = \nabla / \left(\frac{LOA}{100}\right)^3$$

These comparisons are made in Table 2.IV.

It is fairly clear from this table that even though the results have been non-dimensionalised, boats in a different size range cannot be compared directly. This is emphasised by noting that the values of the volumetric displacement/length ratio, show in general lower values for

TABLE 2.IV Comparison between Various High Performance Sailing Craft

Boat	L.O.A. (m)	Sail Area m^2	Δ kg	P_f	$\frac{\text{Sail Area}}{\text{Displacement}}$ (m^2/tonne)	$\frac{\nabla}{\left(\frac{\text{L.O.A.}}{100}\right)^3}$
'Kaa' (prototype) one crew two crew	5.0	19.04	 288 342	 6.7 6.3	 66.1 55.6	 1680 2640
Val class trimaran	9.5	42.3 - 54.8	1000	6.5 - 7.5	42.3 - 54.8	1143
'Three Cheers'	14.0	77.1 - 132.0	3180	7.2 - 9.4	24.2 - 41.5	1130
'Paul Ricard' hydrofoil stabilised trimaran	16.5	196	6000	7.7	32.7	1335
C class catamaran 'Hellcat'	7.6	27.9	478	6.8	58.4	1333
'Mayfly' hydrofoil catamaran	4.6	13.2	190	6.3	69.5	1950
5-0-5	5.05	16.5	287	6.2	57.5	2230
Flying Dutchman	6.05	17.5	314	6.2	55.7	1420
Finn	4.5	10.0	203	5.4	49.3	2230
'NF^2' (Canard hydrofoil)	6.1	27.7 20.3	409 320	6.9 6.5	67.7 63.4	1802 1410
Tornado	6.1	19.04	328	6.3	58.0	1445
Crossbow II (catamaran - holder of record)		111.5	2000	8.3	55.8	

larger boats, one reason for this being that structural weight does not increase in direct proportion to the scale ratio cubed. The performance factor, P_f, is a measure of the power/weight ratio of a craft, since sail area can be considered to vary almost directly with power for similar rigs in the same size range. Comparing values of P_f for boats of a similar length, that is 'Kaa', 'Mayfly' and the three planing dinghies (505, Flying Dutchman and Finn) it can be seen that 'Kaa' has a higher value of P_f especially when sailed singlehanded. The relatively high values of the volumetric displacement/length ratio for 'Kaa', noticeable especially when sailed with two crew are due to her short length in comparison with other similar boats. For example 'Kaa' is over one metre shorter than a Tornado catamaran yet carries the same sail area.

The favourable values of P_f and the volumetric displacement/length ratio of the larger trimarans suggest that applications of hydrofoils to these boats would produce some very fast craft indeed.

The Hydrofoil System

The initial concepts behind the design of the hydrofoil system were based on the experience gained from some tests which were carried out as a final year project (23). This work had also included some work on a prototype boat and from these test results it was decided to design a boat with a four point suspension system with foils at the

bow, sides and stern. It was intended with such a system that the requirements for stability against heeling moments and pitching moments could be separated, the side foils counteracting the effects of heel and the bow and stern foils the effects of pitch. It was also proposed, although never tried out in practice before the foil configuration was changed, that steering could be achieved by rotation of the bow foil as well as the stern foil, alleviating the problems that resulted from the drogue action of the bow foil unit when manoeuvring at low speeds.

Some initial hand calculations similar to those described by Eames (68), based on estimates of the general dimensions and weights of the boat and of the sectional properties for the foil section, NACA 16-412, gave the foil areas given in Table 2.V. These areas, in particular those for the hydrofoils which were in operation only at low speeds, were excessive and it was realised that they could be reduced by designing a system which made use of foil sections with larger camber and of higher aspect ratio. The detailed computer programs which are described in chapter 3 were formulated for rapid calculations on different hydrofoil system designs.

Selection of Hydrofoil Sections

The choice of the hydrofoil sections resulted from limits imposed upon their selection by the estimated maximum speed of the boat and the range of angles of

TABLE 2.V Foil Areas Required at Different Speeds

	Trim (°)	Speed		Bow Foil (m^2)	Side Foils (Total) (m^2)
		ms^{-1}	knots		
Bow begins to rise (take off speed)	2°	3.6	7.1	0.35	
Bow risen	6°	3.6	7.1	0.28	0.81
Craft levels	2°	5.2	10.0	0.09	0.78
" "	2°	6.2	12.0	0.07	0.54
Craft speeds up	2°	10.3	20.0	0.02	0.20
Trim reduced	0°	15.4	30.0	0.03	0.13
	0°	18.0	35.0	0.05	0.05

Stern foil (inverted tee) 0.05 m^2

incidence required at this speed. Coupled with these points was the need to use sections which had a favourable lift/drag ratio as well as relatively high values of the lift coefficients (high camber) over the operating range of angles of incidence. All these are conflicting points and it was necessary to resolve them by the construction of cavitation 'bucket' diagrams which define the range of operation for each section considered (64, 66, 47, 59, 70 and 182). Figure 2.5 shows these curves for the NACA sections 16-1012, 16-412 and the Göttingen profile Gö 14K which is from a circular arc affine series. The two former sections were those chosen for the lifting elements on this system. NACA 16-series sections were chosen because of their uniform pressure distribution at the ideal angle of attack which produced the largest lift coefficients for a section before cavitation occurred.

Each 'bucket' is made up of three curves. The lower curve is the boundary between sub-cavitating operation and cavitation from the underside of the leading edge of the section. The upper curve is the boundary for cavitation to occur from the upper surface of the section near the leading edge. The right hand curve, the bottom of the 'bucket', is the boundary for cavitation to occur from the mid-back position on the low pressure side of the foil. To the left of this last curve and inside the 'bucket' is the range of cavitation free operation. The width of the 'bucket', between the upper and lower curves, defines the range of angles of incidence free from cavitation. The far

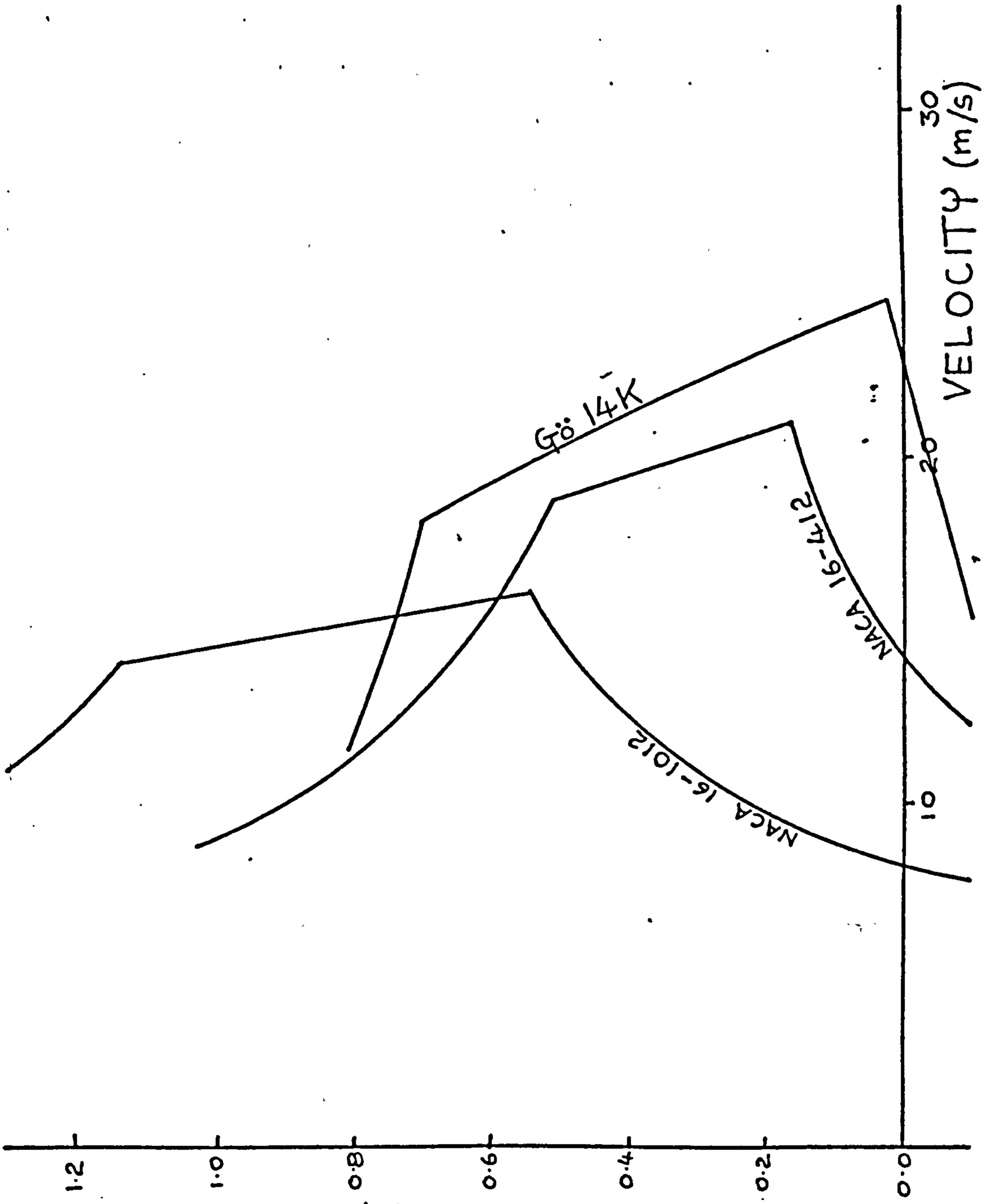

Fig. 2.5 Cavitation Bucket Diagram

right hand corner of the 'bucket' defines the maximum speed that the foil section can operate at without cavitation occurring.

The curves were calculated from the minimum pressure coefficient at these three positions on the section over the range of lift coefficients considered. This calculation used the method of Abbott and von Doenhoff (1). This pressure coefficient or critical cavitation number, σ_c, can be used to find the critical cavitation speed at zero depth, the small depths at which these foils operate make very little difference to the cavitation speed.

Critical cavitation speed (m/sec) $V_c = 13.9/\sqrt{\sigma_c}$

This is calculated from

$$\sigma_c = \frac{\text{atmospheric pressure - vapour pressure}}{\frac{1}{2}\rho V_c^2}$$

The curves are based on a vapour pressure of 1.72×10^3 N/m², but in practice the above expression is fairly insensitive to changes in the vapour pressure of water. An increase of a factor of 10 in the vapour pressure decreases the constant from 13.9 to 12.8. This lack of dependence on the vapour pressure is significant because wide variations in the vapour pressure are experienced especially in sea water due to temperature changes and variations in the amount of entrained air as well as other impurities.

For the prototype, the maximum design speed lay in the range between 30-40 knots (approximately 15-20 m/sec), and the maximum range of angles of incidence expected on the main lifting foils was about ± 3.5 degrees, this angle being made up from ± 1.5 degrees due to variations in the wave orbital velocities and craft motions and ± 2.0 degrees due to the angle of leeway. The NACA 16-1012 section which is free of cavitation up to a speed of 14 m/sec (27 knots) was chosen for the lower speed foils, those that emerged from the water at high speeds, while the NACA 16-412 section (maximum speed 24 m/sec) was used for the higher speed foils such as the cantilever portions of the side foil units.

In practice the width of the 'buckets' is larger than that drawn in figure 2.5 as this marks the boundary at which the pressure on the surface of the hydrofoil just falls to vapour pressure. There is evidence that cavitation is delayed beyond this point (92) and this is also supported by the experimental curve for the section Gö 14K (158) which is a very similar section to NACA 16-412. In any case a limited amount of cavitation may be tolerated, especially if this is intermittent as would be the case for operation in waves, although small areas of cavitation may sometimes increase the initiation of ventilation. Three dimensional and surface effects also enlarge the 'buckets' because of their influence on the low pressure areas on the foil elements. However, on the larger aspect ratio foil elements at mid-span, pressure

reductions may approach those experienced on two dimensional foils and so these results were used as the criterion here.

The Hydrofoil System Design

The design of the initial hydrofoil system is shown in figure 2.6 and 2.7. Figure 2.7 is a detail of the prototype side foil unit which shows an additional strut for extra rigidity which was included on the final design. The curves of drag, trim, height of flight at the position of the origin (the coordinate system which is defined in chapter 3) and lift/drag ratio are shown in figures 2.8,2.9,2.10 and 2.11. Also plotted are the curves for the successful hydrofoil catamaran 'Mayfly' and the drag curves for the hydrofoil trimaran 'NF^2' (30) and a Tornado catamaran. Figure 2.12 shows a redesigned side foil unit which was incorporated in the later foil configurations which are described later in this chapter. Predictions for these later configurations are also shown in figures 2.8,2.9,2.10 and 2.11.

The drag curves (figure 2.8) show the characteristic drag hump for all these configurations which correspond to the high values of bow up trim at take off. The drag for the Tornado catamaran, which comes from some full scale towing trials (30) where the catamaran has both hulls in the water, shows how the drag for this boat increases rapidly and is higher than the drag of the prototype

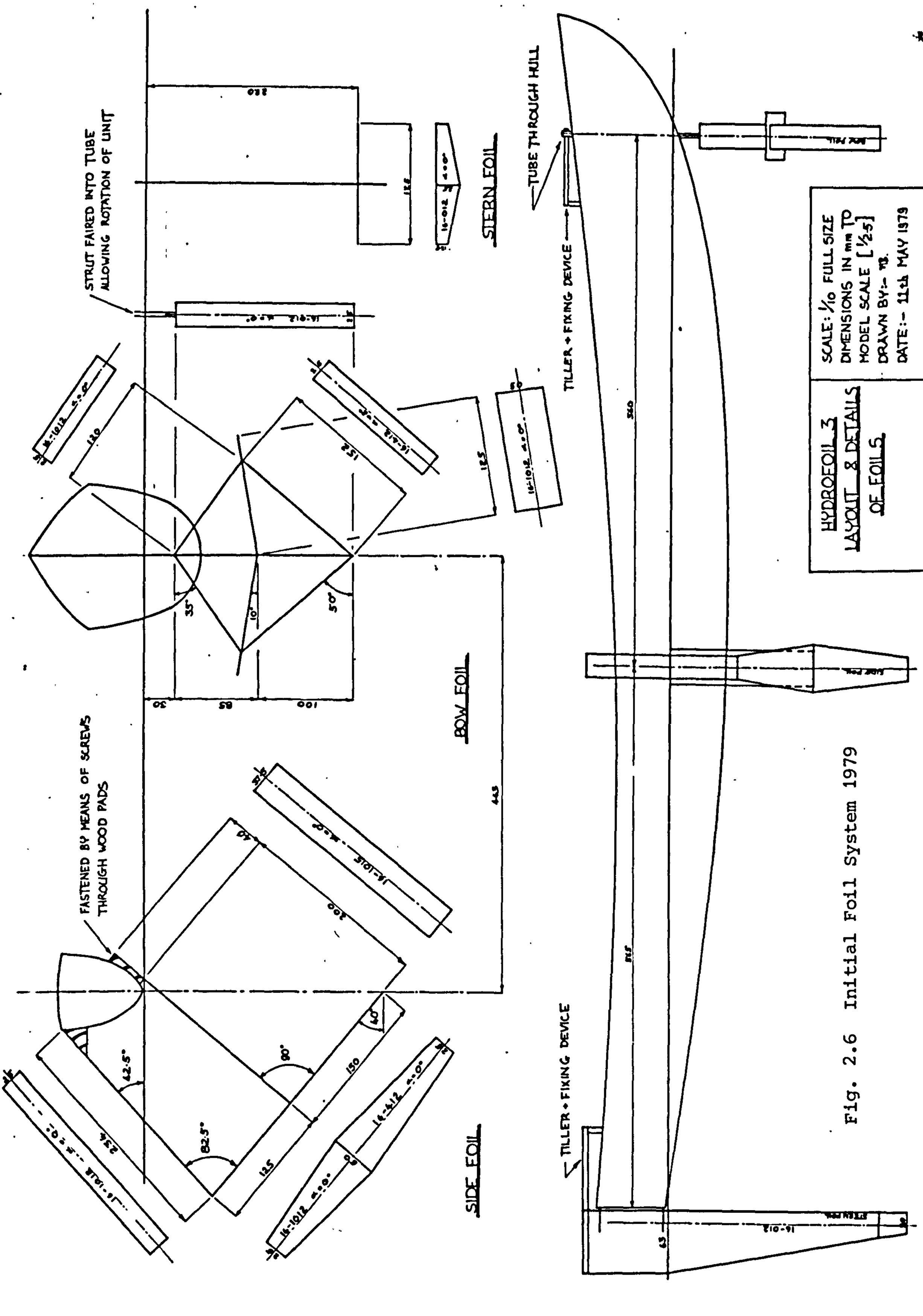

Fig. 2.6 Initial Foil System 1979

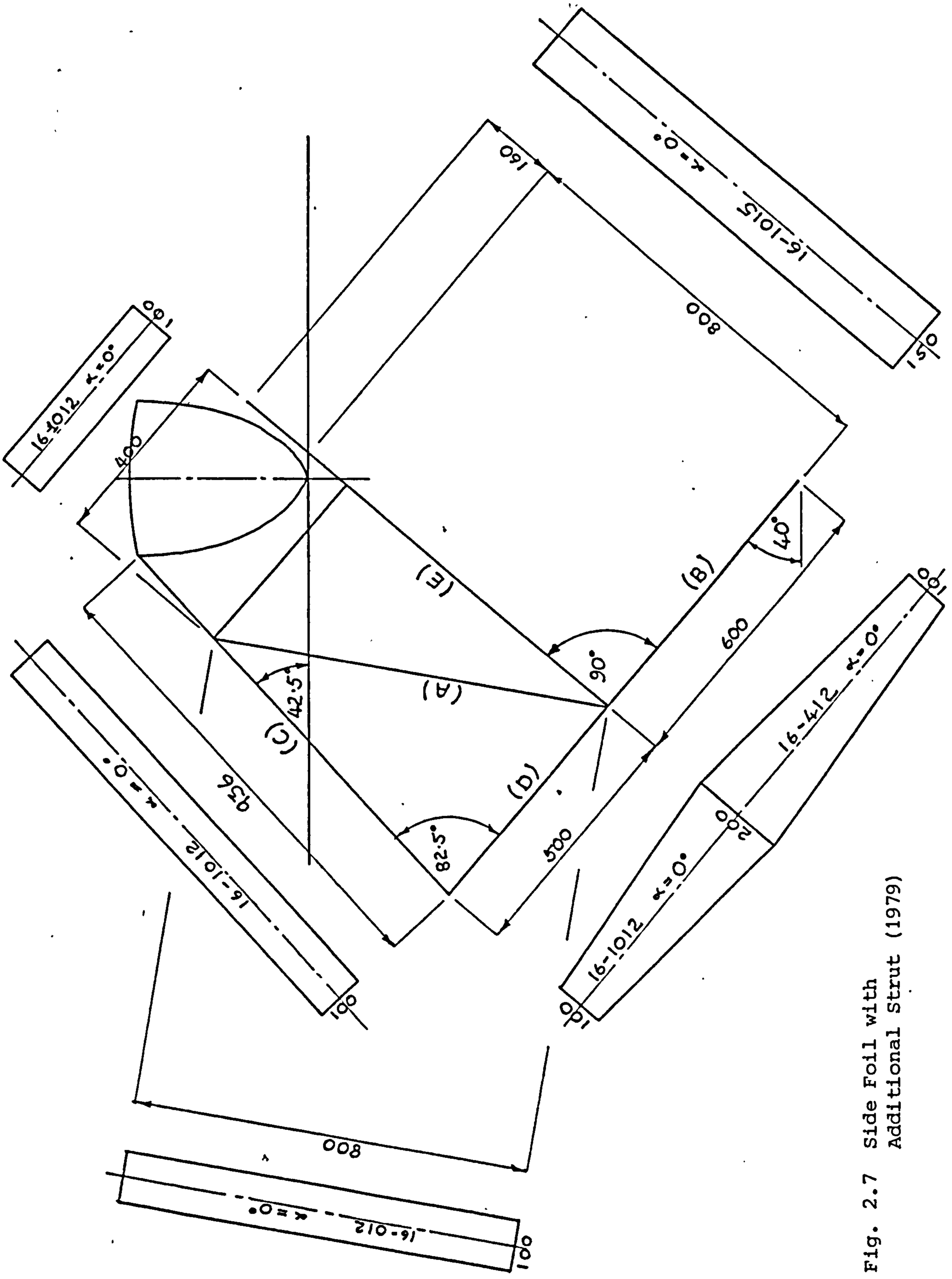

Fig. 2.7 Side Foil with
Additional Strut (1979)

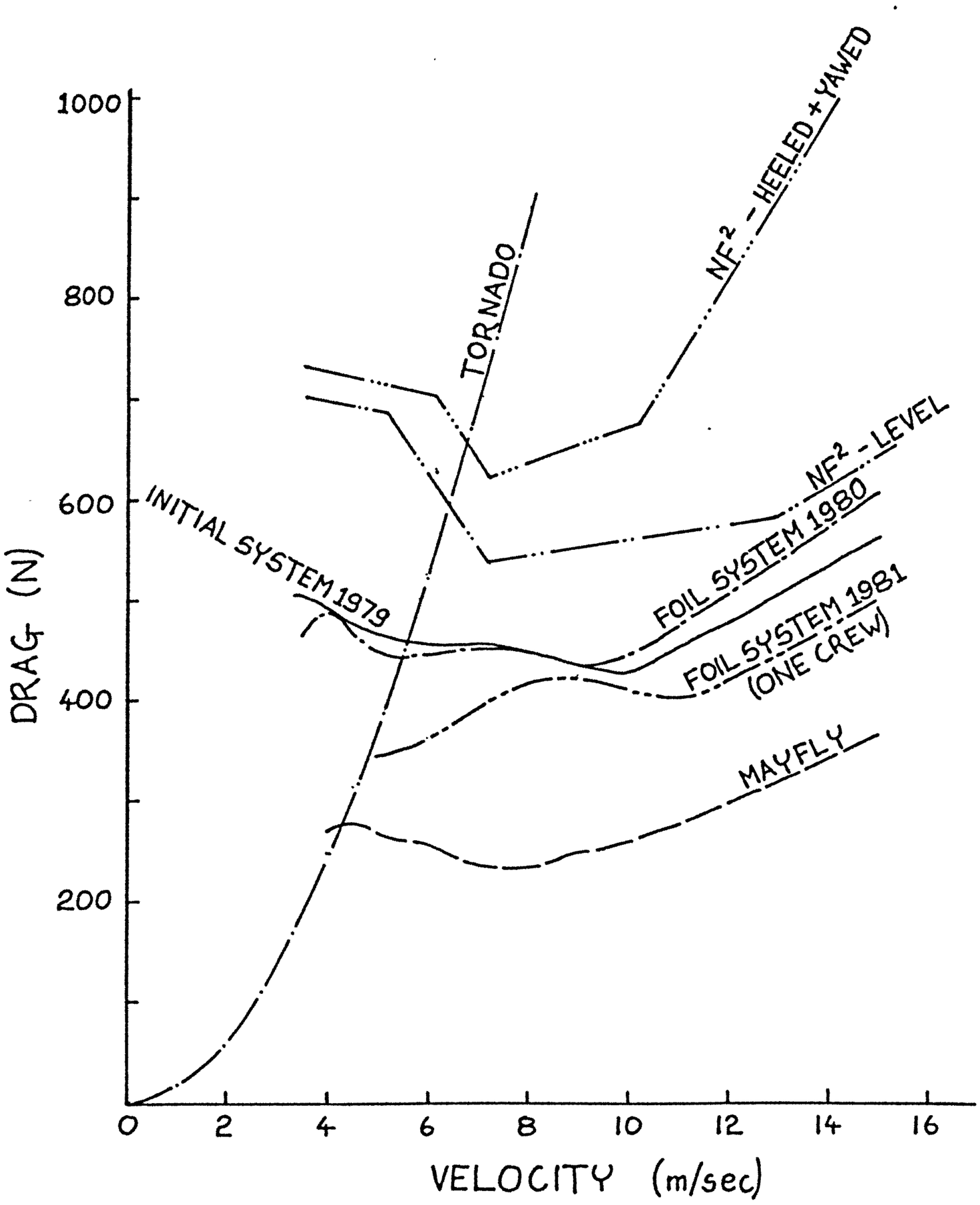

Fig. 2.8 Drag Curves at Zero Heel and Yaw

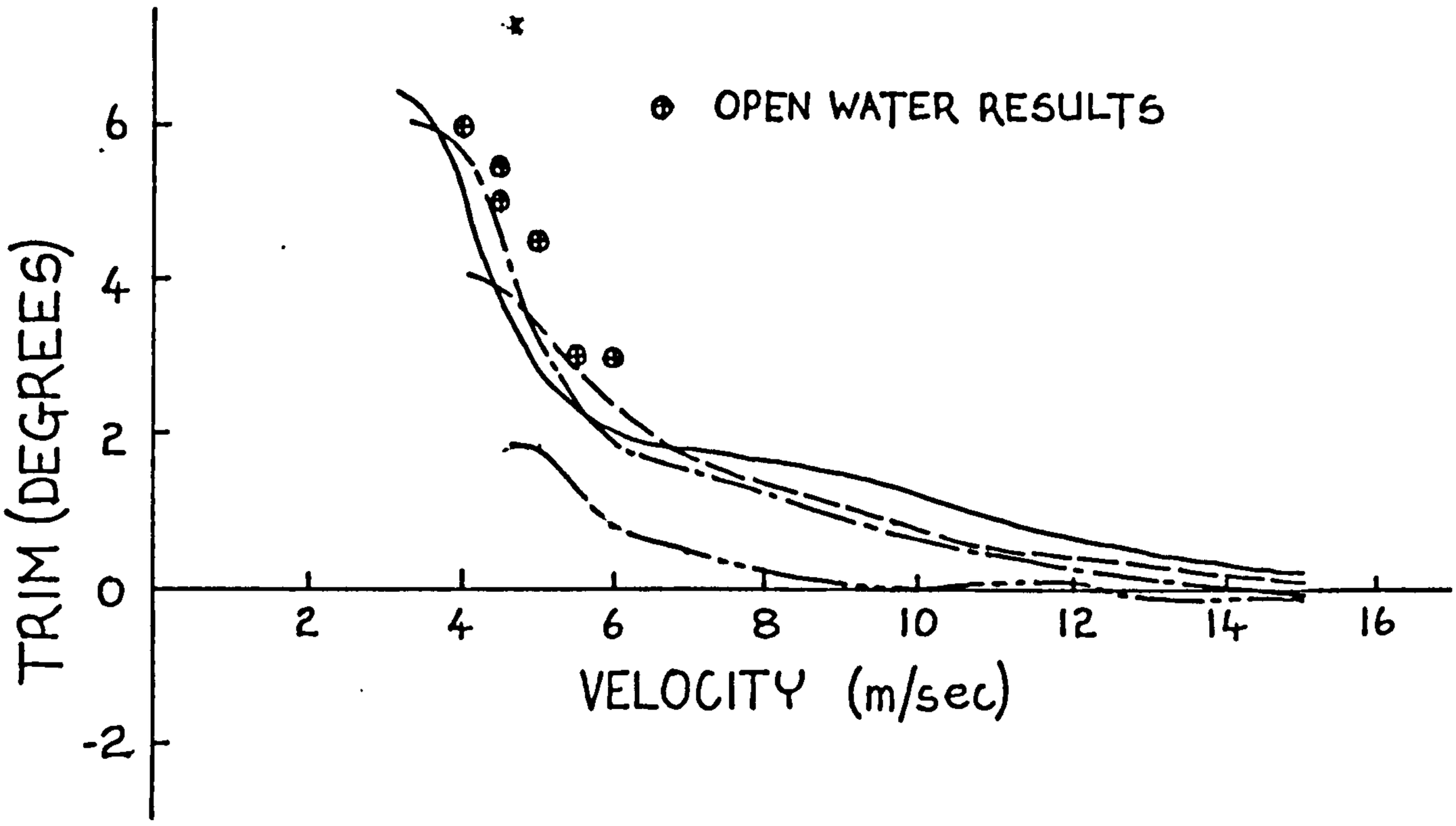

Fig. 2.9 Trim at Zero Heel and Yaw

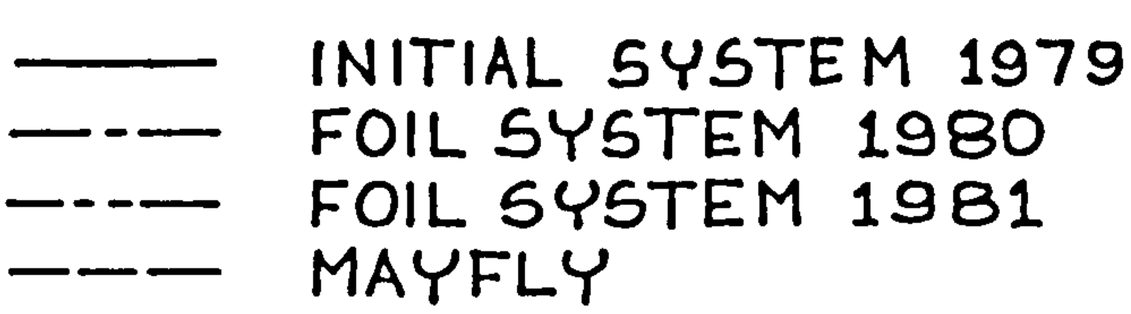

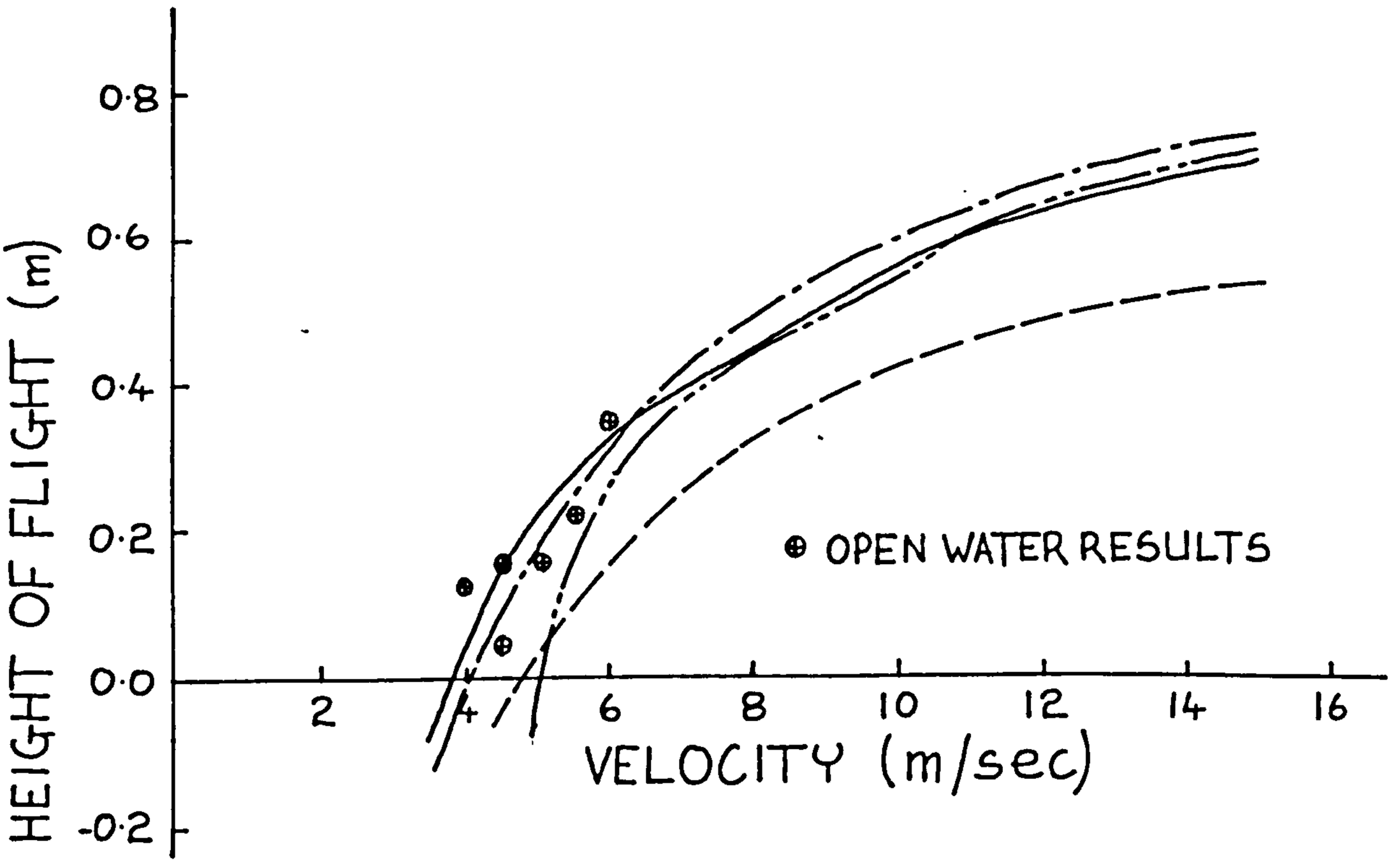

Fig. 2.10 Height of Flight at Zero Heel and Yaw

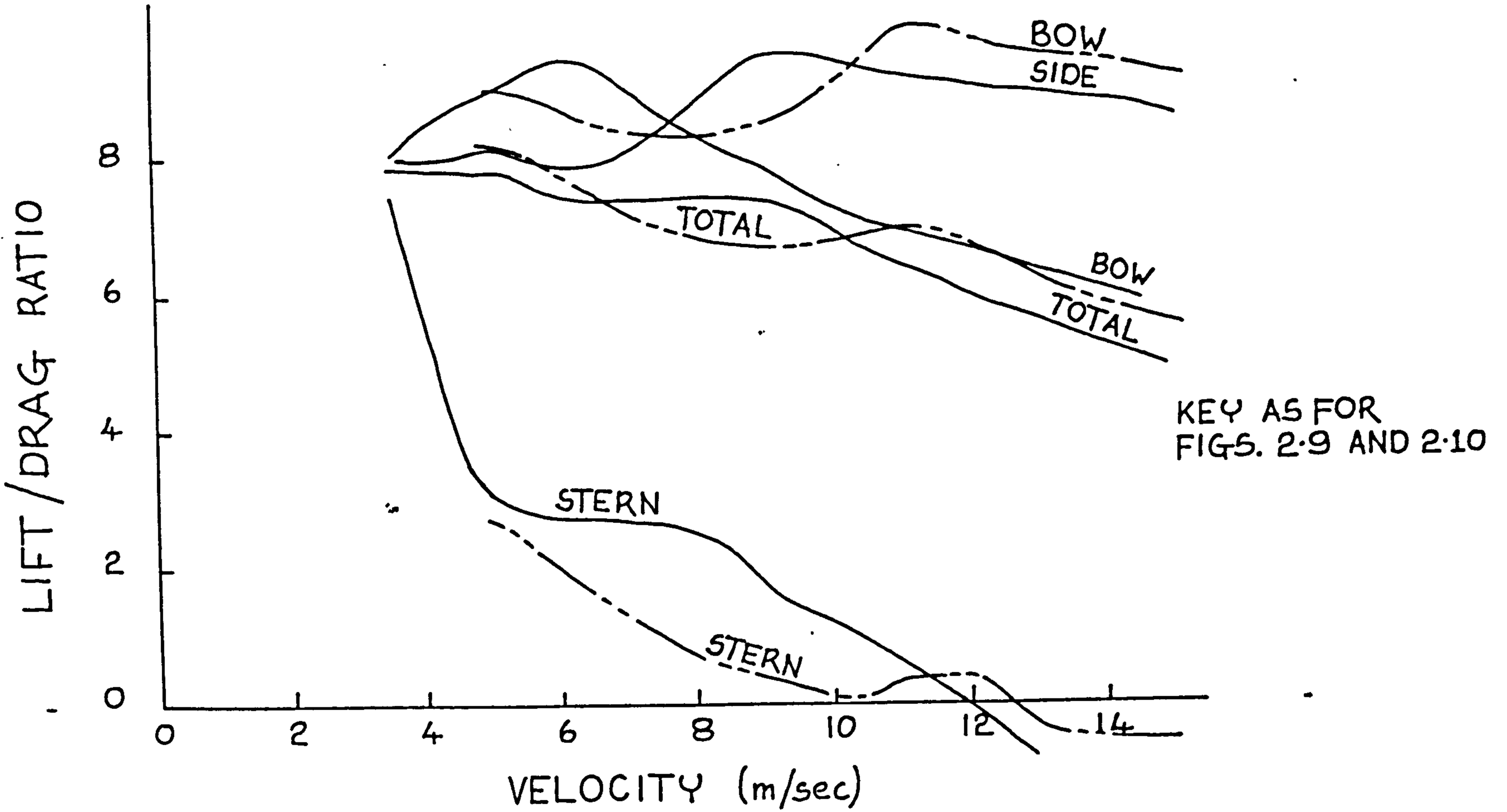

Fig. 2.11 Lift/Drag Ratios for the Foil Systems used in 1979 and 1981

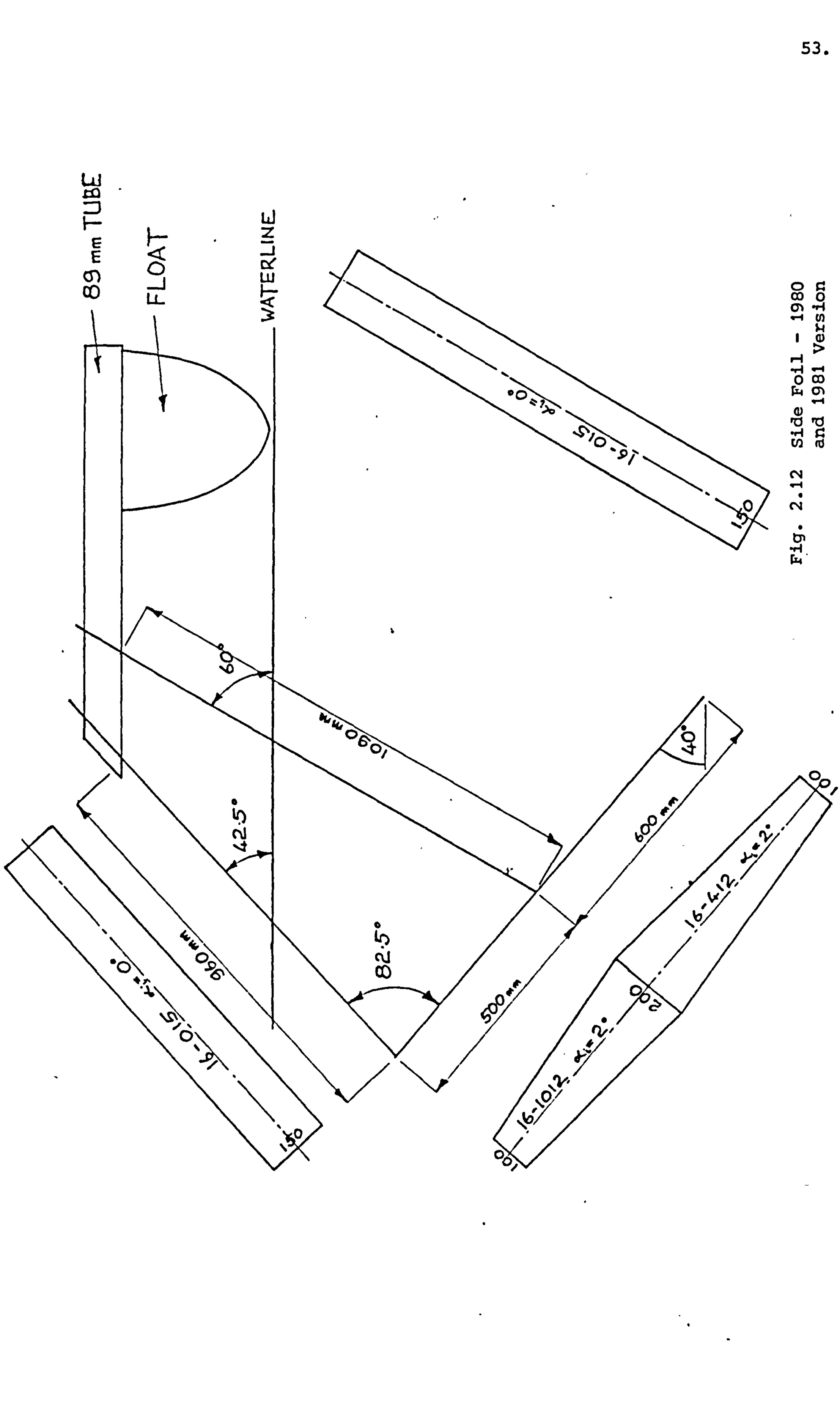

Fig. 2.12 Side Foil - 1980 and 1981 Version

hydrofoil, 'Kaa', above speeds of 6m/sec. In reality this cross over point for a Tornado catamaran sailing at this speed with only the leeward hull in the water would be higher, probably around 7-8 m/sec. The curves for the B class prototype boat fall, as would be expected, mid-way between the A class 'Mayfly' and the C class 'NF^2' (Table 2.IV shows the difference in dimensions between these boats). All the curves were predicted at angles of heel and yaw of zero degrees except for Bradfield's predicted curves for 'NF^2' . These show a large variation between the case for zero heel and yaw and the prediction including heel and yaw angles . Such a large variation was not found to exist in this study and this was a result that was corroborated by the model test results of chapter 4.

Hydrofoil Strength and Construction

From details of the loading on the hydrofoil units, which were found from the lift and drag calculations, it was recognised that the most severe loading occurred on the side foil units. An extreme loading case was considered where a uniformly distributed load of 4000N was wholly supported on the cantilevered tip of this unit. This load was more than the total weight of the boat and could only have occurred if the whole weight of the boat had been supported on the leeward side foil and there were some additional dynamic effects due to operation in waves. A two dimensional frame analysis program was used (35) to analyse the particular hydrofoil unit shown in figure 2.12,

but it was found not unexpectedly that the maximum bending moment occurred at the junction between the cantilevered tip and the lower strut and the value of this moment could have been calculated easily by hand.

The maximum values of the cross-sectional area and the second moment of area for the lower lifting hydrofoil occurred at the connection of the cantilevered tip and the lower strut and were $3.52 \times 10^{-3} m^2$ and $12.6 \times 10^{-8} m^4$ respectively. The cross-sectional area and second moment of area for the two struts were constant along their length and had values of $2.47 \times 10^{-3} m^2$ and $7.62 \times 10^{-8} m^4$. The maximum bending stress in the cantilevered tip was found to be 114 N/mm^2. The maximum end loading of 6464N occurred in the lower strut and was compressive giving a compressive stress in this member of 2.61 N/mm^2. The bending moments in the struts were small.

Although the most convenient material for the construction of these hydrofoils was wood because of the ease by which an accurate section could be achieved, this was obviously totally unsuitable for the lower cantilevered hydrofoil element from strength considerations. The initial design incorporated wooden foil elements only for the struts, but even this compromise turned out to be a catastrophic decision, as will be related later. A search was made for a suitable material for the lower cantilevered foil elements and as it turned out this material was also used for the later struts. The choice was between a fibre

reinforced plastic and a high strength aluminium alloy and the constraints were the ease of achieving a good section and of course the cost of the material and if necessary, of the manufacture. Some properties of the different materials and for the different lay-ups of fibre reinforced materials are given in table 2.VI, (6,50 and 168).

From these figures it can be seen that an aluminium alloy would have been a suitable material, which would have withstood the bending stress in the cantilevered tip with a factor of safety of 2.1. The disadvantages would have been its specific gravity of 2.8 which for solid foils would have lead to foil units of considerable weight and the expense of manufacturing accurate sections. If an alloy such as H30 was used, this expense of milling accurate sections could have been reduced by designing the struts as biogive (double circular arc) sections and welding up lengths of these elements from two rolled plates. Some tentative enquiries were also made about casting hydrofoil elements from a high strength casting alloy.

As for the hulls, though, the decision was greatly influenced by the size of the stocks of glass fibre rovings and resin and it was decided to manufacture hydrofoil elements from uni-directional glass fibre rovings. Reference to table 2.VI shows that the strength of the material is more than adequate. The most critical area was the stress due to bending on the surface of the cantilevered hydrofoil element which was withstood with a

TABLE 2.VI Properties of Materials for Hydrofoil Construction

Properties	Unit	G.R.P. Polyester Resin			Epoxy Resin			Aluminium alloy H30	African Mahogany
		Chopped strand mat	Woven rovings	Unidirectional continuous rovings	Woven Kevlar 49	Unidirectional			
						High modulus carbon fibre	High strength carbon fibre		
Fibre content	% weight	30	45	70					
	% volume	18	29	54	60	60	60		
Specific gravity		1.4	1.6	1.9	1.45	1.6	1.5	2.8	0.5
Tensile strength	N/mm^2	100	250	800	550	930	1620	295 (uts)	
Tensile modulus	kN/mm^2	8	15	40	37	213	148	69	9
Compressive strength	N/mm^2	150	150	350	135				46
Bend strength	N/mm^2	150	250	1000	450				78
Modulus in bend	kN/mm^2	7	15	40	30				
Yield stress	N/mm^2							240	

factor of safety of roughly three. *The most highly loaded lower strut with its end load of 6464N had a factor of safety of 3.9 against failure as an Euler strut. The critical stress was 10.2N/mm^2.

The relatively low value of the modulus (in bend) of this material (40kN/mm^2) meant that deflections were large and with the loading considered here, the tip of the cantilevered portion of the hydrofoil unit was calculated to deflect by 43mm. In reality because the quality of the laminates manufactured for these members was inferior to those of the laboratory tests which formed the basis of Table 2.IV (50), the experience from the full scale trials indicated that the deflections were larger than this value of 43mm which suggested that the actual modulus was lower than 40kN/mm^2. While large deflections were not in themselves harmful, a lack of stiffness in the foil elements would have meant the possibility of torsional loading producing twist in the hydrofoil elements which would have resulted in changes in the angle of incidence of the foils. This would have been detrimental to performance and could even have lead to the premature initiation of ventilation on the foils. The modulus of the laminate could have been increased by the inclusion of a quantity of high modulus carbon fibre to the lay-up, but the proportion required is quite high (171) for a benefit to be obtained and this material is very expensive.

These glass reinforced plastic hydrofoils were made in

split moulds, the first set of which were split about the mid-chord position and the second set about the leading and trailing edges. Each of these methods had its disadvantages. For moulds which were split about the mid-chord position the main problem was that slight mis-alignments between the moulds lead to variations in the camber of the section being moulded but also difficulties were encountered in incorporating woven mat for chordwise reinforcement. For moulds which had their joins at the leading and trailing edges, variations occurred in the thickness/chord ratio of the sections and inaccuracies were apparent in the leading and trailing edges themselves. Alternative methods of splitting the moulds may solve these problems.

The Full Scale Trials

The prototype which was named 'Kaa' was launched and sailed for the first time at the Royal Yachting Association Sailing Speed Week, October 13th-20th, 1979. Details of this event, which includes a complex course and time keeping system which enables timed runs to be sailed in any direction relative to the wind, are given in references 161 and 24. A map of the area is seen in fig 2.13, from which an idea can be obtained of the fetch of the waves for different wind directions.

The first few days were occupied with setting up the boat, but some initial trials were attempted without the

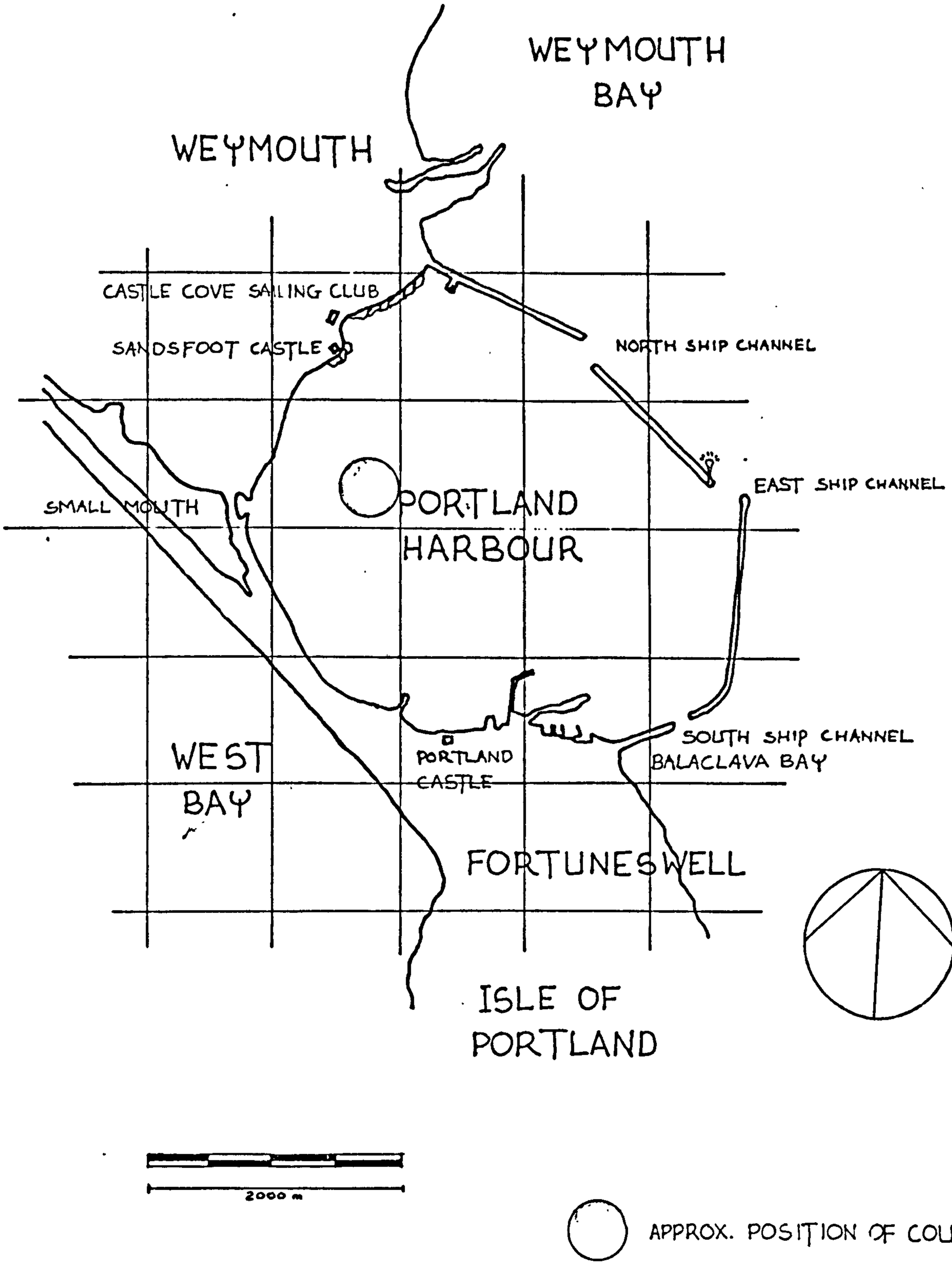

Fig. 2.13 Test Area at Portland Harbour

foil system on the 14th in light winds of 8.5 to 9 knots. No speeds were measured, but the boat performed well in this configuration.

Monday, 15th October - Windspeed 10-15 knots:

This was the first day of sailing with the foil system, but problems were met with overall flexing of the hull and crossbeam structure, mainly associated with racking between the two outer floats. This caused a reduction in the angle of incidence of the leeward side foil and a subsequent lift reduction on this foil.

Tuesday, 16th October - Windspeed 7-10 knots

Video records taken from the support boat:

Extra bracing wires were fitted to counteract this racking problem, but because of the low wind speed, official timekeeping was cancelled. A few runs were made over the course and a speed of around 4 knots was obtained unofficially by the support boat, which could keep station close by.

Wednesday, 17th October - Windspeed 5-7 knots (S.W.)

Video records taken

The angle of incidence of the bow foil unit was increased by 2 degrees. The mainsheet system was re-rigged in a more effective manner. The trapeze system was used

for the first time and the boat flew for the first time. A run was made, but the timekeeping was aborted and so no speed was obtained. Some ventilation was apparent on the bow and side foils.

Thursday, 18th October - Windspeed 5-7 knots

Video records taken

The angle of incidence of the side foils was increased by 0.5 degrees. A jam cleating system was installed for the control of the jib sheets. The boat was sailed single-handed from the trapeze in these light winds, but it did not take off. Two timed runs were made of 4.3 and 3.6 knots respectively. On both occasions the true wind was approximately 90 degrees off the bow.

Friday, 19th October - Windspeed 15-18 knots (S.W.)

Video records taken

No adjustments were made to the boat on this day and there was plenty of wind for take off to occur readily. The boat was sailed with two crew members, one on the trapeze wire and the other, the helmsman, in the centre hull. Two runs were made of 10.9 and 10.5 knots, but a higher speed was obtained during the latter run before the leeward side foil collapsed. This was estimated at 14-15 knots. Some ventilation was apparent on the bow and side foils. The boat sank after the foil broke away.

Figure 2.14 is a photograph of the boat flying on this day. Some data was taken from the photographic and video records which is plotted alongside the theoretical curves of figures 2.9 and 2.10, but these results must be viewed with some caution because they are based on estimates of the speed of the boat which are difficult to judge even from the video tape recordings.

Flexing of the Hull and Crossbeam Structure

This, was mainly associated with a racking movement of the three hulls and interconnecting beam system, the mere flexing or bending of the two cross beams being prevented by the stay wires described previously which can be seen in Figure 2.14. This racking was prounounced because of the lack of torsional rigidity of the centre hull, which was a direct result of the large open cockpit. In an attempt to limit the movement while at the Weymouth trials, two cross wires were fitted spanning the boat from the outboard end of the forward cross beam at one side to the outboard end of the rear cross beam on the opposite side. These wires, while damping the motion, did not prevent the movement altogether.

Variations in the Angle of Incidence of the Hydrofoil Units

The racking of the floats and crossbeam structure caused the angles of incidence of the side foil units to vary considerably, in some cases by as much as ± 2 degrees.

Fig. 2.14 *Kaa* at Weymouth - 1979

In most cases this was a reduction in the angle of incidence of the leeward foil unit which caused a reduction in the lateral stability. With the angle of incidence of these side foils set initially at zero degrees (at an overall trim angle of zero degrees), the lift forces would have fallen to quite low values on these foil elements especially when further variations in the angle of incidence occurred in waves.

During the week certain increases in the angles of incidence of the foil units were made, the bow foil being increased by 2 degrees and the side foils by 0.5 degrees, and these changes certainly improved the performance of the boat in general terms.

The Collapse of the Side Foil Unit

The collapse of this foil was not totally unexpected, but it was considered that in view of the time schedule for the construction, which did not allow a more sophisticated construction method to be used, some useful results would be achieved with wooden struts before a collapse occurred. An extra strut was fitted as an additional support and this can be seen by comparing figures 2.6 and 2.7. The major cause of the collapse was the combined effect of the lift forces, and the drag forces set up when the boat was supported wholly on the lower cantilevered foil element when travelling at speeds above 14-15 knots. This caused failure to occur in the upper strut.

The Sinking

The chain of events which followed the collapse of the side foil unit was as follows.

The port foil broke away during a speed trial, leaving a small hole in the port float. As a consequence the centre compartment of this float slowly filled with water. The speed trial was completed slowly and a final averaged speed of 10.5 knots was recorded. The boat was tacked to head towards the shore and an attempt was made to fly back on the intact starboard foil. The lack of the port foil meant that the boat was unstable and this caused a crash dive, leaving the centre hull cockpit swamped. An attempt was made to bale out this water, but the boat was floating too low in the water. The after decks of the centre hull and port float were below the water surface. A tow was accepted from the support boat. The rear buoyancy compartments slowly filled with water through the deck hatches which were not fully watertight. This led to more hatches lying below the water surface. Halfway to the shore the boat sank, stern first, in 3-4m of water, leaving the three bows pointing skywards. The boat was salvaged, with very little resultant damage, by the much appreciated combined efforts of the rescue boats at the trials.

'Lee Helm'

This is a phenomenon which results from an incorrect

balance between the centre of effort (C.E.) of the sails and the centre of lateral resistance (C.L.R.) of the foil system and hulls, or hulls and centre boards for a more conventional dinghy. In this case the C.E. was forward of the C.L.R. by a small amount, causing 'lee helm'. A symptom of this phenomenon which was troublesome at the trials is that a boat will fail to luff easily into the wind, which leads to difficulty in manoeuvring, particularly at low speeds when rudders are least effective. With 'Kaa' the problem was alleviated by an increase in the rake of the mast.

Restrictions in the Directions of Travel for Foilborne Operation

The prototype could only fly in the wind speeds experienced at Weymouth over a very small band of headings to the true wind. If, while flying, the boat luffed slightly (reducing the heading into the wind - α_W reducing), the angle of heel would increase and the leeward hull would begin to trail in the water. If, on the other hand, the helmsman altered course downwind, the boat would simply lose speed and return gradually to displacement sailing. Although this band of headings was around 25 degrees and would have been increased in higher wind speeds, the highest speeds seemed to be attained when sailing in one direction only and to find this direction was one of the problems associated with sailing fast.

Ventilation

A certain amount of ventilation was observed on the bow and side foil units both by the crew and on the video. Where ventilation occurred on the bow foil it appeared only to affect the particular foil element in contact with the water surface at the time and no dramatic reductions in lift were readily apparent. On the side foils the problem was more widespread and exacerbated by the additional strut which is mentioned previously. No anti-ventilation fences were fitted to the initial version of the foil system. This was in an attempt to judge the effect of any fences which were to be fitted at a later date.

Weymouth Trials 4-11th October 1980

No foil borne sailing was carried out again until the 1980 Sailing Speed Trials which were again held at Weymouth. Before the trials a number of repairs were carried out which were mainly associated with pieces of equipment lost during the sinking, but a series of more substantial alterations were also made.

A deck was fitted to cover in the centre hull cockpit in order to improve the torsional rigidity of this hull and to provide for more reserve of buoyancy. The jib sheet leads and cleating arrangements were improved. The deck hatches were sealed in a more efficient manner. (These hatches which were standard dinghy equipment were far from

satisfactory). Terylene cloth decking was provided in place of the original net between the hulls.

The hydrofoil system was almost completely rebuilt. A new tee piece was constructed and fitted to the stern rudder foil (the original was broken during the sinking). New side foil units were constructed (figure 2.12). These latter were made entirely from uni-directional glass reinforced plastic. Their attachment to the hulls was made by means of an aluminium alloy tube bonded to the two struts and mounted to the deck of the two floats in a similar manner to that of the cross beam mounts. The theoretical performance of this system is shown in figures 2.8, 2.9 and 2.10. Although an improvement over the original system is shown in the lower speed range (drag curve figure 2.8) the drag is actually higher for this system above a speed of 9m/sec. The drag curve is also plotted for this system for the case when the all up weight is lower and the boat is sailed single handed.

The trials at Weymouth (1980) were disappointing for 'Kaa'. Although many more timed runs were made than during the 1979 trials the maximum speed attained was only 10.1 knots. The speeds recorded were 5.5, 9.0, 8.3, 8.1, 8.4, 8.2, 9.9, 9.2, 7.6, 10.0, 7.7, 10.1, 9.9 and 9.1 knots. Take-off was achieved much more readily than during 1979, but once the boat was flying the expected acceleration did not occur. A large amount of ventilation was observed on the new side foil units and it was found that a large

amount of rudder angle was required to keep the boat on course. This latter caused ventilation to occur on the rudder foil. The flight consisted largely of a series of hops with the boat taking off and flying, followed by the formation of ventilated cavities on the side foils which led to crash dives. Later in the week, it was found that the bow foil unit had been badly wrenched and that it was now not aligned accurately with the flow. This would have explained the large angles of helm required to keep a straight course with a resulting higher drag and lower speed.

Some experiments were carried out with nose fences which were fitted to the main lifting element of the side foils during a day when sailing was impossible because of gale force winds. These were fitted according to the recommendations of McGregor et al (117) and they were found to have a beneficial effect by reducing the spread of the ventilated cavities. This reduced the severity of the crash dives.

Some minor adjustments were made during the week and the main boom was repaired after it had been badly split in fairly windy conditions on the Monday, the day before the severe gale.

Loch Lomond Trials August-September 1981

Between October 1980 and August 1981 the foil

configuration was changed from a four point suspension system to a configuration which consisted only of the side foils and the stern foil. The bow foil unit was dispensed with (the mounting sleeve through the hull was blocked off) and the existing side foils were moved forward to be mounted on sleeves on the forward cross beam. This enabled these foil units to retract easily by rotating until they were above the deck level. The stern foil remained as it had been in 1980. These alterations were based on the favourable tank test results which were carried out on this configuration (27) and the experiences gained from two years at Weymouth. Some preliminary tank tests had been carried out on the model with a bow foil, and on a model of the bow foil itself (196), but it was found that this foil system on the model scale was not stable. This was mainly because of difficulties encountered in manufacturing an accurate model of the complex bow foil which had very small chord lengths. This produced a foil which did not have the required lift/drag characteristics.

Repairs were carried out on the hull to deck join where this had suffered damage during operation and during transport. The connections between the cross beams and the hulls were overhauled and the centre hull was repainted where it had been damaged from sitting on the beach at Weymouth.

Nose fences were fitted to the foil system, some of which can just be seen in figure 2.2. These were quarter

chord fences with a height to chord ratio of* approximately 0.06. They were fitted to the strut of the stern foil. One each was fitted to the lower end of the lower struts of the side foils and there were three fitted to the lower lifting sections of these side foils. Although there was no apparent ventilation on the rudder foil during this set of trials, ventilated cavities still formed on the side foils and it was felt that the size of these could be reduced further by an increase in the number of fences on these foil elements.

A map of the test site on Loch Lomond is shown in figure 2.15. The boat was sailed single handed and all the sheet leads and control lines were rigged up to this end. The first two days trials were in fairly light wind conditions. On the third time out there was enough wind for intermittent flight in the gusts and some video recordings were made on this day. It was found that with this foil configuration the boat required a higher speed for take off to occur and this is borne out by the theoretical calculations (figures 2.8,2.9 and 2.10). Figure 2.8 also shows a fairly high drag in the range of speeds from 6-10 m/sec. This is because with all the weight supported on the side foils only, the trim and height of flight were less at a given speed than previously and the lower strut/foil intersection remained submerged until a higher speed around 10m/sec was reached. The boat was found to be more responsive and manoeuvred more easily than before at low speeds.

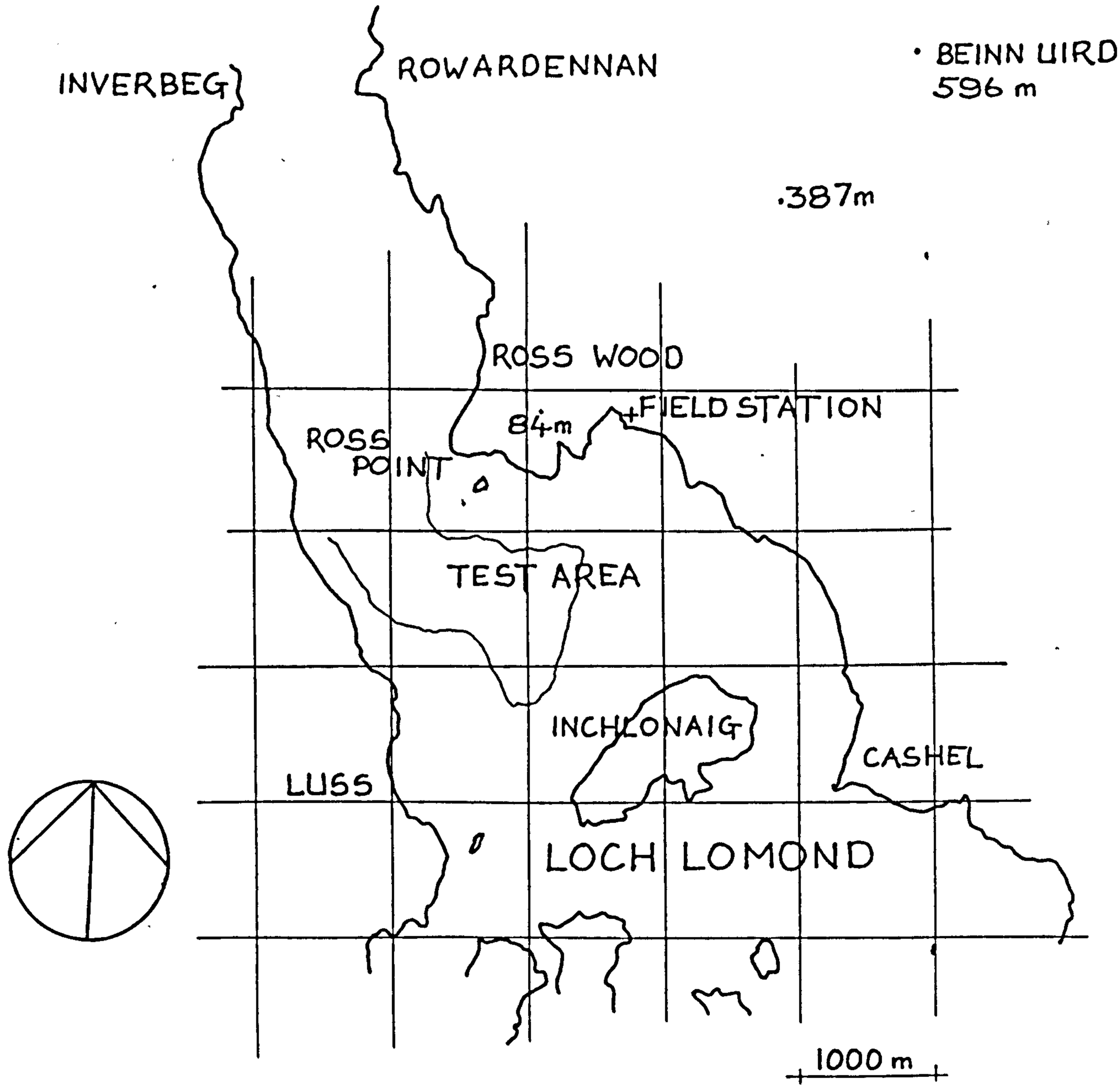

Fig. 2.15 Test Area on Loch Lomond

On the fourth day of trials the wind was of a sufficient strength for sustained flight and 'Kaa' sailed at her best ever speeds, well in excess of 15 knots. Figure 2.16 shows 'Kaa' at speed on this day although the print is poor because of the rain and the magnification of the negative. Shortly after this photograph was taken, the rudder foil broke off because the pintle fittings were not able to withstand the loads imposed on them at these speeds. Although 'Kaa' did not sink this time, because of a fault with the motor of the rescue boat it was necessary to sail her back to the shore rudderless.

This last day of trials indicated that high speeds and manoeuvrability were possible with this design and that the potential of 'Kaa' when rebuilt with a foil system of sufficient structural integrity, would be high.

Fig. 2.16 *Kaa* at Speed on Loch Lomond 1981

CHAPTER 3

The Design Programs - Theoretical Principles

This chapter is mainly concerned with a description of the design programs which made calculations of the forces on a hydrofoil system in calm water assuming steady conditions. These principles were used throughout this study for the force calculations and they will be referred to also from later chapters describing motion studies where to a great extent quasi-steady conditions have been used. All of the computer programs in this study were general programs which could be used for most surface piercing hydrofoil systems. This was necessary not only because of the obvious requirement for versatile computer programs, but because in a design study such as this, it was important to study the effect of changes in the foil system design on the overall behaviour of the craft. The primary calculations were therefore made on a hydrofoil element of constant dihedral angle, but allowing for a linear variation of chord length (figure 3.1).

The approach used for the actual lift and drag characteristics of this element was based mainly on the methods adopted and used by the Defence Research Establishment Atlantic, Canada. These are methods which

were developed from their experience with the various Bras D'Or craft and their predecessors (59,62,63,64,66 and 68). Additional information came from references (7, 10, 18, 21, 32, 46, 72, 75, 76, 88, 101, 112, 183 and 197). This is a lifting line theory where the ideal two-dimensional lift curve slope of 2π is assumed and various corrections are made to this value to account for the various influences that come about because of finite span, the free water surface and viscous flow.

Going back to the hydrofoil element (figure 3.1), defined between its end points A and B with chord lengths and depths c_A ,h_A ,c_B and h_B respectively, and angle of dihedral, Γ , the chord length at any point along its span was expressed in terms of the depth at that point (h) and the end point values alone:

$$\text{Chord length } c = c_A - \frac{(c_A - c_B)(h - h_A)}{(h_B - h_A)} \qquad 3.1$$

where it was assumed that $h_B > h_A$.

Given the ideal 2-D lift curve slope,

$$C_L = 2\pi\alpha_i$$

where the lift coefficient

$$C_L = \frac{L}{\frac{1}{2}\rho S V^2}$$

α_i is the angle of incidence and S is the projected area of the foil onto the horizontal plane.

Since lift was defined in the vertical plane, the angle of

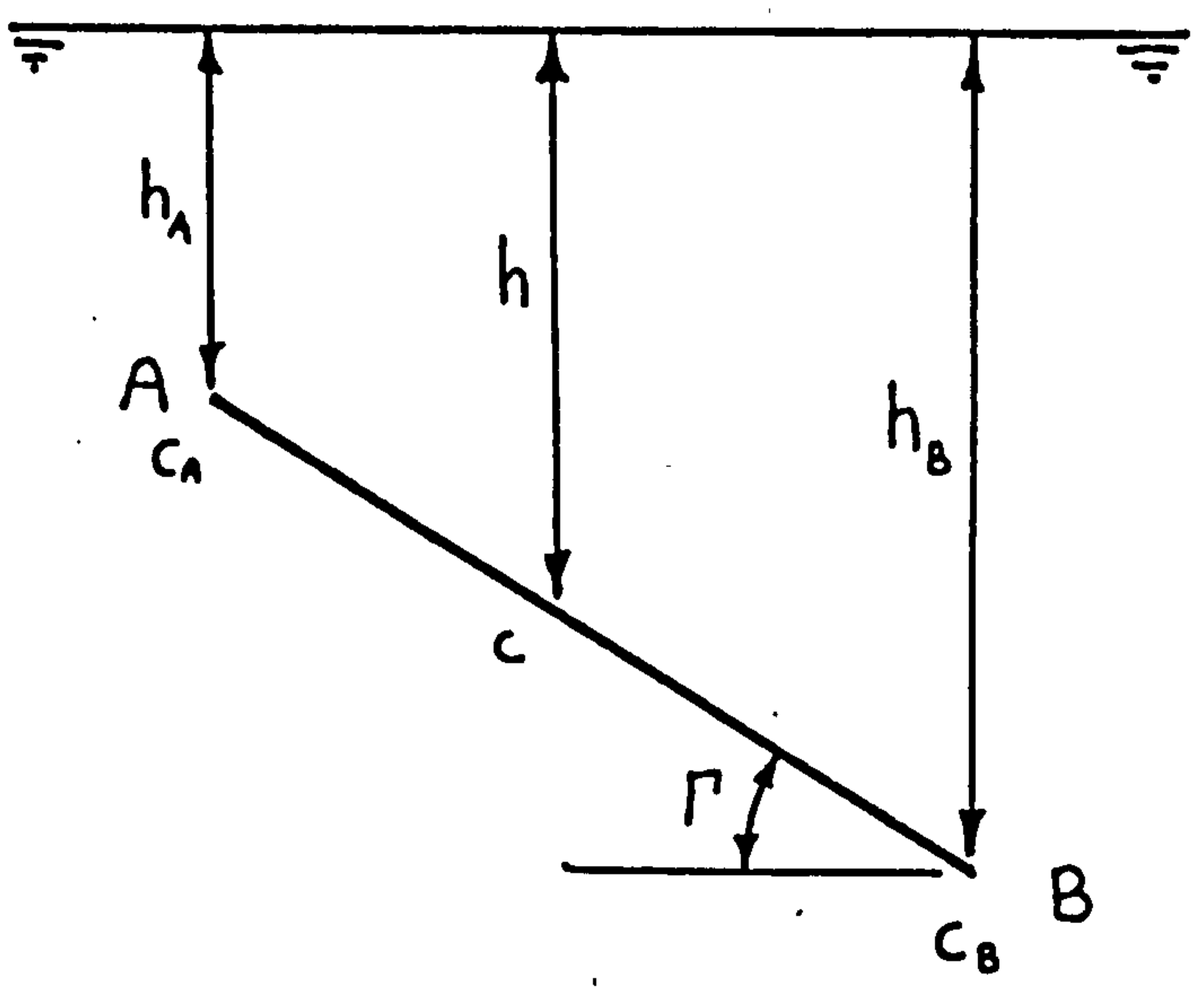

Fig. 3.1 The Hydrofoil Element

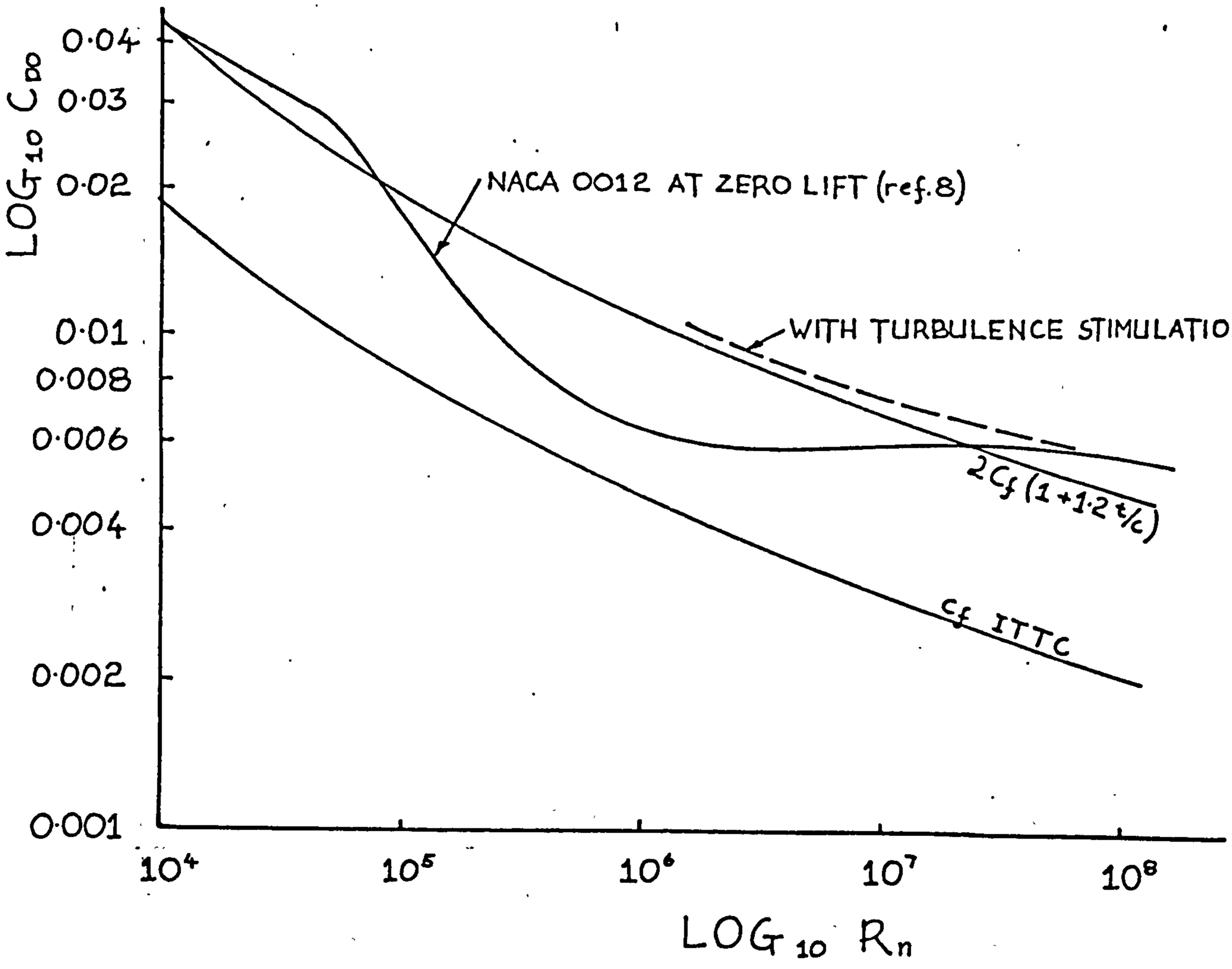

Fig. 3.2 Variation of the Section Drag Coefficient with the Reynold's No.

incidence was first corrected for dihedral angle, Γ, and angle of sweep back γ of the foil:

$$\alpha_i = \alpha_T \cos\Gamma \cos\gamma$$

where α_T is the angle of incidence in the vertical plane. Considering for convenience the inverse of the lift curve slope, the corrections were made as follows:

to the lift equation

$$\frac{\alpha_T}{C_L} = \frac{1}{2\pi \cos\Gamma \cos\gamma} \left(\frac{1}{\bar{K}} + \frac{2}{A^2} \right) + \bar{W} + \frac{1 + \bar{\sigma}}{\pi A}$$

and to the drag equation

$$C_D = C_{DO} + C_L^2 \left(\bar{W} + \frac{1 + \bar{\sigma}}{\pi A} \right)$$

where C_{DO} is the section drag coefficient.

The values $\bar{K}, \bar{W}$ and $\bar{\sigma}$ were corrections averaged over the element and A was the effective aspect ratio of the element. In the majority of the routines, the mean values $\bar{K}, \bar{W}$ and $\bar{\sigma}$ were calculated from the analytically derived definite integrals where the integration was carried out over the range of depth of the element. On some of the later wave work however, this method was unwieldy in applying the variation of the wave parameters with depth (vertical wave orbital velocity, etc.), and resort had to be made to the much more straightforward method of a numerical integration over the depth (using Simpson's Rule), taking five stations over the span of the element. The results were found to be identical to those using the previous methods and the formulation much less complex.

For a hydrofoil, the low pressure field on the upper surface of the foil contributes not only to the lift, but to a distortion of the free water surface which effectively relieves the pressure drop to a certain extent and reduces the lift. This was allowed for by the two corrections $\bar{K}$ and $\bar{W}$, the first an approximation to the lift loss due to the pressure relief and the second a correction to account for the formation of waves.

The value $\bar{K}$ was taken from the factor K due to Wadlin, et al., (17, 187and 188) and averaged over the span

$$\bar{K} = \frac{1}{h_B - h_A} \int_{h_A}^{h_B} \frac{(4h/c)^2}{(4h/c)^2 + 2} + 1 \; dh$$

which gave at constant chord,

$$\bar{K} = 1 - \frac{c}{4\sqrt{2}(h_B - h_A)} \left[\tan^{-1} \frac{2\sqrt{2}\, h_B}{c} - \tan^{-1} \frac{2\sqrt{2}\, h_A}{c} \right]$$

or after substituting in for the chord length from equation 3.1,

$$c = P - Qh$$

where

$$P = c_A + \frac{(c_A + c_B)h_A}{h_B - h_A}$$

and

$$Q = \frac{c_A - c_B}{h_B - h_A}$$

gave

$$\bar{K} = \frac{1}{h_B - h_A}\left[\frac{d'}{a'}(h_B - h_A) + \frac{b'(2d' - a')}{4a'^2}\left\{\log_e\left|\frac{a'h_B^2 - b'h_B + c'}{a'h_A^2 - b'h_A + c'}\right| + \right.\right.$$

$$\left.\left.\frac{b'^2 - 2a'c'}{a'b'}\left(\frac{1}{\frac{c'}{a'} - \frac{b'^2}{4a'^2}}\right)^{\frac{1}{2}}\left(\tan^{-1}\frac{h_B - b'/2a'}{\left(\frac{c'}{a'} - \frac{b'^2}{4a'^2}\right)^{\frac{1}{2}}} - \tan^{-1}\frac{h_A - b'/2a'}{\left(\frac{c'}{a'} - \frac{b'^2}{4a'^2}\right)^{\frac{1}{2}}}\right)\right\}\right]$$

where $a' = 16 + 2Q^2$, $b' = 4PQ$, $c' = 2P^2$, $d' = 16 + Q^2$.

The value of $\bar{W}$ was taken in a similar manner from Vladimirov (36,37,59,173 and 186). This models the wave drag hump of the actual foil element,

$$\bar{W} = \frac{1}{h_B - h_A}\int_{h_A}^{h_B}\frac{1}{2F^2}\exp\left(-\frac{2h}{cF^2}\right)dh$$

which after substituting for chord length and integrating as above gives,

$$\bar{W} = \frac{1}{4(h_B - h_A)}\left[\left(-P + Qh_B + \frac{QV^2}{2g}\right)\exp\left(-\frac{2gh_B'}{V^2}\right)\right.$$

$$\left.+\left(P - Qh_A - \frac{QV^2}{2g}\right)\exp\left(-\frac{2gh_A}{V^2}\right)\right]$$

where P and Q are the same as before.

In both the above cases the simple form was taken for the special case of a horizontal foil, where there was no need for an integration over depth.

Effects of Finite Span and Planform

As for the case of an aerofoil a hydrofoil of finite span undergoes further lift losses which for the realistic assumption of elliptical spanwise loading are given as an increment to the inverse of the lift curve slope as :

$$\Delta\left(\frac{\alpha_i}{C_L}\right) = \frac{1 + \bar{\sigma}}{\pi A}$$

where $\bar{\sigma} = 0$ for a monoplane aerofoil and A is the aspect ratio.

The term $\bar{\sigma}$ was a modification necessary for the influence of the free surface and to a first approximation this could be taken as similar to the effect on the lower wing, of the upper wing of a bi-plane (59 and 78). A numerical approximation to this factor, σ (Prandtl's finite span bi-plane factor) is given by Eames,

$$\sigma = \frac{A}{A + 12^h/c}$$

Again for the mean value,

$$\bar{\sigma} = \frac{1}{h_B - h_A} \int_{h_A}^{h_B} \frac{A}{A + 12^h/c}\, dh$$

and after substituting for the chord length and integrating,

$$\bar{\sigma} = \frac{12AP}{(h_B - h_A)(12 - AQ)^2} \log_e \left| \frac{AP + h_B\ (12 - AQ)}{AP + h_A\ (12 - AQ)} \right| - \frac{QA}{12 - AQ}$$

where P and Q are the same as before. *

Corrections to the above for non-elliptical loading could have been made at this stage, but because of the lack of data available for hydrofoils in this respect and the complex hydrofoil units studied here, it was thought that any correction would not have been justifiable. A small correction was made, however, to bring the calculations of the lifting line theory for moderate aspect ratios more into line with lifting surface theories. The method used, suggested by Eames (59) was to multiply the basic 2-dimensional inverse of the lift curve slope by the factor E, where,

$$E = 1 + 2/A^2$$

(provided A is not small).

Section Drag Coefficient C_{DO}

In the absence of experimental data for all the hydrofoil sections considered, an approximation to the section drag coefficient was obtained from an empirical expression based on the frictional coefficient, C_f, the thickness chord ratio T/c, the design lift coefficient, C_{Li} and the two dimensional lift coefficient for the section at the given angle of attack, C_{L2D}. The basis of this was an expression for the minimum section drag coefficient C_{DOMIN} plus a quantity (normally assumed parabolic) which varied with the section lift coefficient. In reality such formulas tend to be conservative because for a real section

there is a range of angles of attack where C_{DOMIN} is realised whereas the parabolic assumption means that C_{DOMIN} is only held at the design lift coefficient. The choices of the value for the constant of the parabola, CONST, becomes a trade off between modelling the flat part of the curve (where $C_{DO} = C_{DOMIN}$) and the steepness of the ends (i.e. the rate of change of the rise of C_{DO} when away from the minimum value). This value of CONST was left as a variable in all of the computer programs and could be chosen by the operator. However, a value of 0.011 was chosen in most operations of the program. Expressions for the value of the minimum drag coefficient can be found in a number of works (17, 92 and 158), although the curve due to Hoerner (92) and chosen by Eames (59), seemed to be the best fit for experimental data (1 and 158) for NACA and circular arc profiles of moderate thickness/chord ratios. (T/c = 0.07 to 0.15) .

Hoerner gives,

$$C_{DOMIN} = 2C_f \ (1 + 1.2 \ T/c + 70 \ (T/c)^4)$$

where the last term is small at the lower values of T/c.

The curve used was,

$$C_{DO} = 2C_f \ (1 + 1.2 \ T/c) + CONST \ (C_{L2D} - C_{Li})^2$$

where C_f was the skin frictional coefficient taken in this case as the approximation from naval architecture, the I.T.T.C. line,

$$C_f = \frac{0.075}{(\log_{10} R_N - 2)^2}$$

where R_N is the Reynolds number based on chord length.

This curve can be seen plotted at zero lift for a thickness/chord ratio of 0.12 in figure 3.2 together with a plot of C_f and the experimental curve for the section NACA 0012 at zero degrees angle of attack.

Aspect Ratio

It will be noticed that in the above formulations for lift there is a strong dependence on the value of the aspect ratio of the hydrofoil, as would be expected in any theory of aero/hydrofoils. However, a clearly defined method of calculation for the aspect ratio still had to be formulated for the complex surface piercing foil units considered here. In this study this was undertaken by assuming that the effective aspect ratio of the box-plane shown in figure 4a could be taken as,

$$A = b/c\ [1 + h/b(a/b)^3]$$

This expression came from some unpublished work done by Hoerner (67) and it was extended to cover the inclined foil elements of figure 3.3 as follows (25),

$A = b/2c\ [\ 1 + h/b\ ]$ Fig. 3.3b and c

$A = b/c\ [\ 1 + h/b\ ]$ Fig. 3.3d

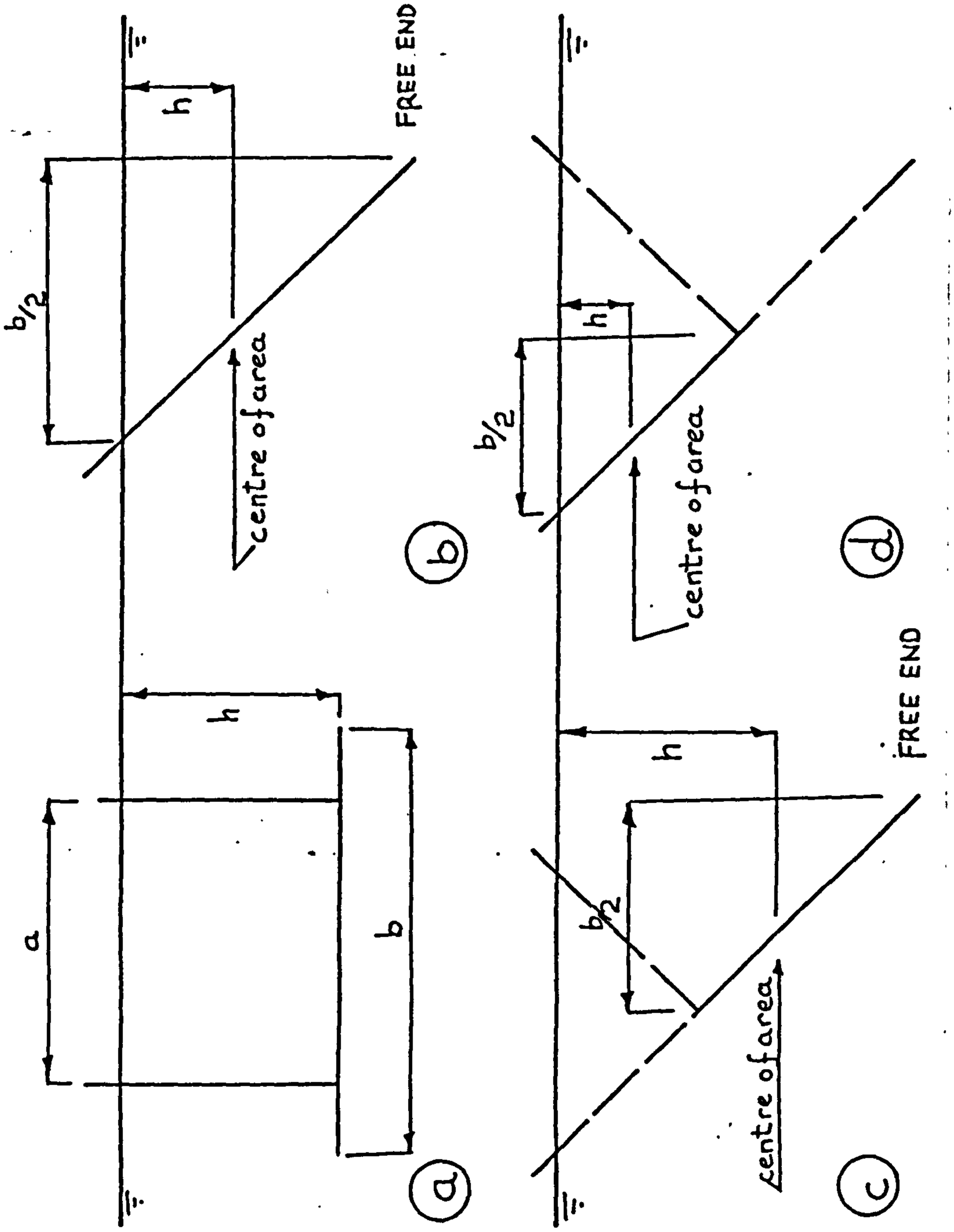

Fig. 3.3 Hydrofoil Element - Aspect Ratio

where h was the depth of the centroid of the area and where the restriction h<b was assumed to apply. In the case when h>b the ratio h/b was taken as unity.

In addition a further reduction in aspect ratio was made for foil elements that cut the free water surface, where it was assumed that the foils had no effect for a depth of 0.1 chord (93),

$$\Delta A = \frac{-0.1}{\tan\Gamma}$$

Spray Drag

Spray Drag was treated as a simple addition to the total drag of the foil element (42,92) and was taken as,

$$\text{Drag due to Spray} = 0.12\ \rho V^2 T^2$$

where ρ is the density of the water. The coefficient 0.12, comes from the work described in the two references given.

Computer Program HYDROFOIL

The above formulations were programmed on a digital PDP 11/40 mini computer as the program designated HYDROFOIL. Three types of foil element were covered, the inclined element of figure 1, as well as the two special cases of a vertical strut and a horizontal foil. This program became the basis of the subroutines FOIL1, FOIL2, FOIL3 , FOIL4, FOIL5 and FOIL6 which will be described

later and which are used throughout this work.

The Calm Water Design Programs (DESIGN 1-5)

The computer programs designated DESIGN1 through 5 were a series of programs which calculated flight orientation of a surface piercing hydrofoil system at a given speed by assuming a quasi-steady balance of forces. They were all variations on the same theme, that is the calculations in each case were very similar, but each one was intended to give the answer to a slightly different question.

DESIGN1,DESIGN3,DESIGN4,(Subroutine FOIL1)

These programs were concerned with the special case of motion where both angles of heel and yaw were zero. DESIGN1 and DESIGN4 provided answers to the flight orientation problem at a given speed. They both had a maximum of 150 iterations, by which time if a balance was not achieved, the values at the 150th iteration were output (DESIGN4 varied from DESIGN1 only in that it could consider a range of speeds for one run of the program). DESIGN3 allowed only one iteration and was useful for obtaining the hydrofoil force situation for a given height of flight and trim.

DESIGN2, DESIGN5 (Subroutines FOIL2, COORD)

These were the full programs incorporating heel, yaw, trim and height of flight displacements. DESIGN2 had a maximum of 100 iterations in a similar manner to the above programs (DESIGN1 and 4), while DESIGN5 provided the force situation after only one iteration for a given orientation of the system. DESIGN5 also had an option for a detailed output of the final foil element coordinates.

The Iterative Technique

These programs used a definition of the hydrofoil system in the form of coordinates of the ends (A,B) of each foil element, figure 3.1. These were referred to a reference system fixed in relation to the boat and designated in the directions x,y,z. The origin of this system was chosen as the intersection of the design waterline, the craft centreline , and the line along which the lift force of the stern foil was assumed to operate. This choice simplified the calculations involving pitching moments, but an allowance in the form of an axis transformation to the centre of gravity had to be made when the same data files were used in the motion studies. This axis system was arranged with the +ve x-direction forwards, +ve y-direction to starboard and the +ve z-direction downwards. This information together with details of the chord length at the ends of the element A and B, foil section type and properties, angle of incidence as well as overall

information such as the mass and mass distribution (positions of the crew for a small sailing hydrofoil craft), centre of gravity and position of the thrust vector were supplied in the form of a data file. The required format of this data file is given in figure 3.4.

In order that calculations could be made on the submerged part of the hydrofoil system only, the coordinates of the foil system described above had to be transformed into an earth axis system (X,Y,Z). This system had its origin at the same position on the craft (it also travelled at the speed of the boat), except that it was displaced vertically to coincide with the instantaneous waterline position. The directions of X,Y,Z, were the same as the x,y,z respectively. The difference between the two systems was due entirely to the height of flight and the trim, yaw and heel angles. A transformation matrix was formulated of the direction cosines of this axis transformation where the order of transformation was yaw followed by trim followed by heel. In this way yaw was considered as rotation about the axis perpendicular to the water surface, trim about the non-heeled but yawed y-axis and heel about the trimmed and yawed x-axis. The only unavoidable inconsistency apparent with this order lying in the fact that heel is not a rotation about an axis parallel to the water surface but about the trimmed axis, but since angles of trim were only small, the error introduced here is negligible. (An excessive angle of trim of 10° would give a correction, cos 10° , of 0.985. An error of 1.5%,

11	Number of Hydrofoil Elements
0.777,0.777,0.777,0.777,0.777,0.777,0.777,0.777	x coordinate of element — End A (m)
0.0,0.0,0.0	
0.517,-0.517,0.585,-0.585,0.758,-0.758,0.655,-0.655	y coordinate of element — End A (m)
0.0,0.063,-0.063	
-0.1,-0.1,-0.1,-0.1,0.058,0.058,0.138,0.138	z coordinate of element — End A (m)
0.0,0.22,0.22	
0.038,0.038,0.038,0.038,0.038,0.038,0.038,0.038	Chord length of element — End A (m)
0.038,0.036,0.036	
0.777,0.777,0.777,0.777,0.777,0.777,0.777,0.777	x coordinate of element — End B (m)
0.0,0.0,0.0	
0.655,-0.655,0.758,-0.758,0.655,-0.655,0.54,-0.54	y coordinate of element — End B (m)
0.0,0.0,0.0	
0.138,0.138,0.058,0.058,0.138,0.138,0.234,0.234	z coordinate of element — End B (m)
0.22,0.22,0.22	
0.038,0.038,0.038,0.038,0.038,0.038,0.038,0.038	Chord length of element — End B (m)
0.038,0.036,0.036	
0.1,0.1,0.1,0.1,0.1,0.1,0.1,0.1	Thickness chord ratio of section
0.2,0.12,0.12	
0.54,0.54,0.54,0.54,0.54,0.54,0.54,0.54	Ideal lift coefficient of section
0.0,0.0,0.0	
0.011,0.011,0.011,0.011,0.011,0.011,0.011,0.011	CONST - normally 0.011 for NACA sections
0.011,0.011,0.011	
6.2,6.2,6.2,6.2,6.2,6.2,6.2,6.2	Zero lift angle (α_o) of section (degrees)
0.0,0.0,0.0	
1.1,1.1,1.6,1.6,3.7,3.7,3.7,3.7	Angle of Incidence (α_i) (degrees)
0.0,-1.0,-1.0	
0.0,0.0,0.0,0.0,0.0,0.0,0.0,0.0	Distance a from figure 3.3a (Horizontal foil elements) (m)
0.0,0.0,0.0	
0.0,0.0,0.0,0.0,0.0,0.0,0.0,0.0	Distance b from figure 3.3b (Horizontal foil elements) (m)
0.0,0.125,0.125	
2,2,2,2,2,2,1,1	Aspect Ratio type - 1 (figure 3.3b and c), 2 (figure 3.3d) and 0 (horizontal elements)
0,0,0	
1,1,1,1,1,1,1,1	Position of element - 1 (bow), 2 (side) and 3 (stern)
3,3,3	
0.0,0.0,51.0,0.0,0.0,0.636,0.0,0.777	Crew weight (N), crew weight (N), boat weight (N), x coord cg.of crew and boat, x coords of side and bow foil units, z_{ce}, Max draught at zero velocity.
0.605,0.24	
-0.15,-0.15,-0.15,-0.15,-0.15,-0.15,-0.15,-0.15	Pitching Moment coefficient of section $C_{MC/4}$
0.0,0.0,0.0	

Fig. 3.4 Data File - This example shows information for the model craft

at the very most).

The transformation matrix required is given below as,

$$\begin{bmatrix} X \\ Y \\ Z \end{bmatrix} = \begin{bmatrix} \cos\tau\cos\lambda & -\sin\lambda\cos\tau & \sin\tau \\ \sin\lambda\cos\theta_h + \cos\lambda\sin\theta_h\sin\tau & \cos\lambda\cos\theta_h - \sin\lambda\sin\theta_h\sin\tau & -\cos\tau\sin\theta_h \\ \sin\lambda\sin\theta_h - \cos\lambda\cos\theta_h\sin\tau & \cos\lambda\sin\theta_h + \sin\lambda\cos\theta_h\sin\tau & \cos\tau\cos\theta_h \end{bmatrix} \begin{bmatrix} x \\ y \\ z \end{bmatrix} - \begin{bmatrix} 0 \\ 0 \\ z_o \end{bmatrix}$$

where

τ is the angle of trim +ve bow up

θ_h is the angle of heel +ve to starboard

λ is the angle of yaw +ve to starboard

z_o is the height of flight at the z-axis.

For a sailing boat, positive angles of heel will occur with negative angles of yaw and vice versa (i.e. a sailing boat is expected to yaw into the wind and heel away from it.)

For programs DESIGN2 and DESIGN5 this matrix was supplied in the form of the subroutine COORD. Programs DESIGN1, DESIGN3 and DESIGN4 used a less complex method where it was only necessary to consider trim and height of flight.

For each value of velocity (V) and from initial values of height of flight (z_o) and trim, yaw and heel angles the programs calculated and summed the total lift, total drag and total side force, itemised between bow, side and stern foils. These were written symbolically as :

$$\text{Total Lift} \qquad L = \sum_{i=1}^{n} l_i$$

$$\text{Total Drag} \qquad D = \sum_{i=1}^{n} d_i$$

and

$$\text{Total Side Force} \qquad SF = \sum_{i=1}^{n} sf_i$$

where l_i, d_i, sf_i are the lift, drag and side force on the ith foil element and n is the total number of foil elements.

In the iterative programs a comparison is then made between the total lift and the all up weight and a correction made to the height of flight accordingly,

$$\begin{aligned} &< W \rightarrow (z_o)_n = (z_o)_o - \Delta z_o \\ \sum_{i=1}^{n} l_i \quad &= W \rightarrow (z_o)_n = (z_o)_o \\ &> W \rightarrow (z_o)_n = (z_o)_o + \Delta z_o \end{aligned}$$

where W is the weight, subscripts n and o denote new and old values respectively, and Δz_o is the change in z_o.

Rotational equilibrium in pitch is then considered, and the trim angle is adjusted until the pitching moments from the various foil units are balanced with the thrust/drag couple from the propulsion system. Assuming a quasi-steady condition exists where the forward thrust from the propulsion system equals the total drag and then taking moments gives,

$$\sum_{i=1}^{n_b} l_{b_i} \begin{cases} < \\ = \\ > \end{cases} \left(M_o W - M_o \sum_{i=1}^{n_s} l_{s_i} - M_o \sum_{i=1}^{n_{st}} l_{st_i} + \sum_{i=1}^{n} d_i \, z_{ce} \right) \Big/ X_{bow} \begin{cases} \rightarrow \tau = \tau_o - \Delta\tau \\ \rightarrow \tau = \tau_o \\ \rightarrow \tau = \tau_o + \Delta\tau \end{cases}$$

where

l_b, l_s, l_{st} are the lifts of the bow, side and stern foil elements respectively,

n_b, n_s, n_{st} are the numbers of the bow, side and stern foil elements respectively ($n_b + n_s + n_{st} = n$),

M_o denotes a moment about the origin,

z_{ce} is the lever between the line of thrust (of the sails in this case) and the hydrodynamic centre through which the drag is assumed to act,

X_{bow} is the x co-ordinate of the bow foil unit and $\Delta\tau$ the change in the trim angle.

In practice because of the position of the origin,

$$M_o \sum_{i=1}^{n_{st}} l_{st_i} = 0$$

The program then iterates to a solution when the above criterion are satisfied within a one percent tolerance, or the maximum number of iterations is reached. This latter may come about at high velocities if the step changes in height and trim values from iteration to iteration are too large for a solution to be reached within the tolerance levels and the program hunts back and forth until it exits at the maximum number of iterations. (In these programs $\Delta z_o = \pm 1$mm and $\Delta\tau = \pm 0.1$ degree). The final values of the total lift, drag and side force, and the new orientation (trim and height of flight) are then presented together with certain other particulars such as the heel and yaw values (neither of which are altered during the computation), lift/drag ratios, mass and velocity. A note is also made of whether the results are within the 1% tolerance or whether the maximum number of iterations was reached.

These programs were used for all of the calm water predictions for both the model and the full scale craft.

CHAPTER 4

Calm Water Model Tests

The hydrofoil formulations and design programs which are described in detail in chapter 3 were used to assess the performance of the variations made in the designs considered in this study. It was considered a necessary requirement that these programs should be checked against quantitative model tests undertaken in a towing tank before the results were extrapolated up to the full scale. It was also felt that useful data would be obtained from the performance of a model of the full scale design. Certain restrictions were encountered both in the construction and the operation of such a model and these were overcome as described below (27).

From the first it was realised that while testing a model at equivalent Froude numbers to the full scale, there would be discrepancies in the Reynolds numbers between the model and full scale craft. On the other hand the smaller the scale ratio, the higher the resulting maximum scale speed of the model. With an absolute maximum carriage speed available of just over 6.5 m/sec certain restrictions were placed on the scale ratio if a relatively high scale speed was to be achieved. Further, the model foils had to

be of a sufficient size to avoid the effects of surface tension forces which would not be present on the full scale. It has been suggested (175) that the minimum hydrofoil chord length to avoid such effects can be taken as 25mm. It can be seen that these are conflicting requirements, the first and third restrictions demanding a large model and the second a small model. The model was built at one quarter full scale.

To enlarge upon the first point, the requirement is for the influences of Reynolds number effects to be similar on the model as on the full scale. With hydrofoils this is a matter of monitoring the position of the laminar/turbulent boundary layer transition so that flow separations occur in the same regions on the model as on the full scale (159). With the NACA 16-series foil sections (these were used on the full scale craft), operation at the design angle of incidence (zero degrees) should produce laminar flow up to the 60% chord point and because of the favourable pressure gradient in this region, this should prevail even for fairly high Reynolds numbers and modest surface roughnesses. Variations from this ideal angle of incidence or in surface roughness will cause wide variations in the transition point and these variations can be expected in the normal operation of a hydrofoil craft. With the model tests undertaken here further complications arose because the model foils were not of the same section as the full scale foils.

Methods of turbulence stimulation* were studied (52,96,116 and 132), but it was realised that compared to ship models and models of solids of revolution, the problem faced here of attaching turbulence stimulators to model hydrofoils of small chord lengths was somewhat different. The most practical solution appeared to be offered by attaching fine wires ahead of and parallel to the leading edge of the hydrofoils but even these would have confused the situation to a certain extent by the addition of their own parasitic drag to the system. Moreover it was not at all clear that stimulators would have been a benefit in this case where the model was operating in the sub-critical flow regime (Reynolds number $\simeq 10^5$) while the full scale craft operated in the transitional flow regime (Reynolds number $\simeq 10^6$). The actual increase in Reynolds number from the model to full scale was a factor of 8. It was for these reasons that it was decided not to fit turbulence stimulators to the model. The calculations were carried out separately for the model and the full scale craft and in this way allowances were made both for the variations in Reynolds number and in the type of foil section used. This course of action, if it had any undesirable effect at all, would have resulted in a slightly conservative estimate of the drag values for the full scale craft which operated in the transitional flow regime (fig. 3.3, chapter 3).

The Model

The model which was constructed for these tests was a one quarter scale model of the 5m long full size boat which is described in detail in chapter 2. The hulls and cross beams of this model were made from balsa wood. The hulls were formed from 12mm thick planks of balsa wood which were shaped to the appropriate waterplane contours, built up sandwich fashion and faired off. The model was equipped with a short mast, the top of which approximated with the position of the centre of effort of the sails. This mast was stayed by four wires to the bow and stern of each outer hull. The model was towed from the top of this mast. The overall length of the model was 1.25m, its mass was 5.2kg and its maximum speed of just over 6.5m/sec corresponded to a speed of approximately 13.0m/sec (25 knots) for the full scale craft. It is shown below the dynamometer in the towing tank in figure 4.1.

The model foils were redesigned because of the difficulties involved in profiling small tapered hydrofoils to NACA sections. Whereas NACA 16-series hydrofoil sections were used on the full scale, the model foils were either ogive or biogive in section (either circular arc upper surface and flat lower surface or circular arc both sides) and they were made from solid aluminium alloy as opposed to the unidirectional G.R.P. foils of the full scale craft. In addition, although tapered foils were employed on the full scale, all the hydrofoils on the model

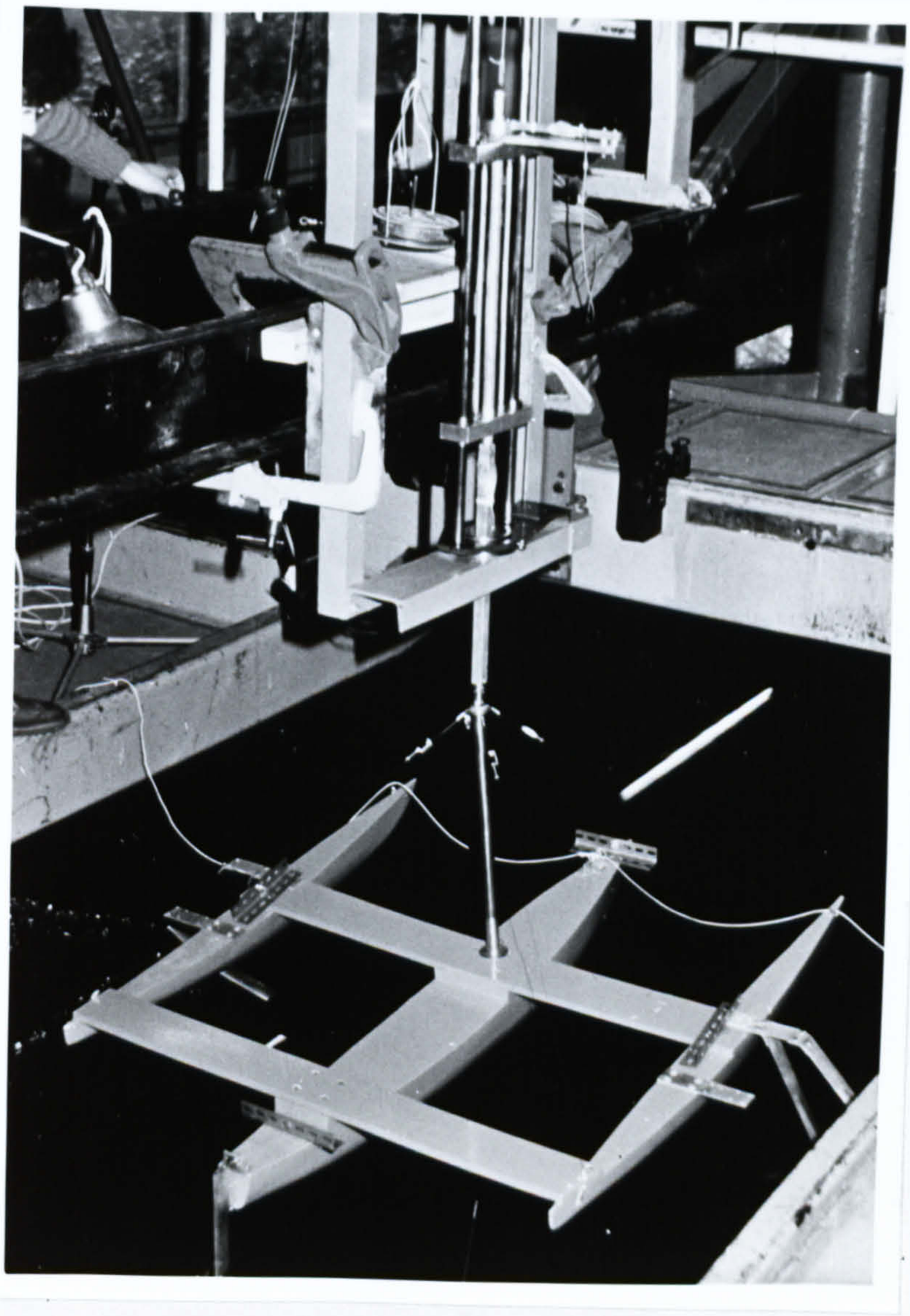

Fig. 4.1 The Test Apparatus and Model

were of constant chord length, 37.5mm. Detailed drawings of the side and stern foils are shown in figures 4.2 and 4.3 respectively. Figure 4.4 shows experimental data for various circular arc and circular arc affine foil sections (Göttingen profiles) which has been extracted from Riegels (158). The ogive sections used on the model had a thickness chord ratio of 0.1 and the data used in the calculations was based on the experimental curve for the section Gö 7K (i.e. α_o = -6.2 degrees, Lift coefficient at α_i = 0° of 0.54).

The dimensions of this model foil system together with various particulars of the foil sections and overall geometry are given in the data file shown in figure 3.5 (chapter 3).

The Dynamometer and Test Rig

The problems of testing any wind propelled vehicle arise from the need to carry out tests at various angles of heel and yaw. Furthermore an additional complication arises because of the relationship between the side force and the downward force from the sails when the craft heels (fig 4.5). This shows up as an increment to the displacement of the craft ΔW where :

$$\Delta W = F_{lat} \tan\theta_h = F_H \sin\theta_h$$

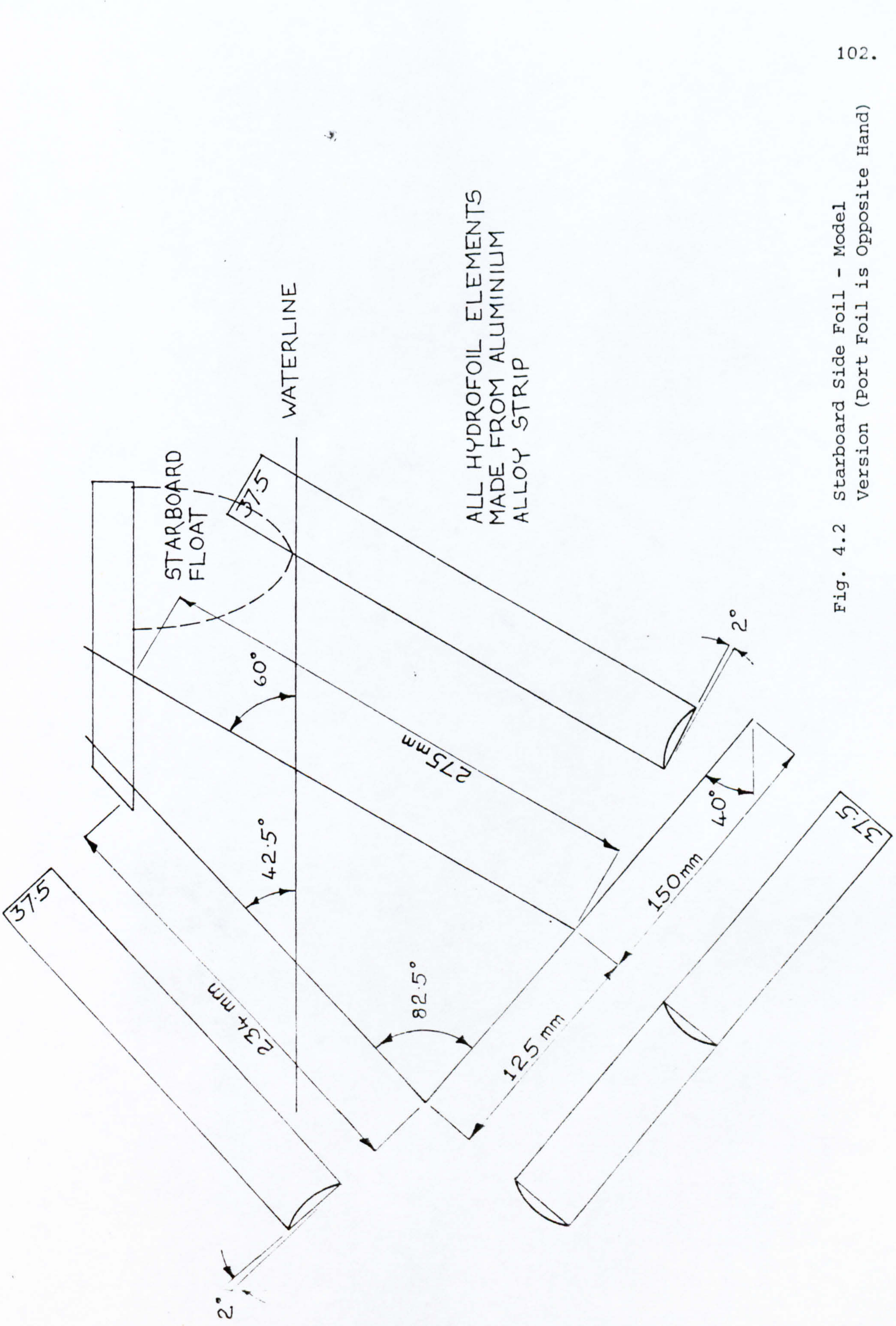

Fig. 4.2 Starboard Side Foil - Model
Version (Port Foil is Opposite Hand)

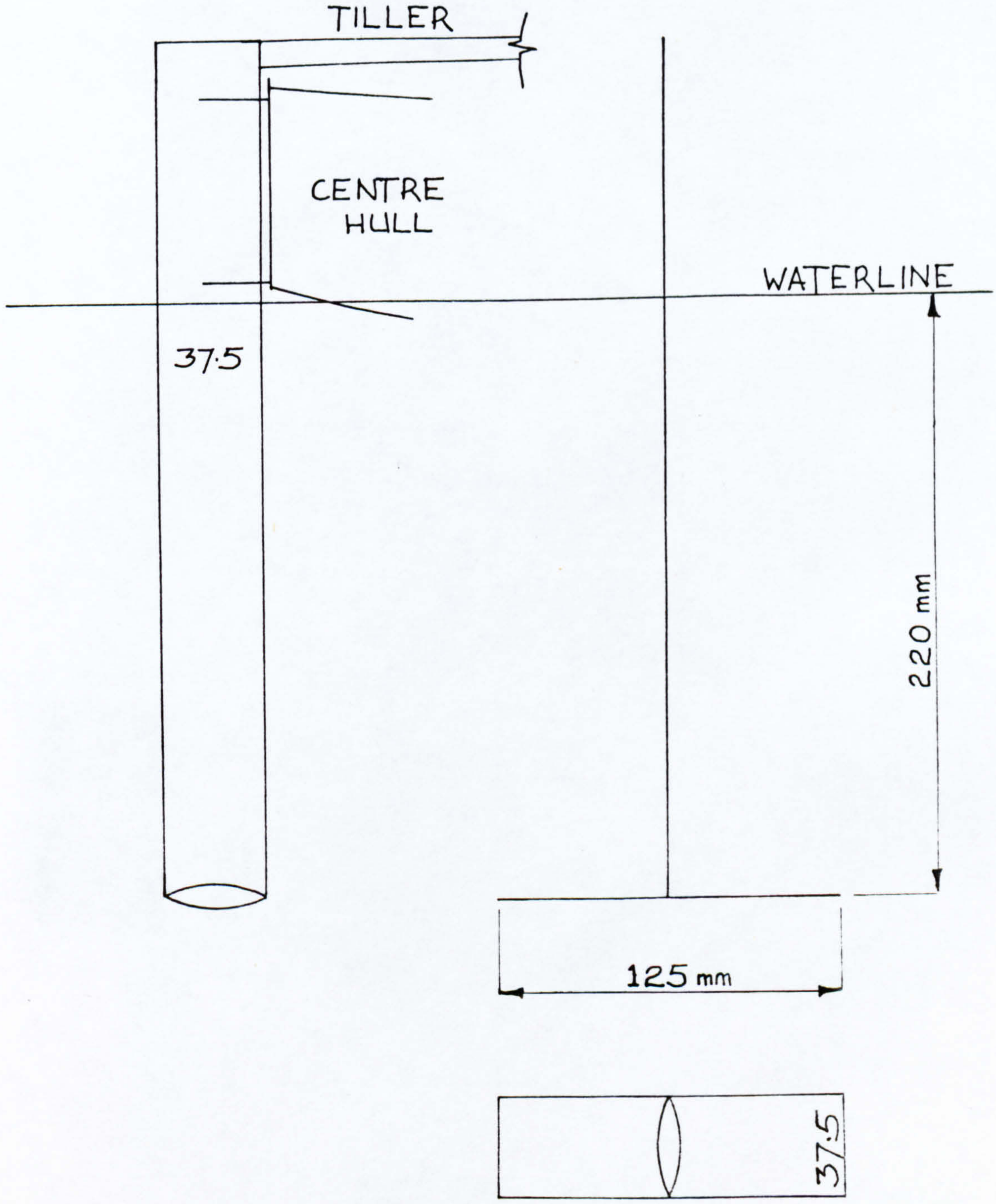

Fig. 4.3 Stern Foil - Model Version

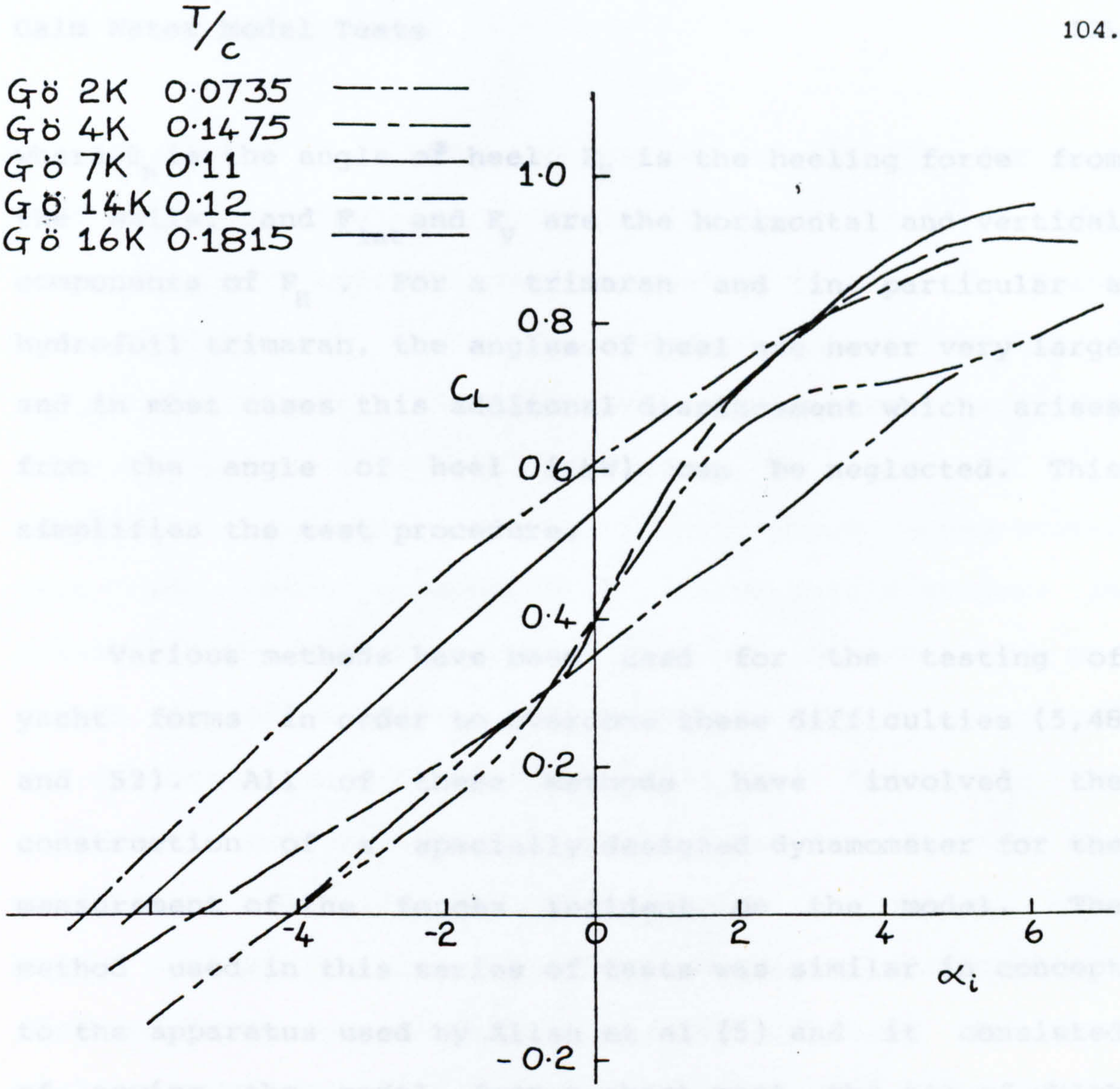

Fig. 4.4 Lift Curve Slopes for Various Circular Arc Göttingen Profiles

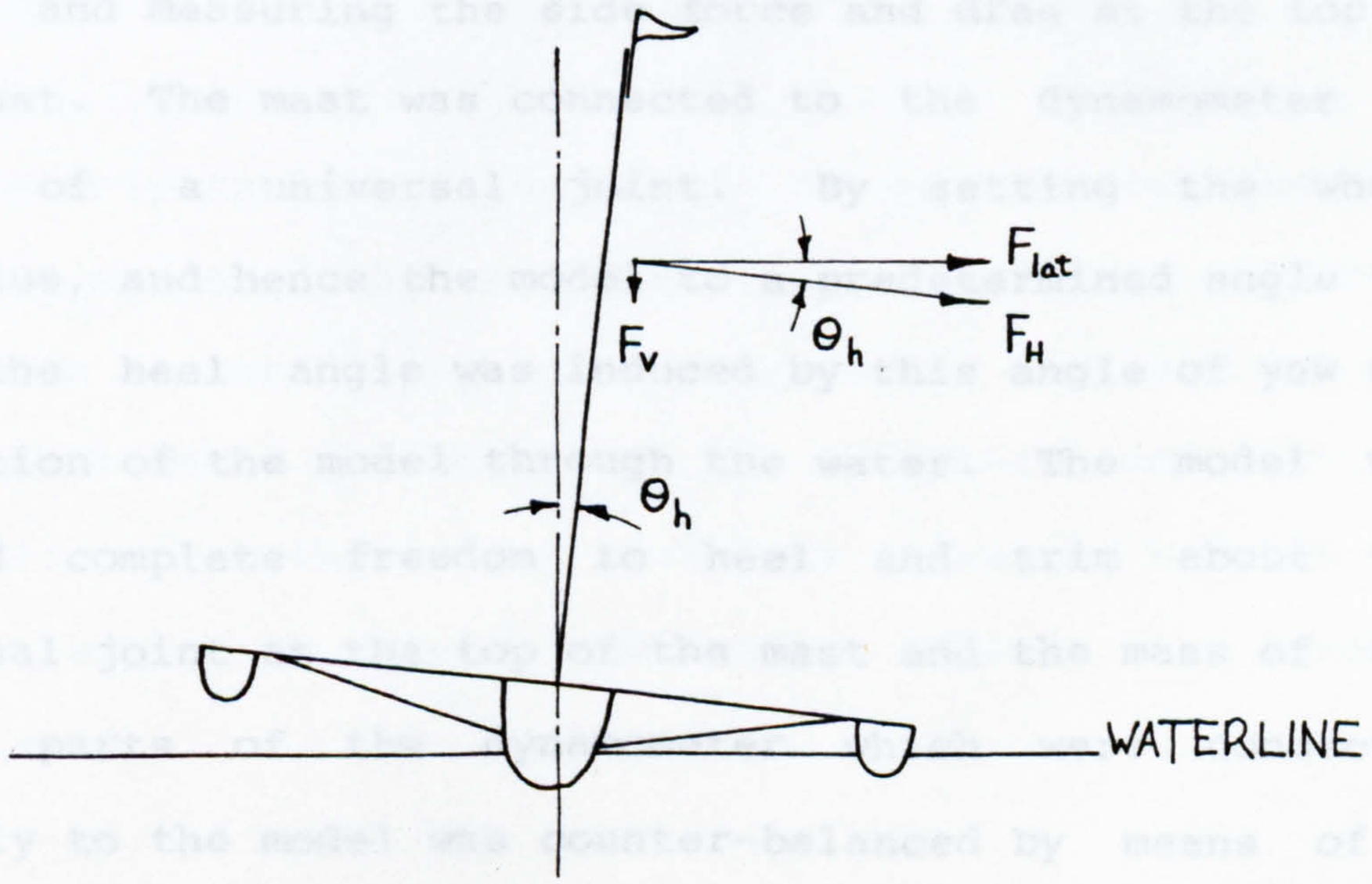

Fig. 4.5 Heeling Forces from the Sail System

where θ_h is the angle of heel, F_H is the heeling force from the sails, and F_{lat} and F_V are the horizontal and vertical components of F_H . For a trimaran and in particular a hydrofoil trimaran, the angles of heel are never very large and in most cases this additonal displacement which arises from the angle of heel (ΔW) can be neglected. This simplifies the test procedure.

Various methods have been used for the testing of yacht forms in order to overcome these difficulties (5,48 and 52). All of these methods have involved the construction of a specially designed dynamometer for the measurement of the forces incident on the model. The method used in this series of tests was similar in concept to the apparatus used by Allan et al (5) and it consisted of towing the model from a short mast, the top of which coincided with the assumed centre of effort position of the sails, and measuring the side force and drag at the top of this mast. The mast was connected to the dynamometer by means of a universal joint. By setting the whole apparatus, and hence the model to a predetermined angle of yaw, the heel angle was induced by this angle of yaw and the motion of the model through the water. The model was allowed complete freedom to heel and trim about the universal joint at the top of the mast and the mass of the moving parts of the dynamometer which were connected directly to the model was counter-balanced by means of a weight on a scale pan.

A drawing of this dynamometer which was built for and used in these tests is shown in figures 4.6 and 4.1. The rollered guides which allowed the model freedom to heave were long enough to allow large variations in heights of flight of the model. All the moving parts were constructed from aluminium alloy in an effort to keep the mass connected to the model to a minimum. Force measurements were made using stragetically placed strain gauges. In particular the bar which was fastened to the model mast was strain gauged at its top end to measure bending moment and was calibrated in such a manner that the forces in two horizontal and orthogonal directions could be found at the position of the universal joint. For the special case where angles of heel and yaw were zero the directions were arranged to be specifically side force and drag, but when angles of yaw were included some resolution of these forces was necessary to obtain the explicit values of side force and drag.

The orientation of the model during an experimental run was measured by means of fine piano wires connected through to linear displacement transducers (L.V.D.T.'s) at four positions on the model, at bow and stern, and port and starboard. From these four positions values of heights of flight, angle of heel, and angle of trim were readily determined.

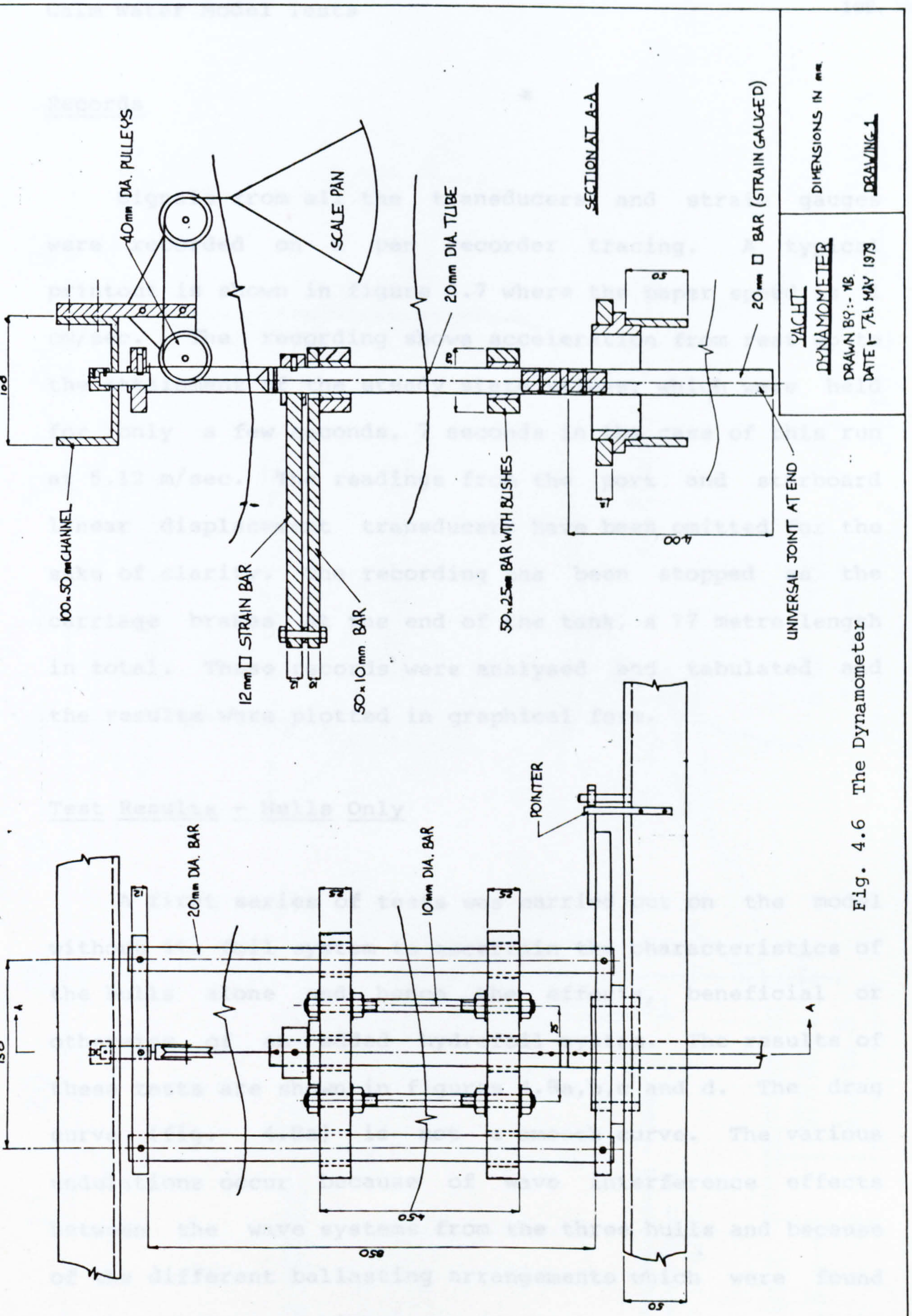

Fig. 4.6 The Dynamometer

Records

Signals from all the transducers and strain gauges were recorded on a pen recorder tracing. A typical printout is shown in figure 4.7 where the paper speed is 1 cm/sec. The recording shows acceleration from rest up to the attainment of the steady state values, which were held for only a few seconds, 7 seconds in the case of this run at 5.12 m/sec. The readings from the port and starboard linear displacement transducers have been omitted for the sake of clarity. The recording has been stopped as the carriage brakes at the end of the tank, a 77 metre length in total. These records were analysed and tabulated and the results were plotted in graphical form.

Test Results - Hulls Only

A first series of tests was carried out on the model without its foil system to ascertain the characteristics of the hulls alone and hence the effects, beneficial or otherwise of an added hydrofoil system. The results of these tests are shown in figures 4.8a,b,c and d. The drag curve (fig. 4.8a) is not a smooth curve. The various undulations occur because of wave interference effects between the wave systems from the three hulls and because of the different ballasting arrangements which were found to be necessary at higher speeds.

Figures 4.8b,c and d are curves of the trim and height

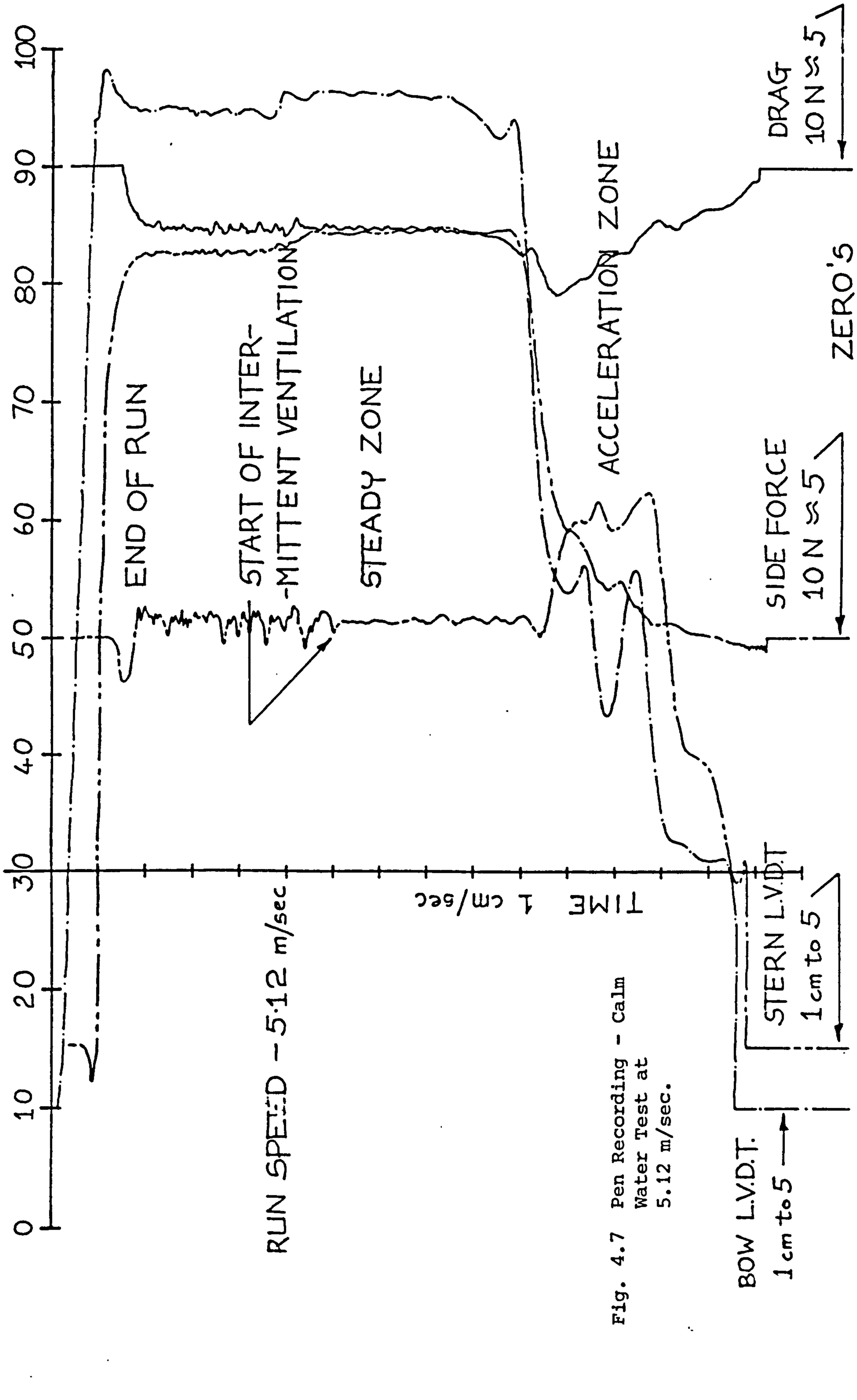

Fig. 4.7 Pen Recording - Calm Water Test at 5.12 m/sec.

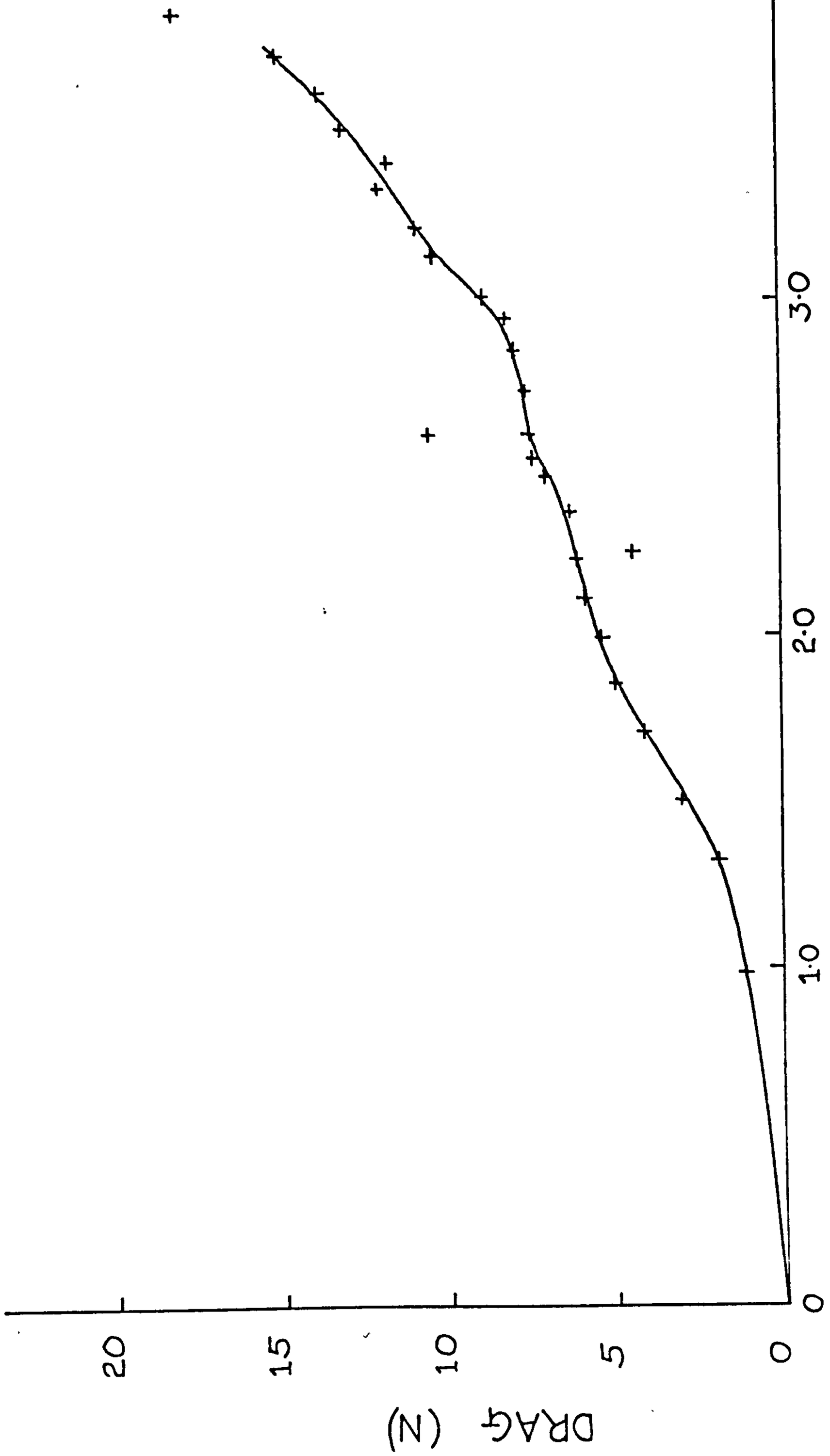

Fig. 4.8a Drag Curve for the Model without the Foil System

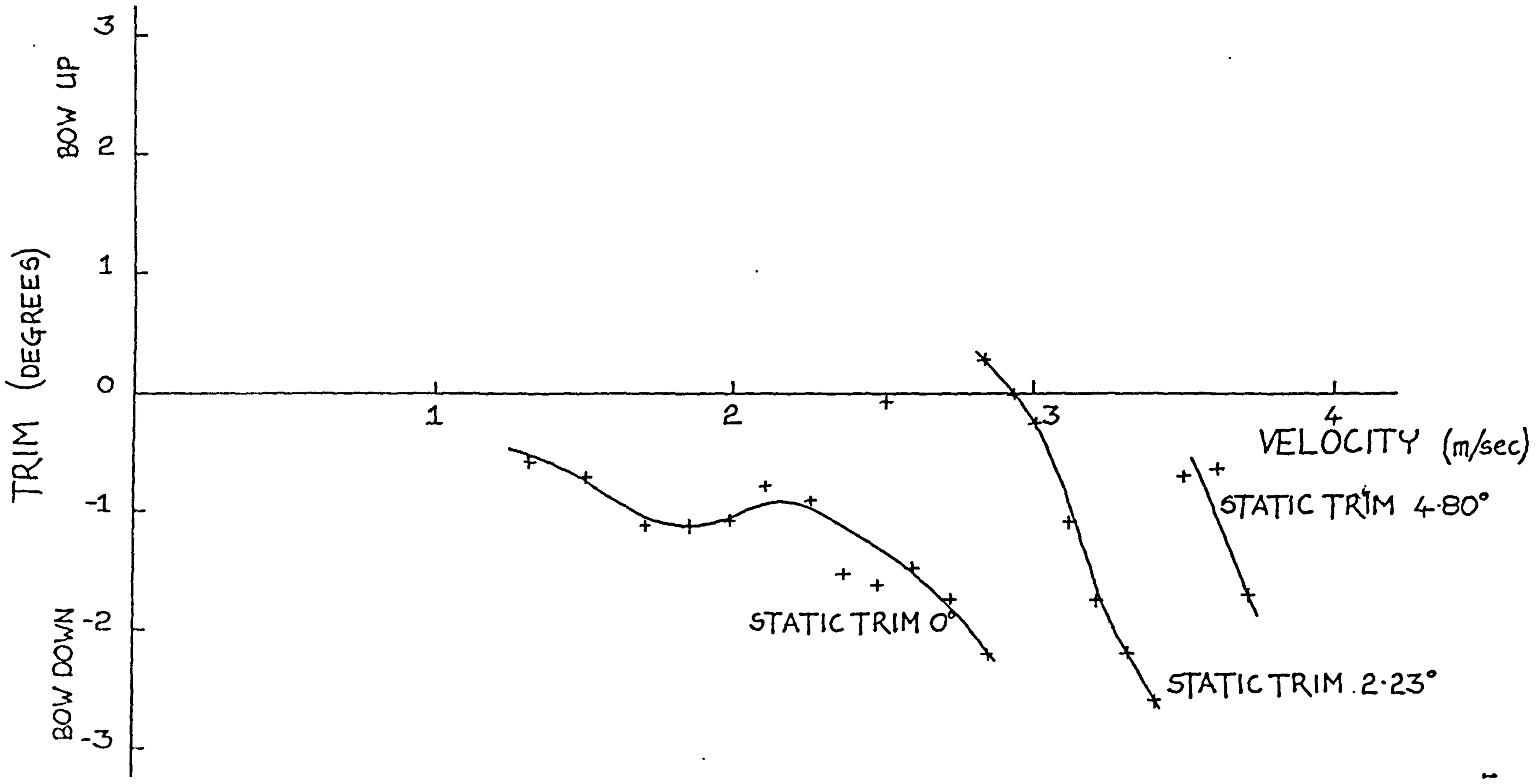

Fig. 4.8b Trim Curve for the Model without the Foil System

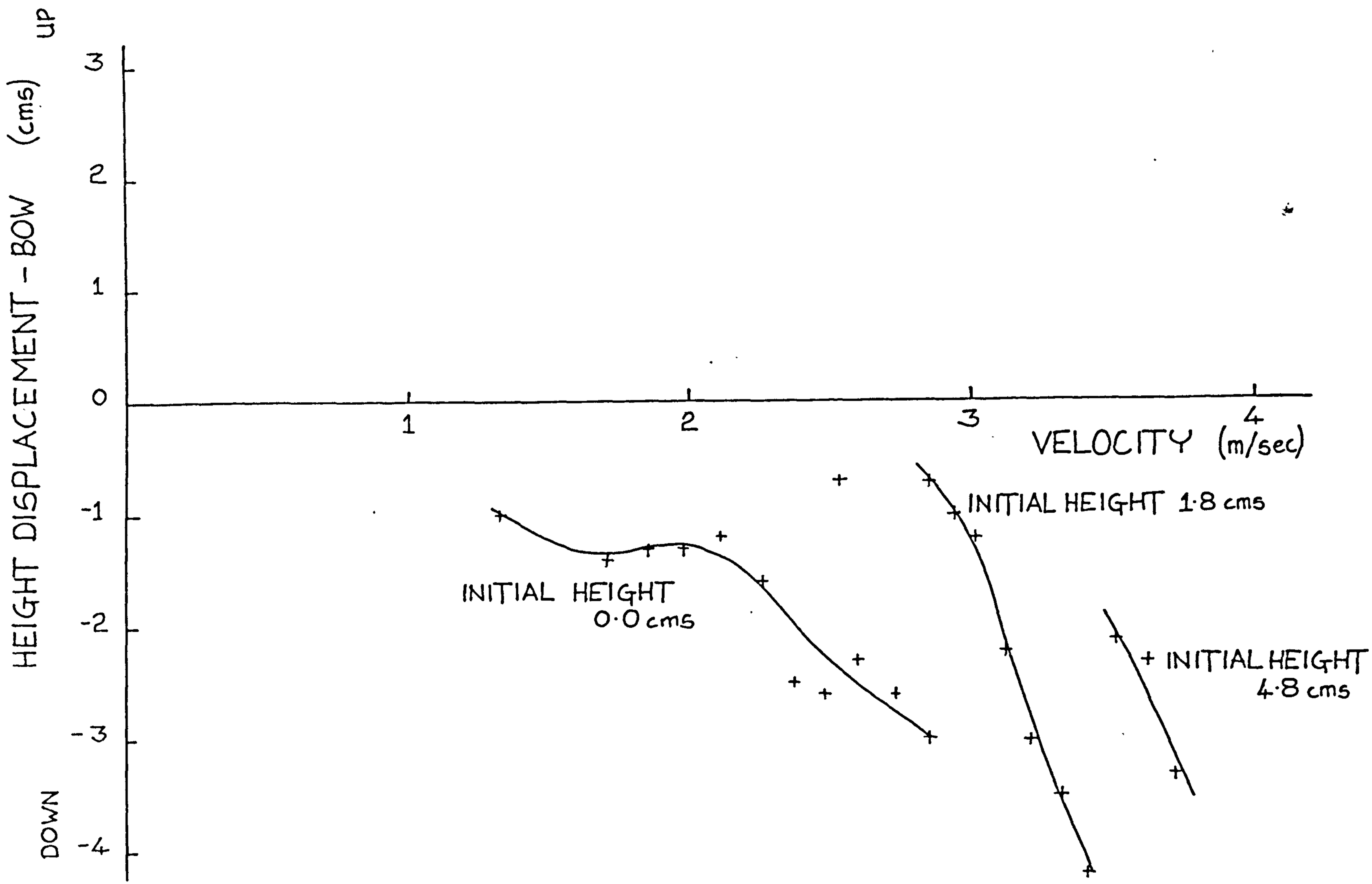

Fig. 4.8c Height of Flight at the Bow - without the Foil System

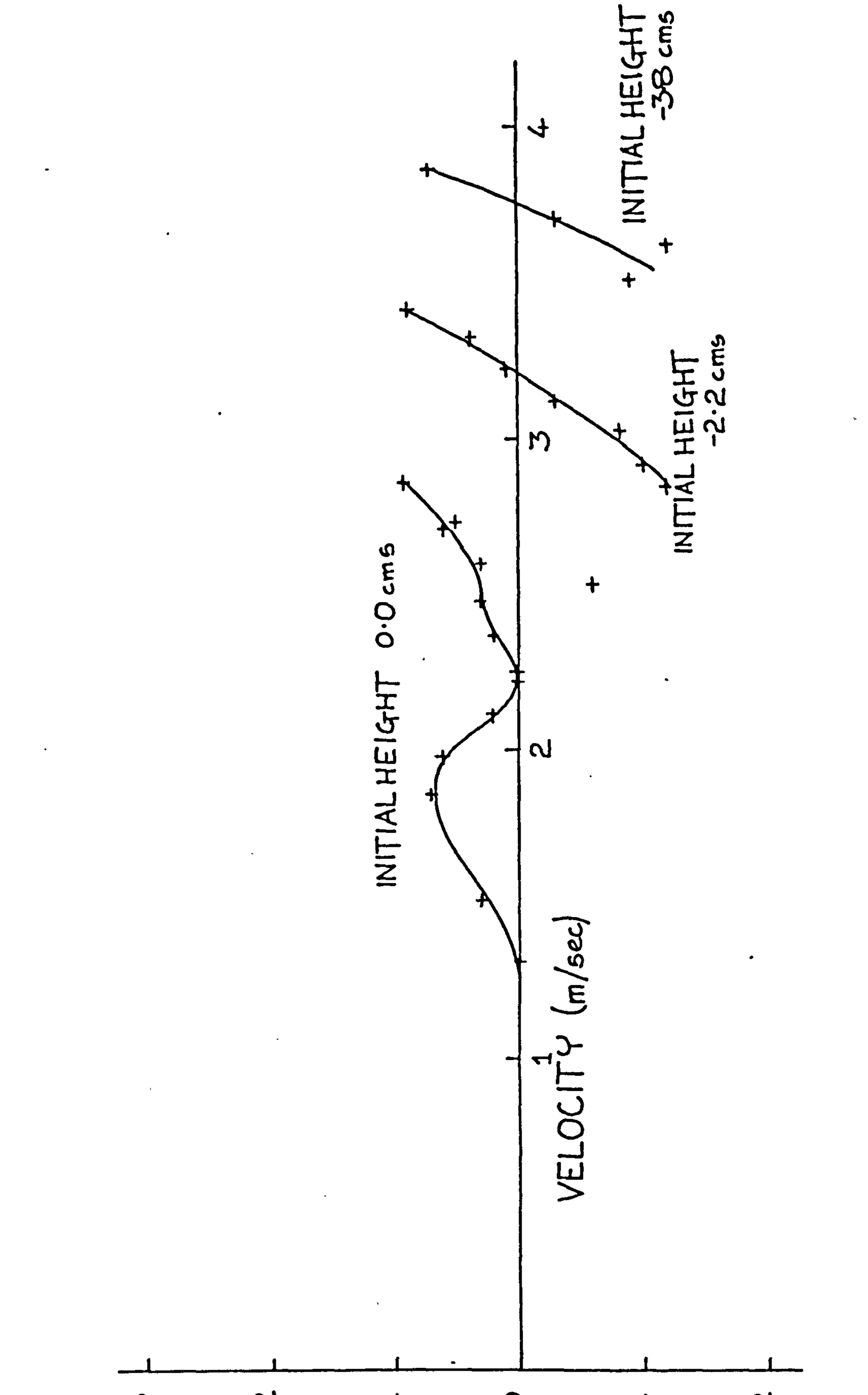

Fig. 4.8d Height Displacement at the Stern - without the Foil System

displacements at the bow and at the stern (the origin of the coordinate system) of the model respectively, also plotted against velocity. As the speed of the model was increased, an angle of trim by the bow developed because of the negative pitching couple which resulted from the height of the tow wire which was positioned at the top of the short mast. When this angle of trim became so severe that the deck edge at the bow was in danger of becoming immersed, the ballast of the model was shifted to counteract the effect and these shifts account for the discontinuities plotted in these figures. This was equivalent to movements of the crew on the full scale. In all two shifts of ballast were made, the second which made speeds up to 3.8 m/sec possible would be explained on the full scale by both crew sitting on the rear cross beam.

Test Results - Hulls and Foils

The foilborne tests can be split into two sections, those incorporating angles of heel and yaw and those where these angles were zero. To deal with the case where there was no heel or yaw first, figure 4.9a is a plot of the drag curve against velocity for a range of speeds from 0 to 7 m/sec. The fastest experimental run was made at almost 6.7 m/sec, at which speed only about a second of steady state conditions were obtained, the majority of the tank length being taken up for acceleration and braking. In fact, the drag results of the fastest two runs are probably slightly higher than would be achieved if a larger period of steady

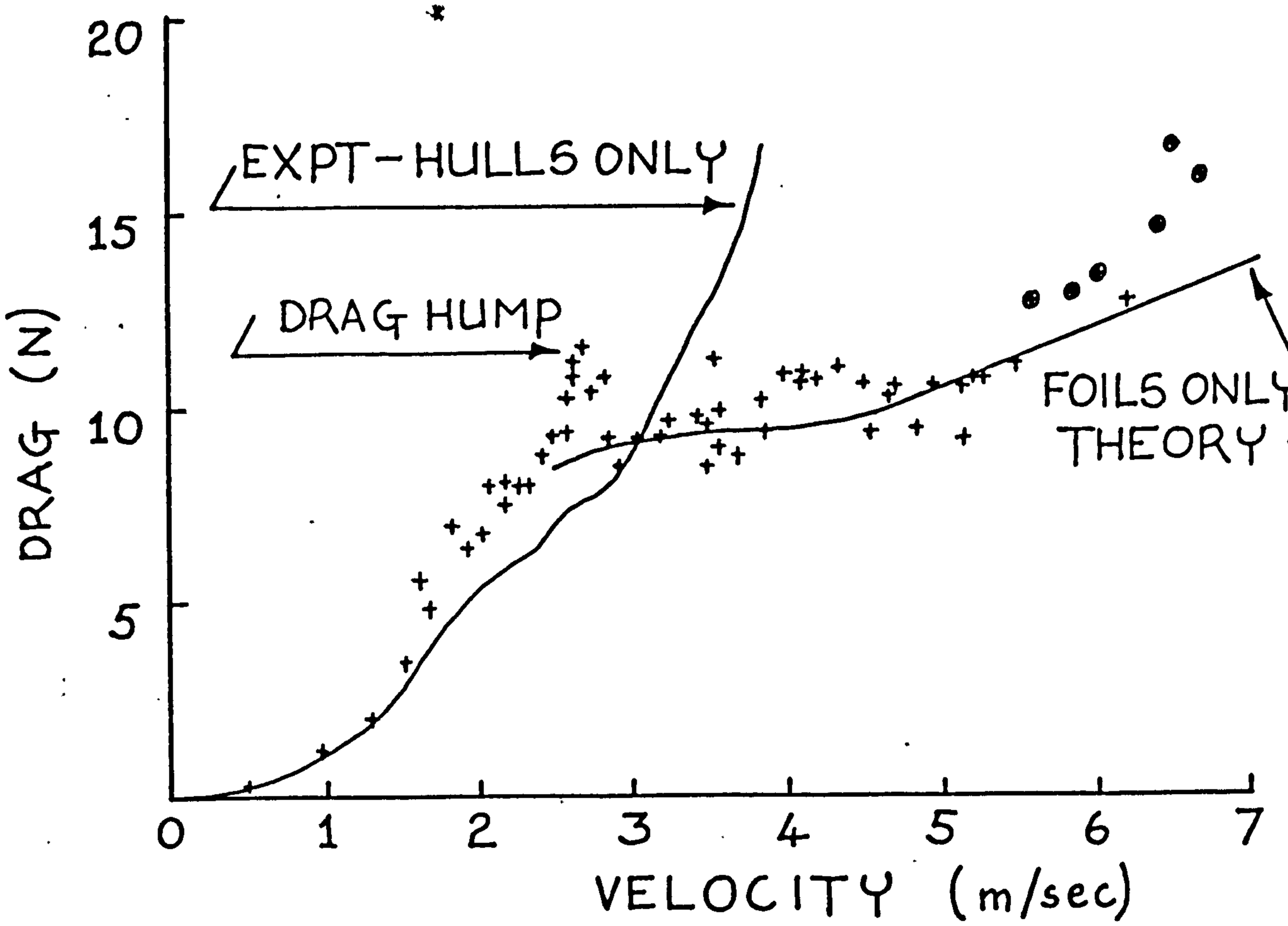

Fig. 4.9a Drag curve at zero degrees heel and yaw

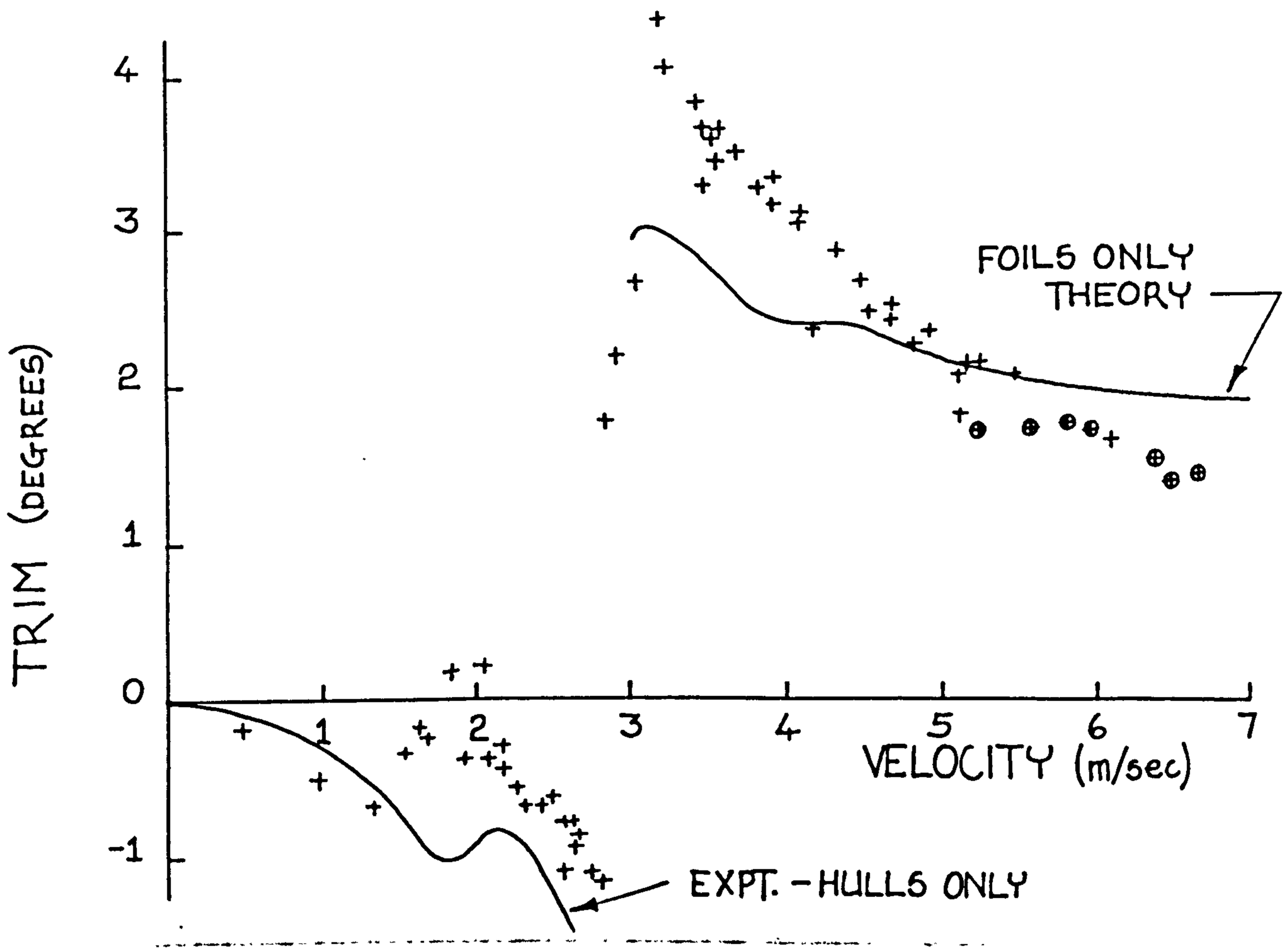

Fig. 4.9b Trim curve at zero degrees heel and yaw

run conditions were obtained, there still being some small quantity of acceleration force present. All the circled points above 5.5 m/sec are results where there was a certain amount of ventilation present on the model foils and this too would add an increment to the drag over that value for the fully wetted flow regime. A fuller discussion of the ventilation experienced during these tests is given later in this chapter.

Altogether about sixty runs were made for this part of the experiment in an effort to reduce the uncertainties produced by the scatter of data. Figure 4.9a shows clearly the drag hump as the model becomes foilborne at a little over 2.5 m/sec. Also shown as a solid line is the drag curve from the experimental runs made without the foil system fitted. At the lower speeds while the model is still hull-borne, the drag as would be expected is less without foils, but the two curves cross just after the model takes off and the curve for the model without foils increases more and more steeply.

Figures 4.9b,c and d are plots of the trim, and height displacements at the bow and stern (the origin of the coordinate system which is described in chapter 3) of the model for the same experimental runs. The difference in flight paths when ventilation occurs on the main lifting foils is clearly seen in figure 4.9c and d, the height of flight being reduced by approximately 3.5 centimetres. The trim curve (figure 4.9b) shows how the trim increases

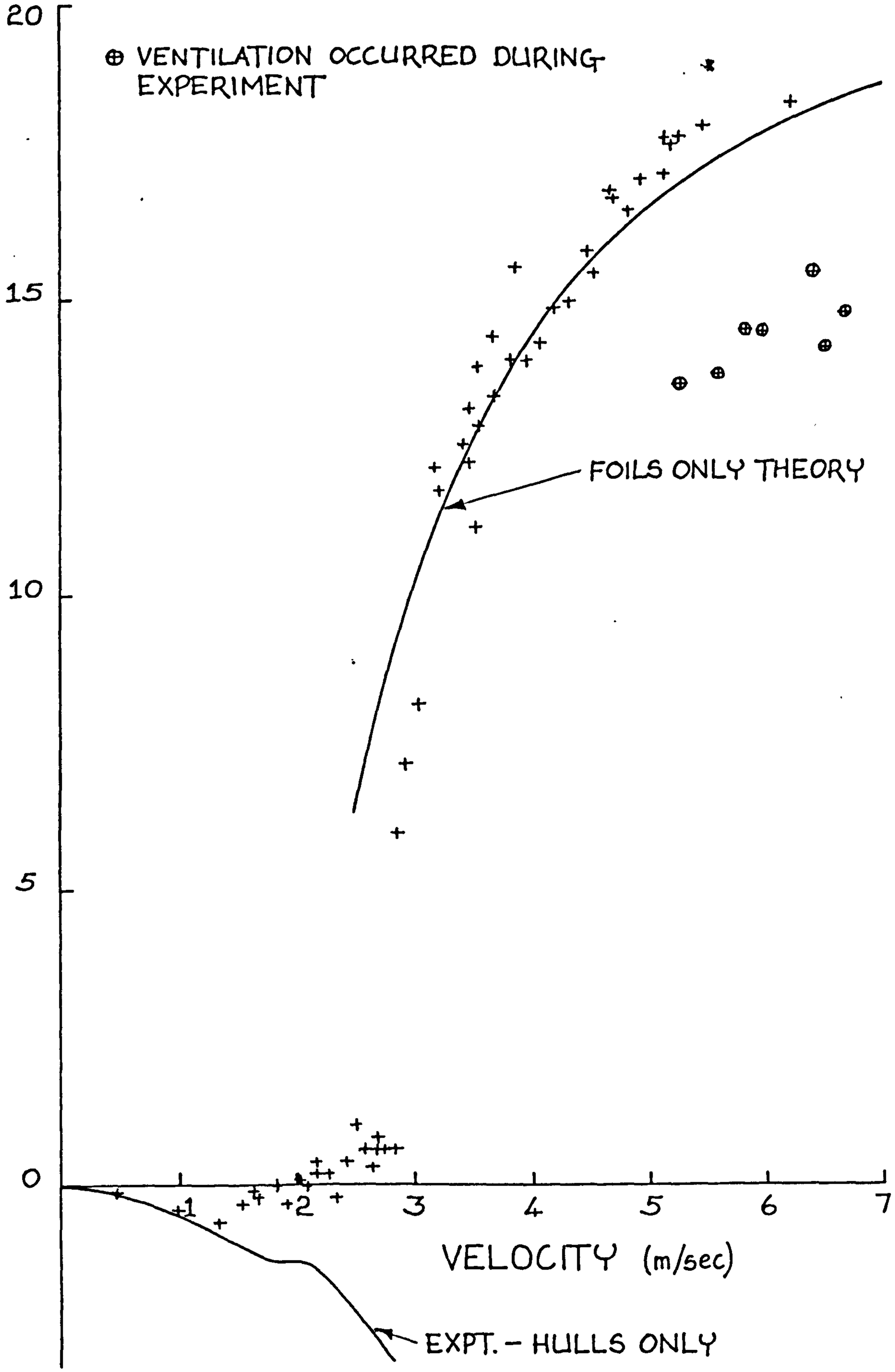

Fig. 4.9c Height of Flight at the Bow - Zero Degrees Heel and Yaw

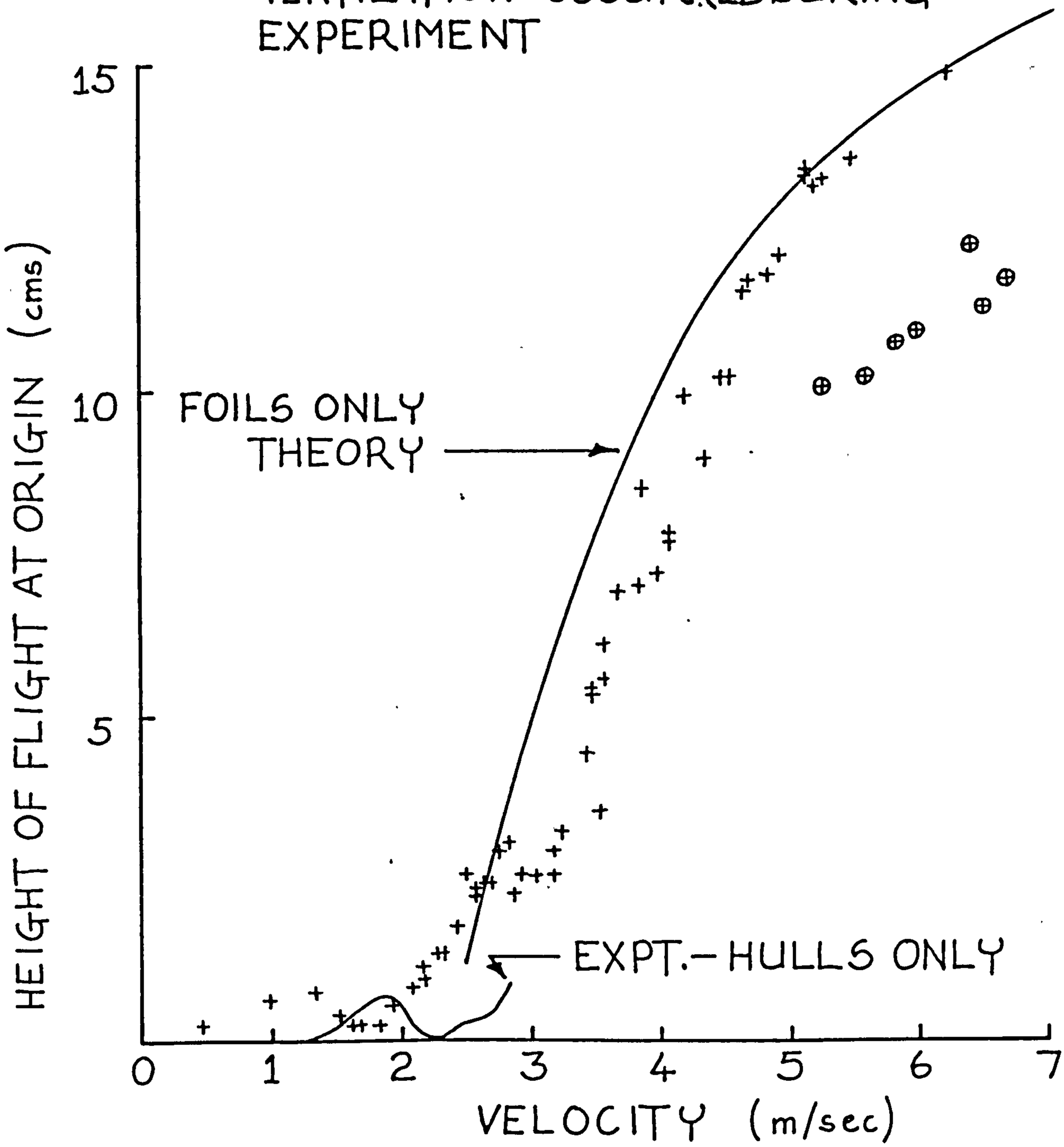

Fig. 4.9d Height of Flight at the Stern (origin) - Zero Degrees Heel and Yaw

dramatically by 5 degrees at take off, but thereafter falls steadily. A stable bow up trim is achieved throughout the speed range where flight occurs. Again the experimental curves for the foil-less model are also given for comparison purposes below the take off speed. These curves emphasise the beneficial effects of the foil system on the orientation of the model even below the take off speed.

All of the graphs described show a theoretical prediction of the situations from the methods which are described in detail in chapter 3 and in most cases the agreement between the experiment and theory is good. The largest variation occurs in the trim prediction where the absolute value of the peak in the experimental results is not quite attained. (fig. 4.9b). This shows up also in the height displacement curve fig. 4.9d, which over predicts the height of flight at the stern by approximately one centimetre in the range of velocity from 3.0 to 4.5 m/sec. Since there is no allowance for the effects of ventilation in the prediction method, the points where ventilation occur fall well below the theoretical curves at higher speeds (figs. 4.9,c and d) although at high speeds where the foils are free from ventilation, the prediction is very good. Similarly the drag prediction (fig. 4.9a) agrees well with the data over the range from take off up until the point where ventilation occurs. In this case though the experimental data is above the theoretical prediction indicating a greater value of drag when ventilation is present.

Test Results - Hulls and Foils at angles of Heel and Yaw

The test results which incorporated angles of heel and yaw are presented in the next series of graphs. The manner in which the tests were carried out meant that the results were obtained over a range of heel and yaw angles. To make sense of this spread of data, the results have been grouped into three different ranges, categorised by their yaw angle. The groups were, 0.0-2.0 degrees yaw, 2.0-3.0 degrees yaw and 3.0-4.5 degrees yaw. The figure numbers are given in table 4.I

Alongside each plotted experimental point the appropriate angle of heel is given except for some runs where this information was unavailable. The theoretical curves are also given, calculated at a mean angle of yaw for the range as given in table 4.I, for heel angles of 0,4 and 8 degrees. (0,2,4 and 8 degrees for the Side force results). For comparison purposes, the experimental curves drawn as the best curve through the data for the zero heel and yaw situation are given below the take off speed (Expt.0°). On the drag curves, the results from the foil-less model are also marked. Circled points mark experiments where there was some measure of ventilation present on the hydrofoils. Overall, there was a much larger spread of experimental scatter in these results compared to the results of the tests where the angles of heel and yaw were zero.

TABLE 4.I

Yaw Group (degrees)	Drag Curve	Trim Curve	Height Displacement at the Origin	Side Force Curve	Theoretical curves calculated at mean Yaw angle (degrees)
0 - 2	4.10a	4.11a	4.12a	4.13a	1°
2 - 3	4.10b	4.11b	4.12b	4.13b	2.5
3 - 4.5	4.10c	4.11c	4.12c	4.13c	3.75

Considering the drag curves (figures 4.10 a,b and c) the theory clearly predicts that angles of heel reduce the drag of the craft. This is because more of the weight of the craft will be supported on the leeward hydrofoils which will be operating at greater depths of immersion and hence will have a larger aspect ratio. These two points lead to higher lift/drag ratios and higher efficiencies. While there is a large amount of scatter in the experimental data, it can be seen that below the take off speed, the drag values are actually greater than those experienced when angles of heel and yaw were zero. When the model is flying the situation is more confused but the trend is for those results at the larger angles of heel to have a lower drag value than those at small angles of heel. There are, however, a number of points where ventilation occurred during a run where the drag value is high despite the large angle of heel present. In general the scatter is greater for the results where ventilation was present. The angle of yaw did not seem to have a significant effect on the drag value itself, although it was inherent in the system that large angles of yaw created large angles of heel (see figure 4.13). At the higher speeds where large angles of heel occurred, the model would be wholly supported on the leeward and stern foils, the windward foil being clear of the water surface.

The curves of model trim against velocity are given in figures 4.11 a,b and c. Here angles of yaw are seen to have some effect on the theoretical curves, where for the

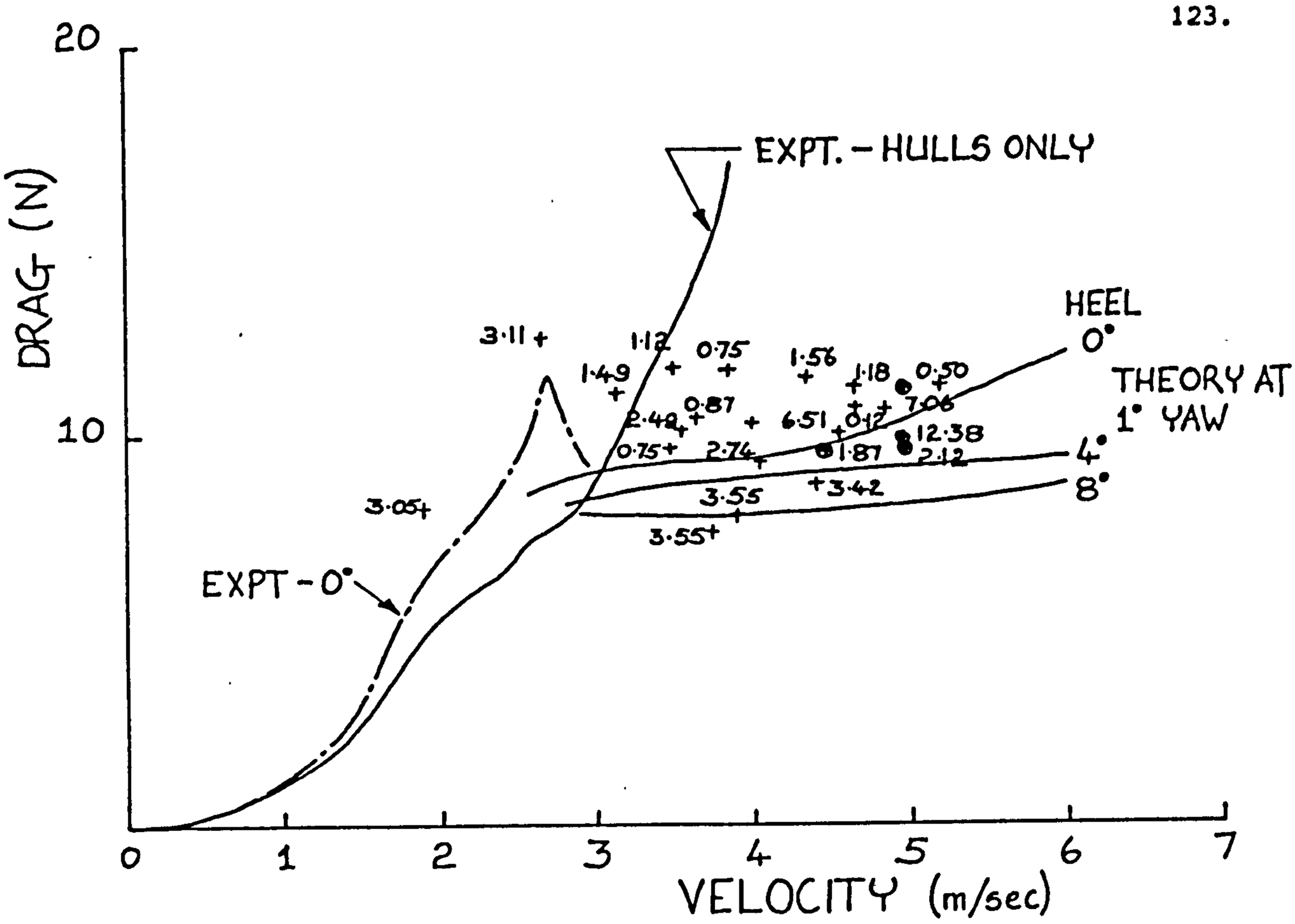

Fig. 4.10a Drag Curve - Yaw Angles 0-2 Degrees

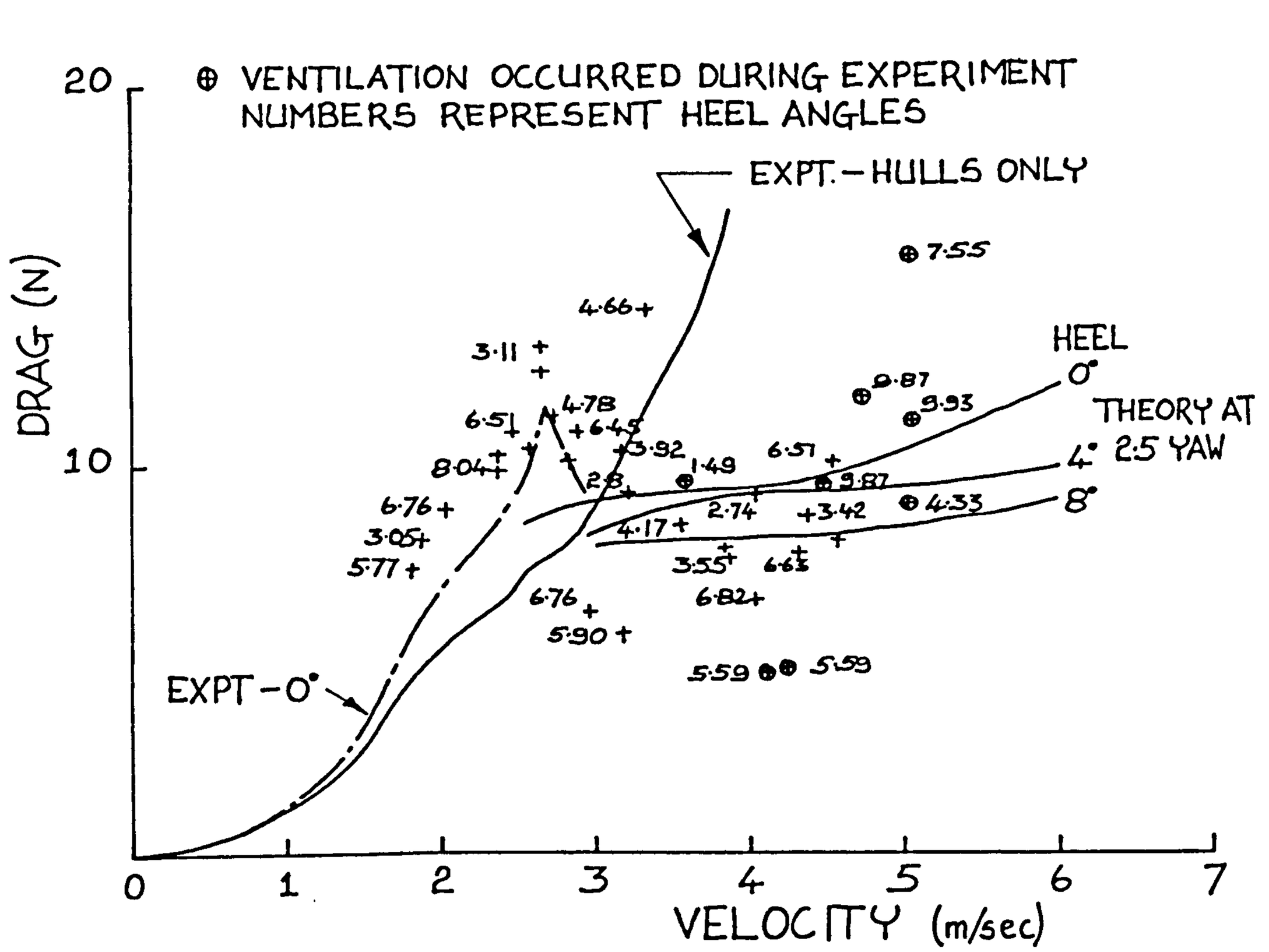

Fig. 4.10b Drag Curve - Yaw Angles 2-3 Degrees

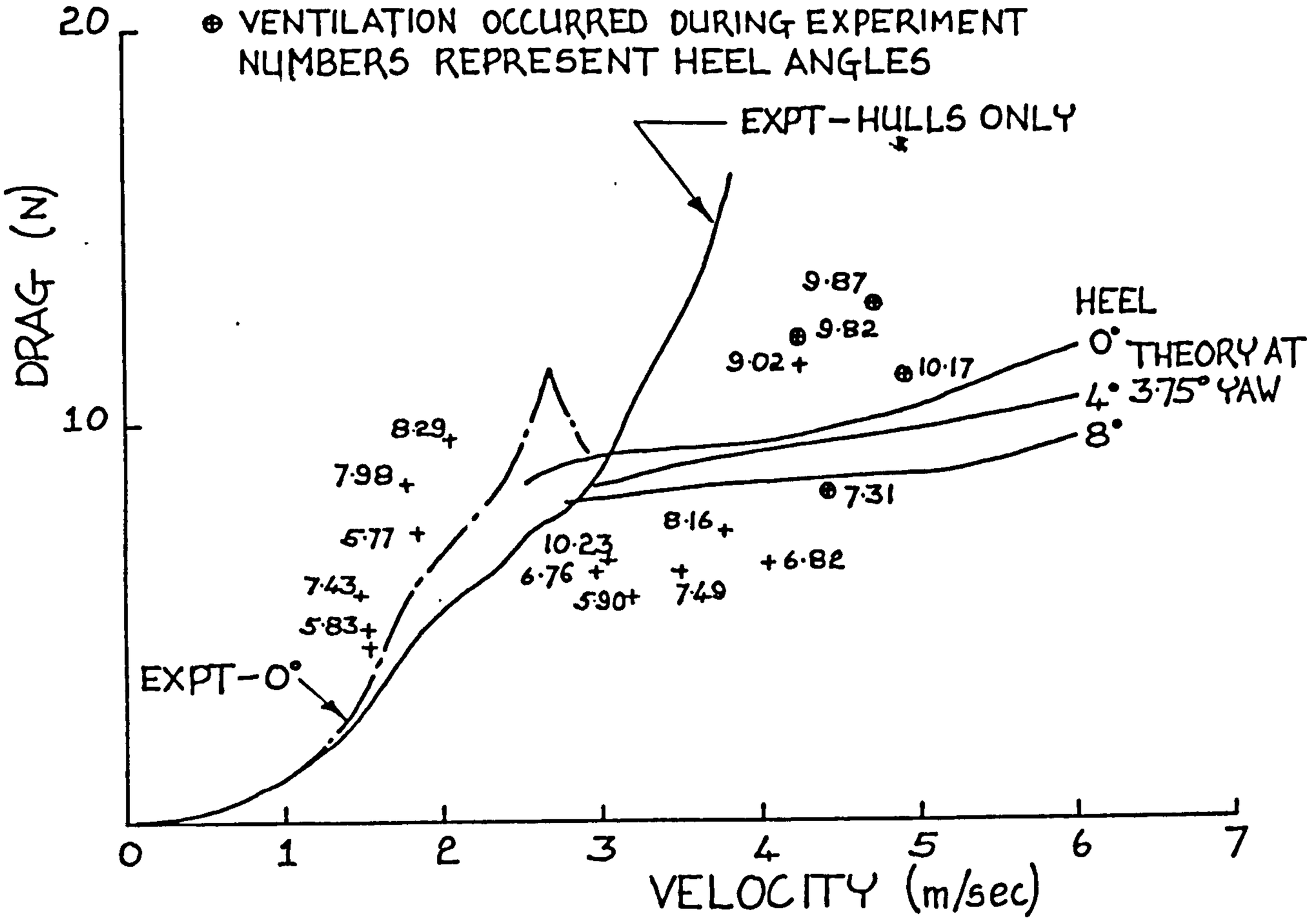

Fig. 4.10c Drag Curve - Yaw Angles 3.0 - 4.5 Degrees

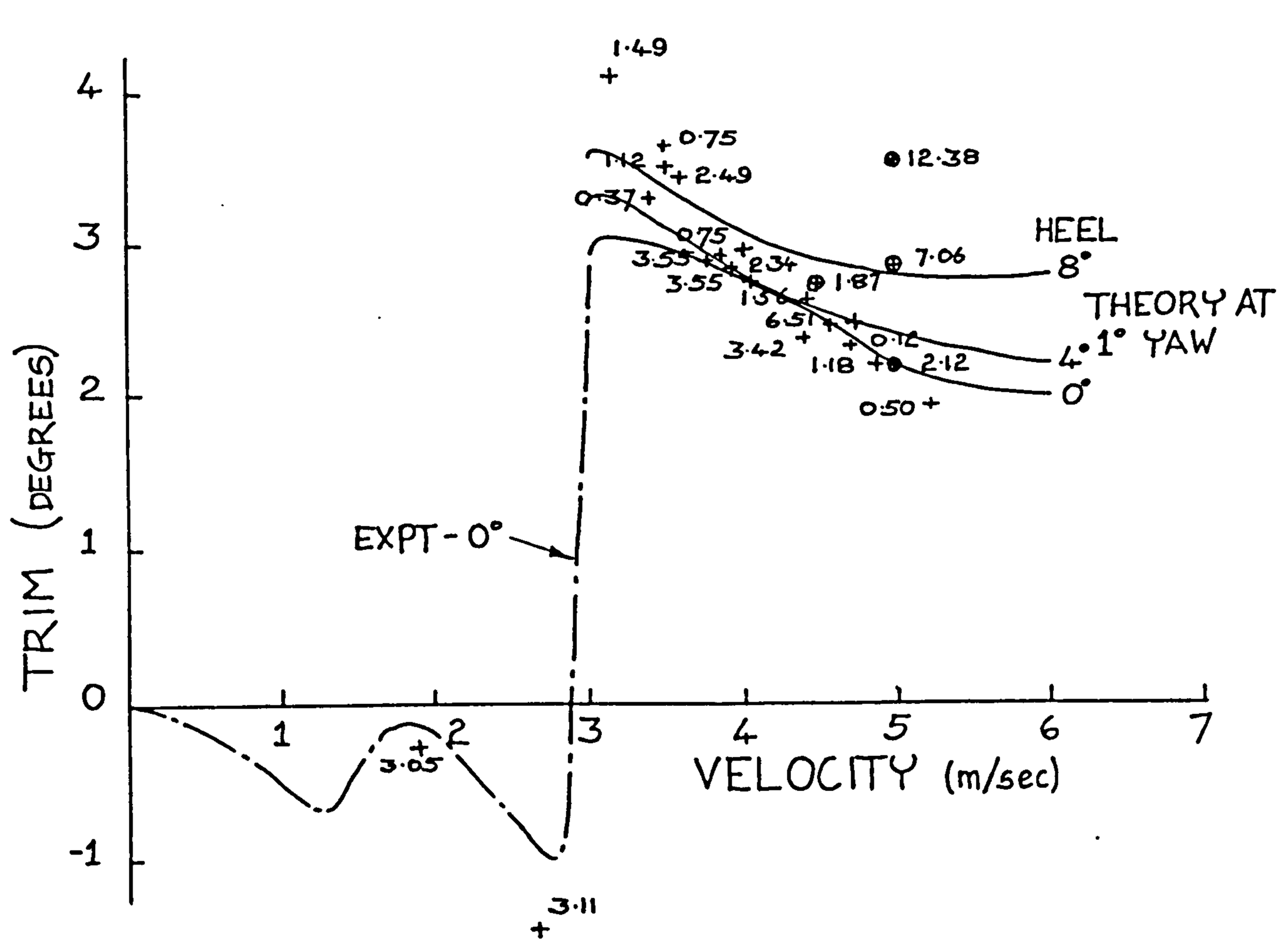

Fig. 4.11a Trim Curve - Yaw Angles 0-2 Degrees

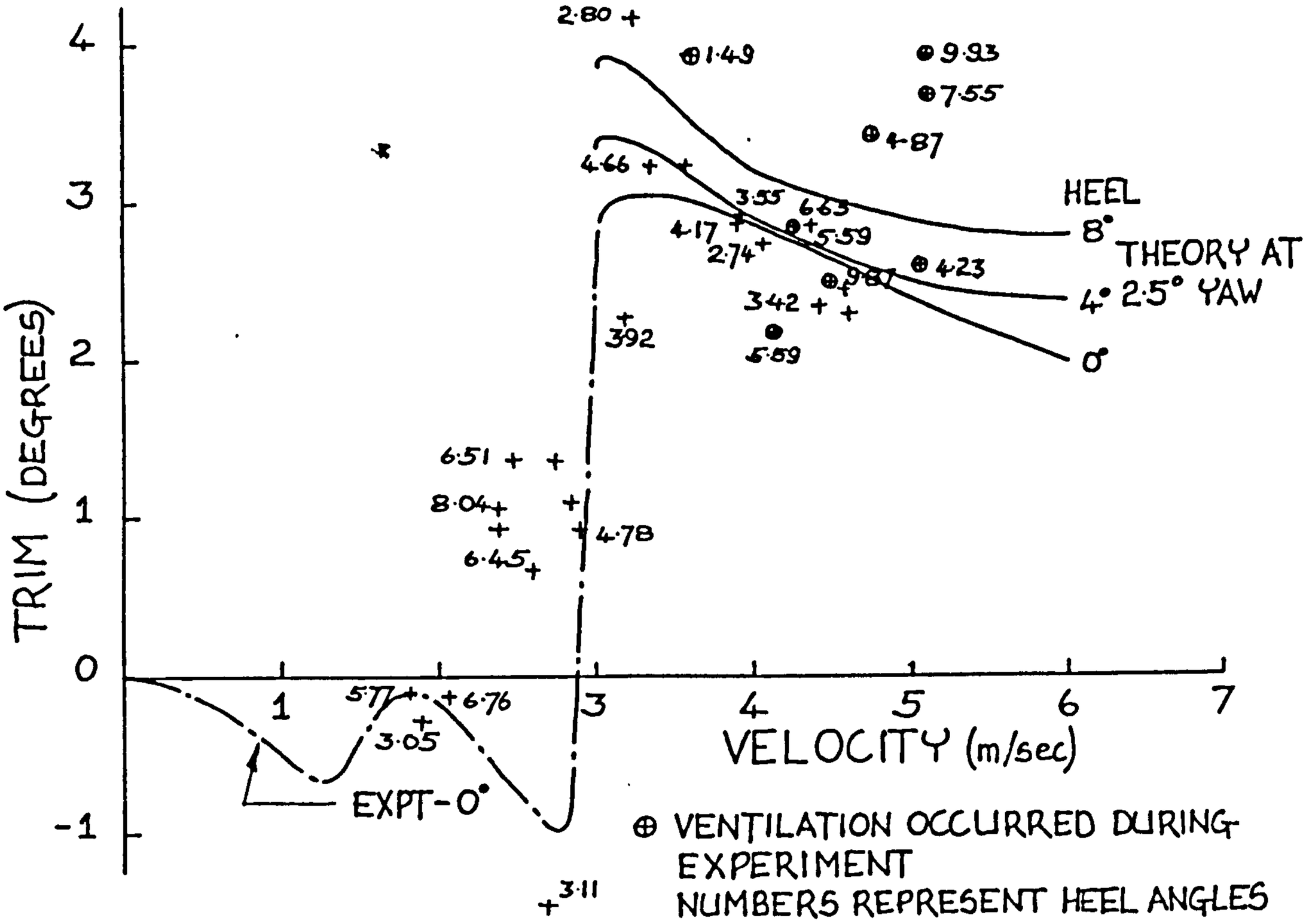

Fig. 4.11b Trim Curve - Yaw Angles 2-3 Degrees

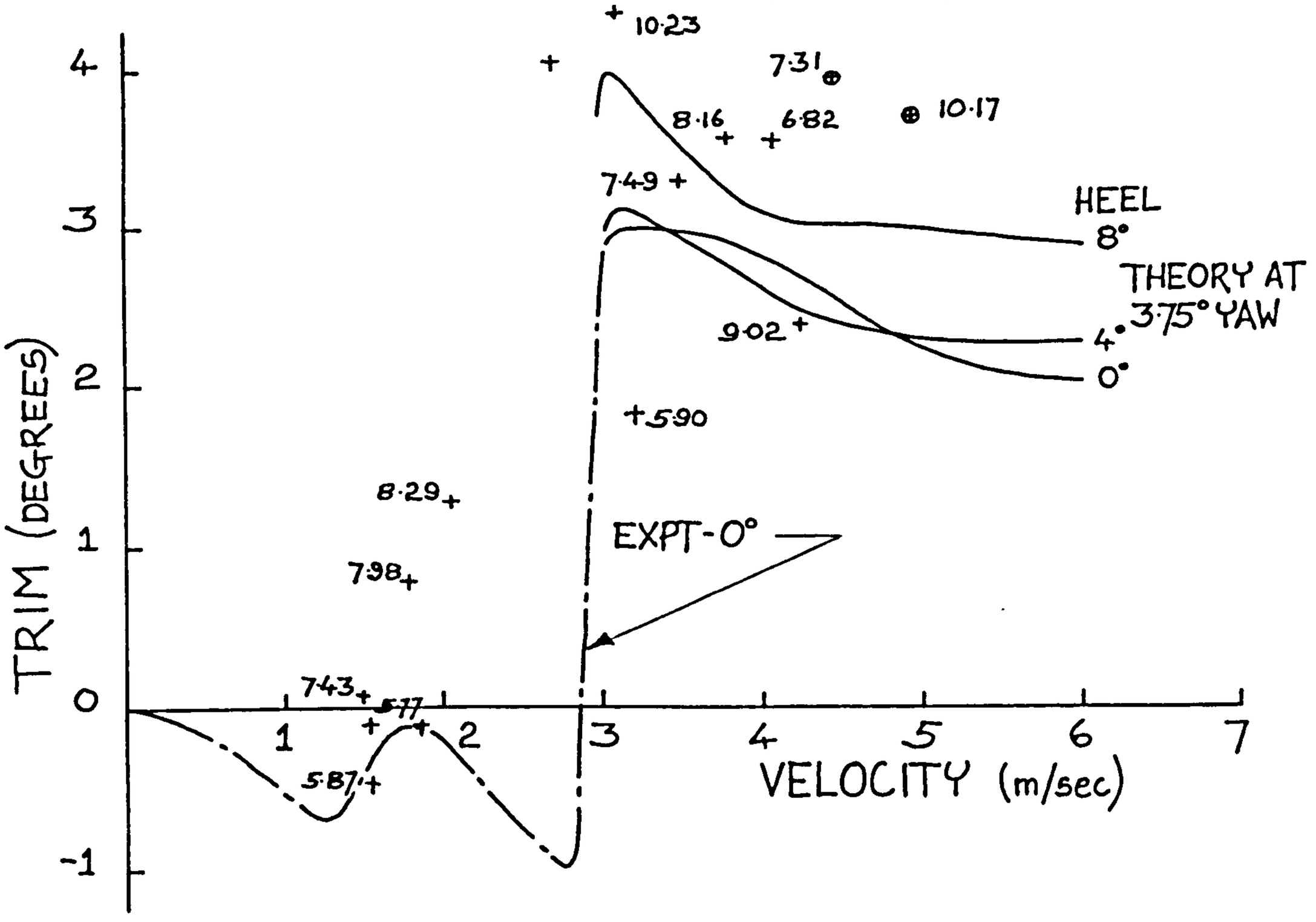

Fig. 4.11c Trim Curve - Yaw Angles 3 - 4.5 Degrees

higher angles of yaw, the trim peak at take off is higher at large angles of heel than for low angles of yaw. The effect of a heel angle is to increase the trim of the model at the same speed. Both these points are borne out to some extent by the experimental results but the agreement tends to be of a qualitative nature, where for example it can be seen that there is a greater proportion of experimental results at a higher angle of heel towards the upper side of the 'cloud' of data. There is a large amount of experimental scatter, especially at the larger angles of yaw where ventilation is more prevalent. As would be expected the data follows the trend of the experimental data for the experiments at zero degrees of heel and yaw more closely than the theoretical curves (see figure 4.9b).

Curves 4.12a,b and c show the height of flight of the model at the position of the origin of the coordinate system or in other words at the stern foil. As for the tests where the angles of heel and yaw were zero the theory over predicts the results in the range of speeds from 3.0 to 4.5 m/sec by approximately one centimetre. If this is taken into account and allowance made for the results where ventilation was present during an experimental run for which there is a larger degree of scatter, the agreement between the experiments and the theory is seen to be good. It can also be seen that the results do not depend to any great extent on the angle of yaw except as stated above that large angles of yaw tend to lead to large angles of heel (see fig. 4.15). This is shown by the fact that most

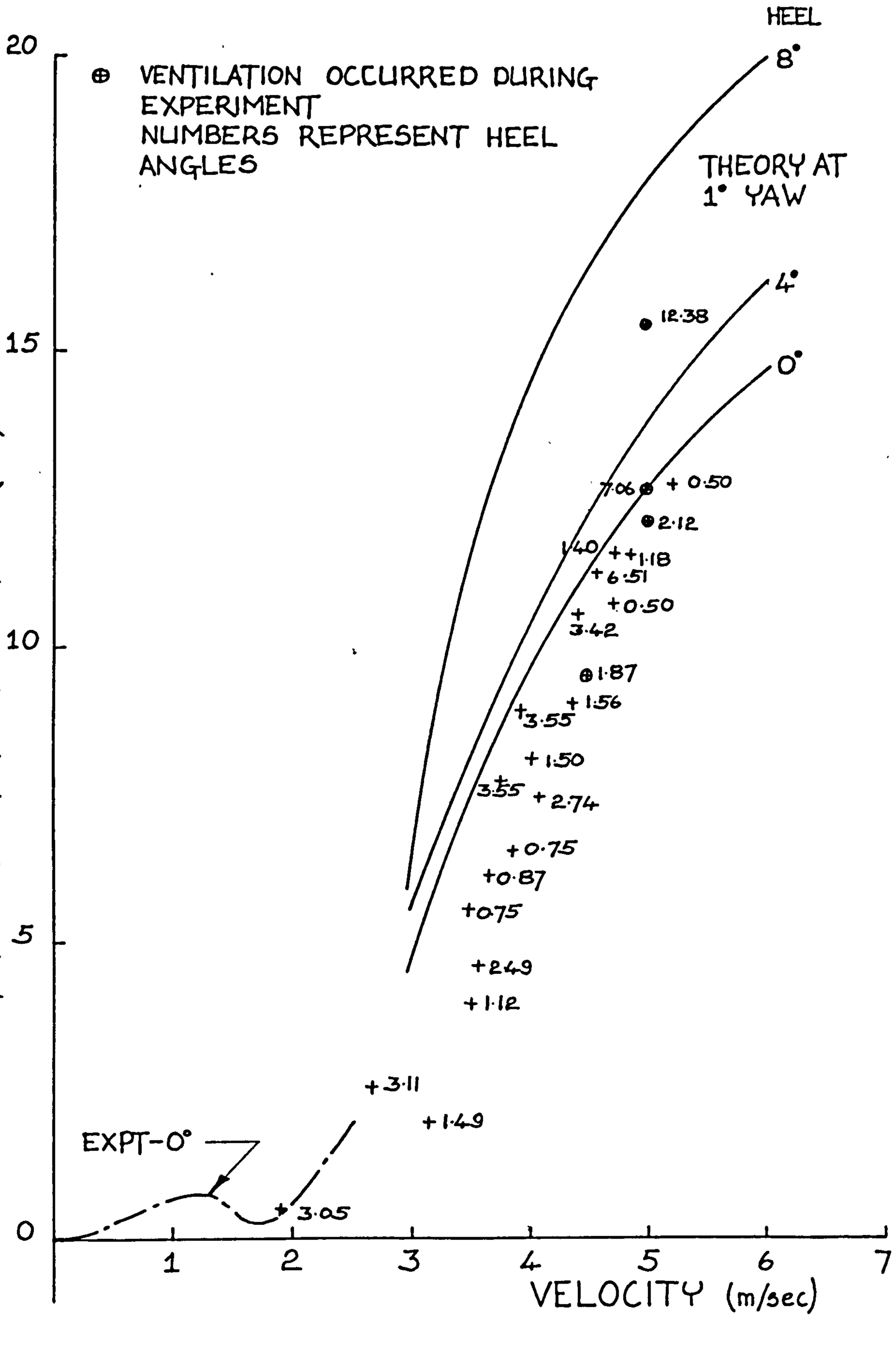

Fig. 4.12a Height of the Flight Path at the Position of the Stern Foil (Origin of the Co-ordinate System) - Yaw Angles 0.2 Degrees

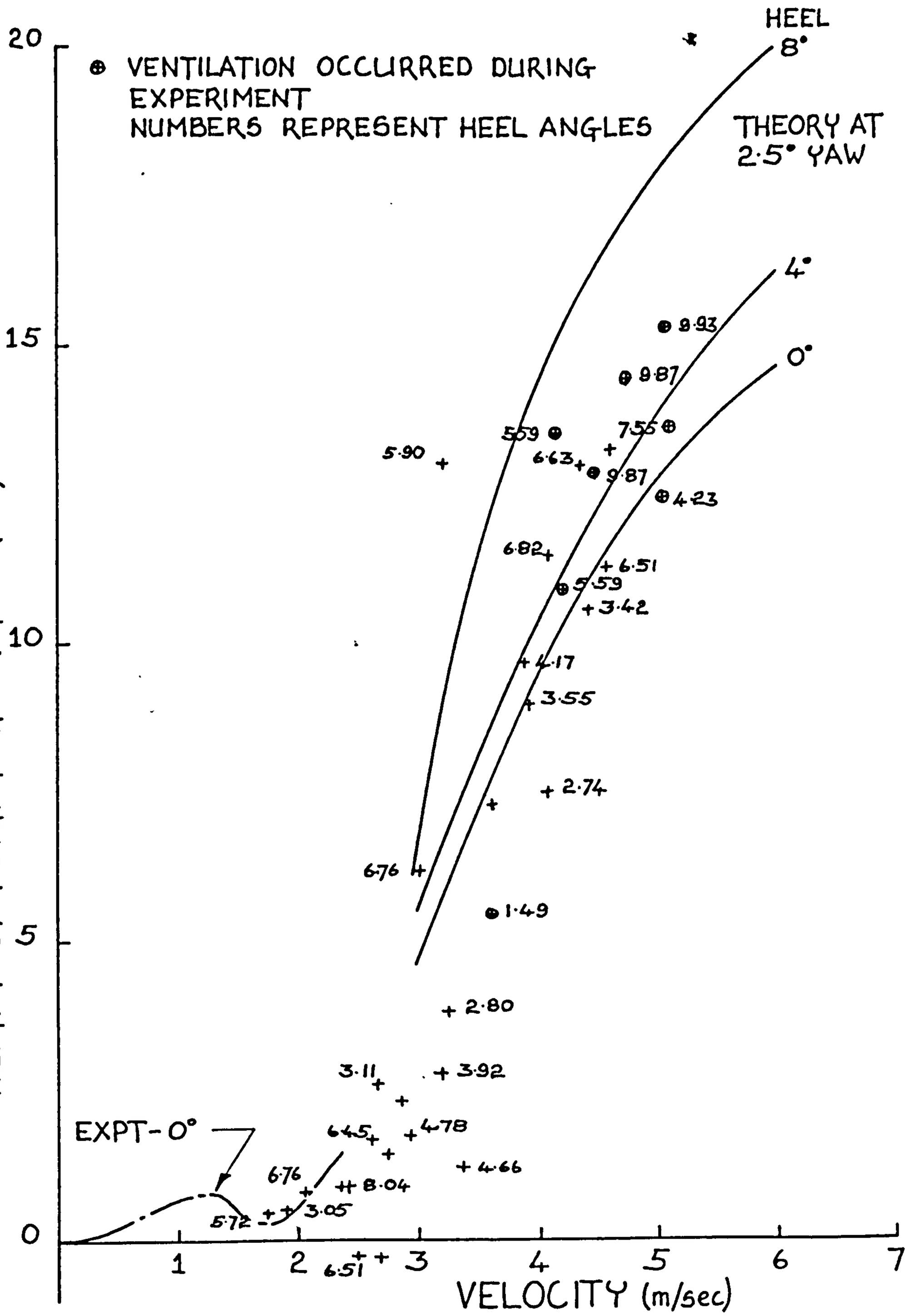

Fig. 4.12b Height of the Flight Path at the Position of the Stern Foil (Origin of the Co-ordinate System) - Yaw Angles 2-3 Degrees

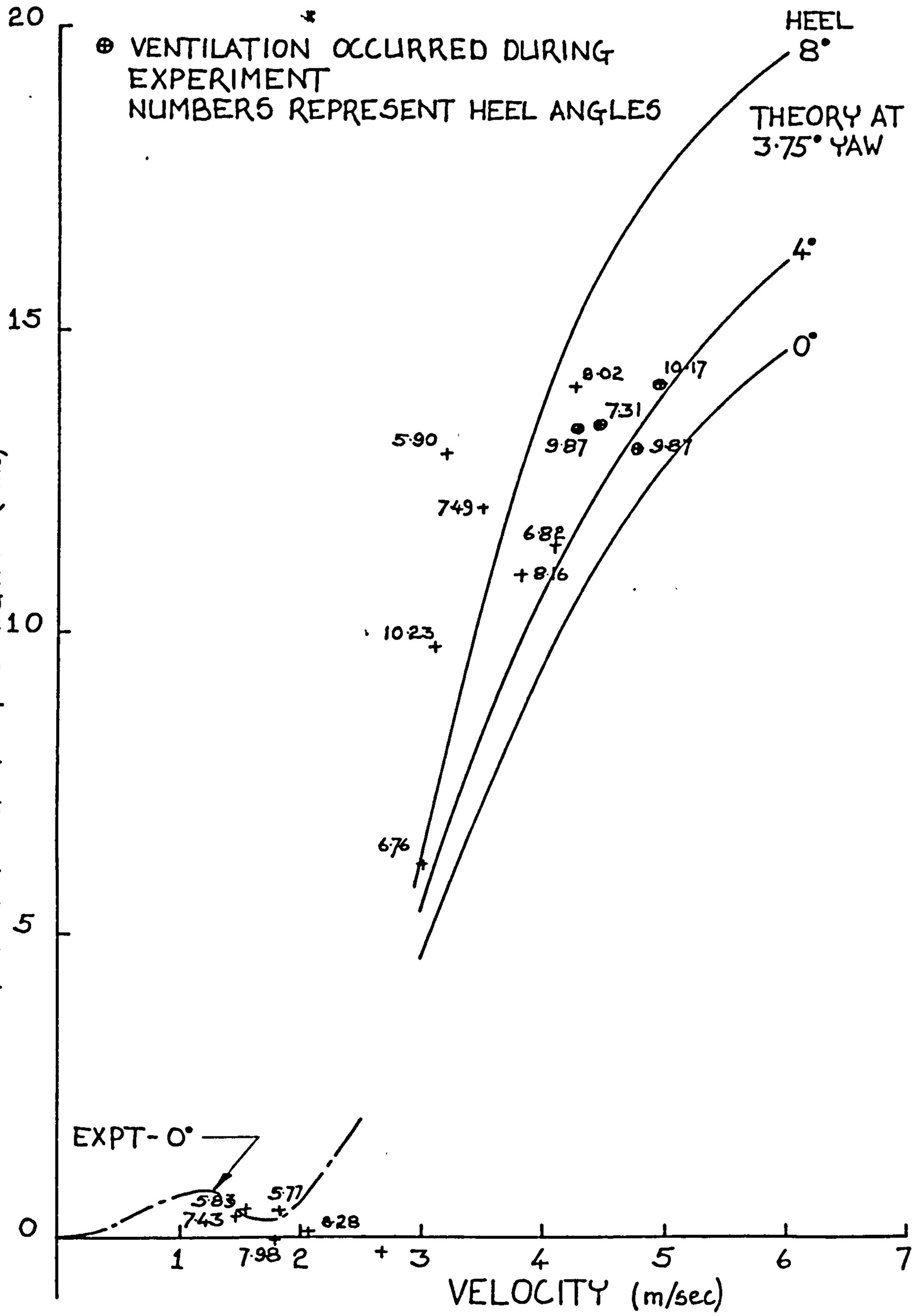

Fig. 4.12c Height of the Flight Path at the Position of the Stern Foil (Origin of the Co-ordinate System) - Yaw Angles 3 - 4.5 Degrees

of the data in figure 4.12a is at low angles of heel and that for figure 4.12c is at high angles of heel.

Results for side force are presented in figures 4.13a,b and c. Here the scatter in the results is very high although again barring some anomalies and the runs where ventilation occurred, qualitatively speaking the results do follow the same trends as those predicted. The maximum values of side force measured are significantly higher than those predicted although again these values mainly occurred in conjunction with some form of ventilation on the model foils. It can be seen from the theoretical predictions that the side force increased to a maximum at about 4 degrees of heel and around a speed of 6 m/sec. At higher values of heel, the maximum value of the side force fell, which can be seen by studying the curves at an angle of heel of 8 degrees. These results are due to different configurations of hydrofoils and struts becoming immersed at the different orientations of the model. The struts which support the main lifting hydrofoil elements make the most contribution to the side force and it is between these angles of heel that the windward struts rise above the water surface.

Figures 4.14 and 4.15 were plotted to assess the relationships which existed between angles of heel, angles of yaw and the velocity of the model. In both cases only experimental data has been used and where two or more 'y' values occur at the same value on the 'x' axis these points

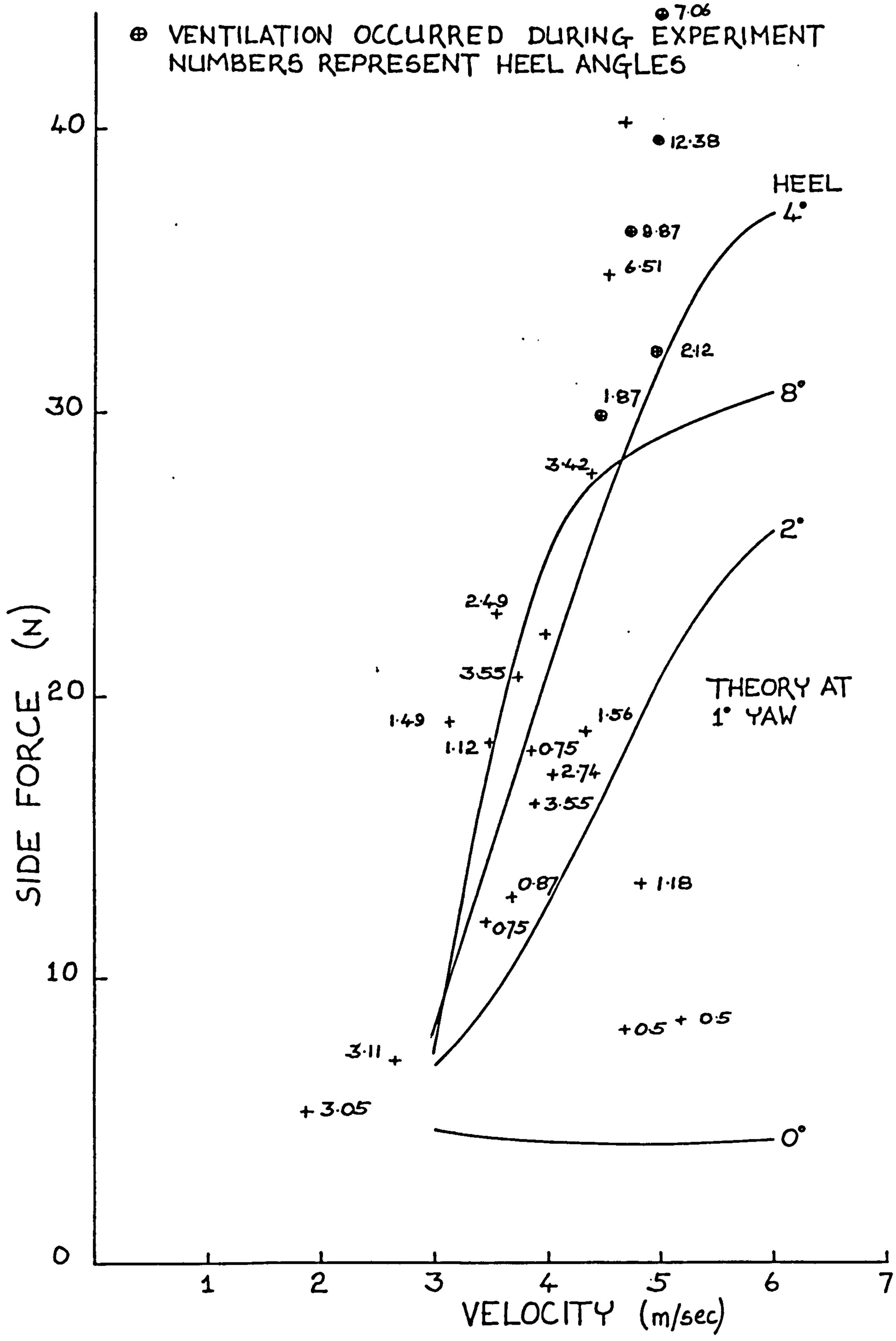

Fig. 4.13a Side Force - Yaw Angles 0-2 Degrees

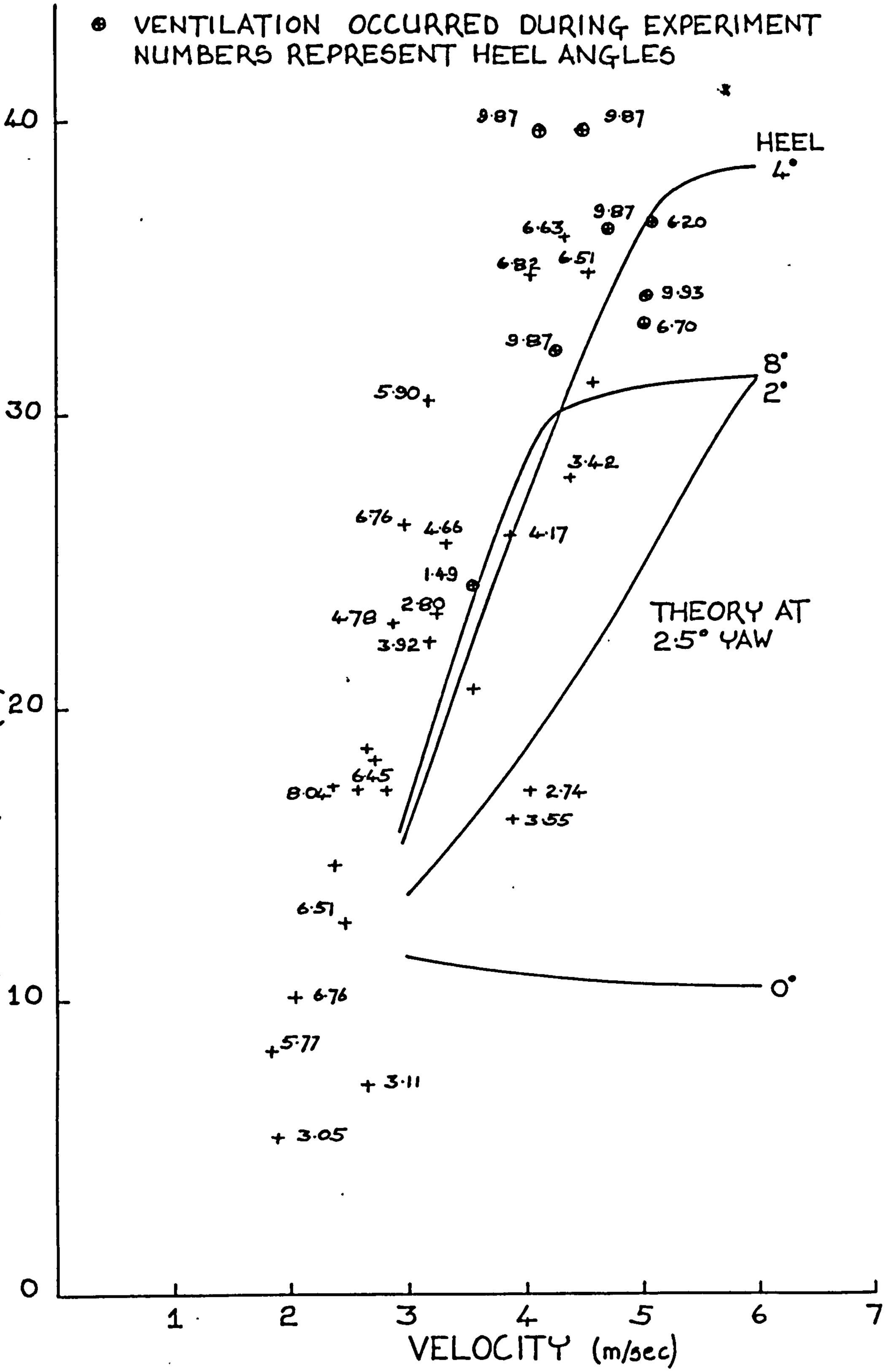

Fig. 4.13b Side Force - Yaw Angles 2-3 Degrees

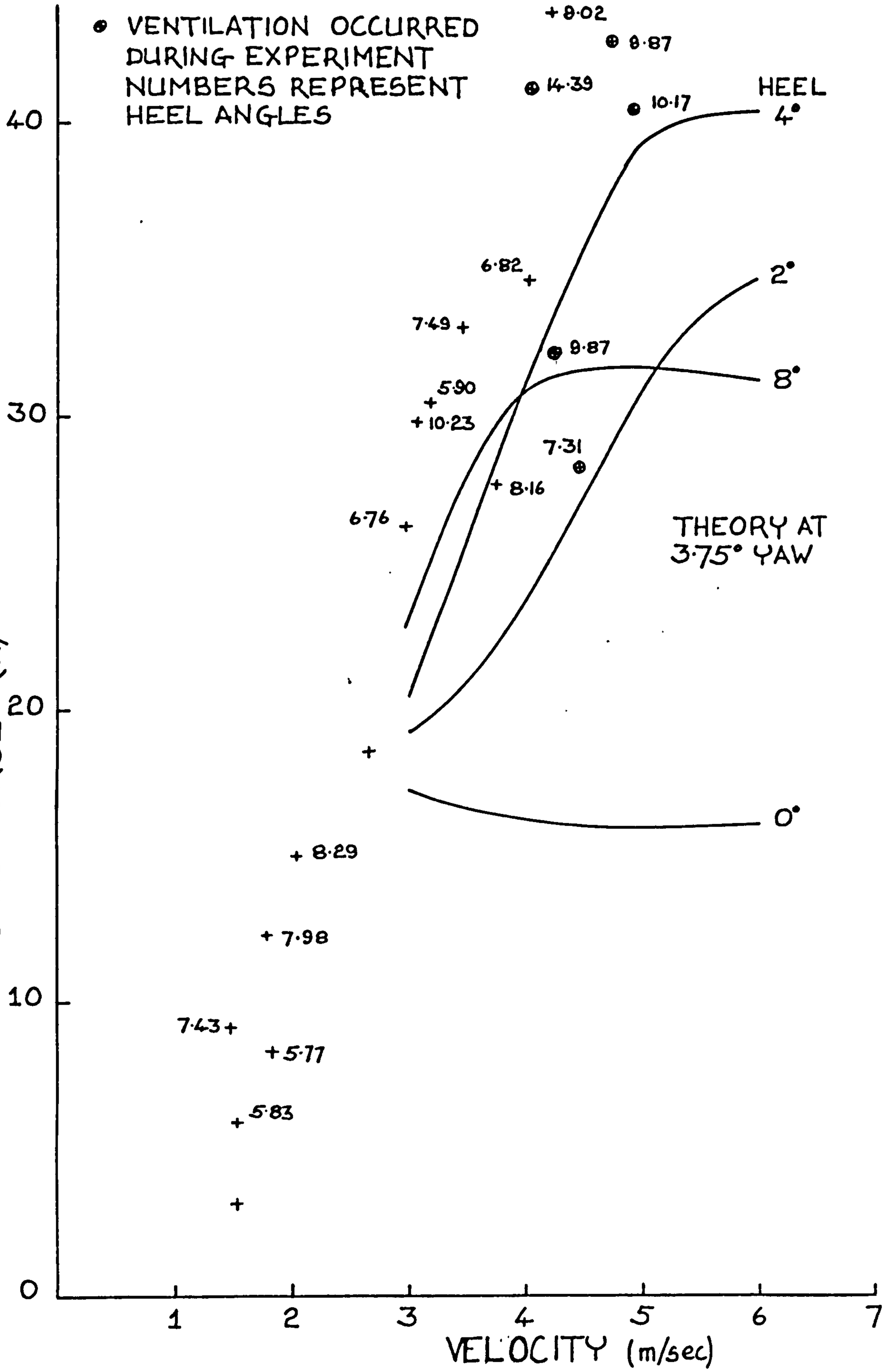

Fig. 4.13c Side Force - Yaw Angles 3 - 4.5 Degrees

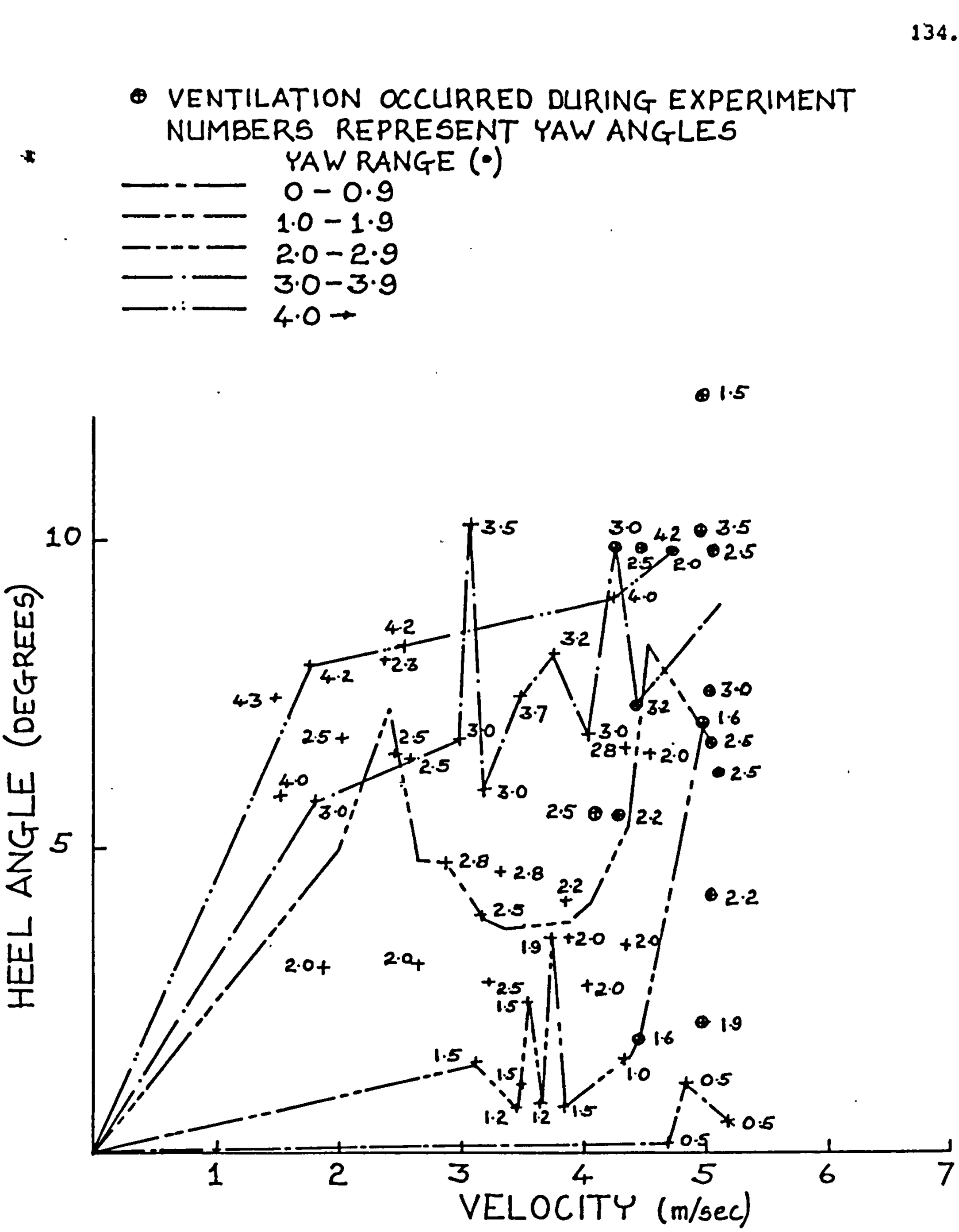

Fig. 4.14 Variation between Heel and Velocity at Different Angles of Yaw

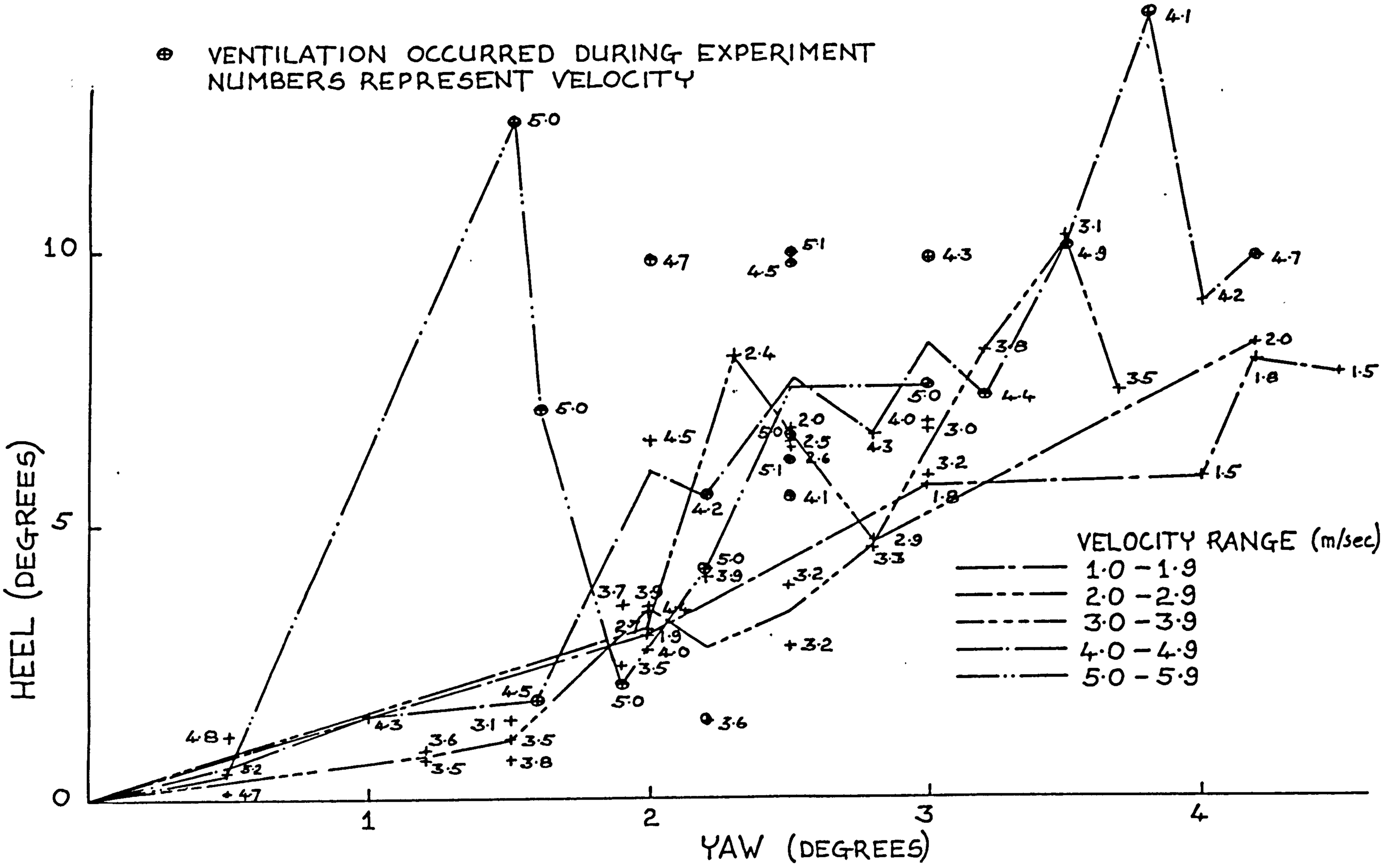

Fig. 4.15 Variation between Heel and Yaw Angles at Different Velocities

have been averaged. All the experimental points have been plotted.

Figure 4.14 is a plot of the heel angle against velocity. The curves shown join all the results which lie in a designated range of yaw values. The yaw value ranges are denoted on the graph and the numbers next to the data points are the actual yaw value for the run. The end result is a family of curves which show that the angle of heel is a function of both the yaw angle and the velocity. Higher angles of heel were produced at larger angles of yaw for the same speed of the model.

Figure 4.15 extended the same idea to see how the angle of heel varied with the angle of yaw at different speeds. The speed ranges are denoted on the graph and the numbers next to the points are the actual speeds of the experimental runs. If the large variations in the curve for the speed range 5.0-5.9 m/sec are disregarded at speeds below 2 m/sec, it can be seen that all the curves follow more or less the same course which can be approximated to a straight line or a very shallow parabola.

Ventilation

Throughout this chapter reference has been made to ventilation, the formation of air cavities, on the surface of the model hydrofoils and their detrimental effects on the performance of the craft. The most comprehensive study

on the ventilation phenomenon and its causes and effects was carried out at the University of Leeds, Dept. of Mechanical Engineering, for the Canadian 'Bras D'Or' hydrofoil project. A description of the phenomenon together with the important results from this programme of work have been published in the papers listed in the references (59,117,119,166,174 and 175).

In the model tests described here, ventilation occurred most frequently on the upper part of the main lifting foils (side foil units), that portion with 40 degrees dihedral angle positioned between the two struts (fig. 4.2). At even higher speeds or at larger angles of heel and yaw, these ventilated cavities would spread to the lower main lifting foil, with a subsequent loss in lift and height of flight. (fig. 4.16). Depending on the flow conditions and speed at the time of the 'crash' (the model never fully crashed to the extent that the hulls re-entered the water) the ventilated cavity would either 'wash out' and the model regain its former attitude or the run would be completed at the new orientation, the foils operating in their ventilated state. In some cases small intermittent cavities would form on a portion of the foil system, the cavities alternately forming, 'washing out' and then reforming.

A small amount of bluff body ventilation was also noted at times at the higher speeds behind the trailing edge of the main strut of the stern foil, but this never

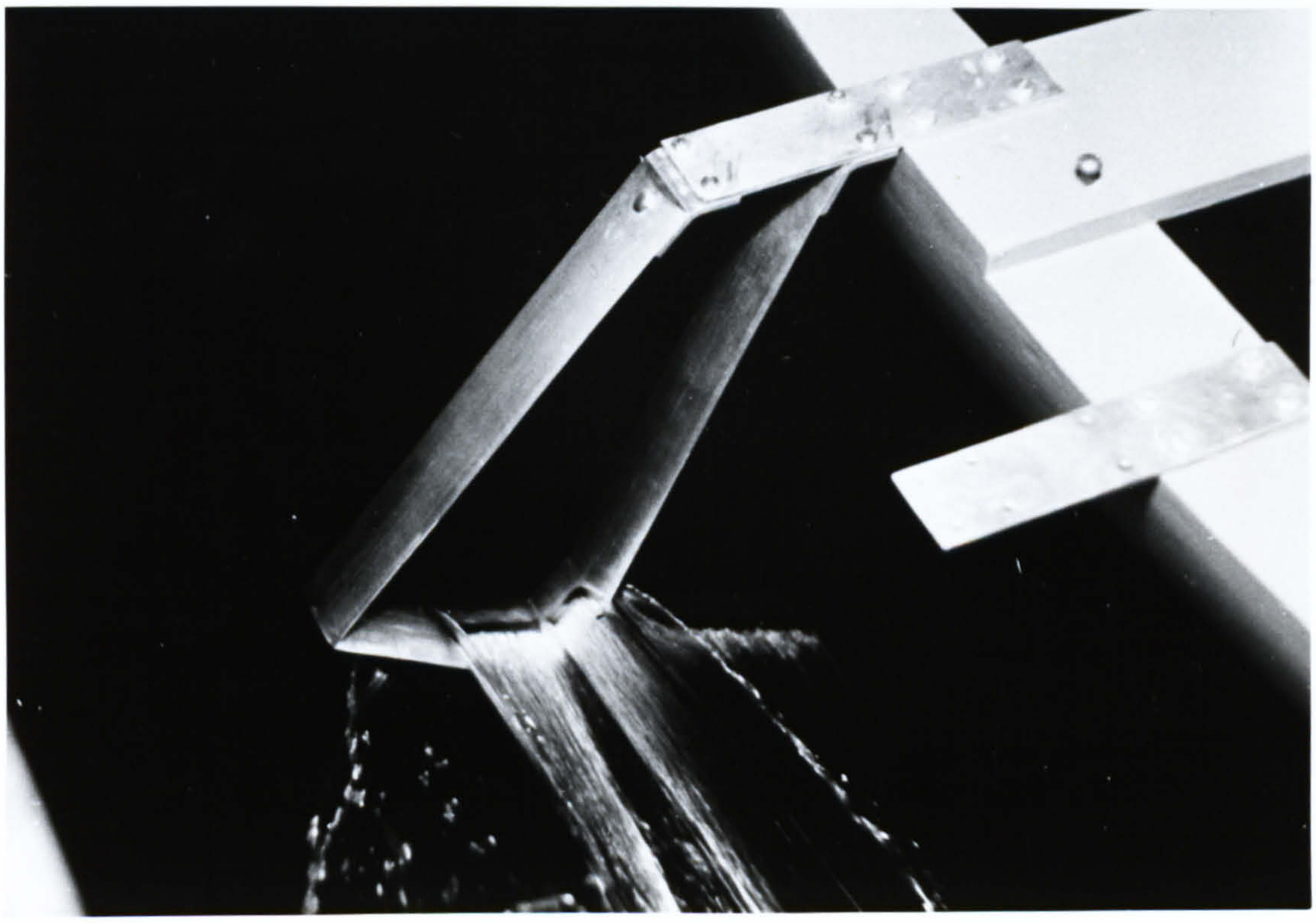

Fig. 4.16 Ventilation on the Model Side Foil in the Towing Tank

spread to the tee foil. Experiments were not undertaken with model fences as it was felt that because of the small size of the fences required, no meaningful results would have been obtained. The extensive differences between the behaviour of ventilated regions on hydrofoils on the full scale and in the model tank are emphasised by Rothblum (160). Because of these scale effects any studies of the ventilation situation on the full scale system and the positioning of anti-ventilation fences had to be undertaken from the results of the full scale trials and not from information gained in the towing tank.

Conclusions

The foregoing results show how the formulations of chapter 3 can be regarded as an efficient and generally accurate method for the calculation of the forces incident on complex surface piercing hydrofoil systems. The predictions of the drag and orientation of the model agree well with the experimental results for the case when angles of heel and yaw are zero although there are small variations of the order of one degree in the results of the trim predictions.

When angles of heel and yaw are included the scatter in the experimental results is higher and as a consequence their agreement with the theoretical predictions is not as accurate as for the previous case. However, trends in the experimental results are predicted correctly and in most

cases the experimental results fall within a well defined scatter band.

Ventilation on parts of the hydrofoil system affected the experimental results significantly and was in all cases detrimental to the performance of the model. Experimental runs where ventilation occurred normally yielded results with a high degree of scatter.

CHAPTER 5

Wind Propulsion

This chapter on wind propulsion covers two different types of wind propulsion systems. The first, a soft sail rig, was the type of system that was used on the prototype craft. The second which consisted of a wind turbine connected via a suitable gear train and shaft arrangement to a water propeller was not constructed, but its performance was considered analytically and compared with the performance of the sail rig.

Sails - Performance Prediction

There has been a considerable amount of work carried out on the aerodynamics of sails and the estimation of the performance of sailing yachts, some of which is described in the references , (28, 29, 31, 34, 39, 43, 52, 55, 69, 83, 84, 86, 102, 109, 122, 123, 124, 126, 130, 134, 172, 176 and 195.) In some cases this has involved work of considerable complexity, a good example are the lifting surface theories used by Milgram, (130) which were used for the tabulation of data for a variety of rigs of different aspect ratios and types. It was felt by the author that such complexity was unnecessary in this study. While every

effort was made to design an efficient rig (chapter 2), the actual values of the force coefficients from the sails were still unknown quantities and they would alter substantially with changes in sheeting angles, camber and twist of the sails, and with the unsteady forces arising from variations in the wind velocity and direction and motions of the boat.

The method adopted here was to use the sail force coefficients C_{TA} and aerodynamic drag angles ε_A which were formulated by Bradfield, (31), from various sources which included Davidson's 'Gimcrack' tests, (52) for the calculation of the sail forces on a day sailing catamaran, a rig very similar to that used on the prototype craft in this study. These coefficients which predicted results which agreed well with the results from a full scale experiment carried out by Bradfield are plotted in figure 5.1 against β_A, the heading angle to the apparent wind, and they were considered to be typical of the averaged steady values experienced. Plotted alongside this data for comparison are values from the tables of Milgram, (130), (based on a lifting surface theory) for two conditions, that of a sloop rig and that of an 'una' rig (mainsail only) for a mainsail aspect ratio of 3.0. The actual mainsail aspect ratio was 3.32 and this would produce larger values of the force coefficient and smaller values of the aerodynamic drag angle than those predicted for an aspect ratio of 3.0. Bearing this in mind, the results from Milgram are seen to agree well with the coefficients used by Bradfield. This method neglects the effect of

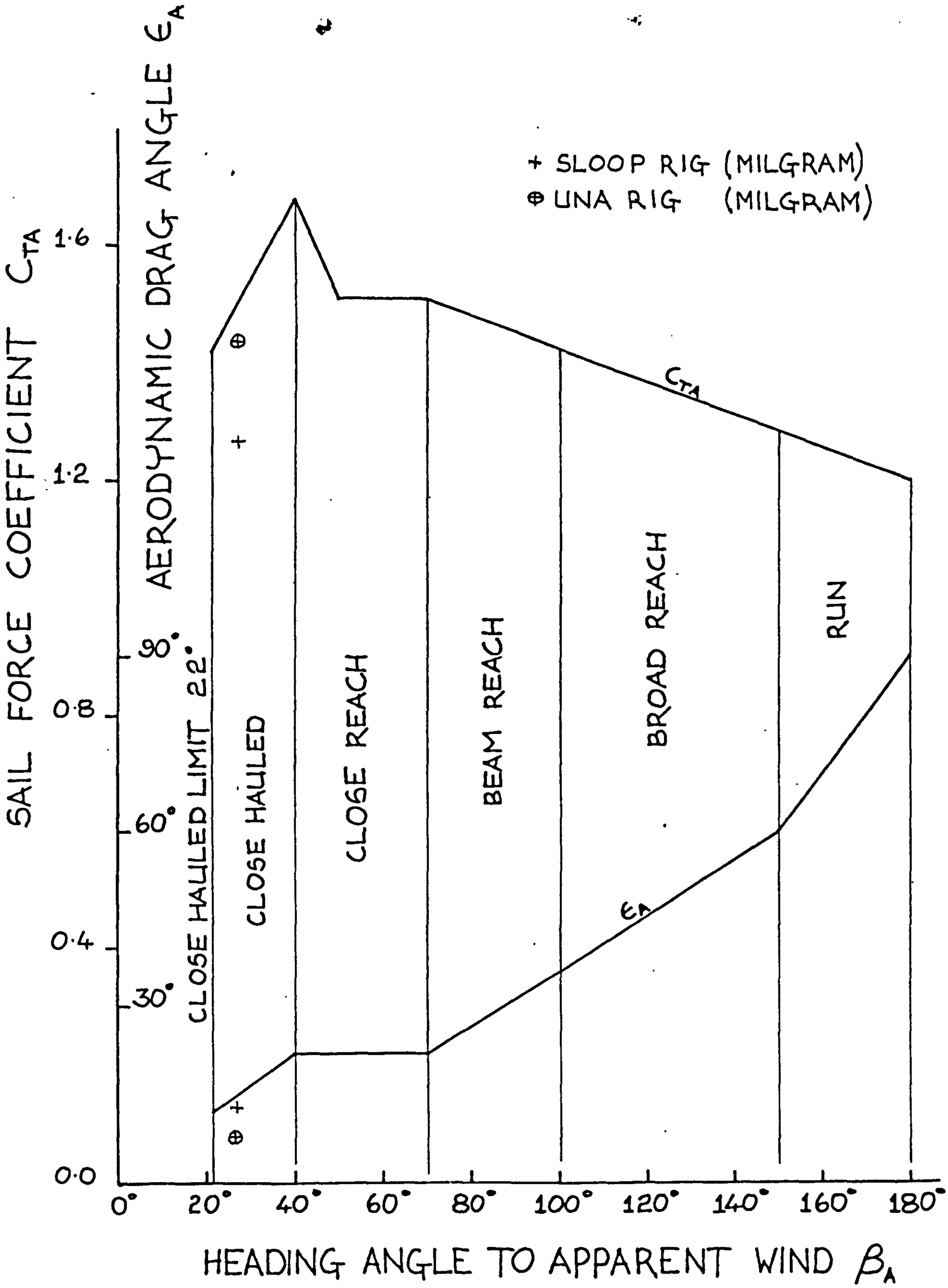

Fig. 5.1 Estimated Values of C_{TA} and β_A used in the Sail Force Calculations (Bradfield)

unsteady forces due to variations in the wind strength and direction and the motion of the craft is assumed to be steady and in a straight line. The sail camber and twist and hence the sail characteristics, are assumed not to vary with the wind strength. This is not unreasonable for a fully battened mainsail over the wind speed range of importance. The sails are at all times assumed to be set and trimmed in their most efficient manner.

The coefficients which are plotted in figure 5.1, assume the close-hauled limit to be at a heading angle to the apparent wind, β_A, of 22 degrees. Between a heading angle, β_A, of 22 degrees and 40 degrees, the boat is assumed to be close hauled and the angle of incidence of the sails increases steadily although the sheeting angles are not altered. This produces an increase in the force coefficient and drag angle which are assumed to vary linearly with the angle of incidence. Above a heading angle, β_A, of 40 degrees, which is assumed to be the upper limit of close hauled sailing, the sheeting angles of the two sails are increased in order that the angle of incidence of the sails does not increase to the extent that the sails begin to stall. The sail camber and twist are preserved over this range by the use of efficient sheeting arrangements (e.g. by use of a mainsheet track) and adjustable jib sheet fair leads, but the force coefficient, C_{TA}, falls because of the decreasing interaction between the mainsail and the jib. (i.e. the velocity of the airflow over the low pressure side of the mainsail

decreases as the 'slot' between the two sails widens). As the heading angle, β_A , increases beyond 70 degrees the mainsail begins to twist and stall. Little information is available for thin and flexible aerofoils operating in this region and Bradfield assumed the curves to vary linearly over the reach and the run. The sail force coefficients at a heading angle, β_A , of 180 degrees, pure downwind sailing, where the sails are operating as purely drag devices was taken as 1.2, (123) and the aerodynamic drag angle was 90 degrees in this mode.

Referring to figure 5.2 which shows the equilibrium of forces and the velocity triangle between the wind and the boat speed vectors for a sailing yacht while close hauled, the sail force coefficient, C_{TA} , is defined as :

$$C_{TA} = \frac{T_A}{\frac{1}{2}\rho_A V_A^2 S_A}$$

where T_A is the total sail force, ρ_A is the density of the air, V_A is the apparent wind speed and S_A is the total sail area.

Resolving the total sail force into a driving force, R, and a heeling force, F_H , we get:

$$\text{Driving Force } R = T_A \sin (\beta_A - \varepsilon_A)$$

$$\text{Heeling Force } F_H = T_A \cos (\beta_A - \varepsilon_A)$$

and the driving and heeling force coefficients C_R, C_H:

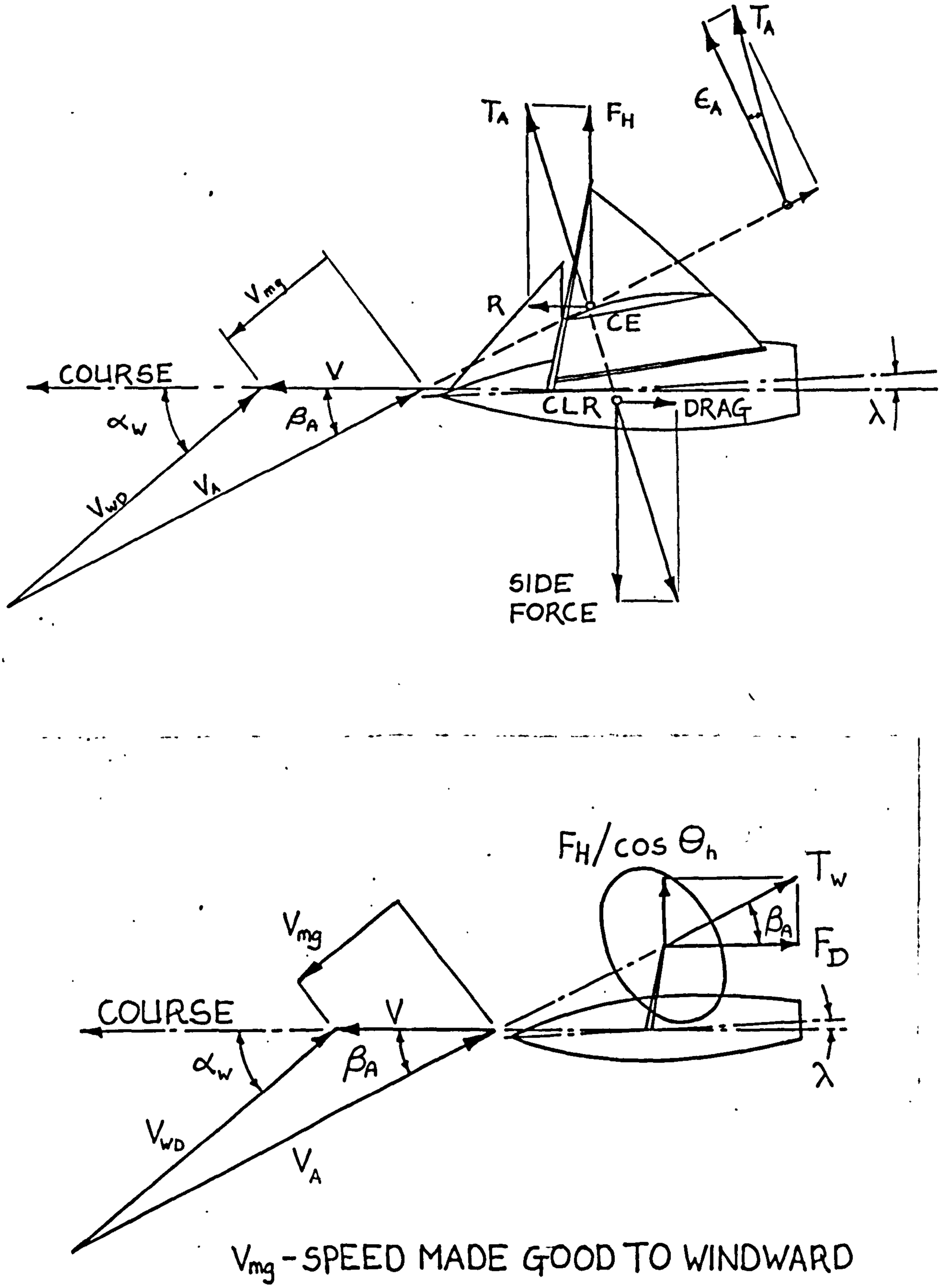

Fig. 5.2 Sail and Windmill - Velocity Triangle and Drag Forces

$$C_R = C_{TA} \sin(\beta_A - \varepsilon_A)$$
$$C_H = C_{TA} \cos(\beta_A - \varepsilon_A)$$

The apparent wind angle and the apparent wind speed are given for any moving vehicle in the plane perpendicular to the mast as (86):

$$\tan\beta_A = \frac{V_{WD}}{V} \sin\alpha_W \cos\theta_h \Big/ \left(\frac{V_{WD}}{V} \cos\alpha_W + 1\right)$$

$$V_A = V \sqrt{\left(\frac{V_{WD}}{V} \sin\alpha_W \cos\theta_h\right)^2 + \left(\frac{V_{WD}}{V} \cos\alpha_W + 1\right)^2}$$

where V is the speed of the boat, V_{WD} is the true wind speed, α_W is the angle of the boats course to the true wind direction and θ_h is the angle of heel.

These take into account the angle of heel because the sail coefficients are defined at angles of incidence which are measured in the plane which is perpendicular to the mast. In all cases in this study it was possible to assume that the angle of heel was zero, and this was a realistic assumption because the prototype craft was always sailed either upright or at very small heel angles.

These formulations were incorporated into the computer program WIND and its subroutine SAIL. The computations were carried out at different values of the boat speed and the wind speed for directions of the boats course relative to the true wind direction, α_W, of 0,30,45,60,90,120,150

and 180 degrees. The wind speed values were 3,6,9,12 and 15 m/sec. The boat speeds could be chosen by the operator. The program WIND also carried out a similar calculation for a windmill using a different subroutine WMILL.

Windmills - Performance Predictions

Recent developments in wind propulsion systems for sailing craft have included a number of relatively novel and potentially efficient types of rig. Among these have been solid aerofoil rigs, kite sail rigs, vertical and horizontal axis wind turbine rigs and inclined sail rigs, some examples of which are described in the references (8, 11, 12, 13, 14, 26, 30, 34, 71, 74, 94, 125, 135, 145, 146, 147, 152, 176, 177, 178, 179, 185, 189 and 192.) From this list, the most worthwhile contenders against the fully battened soft sail rig employed here, appeared to be either a solid aerofoil rig or a wind turbine rig. It was realised that an efficiently designed solid aerofoil rig which included facilities for camber control, which in their simplest form would involve trailing edge flaps, offered the best scope for the propulsion of a craft which would be capable of very high speeds over a limited range of courses relative to the true wind direction. This was borne out by the experiences which have been gained from the races of the Little America's Cup on 'C' class catamarans (34 and 152). The overall aim of this study was to design a versatile craft and the wind turbine rig seemed an attractive proposition for this and one worthy of

further study. The reasons behind this decision were as follows. A wind turbine propulsion system is able to propell a craft at any direction relative to the true wind direction. Control of the wind turbine, both pitch control and orientation of the rotor with the wind direction, can be arranged from a remote positon such as a cockpit or wheelhouse. Pitch control or the feathering of the blades of the rotor is essentially a form of reefing or of reducing the effectiveness of the system which is necessary as the wind strength increases. Little work had been carried out in order to ascertain the potential of the wind turbine rig.

A horizontal axis wind turbine or windmill was chosen mainly because it was expected that the efficiency of this type of rotor (the ratio of rotational power output to the work done on the drag component of the windmill force) and hence the windward performance would be greater than for a vertical axis rotor. This is especially true in higher windspeeds when the pitch and hence the efficiency (figure 5.3) of the horizontal axis rotor are increased in order to reduce the power absorbed by the windmill. The vertical axis rotor of the straight bladed type (137 and 138) in the same conditions, reduces its effectiveness by adjusting the angle of the blades to the vertical and this reduces its efficiency. These are controversial points and they were discussed at length at the recent RINA Symposium on the Wind Propulsion of Commercial Ships (176, papers 8,11 and 15).

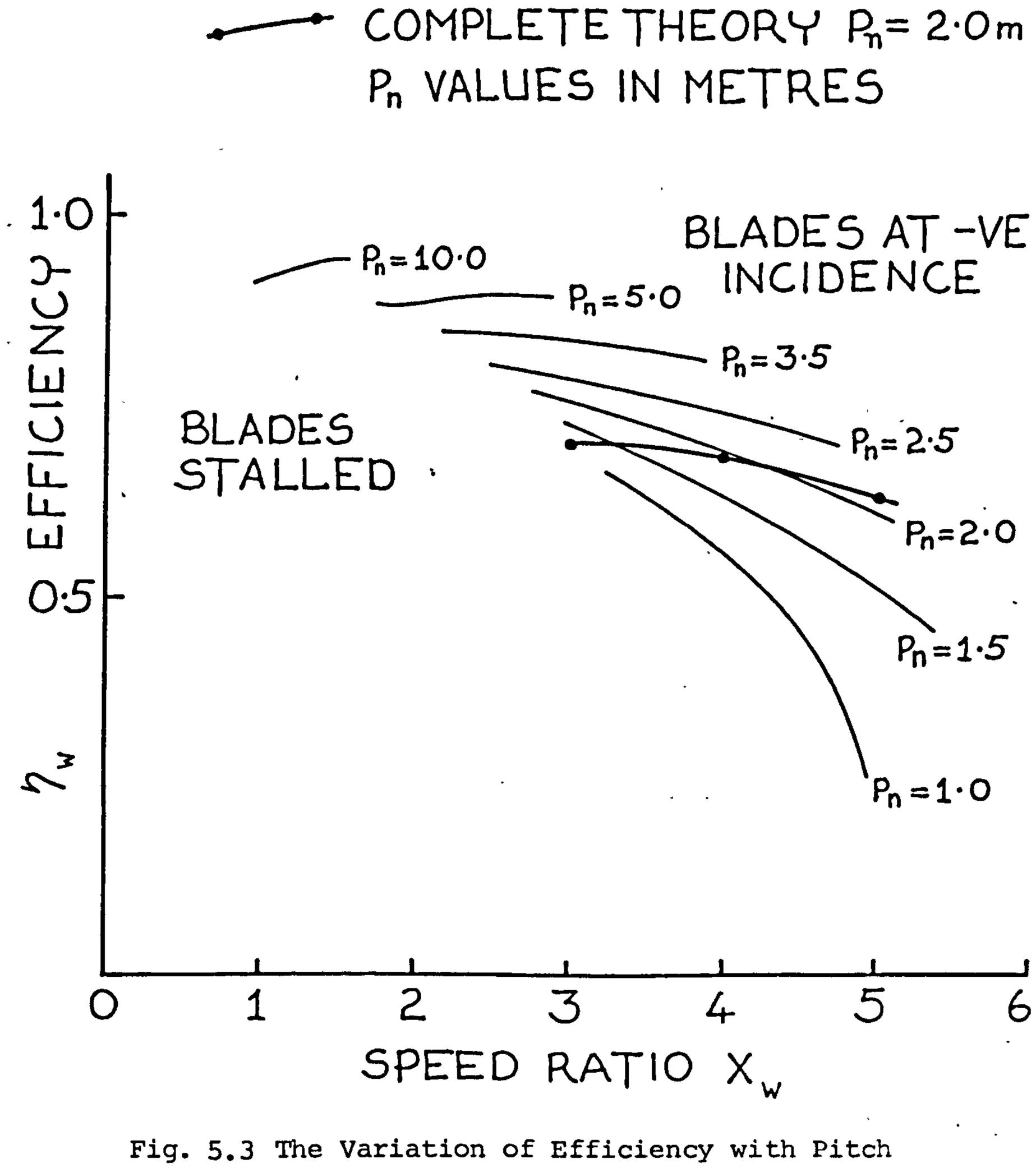

Fig. 5.3 The Variation of Efficiency with Pitch

Other points which affect the choice of the rotor are the relative heights of the centres of pressure between the two designs, which influences the heeling moment, the amount of weight aloft and the alignment of the rotor with the wind direction. The vertical axis wind turbine gains from having no requirement for a gear box aloft, but loses to the horizontal axis windmill because of its requirement for a horizontal strut to support its blades. This coupled with the mechanism for adjusting the inclination of the blades and the more severe structural loading, which is strongly periodic as the loading on the blades alters over the cycle, for the vertical axis rotor reduces any weight differences which may exist between the two designs in theory. Self-alignment with the wind direction is a true advantage of the vertical axis rotor, but alignment of the horizontal axis windmill is not expected to cause any significant problems in practice. Some of these aspects are discussed in the following references (12, 13, 26, 19, 73, 79, 98, 120, 137, 140 and 180).

The vortex theory of the windmill, as in the case of the propeller (19,60,98,193), is based on the conception that trailing vortices spring from the rotating blades of the rotor and pass downstream in the form of helical vortex sheets. The aerodynamic forces on the blades are calculated from the two dimensional aerofoil characteristics in association with the modified system of velocities which are derived from the induced velocity of the vortex system. The calculation of these induced

velocities is very complex and because of this the analysis is based on the assumption that the rotor has a large number of blades. This implies that the velocity has a uniform value around any annulus of the windmill disc and the vortex theory becomes almost identical with the blade element theory, but where the calculation of the induced velocities is made from the momentum theory. The periodicity of the flow which is encountered with a rotor having a small number of blades may be estimated subsequently as a correction to this simplified form of analysis.

Consider an element of the windmill blade at a radius r_w, figure 5.4, the effective velocity, W_w, of this element can be found as the vector sum of the axial and tangential components of the inflow velocity. The axial velocity is reduced from V', ahead of the windmill to $V'(1 - \delta)$ at the windmill. The rotational velocity of the wind increases as it passes through the windmill, but its direction behind is opposite to the direction of rotation of the windmill. Using the axial and rotational interference factors δ and δ'

$$W_w \sin\phi = V' (1 - \delta)$$

$$W_w \cos\phi = \Omega r_w (1 + \delta')$$

where ϕ is the angle of the inflow velocity defined on figure 5.4 and Ω is the angular velocity of the rotor. Hence the speed ratio (the inverse of the conventional value taken for propellers) is :

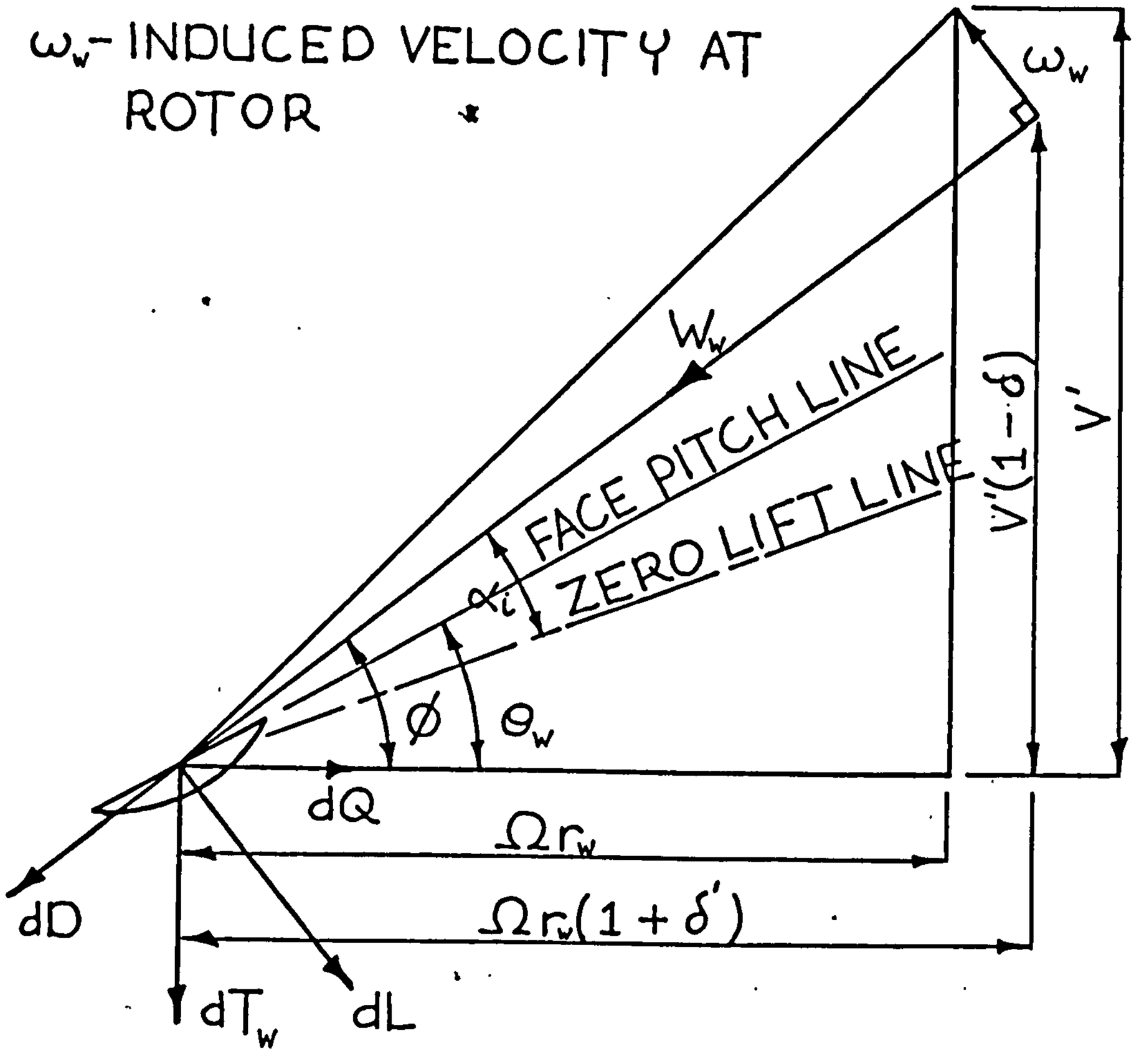

Fig. 5.4 Forces on the Blade Element.

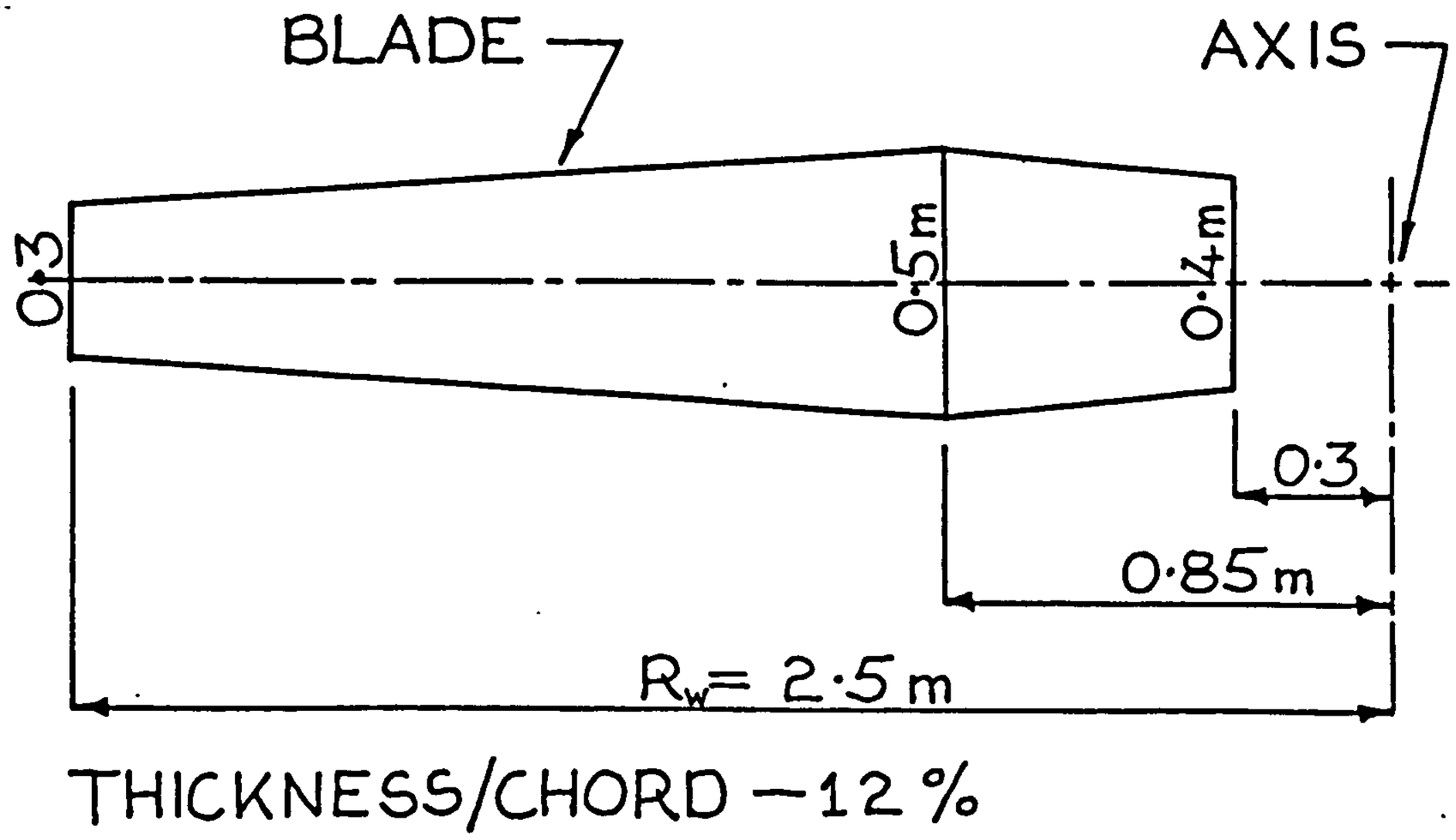

Fig. 5.5 Geometry of the Windmill Blade

$$\text{Speed Ratio } X_w = \frac{\Omega R_w}{V'} = \frac{R_w}{r_w} \frac{(1 - \delta)}{(1 + \delta')} \cot\phi$$

where R_w is the radius of the windmill rotor.

Considering the lift and drag forces operating on the blade element, the thrust, T_w and torque, Q can be found as :

$$\frac{dT_w}{dr_w} = \tfrac{1}{2} B c \rho_A W_w^2 (C_L \cos\phi + C_D \sin\phi)$$

$$\frac{dQ}{dr_w} = \tfrac{1}{2} B c \rho_A W_w^2 r_w (C_L \sin\phi - C_D \cos\phi)$$

where B is the number of blades, c is the chord length and C_L and C_D are the lift and drag coefficients respectively.

To non-dimensionalise these equations, the chord is replaced by the element solidity, σ :

$$\sigma = \frac{B c}{2\pi r_w}$$

and the thrust and torque coefficients T_{wc} and Q_c are taken as :

$$T_{wc} = \frac{T_w}{\pi R_w^4 \rho_A \Omega^2} \qquad Q_c = \frac{Q}{\pi R_w^5 \rho_A \Omega^2}$$

Also the components of the aerodynamic force normal and parallel to the axis of the windmill can be written respectively as:

$$C_x = C_L \sin\phi - C_D \cos\phi$$

$$C_y = C_L \cos\phi + C_D \sin\phi$$

Hence: $$R_w \frac{dT_{wc}}{dr_w} = \sigma \left(\frac{r_w}{R_w}\right)^3 (1 + \delta')^2 C_y \sec^2\phi$$

$$R_w \frac{dQ_c}{dr_w} = \sigma \left(\frac{r_w}{R_w}\right)^4 (1 + \delta')^2 C_x \sec^2\phi$$

From energy and momentum considerations, the rotational and axial interference factors can be found in a similar manner to that of the propeller (60).

$$\frac{\delta'}{1 + \delta'} = \frac{\sigma C_x F_W}{4\sin\phi \cos\phi}$$

$$\frac{\delta}{1 - \delta} = \frac{\sigma C_y F_W}{4\sin^2\phi}$$

where F_W is a correction made to represent approximately the losses which arise due to a finite number of windmill blades (60 and 143)

$$F_W = \frac{2}{\pi} \arccos e^{-f}$$

$$f \simeq \frac{B}{2} \frac{R_w - r_w}{r_w \sin\phi}$$

Detailed thrust and torque curves can then be calculated by taking a number of stations along the blades. The chord, radius and face pitch angle ($\theta_W = \tan^{-1} P_n / 2\pi r_w$) at each station will be known, together with the two dimensional lift and drag coefficients for the section at each value of the angle of incidence. For a range of angles of incidence at this station, the calculation is carried out for the inflow angle, the aerodynamic force coefficients parallel and normal to the axis of the

windmill, the axial and rotational interference factors, the speed ratio and then finally the element thrust and torque coefficients. These calculations were carried out in the computer programs VORTEX and VORTEX1.

These thrust and torque coefficients can then be plotted against the speed ratio, X_w , for each station. For a given value of the speed ratio, the variation of the thrust and torque coefficients can then be found over the span of the blades and these values can be integrated numerically to obtain the overall thrust and torque of the windmill.

This approach is unwieldy, however, for a long series of calculations on different windmills and as with the propeller (60), for comparison purposes, the calculations can be made on the blade section at $r_w = 0.7R_w$. Then the overall thrust and torque coefficients can be taken approximately as:

$$T_{wc} = 0.57\, R_w \frac{dT_{wc}}{dr_w} \qquad Q_c = 0.57\, R_w \frac{dQ_c}{dr_w}$$

the value of the constant, 0.57, being valid only for blades of constant pitch along the blade span and for certain blade shapes.

In order to make comparisons between different windmill configurations, the terms of interest are the efficiency and the power ratio of the windmill.

Efficiency

This is the ratio of the rotational power output to the work done on the drag component of the windmill force:

$$\eta_W = \frac{\Omega Q}{T_w V'} = \frac{X_w Q_c}{T_{wc}}$$

In the case of a windmill mounted on a moving vehicle, this efficiency is strictly appropriate as a true parameter only when the vehicle is moving to windward. This is because on all other courses relative to the apparent wind direction, the drag force from the windmill does not directly oppose the motion of the vehicle. At an apparent wind angle, β_A, (Figure 5.2) of 90 degrees this rotor drag contributes solely to the heeling moment and at angles greater than 90 degrees it contributes some value to the driving force. However, for the best windward performance it is important to have a high value of this parameter.

Power Ratio

The second term of interest is the ratio of the actual power output to the maximum power output of an ideal windmill of the same proportions. This latter is calculated from the momentum theory of a windmill, which ignores rotational motion of the air, and it occurs at a value of the axial interference factor, δ , equal to 1/3.

$$P_{MAX} = \frac{8}{27} \pi R_w^2 \rho_A V'^3$$

$$\text{Power Ratio } \frac{P}{P_{MAX}} = \frac{27}{8} X_w^3 Q_c$$

A high value of the power ratio is necessary especially at low wind speeds. When the energy of the wind is low it is important for the windmill to absorb as much of this energy as possible. At higher windspeeds, this is not so critical and the pitch of the windmill can be altered so that a higher efficiency and lower power ratio are achieved.

A Windmill Mounted on a Moving Vehicle

When a windmill is mounted on a moving vehicle and operates in the windmill mode, the velocity and force diagrams are as shown in figure 5.2. The formulation for the apparent wind angle β_A and the apparent windspeed V_A is the same as that for a sailing boat and is given previously in this chapter.

The drag and heeling forces from the rotor are respectively :

$$F_D = T_W \cos\beta_A$$

$$F_H = T_W \sin\beta_A \cos\theta_h$$

This leads to the overall driving force from the rotor in the windmill mode of:

$$F_T = Pe/V - F_D$$

where V is the velocity of the craft and e is the product of the transmission efficiency between the windmill and the propeller, and the efficiency of the water propeller. In this analysis, the transmission efficiency was taken as 0.9 and a brief analysis of the propeller operating conditions led to a propeller efficiency of between 0.65-0.68. The value of e was taken as 0.6.

This part of the calculation was calculated in the subroutine WMILL which as for the sail calculations ran in conjunction with the main program WIND.

Other modes of operation of the windmill are discussed later in this chapter.

Windmill Propulsion for the Hydrofoil Trimaran

The windmill design discussed here was developed for the hydrofoil trimaran which had been previously sailed using the conventional cloth sails which are described in chapter 2. This design consisted of a two bladed rotor, of radius equal to 2.5m, giving a swept area of $19.63m^2$ which is close to the original sail area of the boat of $19.05m^2$. The shape of the blades and chord lengths are given in figure 5.5.

The propeller chosen for use with the windmill had a

diameter of 0.5$m and controllable pitch. Two conditions of operation were briefly considered at boat speeds of 4 and 12 m/sec . The increase in rotational speed between the propeller and the windmill was 5:1, the windmill speed being 150 and 360 rpm respectively. The efficiency was found to be in the range 0.65-0.68 for both conditions. A value of 0.67 was taken in the following predictions of available driving force.

The main features of this design were chosen after a study using the short approach described above for calculations on a series of different windmills. Comparisons were made between windmills of different sectional properties, solidity and pitch.

The variation of the efficiency and power ratio with the solidity (at r_w/R_w = 0.7) of the windmill is shown in figure 5.6 at a pitch/diameter setting of 0.5 and a speed ratio X_w = 3.5. The power ratio reaches a maximum at a value of solidity of 0.1. The efficiency on the other hand increases steadily with decreasing solidity. For a windmill operating as a propulsion device it is important to maintain a high value of efficiency especially when working directly upwind, but it is also important to maintain a fairly high power ratio as this parameter affects the ultimate power available from the windmill. In this case a compromise was achieved by selecting a solidity of 0.07, where the two curves cross. Similarly referring to figure 5.7 which compares sections of differing camber,

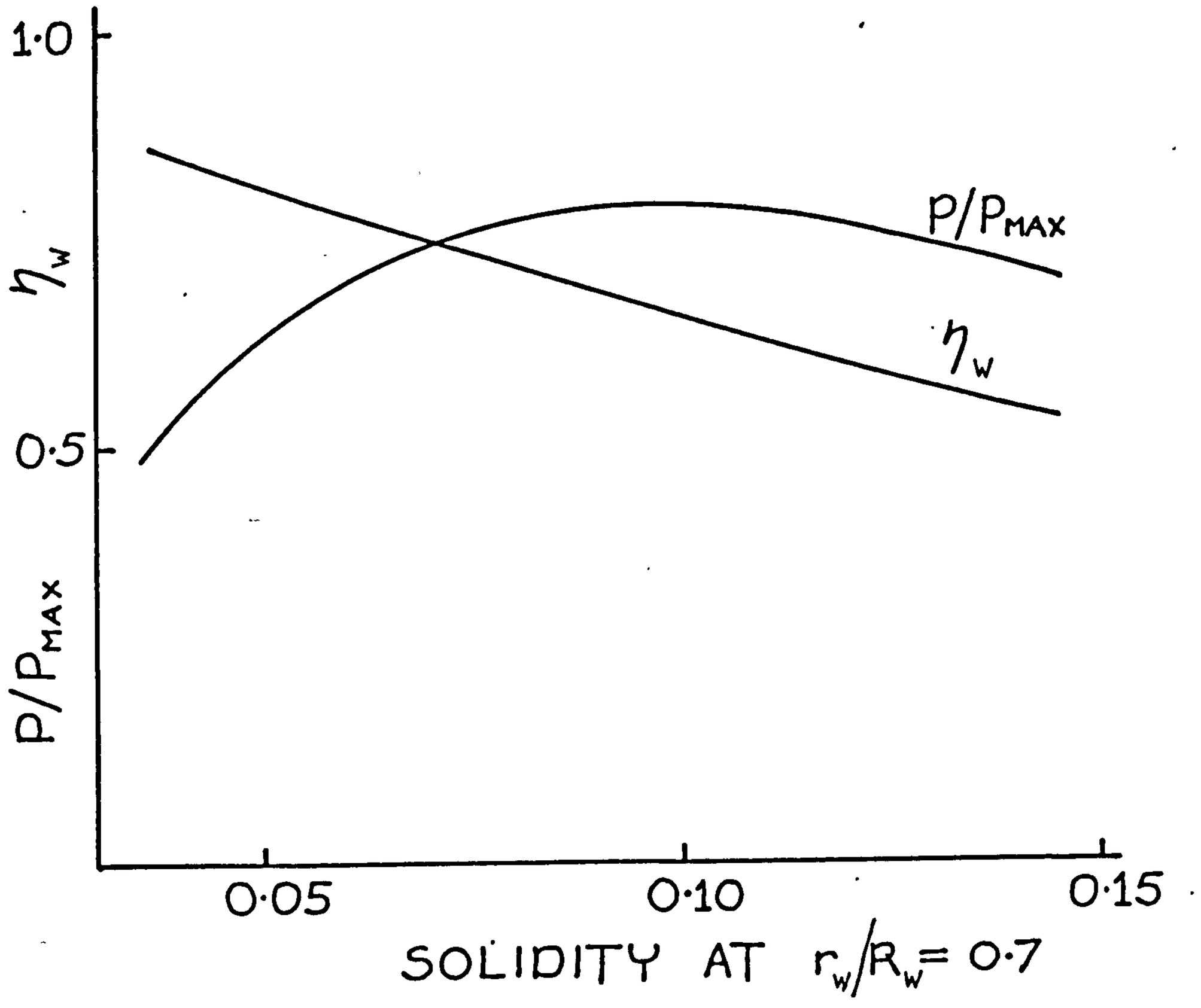

Fig. 5.6 Variation of the Power Ratio and Efficiency with Solidity at $X_w = 3.5$

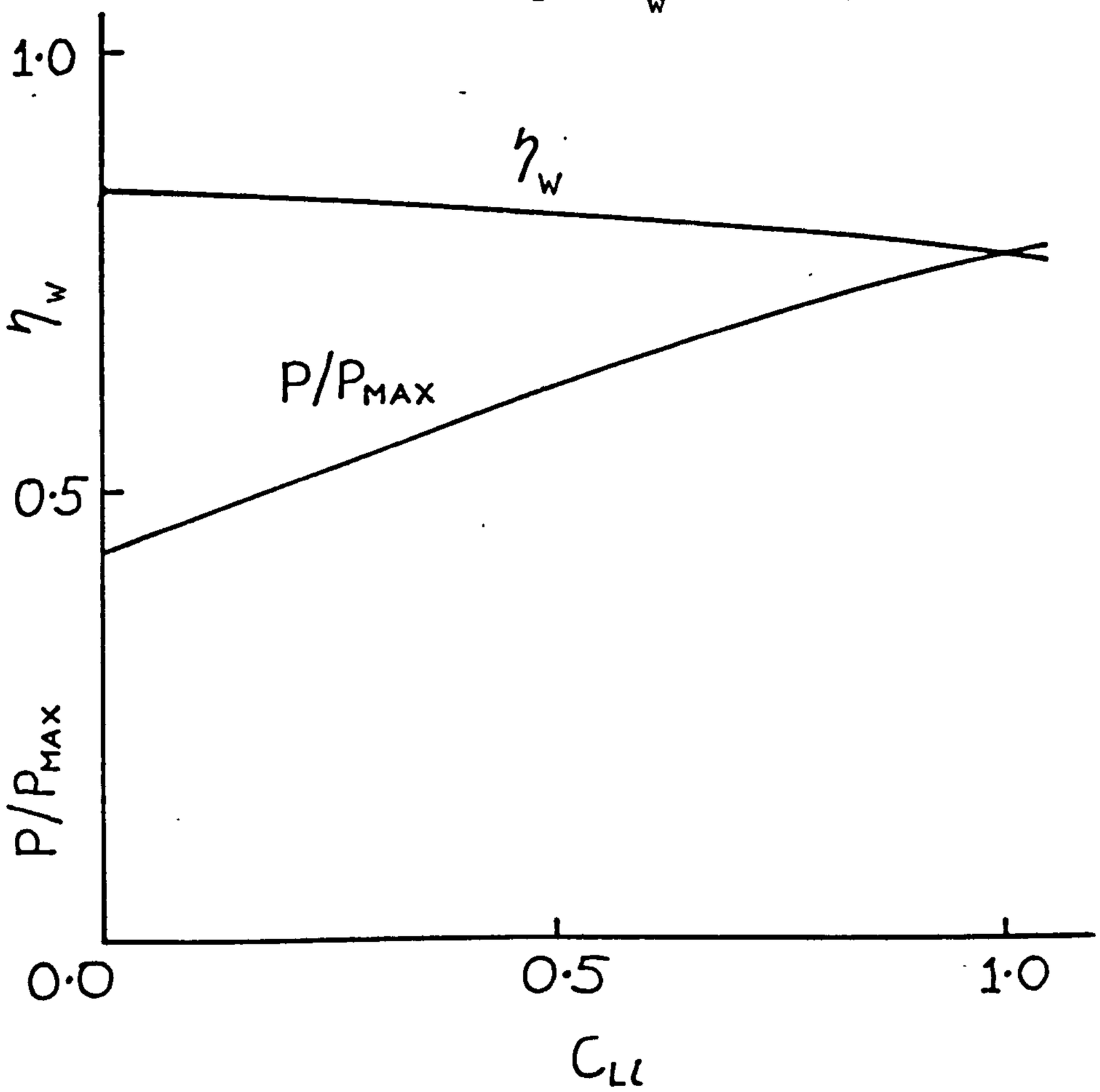

Fig. 5.7 Variation of the Power Ratio and Efficiency with Design Lift Coefficient at $X_w = 3.5$

a section of high camber was chosen (C_{L_i} = 1.0). This section while operating at a slightly lower efficiency than the other sections considered had a much higher power ratio over the range of operation considered.

In figures 5.3 and 5.8 efficiency and power ratio are plotted against the speed coefficient X_w for a range of pitch/diameter settings. It must be remembered that in each case, the pitch value is as if the windmill was designed for that pitch, and the values would be slightly different for a controllable pitch windmill. In the latter case, the windmill would be designed for optimum performance at a pitch of between 1.5 and 2.5m and at higher pitch settings the actual pitch would vary over the span of the blades. In the design considered here, it was considered necessary to allow the blades to 'weather cock' with the wind (infinite pitch) and operate down to a pitch setting of 1.5m for maximum power output. In higher wind speeds therefore and when lower power is required, say for manoeuvring, a higher pitch setting could be selected thus reducing power output and drag. The windmill would operate at a higher efficiency at these higher pitch settings.

The optimum pitch of the windmill was selected as 2.0m (P_n/D_W = 0.4) and the variation of blade angle along the blade was designed accordingly. The detailed curves were calculated for this condition and can be seen plotted in figures 5.3 and 5.8 also. The agreement between these and the curves found by the approximate method is mainly good

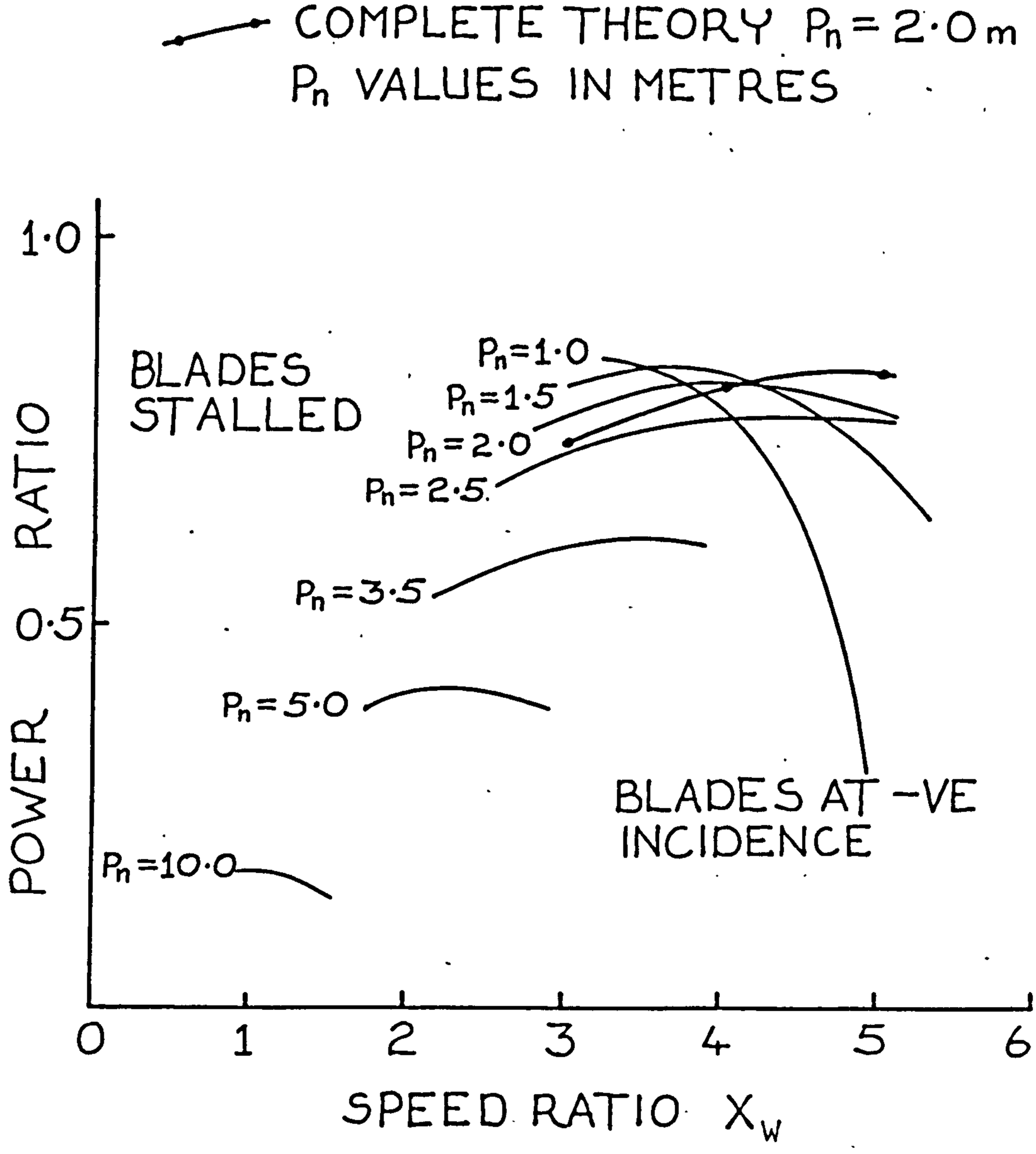

Fig. 5.8 The Variation of Power Ratio with Pitch

although there is a variation of about 7% between the efficiency curves at high values of blade incidence.

The Performance of the Windmill as a Propulsion Device

Windmill polar diagrams could now be calculated and plotted for a variety of boat speeds. The graphical results are presented here for two speeds only 4.0 m/sec (7.8 knots) and 10.0 m/sec (19.5 knots). These correspond to the speed at which the hydrofoil boat takes off and to a speed that is relatively high for a sailing boat, although well within the range expected with this craft. The results are shown in figures 5.9, 5.10, 5.11 and 5.12.

In figure 5.9 at a boat speed of 4.0 m/sec two curves are shown, both for a true wind speed of 9 m/sec (Beaufort 5), but for different operating points of the windmill. These operating points are shown for all the curves in Table 5.I.

Table 5.I

	Speed Wind Speed V_{WD} (m/sec)	Ratio X_w	Efficiency η_W	Power Ratio P/P_{MAX}	P_n Pitch (m)
WA - 9	9	4.0	0.69	0.81	2.0
WB - 6/9/15	6/9/15	4.0	0.74	0.81	2.5
WC - 12/15	12/15	2.5	0.89	0.42	5.0

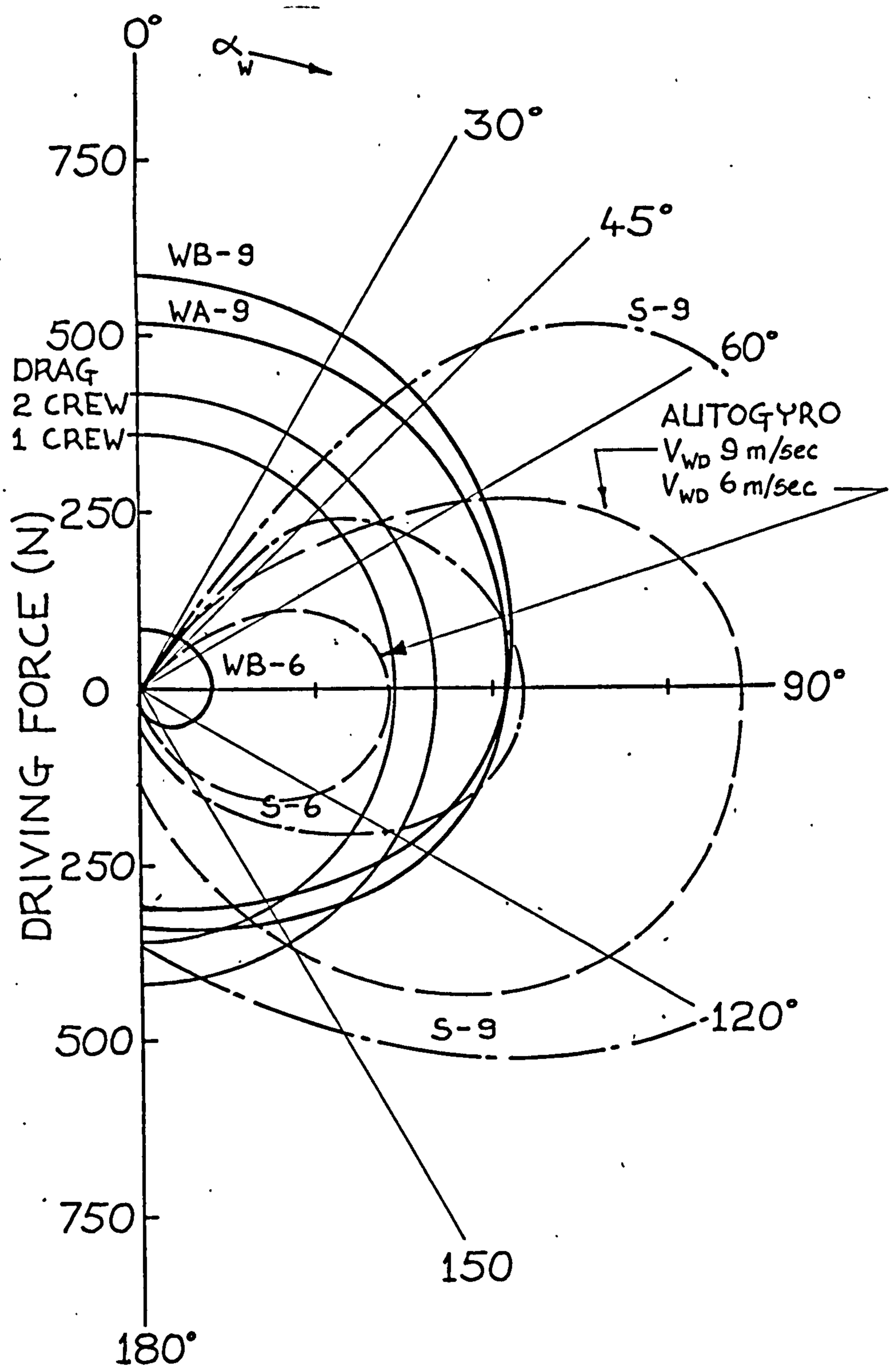

Fig. 5.9 Windmill and Sail Polars at a Boatspeed of 4 m/sec.

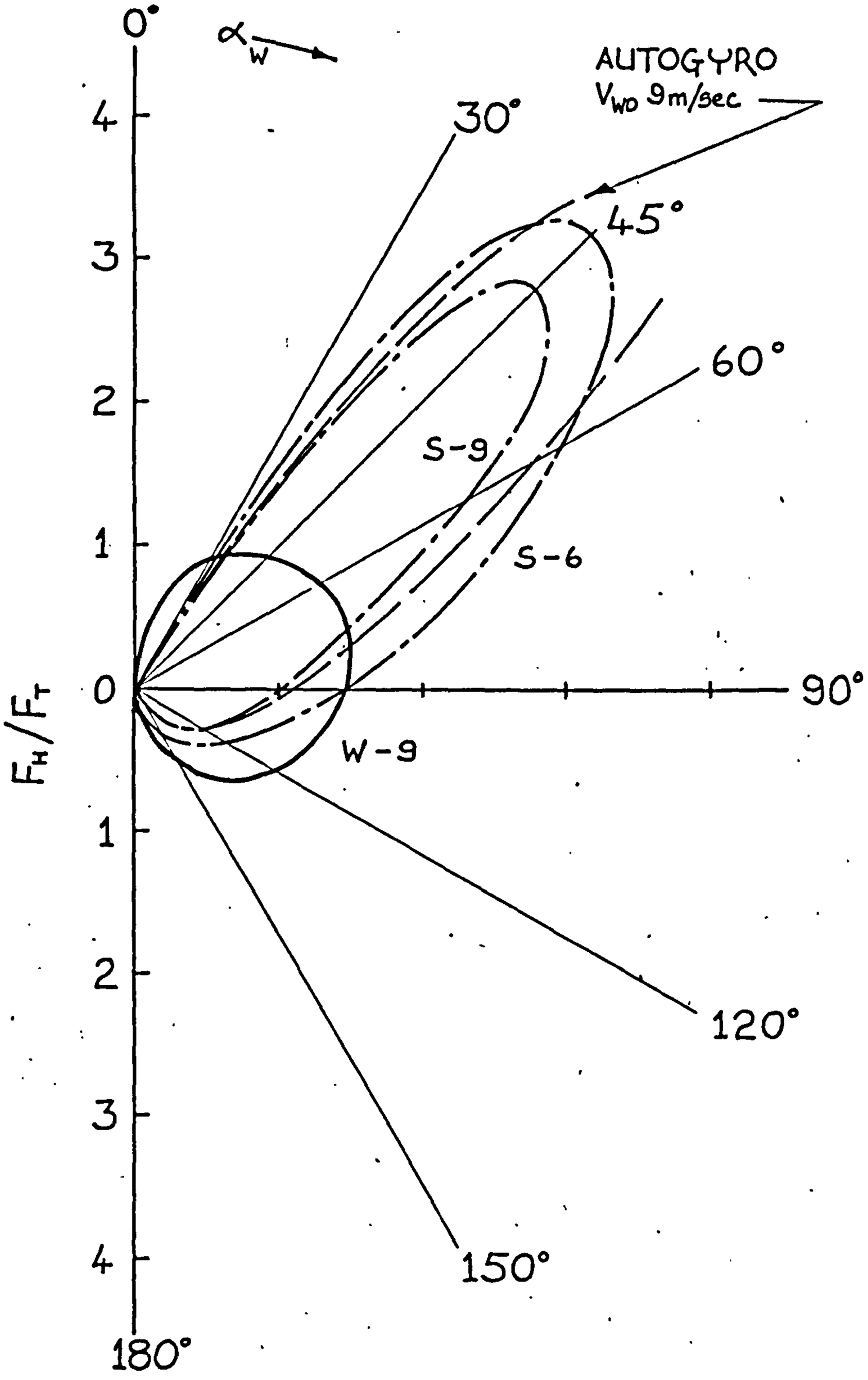

Fig.5.10 The Ratio F_H/F_T at a Boatspeed of 4 m/sec.

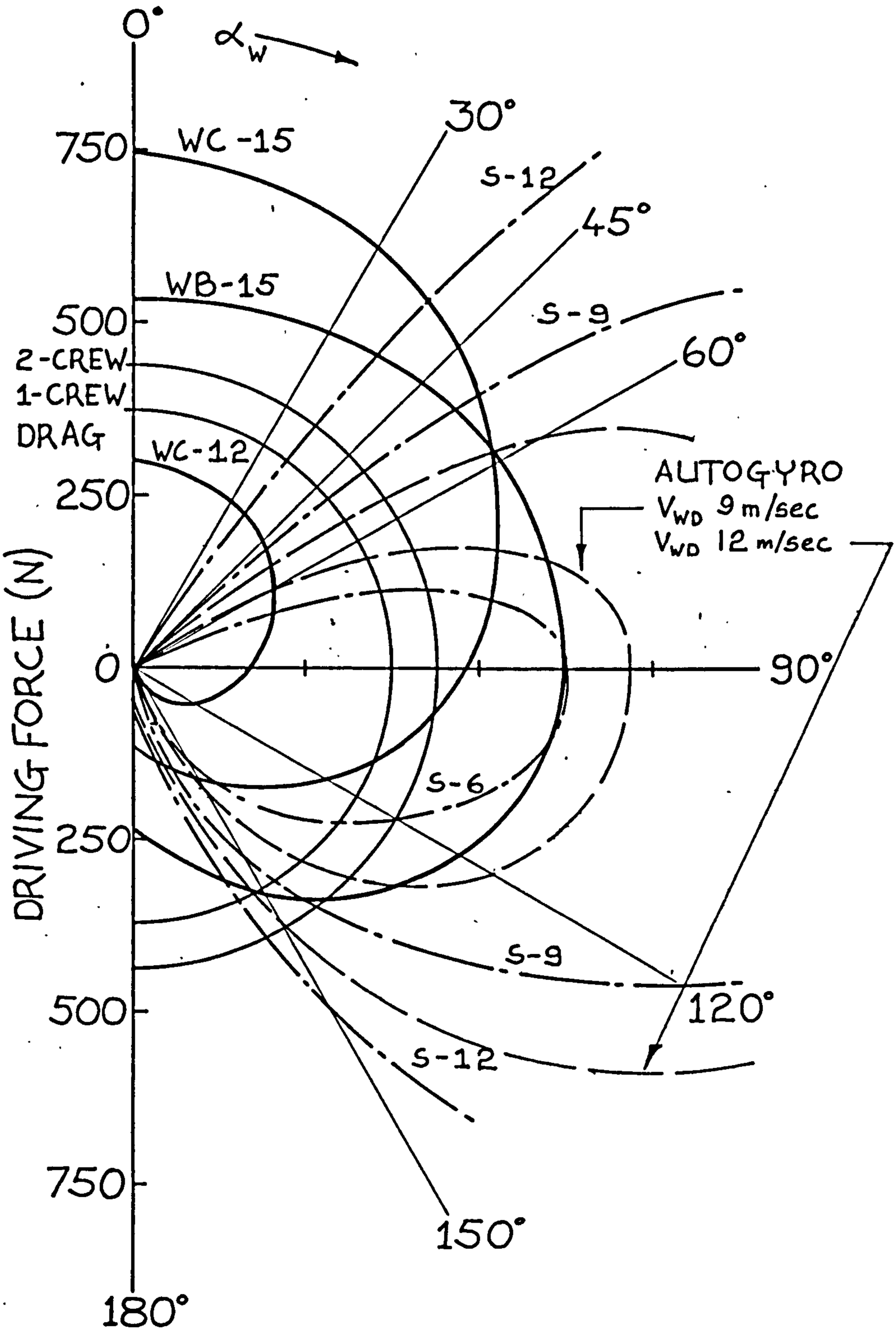

Fig. 5.11 Windmill and Sail Polars at a Boatspeed of 10 m/sec.

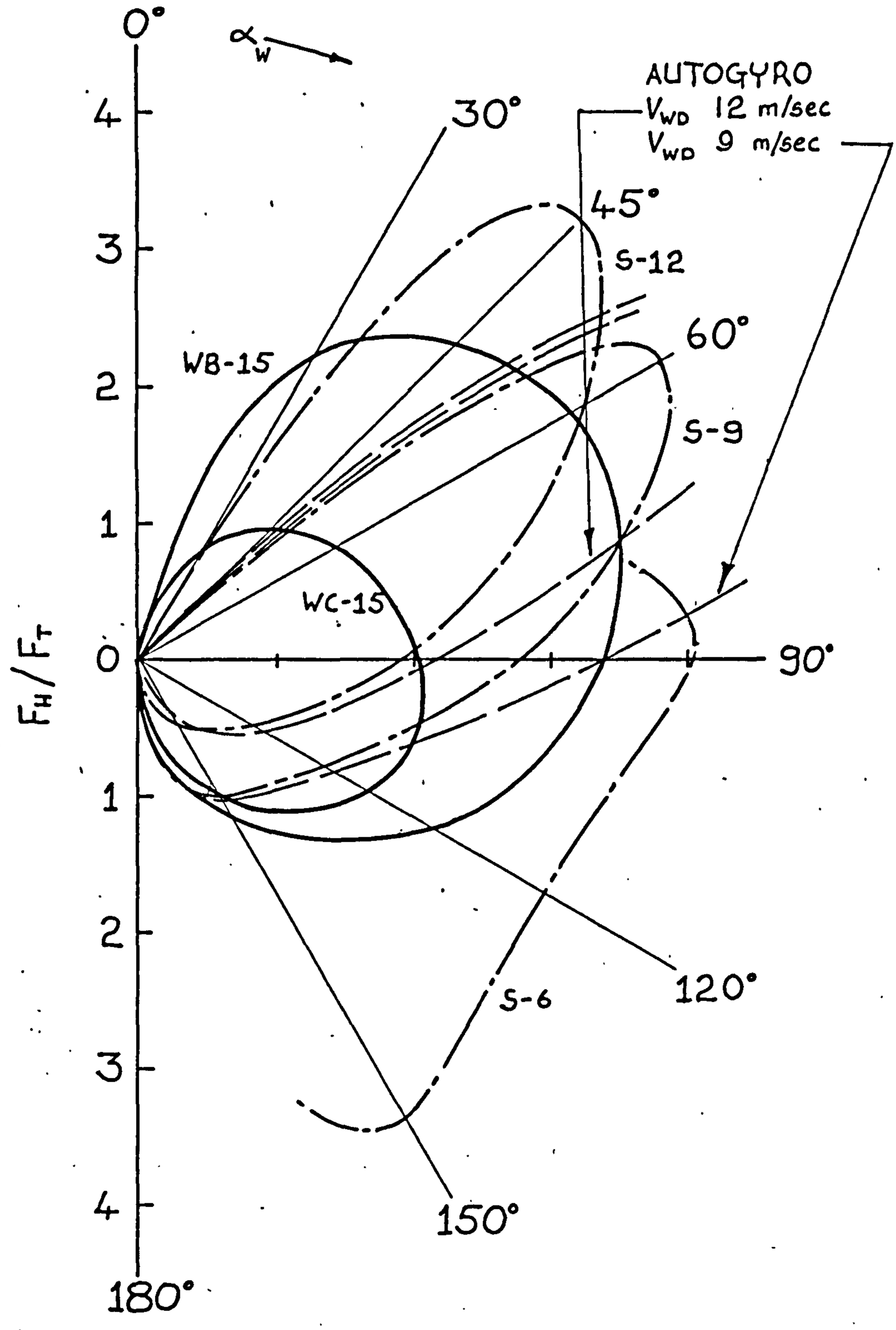

Fig. 5.12 The Ratio F_H/F_T at a Boatspeed of 10 m/sec.

Both these curves show an excess of driving force over resistance from zero to approximately 130 degrees heading angle and acceleration would be expected. However, it was found that this driving force was much reduced for lower windspeeds and forward speeds could not be expected at wind speeds much less than 9 m/sec , the curve for WB - 6 (i.e. V_{WD} = 6 m/sec) emphasises this. The driving force is fairly constant over the range of heading angles 0-90 degrees, a significant point which shows that the boat can sail directly to windward as easily as at 90 degrees to the true wind. Above 90 degrees, the force falls until after about 130 degrees, it is less than the resistance of the boat. (This latter angle is greater if the resistance of the boat sailed single handed is considered) . The boat cannot be sailed directly downwind at 4 m/sec in this windspeed unless some other form of propulsion is used or the windmill is operated in a different fashion.

Figure 5.11 shows the position at a boat speed of 10.0 m/sec . It is clear that a much higher wind speed is required for forward motion, the curves are drawn at a windspeed of 12 and 15 m/sec (Beaufort 6 and 7). Also noticeable is the large difference in performance when the pitch is altered from 2.5 to 5.0m. The greater pitch leads to a greater efficiency and an improvement in the windward performance. Better performance is attained down wind by reducing the pitch. The combined effect is a range of performance from zero to almost 140 degrees heading angle. Again the driving force decreases on courses downwind.

Figures 5.10 and 5.12 show the variation of the ratio of the heeling force to the driving force (F_H / F_T) over the range of heading angles. This ratio is high in figure 5.12 for the windmill of lower pitch, but over the range where it is highest, the pitch would be increased and ratio reduced to that of the lower curve.

The Performance of Sails as a Propulsion Device

Estimates of the performance of the soft sail rig which is described in detail in chapter 2 and has a total sail area of 19.05 sq.metres were made using the theory which has been described earlier in this chapter. The results of these calculations are plotted alongside the windmill data in figures 5.9, 5.10,5.11 and 5.12. The curves are denoted S-6/9/12 the number denoting the wind speed in m/sec.

No sail can propel a craft directly to windward and even at the lowest possible heading angles of 40 - 70 degrees the ratio F_H / F_T (heeling force/ driving force) is high, of the order 4-5. Neither of these problems are encountered by the windmill. The sails on the other hand have the ability to provide sufficient driving force for acceleration to occur even at low values of wind speed, albeit for a low range of heading angles, note the curves at a windspeed of 6m/sec . At the higher boat speed of 10 m/sec the windmill is unable to provide sufficient driving force until a wind speed above 12 m/sec is reached

(Beaufort 6-7). In other words the windmill powered boat would not reach this speed until the wind had reached Beaufort 6-7, but the sail powered boat could possibly have flown at this speed in Beaufort 4 at a heading angle of 90 degrees if sufficient heel restoring moment could be provided to counteract the large heeling force (F_H/F_T= 4.0). Values of F_H/F_T of this order are counteracted by the foil system and can be seen in the results from the model tests, chapter 3.

At higher wind speeds the sail force predictions are optimistic. At Beaufort 6 reefing of the sails would be necessary and this would increase the ratio of drag to lift force from the sails. This in turn would decrease driving force and increase the ratio F_H/F_T. The range of useful heading angles over which sufficient driving force is obtained would be reduced.

Reducing the effectiveness or reefing the windmill on the other hand would be achieved by increasing the pitch and this would increase the efficiency, η_W , and hence reduce the drag of the rotor. In direct contrast to the sail rig, it can be seen that the performance of a wind turbine propulsion system should improve with increasing wind speed .

The Windmill as an Autogyro

The foregoing discussion has shown how for most

courses relative to the true wind, the soft sail rig (or a fixed aerofoil rig) is the best choice of propulsion for a high speed boat to operate in low wind speeds. This is especially true of a boat which is explicitly designed to sail very fast in one direction relative to the wind, such as a design for a boat in which it is intended to make attempts at the sailing speed records. For a more versatile boat or for a wind propelled commercial ship, the windmill rig is an attractive system mainly because of its ability to sail at any course relative to the wind direction. This potential would be increased if the performance of the system could be improved especially in beam wind and downwind conditions.

Improvements mainly in the windward performance of the wind turbine propulsion system can be made by increasing the transmission and propeller efficiency, e, increasing the efficiency of the rotor either by decreasing the solidity or by increasing the pitch, or by increasing the diameter of the rotor. These adjustments increase the maximum boat speed that can be achieved in a given windspeed. In particular the driving force, F_T , is very sensitive to changes in e, the transmission and propeller efficiency, but even small changes in e may be difficult if not impossible to achieve. Neither decreasing the solidity or increasing the pitch of the rotor have quite the same beneficial effect as increases in e and they are both made at the price of reducing the power ratio. Increasing the diameter of the windmill does not increase the boat speed

at which F_T falls to zero, but for a boat speed lower than this, a higher driving force is realised for the same wind speed. Increased diameter also leads to higher heeling forces. Improvements in performance may also be made by the installation of concentrator systems such as tip vanes which have a similar effect on the performance of a wind turbine as a duct on a water propeller (184).

Much larger improvements in the performance of the windmill system in beam wind conditions can be achieved by the operation of the windmill in the autogyro or lifting windmill mode (54,60). To do this, the windmill rotor is disconnected from the water propeller and the pitch is reduced, in the case of the design considered here to a value of around 0.5m, and the windmill is inclined at an angle of incidence to the flow rather than at an angle of 90 degrees to the flow as it is when it operates in the windmill mode. The windmill is then similar in its mode of operation to an aerofoil rig and there is a lift and drag force associated with the operation, although in most cases the force coefficients and lift/drag ratios obtained would be inferior to those obtained with a pure aerofoil rig.

A detailed analysis of this mode of operation was not carried out, but a brief study based on the lift and drag coefficients presented by Glauert (60) for a similar rotor was undertaken and the results are also plotted in figures 5.9, 5.10, 5.11 and 5.12. It is apparent from a study of these curves that the performance of the wind turbine

system has been considerably improved in beamwind and reaching conditions. In particular the operation of the wind turbine in this mode allows the craft to operate at high speeds in beam winds although not to quite the same extent as the sail rig (figure 5.11). On the other hand the maximum values of the heeling force/driving force (F_H / F_T) are much higher than for the sail rig (figure 5.10 and 5.12), but because these high values occur over a very small range of heading angles, this would not be a significant problem in practice except to the extent that close hauled operation in the autogyro mode would be restricted.

These calculations were carried out in a similar manner to the sail performance calculations. The difficulty was to obtain the best operating point for the windmill in this mode. A number of trial calculations showed this to be at an angle of incidence of the rotor to the incoming flow of 25 degrees. The total aerodynamic force coefficient, C_{TA}, and the aerodynamic drag angle ε_A were 1.05 and 25 degrees at this angle of incidence.

It has been suggested (86 and 176 paper 8) that it may be possible to achieve similar improvements in the downwind performance of a wind turbine propulsion system by operating the windmill in the airscrew mode where the windmill is driven by the water propeller. Although this may at first appear to be a form of perpetual motion machine, Hammitt (86) explains that while the boat is

travelling downwind faster than the windspeed, and the air is accelerated backwards by the airscrew, the speed of the wind relative to the water surface is actually reduced and hence power is still extracted from the wind. This mode of operation was not studied in any depth.

CHAPTER 6

Seakeeping Studies - Linear Solutions in the Frequency Domain

The basic requirement of these studies on hydrofoil craft subject to wave motions was to ascertain the performance of the various designs of the craft considered in this study. Although there has been a considerable quantity of work on hydrofoils in waves, (9, 15, 16, 40, 53, 58, 89, 91, 104, 105, 108, 111, 134, 148, 164, 165, 166, 167 and 190), much of the more recent and more detailed work remains unpublished because of its military or commercial importance. For example there is very little available information from the Boeing Company even though they are producers of some of the most advanced hydrofoil craft at the present day. The most useful references to these studies from work directly on hydrofoils was the linear work of Ogilvie (148), the non-linear time domain solutions of Keuning (108) and the various methods used on the Canadian hydrofoil research programme (53, 164, 165 and 166). Input from work on seakeeping outside the realm of specific hydrofoil studies came from references (2, 20, 51, 129 and 136).

In this work two different approaches were made to the problem, the first a linear solution involving linearised

equations of motion with constant coefficients and the second a time domain solution involving time varying coefficients and forcing functions which were not necessarily sinusoidal. It is understandable that it was from the second method that the most realistic solutions were obtained, but even these were not entirely satisfactory over the whole frequency range especially in following seas. In particular, effects due to oscillatory forces on foils near the free surface are still not entirely understood and they can become very important especially at the higher frequencies of encounter. These and other problems such as wave impacts on the hulls will be discussed in greater length in chapters 7 and 8.

The Linearised Equations of Motion

From three dimensional rigid body dynamics the force and moment equations for seakeeping allowing only three degrees of freedom, surge, heave and pitch for head and following seas, were (2):

Surge force $$X_F = m(\dot{u} + qw - q^2 X_G + \dot{q} Z_G) \quad 6.1$$

Heave force $$Z_F = m(\dot{w} - qu - Z_G q^2 - X_G \dot{q}) \quad 6.2$$

Pitching moment $$M = I_y \dot{q} + m[Z_G(\dot{u} + qw) - X_G(\dot{w} - qu)] \quad 6.3$$

where u and w were the surge and heave velocities,

q was the pitch angular velocity,

X_G and Z_G were the coordinates of the centre of

gravity,

I_y was the moment of inertia of the craft about the y-axis,

and m was the mass of the craft.

The dot denotes differentiation w.r.t. time and the axis system (x,y,z) was as described in Chapter 3.

Since the linearised equations of motion were set up, only the linear terms of the above equations were of interest. The variables present were :

$$x,\ z,\ \theta,\ u,\ w,\ q,\ \dot{u},\ \dot{w},\ \dot{q}$$

(x,z and θ were displacements in surge, heave and pitch respectively) and they could be represented by :

$$u = U_o + \Delta u$$

$$w = w_o + \Delta w \quad \text{etc.}$$

where the o subscript denotes the value at the equilibrium condition, but also where these variables except u have equilibrium values of zero, (i.e. the equilibrium value of u is not zero because there is a constant forward speed).

Substituting these into equations 6.1, 6.2 and 6.3 gives, for example for the Heave equation :

$$Z_F = m[(\dot{w}_o + \Delta w) - (q_o + \Delta q)(U_o + \Delta u) - Z_G(q_o + \Delta q)^2 - X_G(\dot{q}_o + \Delta\dot{q})]$$

but $w_o = q_o = \dot{u}_o = \dot{w}_o = \dot{q}_o = 0$

as above, which neglecting second order terms (e.g. $\Delta q\ \Delta u$) gives:

$$Z_F = m[\dot{w} - U_o\, q - X_G\, \dot{q}] \qquad 6.4$$

and similarly

$$X_F = m[\dot{u} + Z_G\, \dot{q}] \qquad 6.5$$

$$M = I_y\, \dot{q} + m[Z_G\, \dot{u} - X_G\, \dot{w} + X_G\, U_o\, q] \qquad 6.6$$

in which Δu, Δw, Δq, $\Delta \dot{u}$, $\Delta \dot{w}$ and $\Delta \dot{q}$ have been written as $\Delta u, w, q, \dot{u}, \dot{w}, \dot{q}$ respectively.

The left-hand side of the above equations 6.4, 6.5 and 6.6 could also be written down assuming only the linear terms from the Taylor expansion. These were equated to the right hand-side of the equations 6.4, 6.5 and 6.6 written in terms of the three independent variables $\Delta u, z$ and θ where z was taken to represent heave perpendicular to the water surface and was a function of both w and U_o.

That is :

$$w = \dot{z} + U_o\, \theta$$

$$\dot{w} = \ddot{z} + U_o\, \dot{\theta} = \ddot{z} + U_o\, q$$

(assuming small angles of pitch, θ).

The three equations of motion were :

Surge

$$[(X_{\dot{u}} - m)\ D + X_u]\ \Delta u + [X_{\dot{w}}\ D^2 + X_w\ D + X_z]\ z$$

$$+ [(X_{\dot{q}} - m\ Z_G)\ D^2 + (X_q + X_{\dot{w}}\ U_o)\ D + (X_\theta + X_w\ U_o)]\ \theta = 0 \qquad 6.7$$

Heave

$$[Z_{\dot{u}}\ D + Z_u]\ \Delta u + [(Z_{\dot{w}} - m)\ D^2 + Z_w\ D + Z_z]\ z$$

$$+ [(Z_{\dot{q}} + m\ X_G)\ D^2 + (Z_q + U_o\ Z_{\dot{w}})\ D + (Z_\theta + U_o\ Z_w)]\ \theta = 0 \qquad 6.8$$

Pitch

$$[(M_{\dot{u}} - m\ Z_G)\ D + M_u]\ \Delta u + [(M_{\dot{w}} + m\ X_G)\ D^2 + M_w\ D + M_z]\ Z$$

$$+ [(M_{\dot{q}} - I_y)\ D^2 + (M_q + U_o\ M_{\dot{w}})\ D + (M_\theta + M_w\ U_o)]\ \theta = 0 \qquad 6.9$$

where the D's are the D operator and denote differentiation w.r.t. time (i.e. :— d/dt) and the notation Z_θ, for example, means the derivative of the Z force w.r.t. the θ displacement.

Equations 6.7, 6.8 and 6.9 are the homogenous equations of motion and must be equated to their respective exciting forces which were assumed to be sinusoidal and to act at the forcing frequency, the frequency of encounter of the waves, but with a phase lag to the oncoming wave train. To reduce the mathematical complexity at this stage, the effect of surge motions on the response was assumed to be small and the origin was assumed to be at the centre of gravity. The two equations of motion in heave and in pitch which were solved in the frequency domain, including the exciting forces were finally :

$$\text{Pitch } M_p(t) = \frac{\begin{vmatrix} a_{11} & Z_1 e^{-i\varepsilon_Z} e^{i\omega_e t} \\ a_{21} & M_1 e^{-i\varepsilon_M} e^{i\omega_e t} \end{vmatrix}}{\begin{vmatrix} a_{11} & a_{12} \\ a_{21} & a_{22} \end{vmatrix}} \qquad 6.13$$

where the values a_{11} ,a_{12} ,a_{21} and a_{22} are the coefficients of z and θ in the equations of motion 6.10 and 6.11 and the denominator is the solution of the homogenous equations of motion, the stability equation, which is a quartic in D (the D operator) and this has a solution of the form:

$$C_4 (D-\sigma_4)(D-\sigma_3)(D-\sigma_2)(D-\sigma_1) = 0 \qquad 6.14$$

where C_4 is the coefficient of D^4,

σ_1 , σ_2 , σ_3 and σ_4 are the roots of the quartic in D.

The system is stable if all the roots are negative (real roots) or the real part of the roots are negative (complex roots).

Both the solutions Z_H and M_P take the form :

$$Z_H(t),\ M_P(t) = \frac{(A + i\ B)\ e^{i\omega_e t}}{C_4 (D-\sigma_4)(D-\sigma_3)(D-\sigma_2)(D-\sigma_1)}$$

which on integrating gives :

$$Z_H(t),\ M_P(t) = \frac{(A + i\,B)\ e^{i\omega_e t}}{C_4 (i\omega_e - \sigma_4)(i\omega_e - \sigma_3)(i\omega_e - \sigma_2)(i\omega_e - \sigma_1)} + \sum_{i=1}^{4} G_i\ e^{\sigma_i t}$$

where G_1 , G_2 , G_3 and G_4 are constants.

If σ_1, σ_2 , σ_3 and σ_4 are stable roots, the transient $\sum_{i=1}^{4} G_i\ e^{\sigma_i t}$ dies out in time and the oscillatory term is left. This takes the form :

$$Z_H(t),\ M_P(t) = (\alpha + i\beta)\ e^{i\omega_e t}$$

6.15

where

$$\alpha = \frac{1}{C_4 (\sigma_4^2 + \omega_e^2)(\sigma_3^2 + \omega_e^2)(\sigma_2^2 + \omega_e^2)(\sigma_1^2 + \omega_e^2)} [A\sigma_4\sigma_3\sigma_2\sigma_1 - A\sigma_4\sigma_3\ \omega_e^2$$

$$- A\omega_e^2\sigma_2\sigma_1 + A\omega_e^4 - A\omega_e^2\ (\sigma_4 + \sigma_3)(\sigma_2 + \sigma_1) - B\omega_e\sigma_4\sigma_3\ (\sigma_2 + \sigma_1)$$

$$+ B\omega_e^3\ (\sigma_2 + \sigma_1) - B\omega_e\sigma_2\sigma_1\ (\sigma_4 + \sigma_3) + B\omega_e^3\ (\sigma_4 + \sigma_3)]$$

$$\beta = \frac{1}{C_4 (\sigma_4^2 + \omega_e^2)(\sigma_3^2 + \omega_e^2)(\sigma_2^2 + \omega_e^2)(\sigma_1^2 + \omega_e^2)} [B\sigma_4\sigma_3\sigma_2\sigma_1 - B\sigma_4\sigma_3\ \omega_e^2$$

$$- B\omega_e^2\sigma_2\sigma_1 + B\omega_e^4 - B\omega_e^2\ (\sigma_4 + \sigma_3)(\sigma_2 + \sigma_1) + A\omega_e\sigma_4\sigma_3\ (\sigma_2 + \sigma_1)$$

$$- A\omega_e^3\ (\sigma_2 + \sigma_1) + A\omega_e\sigma_2\sigma_1\ (\sigma_4 + \sigma_3) - A\omega_e^3\ (\sigma_4 + \sigma_3)]$$

where the A's are A_H and A_P for the solution of Z_H and M_P respectively, the B's are B_H and B_P for the solution of Z_H and M_P respectively and the imaginary parts from the complex conjugate pairs of roots, σ_1 and σ_2 , σ_3 and

σ_4 cancel out in the above equations.

Equation (6.15) could be written in the form (where the real part gives the solution):

$$Z_H(t),\ M_P(t) = r_o\ e^{i(\omega_e t + \varepsilon)}$$

where $r_o = \sqrt{\alpha^2 + \beta^2}$ and $\varepsilon = \tan^{-1} \beta/\alpha$

(care had to be taken with ε to avoid errors of π).

The values of A_H , A_P , B_H and B_P were found from the determinants in the numerators of equations (6.12) and (6.13) :

$$A_H = Z_1\ [-\ (M_{\dot{q}} - I_y)\ \omega_e^2\ \cos\varepsilon_Z + (M_\theta + M_w\ U_o)\ \cos\varepsilon_Z$$

$$+\ (M_q + U_o\ M_{\dot{w}})\ \omega_e\ \sin\varepsilon_Z] - M_1\ [-\ Z_{\dot{q}}\ \omega_e^2\ \cos\varepsilon_M$$

$$+\ (Z_\theta + U_o\ Z_w)\ \cos\varepsilon_M + (Z_q + U_o\ Z_{\dot{w}})\ \omega_e\ \sin\varepsilon_M]$$

$$B_M = Z_1\ [(M_q + U_o\ M_{\dot{w}})\ \omega_e\ \cos\varepsilon_Z + (M_{\dot{q}} - I_y)\ \omega_e^2\ \sin\varepsilon_Z$$

$$-\ (M_\theta + M_w\ U_o)\ \sin\varepsilon_Z] - M_1\ [(Z_q + U_o\ Z_{\dot{w}})\ \omega_e\ \cos\varepsilon_M$$

$$+\ Z_{\dot{q}}\ \omega_e^2\ \sin\varepsilon_M - (Z_\theta + U_o\ Z_w)\ \sin\varepsilon_M]$$

$$A_P = M_1\ [-\ (Z_{\dot{w}} - m)\ \omega_e^2\ \cos\varepsilon_M + Z_{z_o}\ \cos\varepsilon_M$$

$$+\ Z_w\ \omega_e\ \sin\varepsilon_M] - Z_1\ [-\ M_{\dot{w}}\ \omega_e^2\ \cos\varepsilon_Z$$

$$+\ M_{z_o}\ \cos\varepsilon_Z + M_w\ \omega_e\ \sin\varepsilon_Z]$$

$$B_P = M_1\ [Z_w\ \omega_e\ \cos\varepsilon_M + (Z_{\dot{w}} - m)\ \omega_e^2\ \sin\varepsilon_M$$

$$-\ Z_{z_o}\ \sin\varepsilon_M] - Z_1\ [M_w\ \omega_e\ \cos\varepsilon_Z$$

$$+\ M_{\dot{w}}\ \omega_e^2\ \sin\varepsilon_Z - M_{z_o}\ \sin\varepsilon_Z]$$

Application of the Equations of Motion to a Real Hydrofoil Problem

Having set up the equations of motion and their solution, it remained necessary to apply these to the problem of a real hydrofoil system. To do this the coefficients or hydrodynamic derivatives in the equations of motion (6.10 and 6.11) had to be calculated together with the amplitudes and the phase lags of the forcing functions (M_1, Z_1, ε_M and ε_Z). From these values of the derivatives and the mass and moment of inertia (I_y), the roots of the stability equation could be found and the solutions as given above, finally computed for each value of frequency considered.

Hydrodynamic Derivatives

In the absence of experimental data, the hydrodynamic derivatives were calculated using methods similar to those used by Schmitke (164, 165 and 166). (Schmitke advocates the use of these derivatives only for the solution of the linear stability equation, his calculations for the motion response were based on a non-linear analogue computer solution). The derivatives of interest were, Z_w, Z_z, Z_q, Z_θ, M_w, M_z, M_q and M_θ and in this study the added mass or inertia coefficients (and cross coupled inertia coefficients) were also included $X_{\dot{u}}$, $X_{\dot{w}}$, $X_{\dot{q}}$, $Z_{\dot{u}}$, $Z_{\dot{w}}$, $Z_{\dot{q}}$, $M_{\dot{u}}$, $M_{\dot{w}}$ and $M_{\dot{q}}$ (the surge values were required for the pitching moment calculations which included the drag

force). These latter derivatives, particularly the surge and cross coupled terms were found to have only a very small effect on the forces, but they were included for completeness. Because of this the simple approaches outlined below for the calculation of these terms were felt to be justified and variations with frequency were also neglected. Writing the acceleration forces due to the added virtual mass terms as X_a , Z_a and M_a :

$$\begin{bmatrix} X_a \\ Z_a \\ M_a \end{bmatrix} = - \begin{bmatrix} X_{\dot{u}} & X_{\dot{w}} & X_{\dot{q}} \\ Z_{\dot{u}} & Z_{\dot{w}} & Z_{\dot{q}} \\ M_{\dot{u}} & M_{\dot{w}} & M_{\dot{q}} \end{bmatrix} \begin{bmatrix} \dot{u} \\ \dot{w} \\ \dot{q} \end{bmatrix} = - \begin{bmatrix} \frac{\rho\pi}{4}(T^2 + c^2\alpha_i^2) & 0 & Z_i \frac{\rho\pi}{4}(T^2 + c^2\alpha_i^2) \\ 0 & \frac{\rho\pi}{4} c^2 & - x_i \frac{\rho\pi}{4} c^2 \\ Z_i \frac{\rho\pi}{4}(T^2 + c^2\alpha_i^2) & - x_i \frac{\rho\pi c^2}{4} & \frac{\rho\pi}{128} (c^2 - T^2)^2 \end{bmatrix} \begin{bmatrix} \dot{u} \\ \dot{w} \\ \dot{q} \end{bmatrix}$$

where x_i and z_i are the coordinates of the foil element from the centre of gravity of the craft and all values are taken per unit length of the foil element.

Referring to figure 6.1, $Z_{\dot{w}}$ was taken as the added virtual mass of a flat plate oscillating normal to its surface:

$$Z_{\dot{w}} = \frac{\rho\pi c^2}{4} \quad \text{(per unit length)}$$

which is the same for a cylinder of radius c/2 and an ellipse also.

$Z_{\dot{u}}$ was taken as the added virtual mass of an ellipse oscillating at an angle α_i to the major axis:

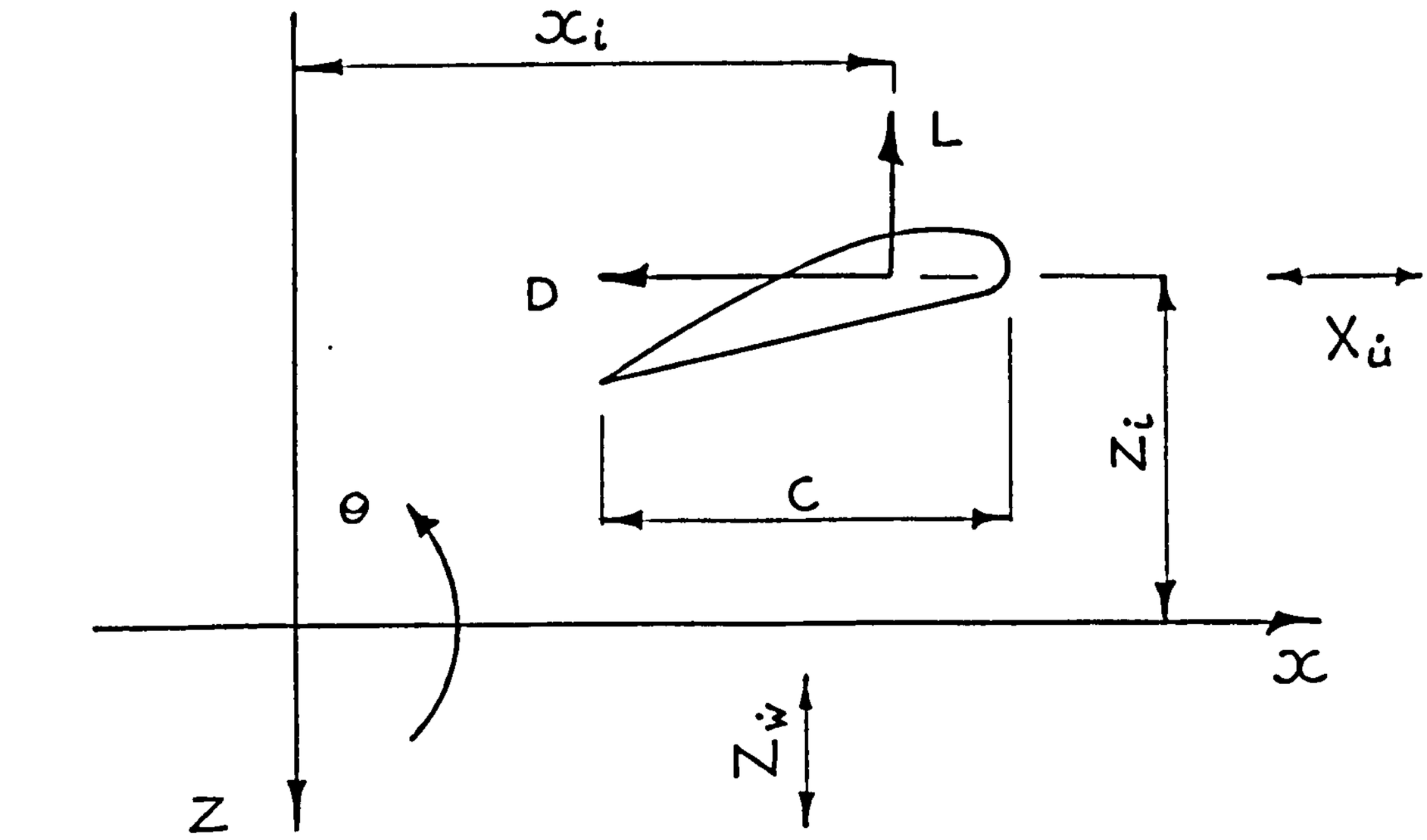

Fig. 6.1 Sign Convention of the Hydrofoil Element

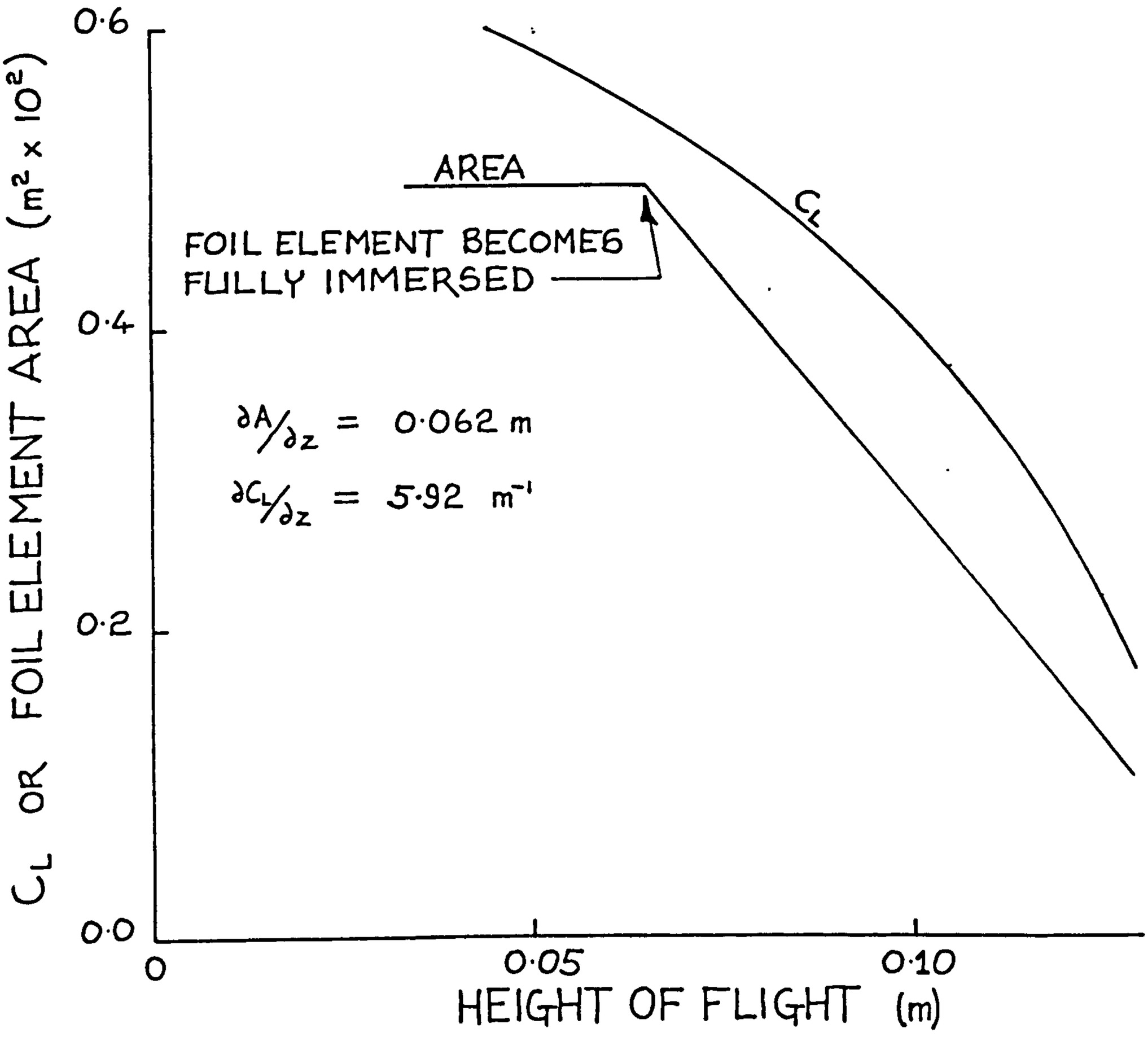

Fig. 6.2 Example of the Variation of Area and Lift Coefficient with Depth of Immersion for a Foil Element

$$AVM_{ellipse} = \rho\pi \left[(T/2)^2 \cos^2\alpha_i + (c/2)^2 \sin^2\alpha_i \right]$$

which for small angles of incidence gives:

$$X_{\dot{u}} = \frac{\rho\pi}{4} (T^2 + c^2\alpha_i^2)$$

where α_i the angle of incidence is in radians.

$X_{\dot{q}}$, $Z_{\dot{q}}$, $M_{\dot{u}}$ and $M_{\dot{w}}$ are derivations of the above two, $X_{\dot{w}}$ and $Z_{\dot{u}}$ were assumed to be zero and $M_{\dot{q}}$ was taken from the rotational coefficient for an ellipse:

$$M_{\dot{q}} = \frac{1}{128} \rho\pi (c^2 - T^2)^2$$

To go back to the eight velocity and displacement derivatives described above, these were calculated for a foil element from the expressions below, which are similar to those of ref. 164:

$$Z_z = - \frac{1}{2} \rho V^2 \left(C_L \frac{\partial S}{\partial z} + S \frac{\partial C_L}{\partial z} \right)$$

$$Z_w = - \frac{1}{2} \rho A_A V \left(\frac{\partial C_L}{\partial \alpha_i} \cos^2\Gamma + C_D \right)$$

$$Z_\theta = \frac{1}{2} \rho V^2 x_i \left(C_L \frac{\partial S}{\partial z} + S \frac{\partial C_L}{\partial z} \right)$$

$$Z_q = \frac{1}{2} \rho V A_A \left[2 C_L Z_i \cos\Gamma. + x_i \left(\frac{\partial C_L}{\partial \alpha_i} \cos^2\Gamma + C_D \right) \right]$$

$$M_z = - Z_z x_i + \frac{1}{2} \rho V^2 \left(A_A c \frac{\partial C_M}{\partial z} + C_M \frac{\partial (c A_A)}{\partial z} \right) \cos\Gamma$$

$$M_w = - Z_w x_i + \frac{1}{2} \rho A_A Vc \cos^2\Gamma \frac{\partial C_M}{\partial \alpha_i}$$

$$M_\theta = - Z_\theta x_i + \frac{1}{2} \rho V^2 x_i \left(A_A c \frac{\partial C_M}{\partial z} + C_M \frac{\partial (c A_A)}{\partial z} \right) \cos\Gamma$$

$$M_q = - Z_{\dot{\theta}} x_i + \frac{1}{2} \rho A_A V^2 c \cos\Gamma \frac{\partial C_M}{\partial \dot{\theta}}$$

Some of these differ from the results of Schmitke, the most notable differences occurring in M_w and M_q, although there were some sign changes in other derivatives mainly because of differing sign conventions. In M_w and M_q the variations were due to the $\frac{\partial C_M}{\partial \alpha_i}$ and $\frac{\partial C_M}{\partial \dot{\theta}}$ terms, which to be rigorous should be included (97), but which in fact reduced to Schmitke's values in practice because $\frac{\partial C_M}{\partial \alpha_i} = 0.0$ over the expected range of lift coefficients and the value of $\frac{\partial C_M}{\partial \dot{\theta}}$ is small. As an example of how these expressions were obtained the derivation of M_Z is given below. (fig. 6.1):

$$M = \frac{1}{2}\rho A_A V^2 C_L x_i \cos\Gamma - \frac{1}{2}\rho A_A V^2 C_D Z_i + C_M \frac{1}{2}\rho A_A V^2 c \cos\Gamma$$

$$= - Z x_i + X Z_i + C_M \frac{1}{2}\rho A_A V^2 c \cos\Gamma$$

Differentiating w.r.t. z

$$M_Z = \frac{\partial M}{\partial z} = - Z_z x_i + X_z Z_i + \frac{1}{2}\rho V^2 \cos\Gamma \left[A_A c \frac{\partial C_M}{\partial z} + \frac{C_M \partial (c A_A)}{\partial z} \right]$$

where for the heave and pitch coupled equations only, $X_Z = 0.0$, A_A was the actual area of the foil element and C_M was the pitching moment coefficient.

These hydrodynamic derivatives were calculated for the whole craft using the computer program DESIGN6 and its associated subroutines FOIL3 and DES6 for which a block diagram can be seen in fig. 6.4. This program calculates all the values of all the derivatives on all the foil elements and sums them, presenting the results in total as well as the sub-totals itemised between bow, side and stern foils. Input data was in the form of the data file shown in fig 3.4 of Chapter 3 with the addition of the last line for the pitching moment coefficient about the 1/4 chord point ($C_{Mc/4}$). Various other data was also required, including the speed, orientation and z-coordinate of the centre of gravity from the origin of the coordinate system used in the formation of the data file.

This program was developed from the program DESIGN2 (chapter 3), and was essentially a similar calculation although there were no iterations, where the main program

summed the derivatives as well as the lift and drag values. The subroutine DES6 was invoked to obtain values of the area, the lift coefficient and the pitching moment coefficient at an increment of draught either side of the steady state value, and these were used to obtain $\frac{\partial S}{\partial z}$, $\frac{\partial(c\ A_A)}{\partial z}$, $\frac{\partial C_L}{\partial z}$ and $\frac{\partial C_M}{\partial z}$. The values obtained in this way were a linear fit to the curve at the steady state value. The variations of the area with depth was of course linear for the types of foil element considered here, although there were discontinuities at the point where a foil became completely immersed. The slopes $\frac{\partial C_L}{\partial z}$ and $\frac{\partial C_M}{\partial z}$ varied in a more complicated fashion and continued to vary even after the foil became completely immersed. This was because the surface influenced the lift behaviour even at a depth of immersion. An example of the variation of the lift coefficient and the area with the height of flight for one foil element is given in Figure 6.2.

Table I shows the computed derivatives for the one quarter scale model craft itemised between the main bow foils (there were two main foils which were designated bow foils, one on each of the outer hulls) and the stern foil. This itemisation is useful in deciding in global terms what contribution each foil makes to a certain aspect of the dynamical behaviour. For example Z_z is a measure of the vertical stiffness of the foil units and it can be seen that the dihedral bow foils are much 'stiffer' than the stern foil unit. Z_w on the other hand is a measure of the vertical damping and it can be seen that all of the foil

TABLE 6.I Stability Derivatives - Model Craft

	kg	Ns/m	N/m	kgm	Ns	N
	$Z_{\dot{w}}$	Z_w	Z_z	$Z_{\dot{q}}$	Z_q	Z_θ
Bow Foils	-0.3046	-51.61	-532.6	0.0441	13.82	76.53
Stern Foil	-0.1283	-30.98	- 0.2104	-0.0809	-19.45	- 0.1327
Total	-0.4329	-82.59	-532.9	-0.03686	- 5.635	76.40

	kgm	Ns	N	kgm^2	Nms	Nm
	$M_{\dot{w}}$	M_w	M_z	$M_{\dot{q}}$	M_q	M_θ
Bow foils	0.0441	7.481	79.36	-1.35×10^{-5}	- 2.003	-10.59
Stern Foil	-0.0809	-19.55	- 0.1327	-0.50×10^{-5}	-12.27	- 0.0838
Total	-0.0369	-12.07	79.22	-1.85×10^{-5}	-14.28	-10.67

units play a significant role in damping. Similar arguments hold for the pitch motion and the derivatives M_q and M_θ.

The Exciting Forces

The exciting forces were obtained from the program DESIGN7 (Subroutines FOIL4,WAVE1,WAVE2,COORD), the basis of which again came from DESIGN2 and the majority of the data was again supplied from the same data file as before. A block diagram of this program is shown in fig. 6.5. For each wave at a given frequency and amplitude, which could be either a head or a following sea, the period was calculated and divided into twelve time steps. The total lift, drag and pitching moment were calculated and output for each of these time steps.

One of the calm water programs such as DESIGN2 was first run at the speed of interest to obtain the steady state height of flight and orientation of the craft at this speed. At this orientation, the input wave was considered to run past the craft in the twelve time steps referred to above and the forces on the foil system were calculated as if the craft did not react. Since the craft was moving in the wave system, the frequency of encounter of the waves differed from the actual frequency of the waves. The frequency of encounter was given as below

in head seas :

$$\omega_e = \omega \left(1 + \frac{\omega V}{g}\right)$$

in following seas :

$$\omega_e = \omega \left(1 - \frac{\omega V}{g}\right)$$

where ω was the frequency of the waves,
g was the gravitational acceleration and
V was the velocity of the hydrofoil craft.

This gave negative frequencies of encounter when the craft overtook the waves in a following sea.

The wave particulars were expressed with reference to the axis system moving with the craft, hence the height of the water surface as a function of the position, x, and the time t was given by :

$$\eta(x,t) = a_w \cos (kx \pm \omega_e t) \qquad 6.16$$

where a_w was the amplitude of the wave and k was the wave number. The wave was taken to be in phase with the origin of the axis system and the +ve and -ve signs denoted head and following seas respectively.

(The actual wave this corresponded to had a frequency of ω , the above equation was the wave as encountered by the hydrofoil craft).

This gave the wave particulars:

Horizontal water particle velocity

$$u_w = \mp k\, c_w\, a_w\, e^{kh_w} \cos(kx \pm \omega_e t)$$

Vertical water particle velocity

$$v_w = \mp k\, c_w\, a_w\, e^{kh_w} \sin(kx \pm \omega_e t)$$

Horizontal water particle acceleration

$$a_{h_w} = \ddagger k^2\, c_w^2\, a_w\, e^{kh_w} \sin(kx \pm \omega_e t)$$

Vertical water particle acceleration

$$a_{vw} = \mp k^2\, c_w^2\, a_w\, e^{kh_w} \cos(kx \pm \omega_e t)$$

Pressure force (ex. hydrostatic pressure) =

$$a_w\, \rho g\, e^{kh_w} \cos(kx \pm \omega_e t)$$

where c_w was the wave celerity,

h_w was the depth in the wave from the undisturbed water surface and the upper and lower signs denoted head and following seas respectively.

Wave pressure forces on the hydrofoils were neglected because the variation in wave pressure between the upper and lower surfaces of a foil element is minimal and the pressure forces were assumed to cancel each other out. Buoyancy forces of the hydrofoils in this and in all other analyses in this work were assumed to be a negligible proportion of the total lift and were therefore neglected also. The waves were assumed to affect the forces on the hydrofoil system by :

1) A variation in immersed foil area

2) A variation in the velocity over the foil surface

3) A variation in the angle of attack of the foil elements due mainly to the vertical water particle velocity.

4) The effect of the acceleration forces on the added virtual masses associated with the foils.

These forces were calculated in DESIGN7 using the subroutine FOIL4 which called the subroutine WAVE1 for the variations due to the wave particle velocities and the subroutine WAVE2 for the variations due to the wave particle accelerations. FOIL4 differed from FOIL1,2,3 in that a numerical integration over depth was used (Chapter 3). This was to enable the effects of water particle motions to be applied at each depth (step) of the numerical integration so that an integration of these effects was also achieved.

The force variations in 1 - 4 above were calculated as described below. It was assumed that the foil chord length was small with respect to the wave length, or in other words that the wave particulars could be assumed to be constant over the chord length:

1) Variation in immersed foil area.

This was calculated by allowing for the variation in immersion at each foil element calculated from equation (6.16).

2) Variation in the local velocity.

The local velocity over the surface of the foil elements was taken as the vector sum of the forward velocity of the hydrofoil and the horizontal component of the water particle velocity at the position of the element:

$$V_w = V \pm k\, c_w\, a_w\, e^{kh}{}_w \cos\,(kx \pm \omega_e t)$$

where the upper and lower signs are for head and following seas respectively.

3) Variations of angle of attack.

For cases where the value of the wave orbital velocity could be considered small with respect to the forward velocity of the hydrofoil elements (all practical cases) the change in the angle of attack in waves ($\delta\alpha_i$) was given by:

$$\delta\alpha_i = \mp \frac{k\, c_w\, a_w\, e^{kh}{}_w \sin\,(kx \pm \omega_e t)}{V \pm k\, c_w\, a_w\, e^{kh}{}_w \cos\,(kx \pm \omega_e t)}$$

where $\tan\delta\alpha_i \simeq \delta\alpha_i$ in radians,

the upper and lower signs are again for the head and following sea cases respectively and a positive value of $\delta\alpha_i$ denotes an increase in the angle of attack.

4) Acceleration Forces.

These were calculated as the product of the particle accelerations and the appropriate added virtual masses. Horizontal and vertical components were considered only.

Pitching Moments

The main contribution to the pitching moments from the foil elements came from the lift and drag forces and their respective levers to the centre of gravity. However, there was also a smaller contribution from the pitching moment owing to the section itself which for thin wing theory where the aerodynamic centre can be assumed to be at the quarter chord point (1) can be given by:

$$M_{c/4} = 1/2\,\rho V^2\, Sc\; C_{Mc/4}$$

This was a two dimensional value of the pitching moment coefficient about the quarter chord point. Glauert shows (78) how the two dimensional value of this coefficient is not altered for the three dimensional case of a rectangular wing. In the absence of more detailed

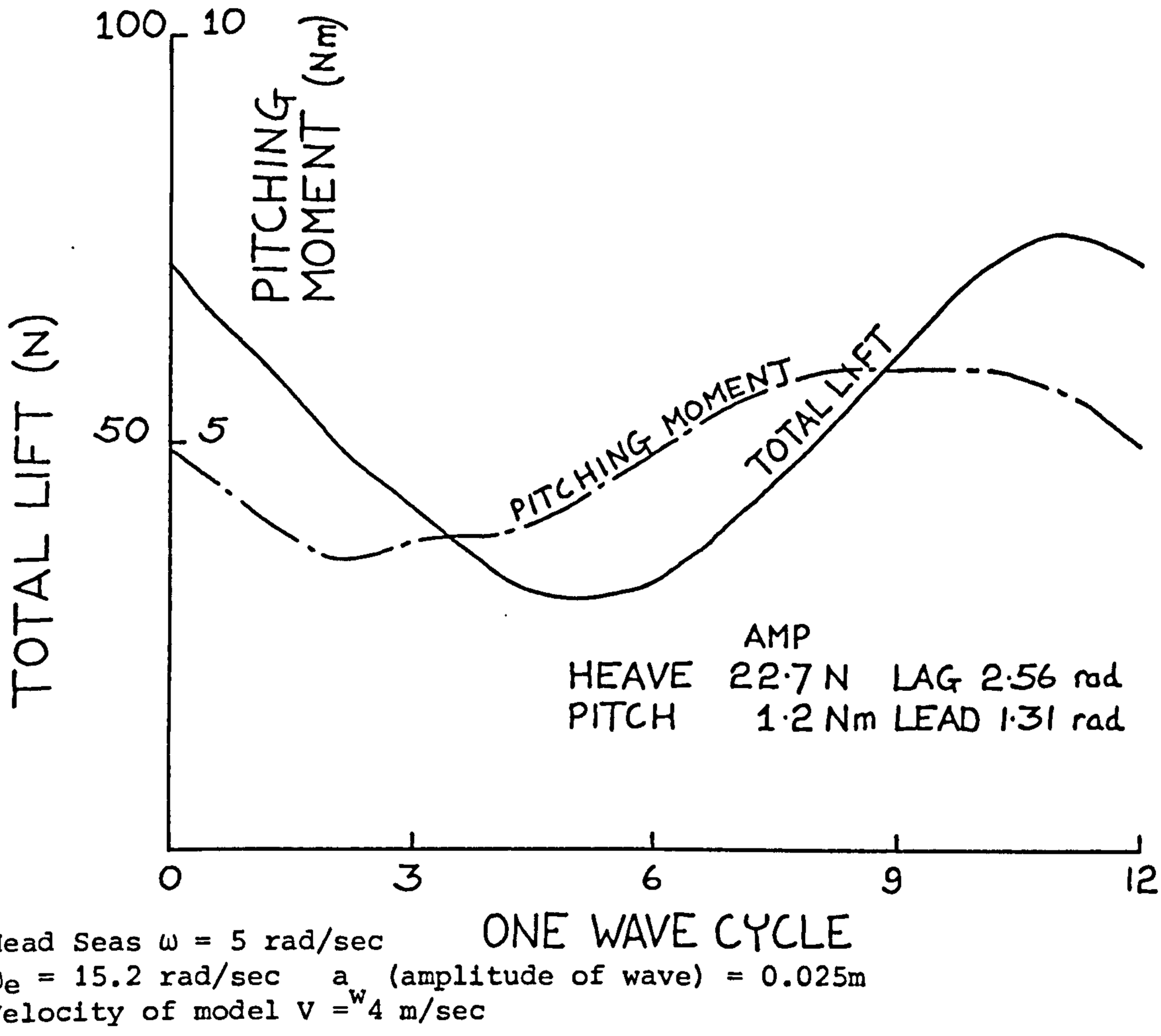

Head Seas ω = 5 rad/sec
ω_e = 15.2 rad/sec a_w (amplitude of wave) = 0.025m
Velocity of model V = 4 m/sec

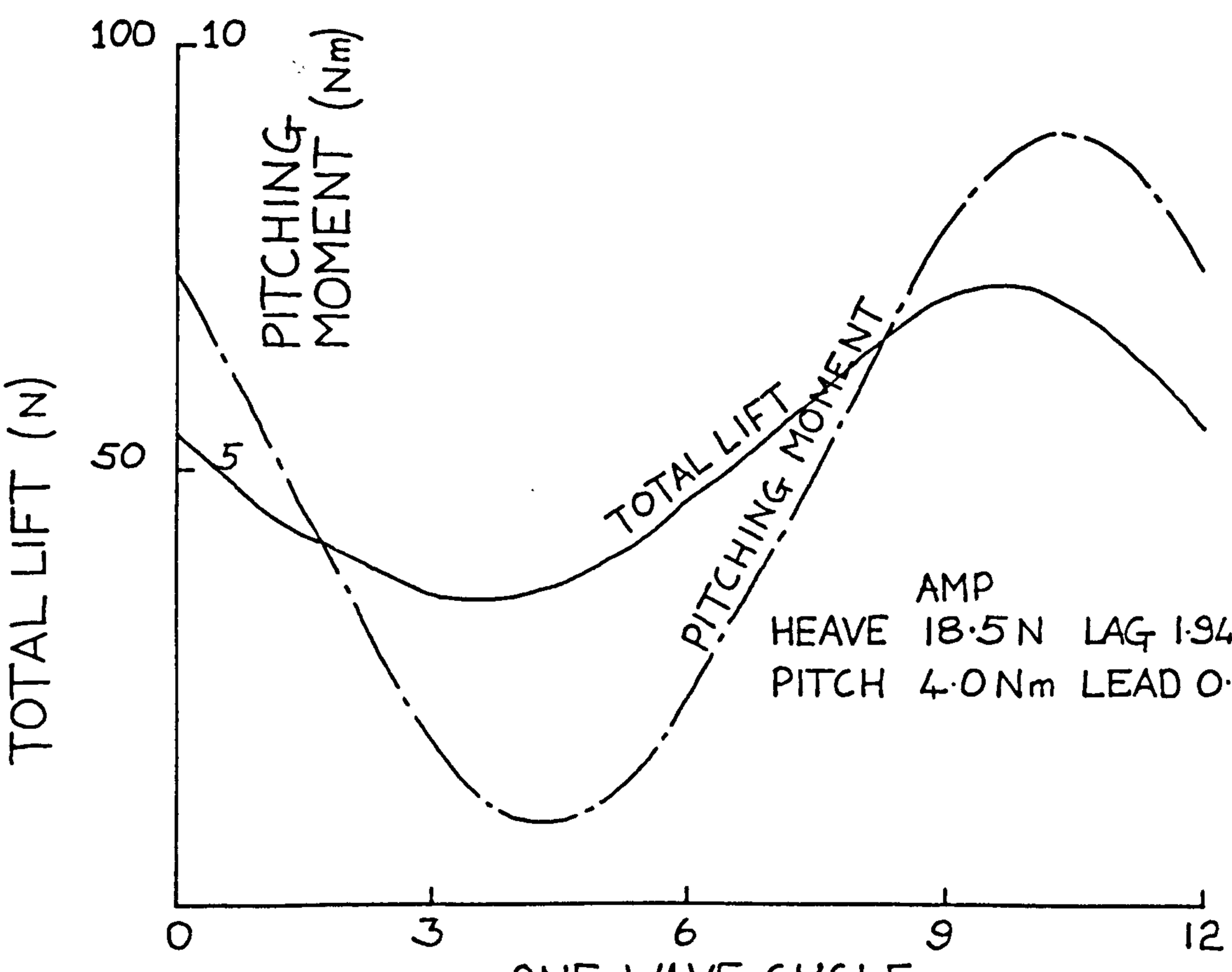

Head Seas ω = 8 rad/sec
ω_e 34.1 rad/sec a_w (amplitude of wave) = 0.025m
Velocity of model V_w = 4 m/sec

Fig. 6.3 Examples of the Variation of Total Lift and Total Pitching moment for the Model in Waves

Fig. 6.4 Block Diagram for Program DESIGN6 - calculation of stability derivatives

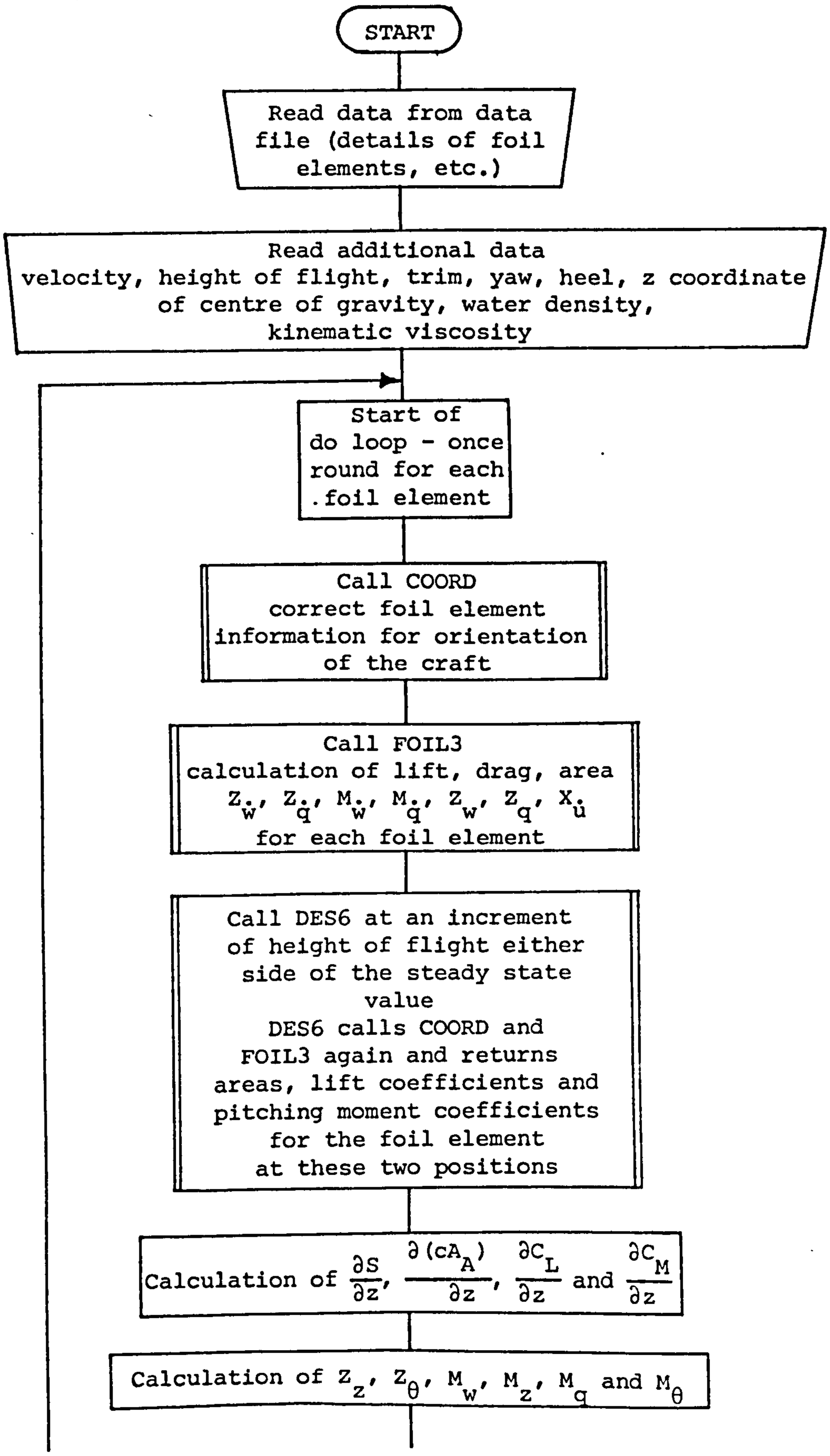

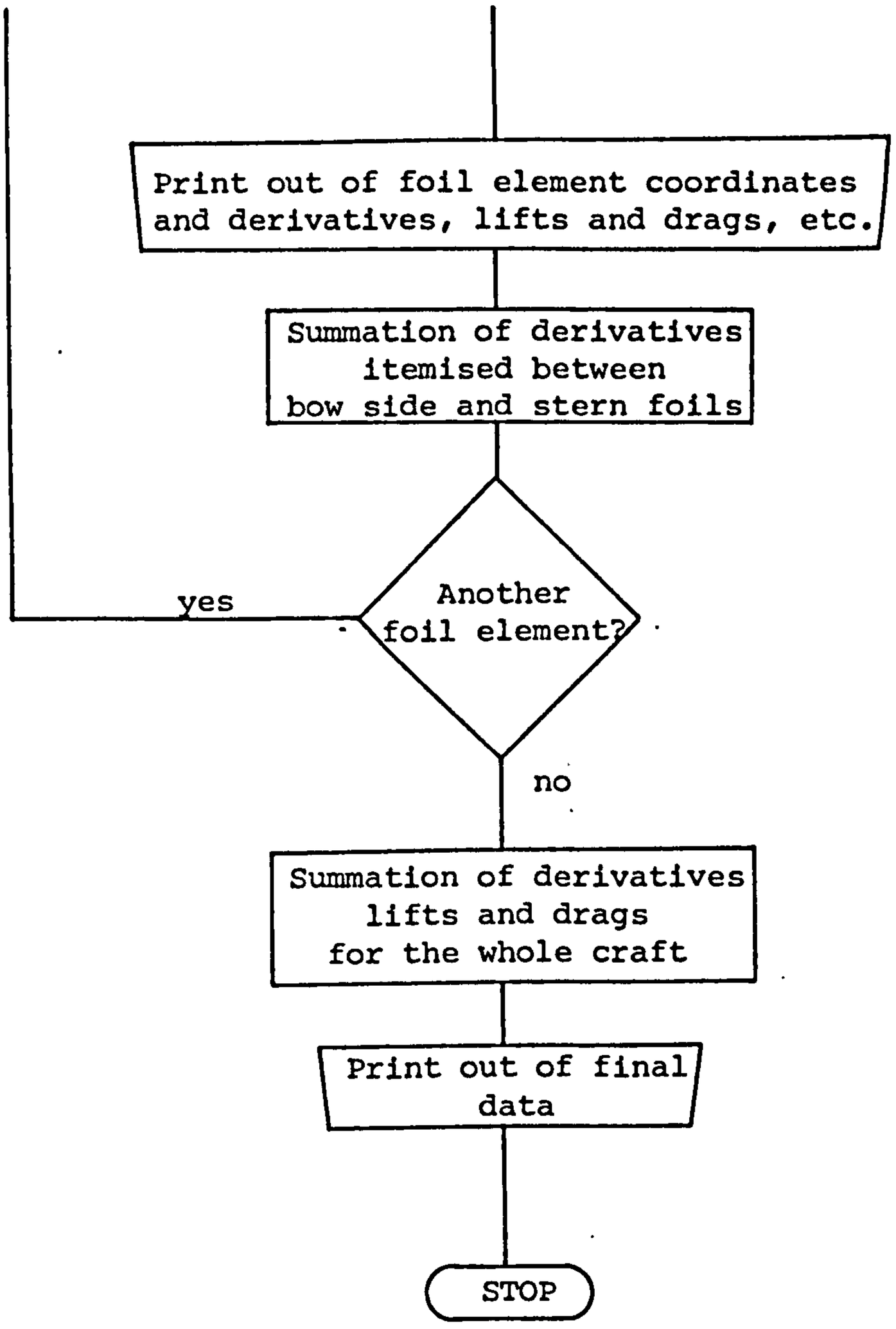
Print out of foil element coordinates and derivatives, lifts and drags, etc.
Summation of derivatives itemised between bow side and stern foils
Another foil element?
yes
no
Summation of derivatives lifts and drags for the whole craft
Print out of final data
STOP

Fig. 6.5 Block Diagram for Program DESIGN7 - calculation of exciting forces

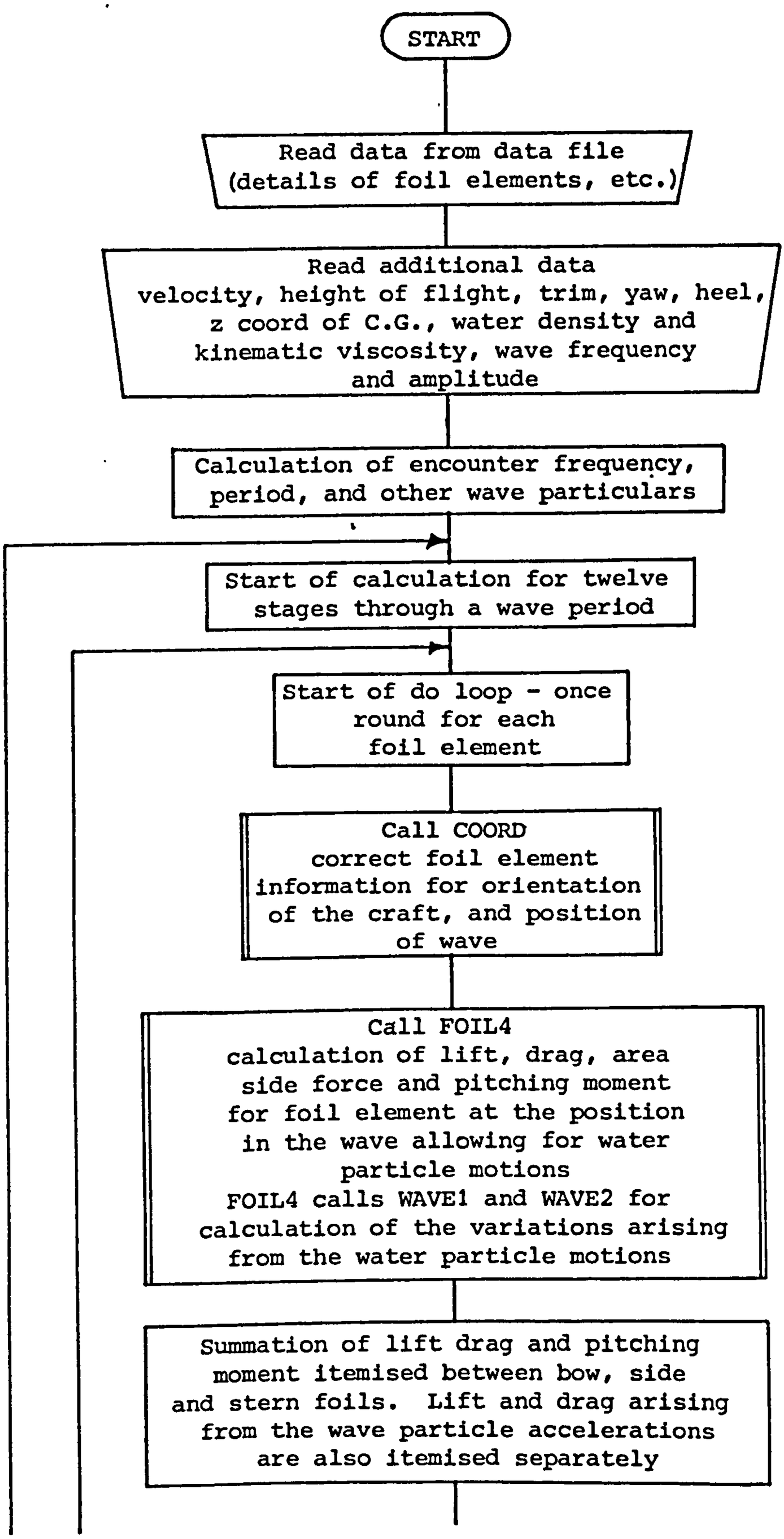

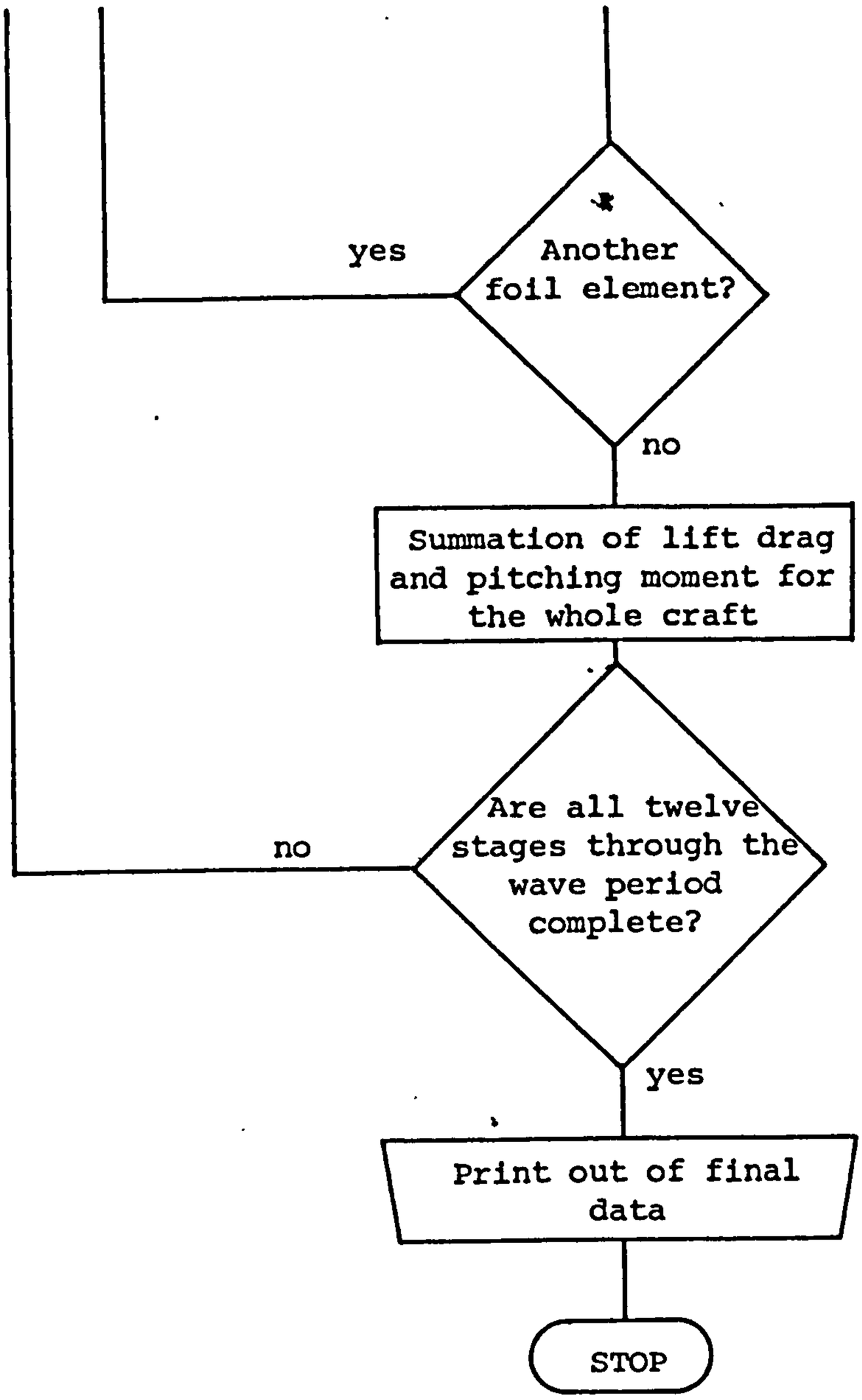
Another foil element?
yes
no
Summation of lift drag and pitching moment for the whole craft
Are all twelve stages through the wave period complete?
no
yes
Print out of final data
STOP

information the effects of finite span and the proximity of the free water surface were assumed not to affect the values of the pitching moment coefficient.

Where experimental values of $C_{Mc/4}$ did not exist (1 and 158) for a section type, this was calculated using the approximate method due to Pankhurst (1,page 72):

$$C_{Mc/4} \simeq \Sigma B_{PK} (U_c + L_c)$$

where B_{PK} are Pankhurst's constants (1,page 72)

U_c and L_c are the upper and lower ordinates of the wing section in fractions of chord.

Some results of these exciting force calculations for the one quarter scale model are shown in figure 6.3, where the pitching moment and total lift curves are plotted over one cycle. It will be noticed that these curves are not necessarily sinusoidal, but that they can be approximated to a sinusoid to a greater or lesser degree depending on the frequency in order to use the linear solution described here. Values of amplitudes and phase differences were lifted off these curves.

Solution of the Stability Equation

The stability equation which has a solution of the

Seakeeping Studies - Linear Solutions in the Frequency Domain

form given in equation (6.14) was a quartic in the D-operator with coefficients as below:

$$[(Z_{\dot{w}} - m)(M_{\dot{q}} - I_y) - Z_{\dot{q}} M_{\dot{w}}] D^4 +$$

$$[(Z_{\dot{w}} - m)(M_q + U_o M_{\dot{w}}) + Z_w (M_{\dot{q}} - I_y) - Z_{\dot{q}} M_w - (Z_q + U_o Z_{\dot{w}}) M_{\dot{w}}] D^3 +$$

$$[(Z_{\dot{w}} - m)(M_\theta + M_w U_o) + Z_w (M_q + U_o M_{\dot{w}}) + Z_z (M_{\dot{q}} - I_y) -$$

$$Z_{\dot{q}} M_z - (Z_q + U_o Z_{\dot{w}}) M_w - (Z_\theta + U_o Z_w) M_{\dot{w}}] D^2 +$$

$$[Z_w (M_\theta + M_w U_o) + Z_z (M_q + U_o M_{\dot{w}}) - (Z_q + U_o Z_{\dot{w}}) M_z - (Z_\theta + U_o Z_w) M_w] D +$$

$$[Z_z (M_\theta + M_w U_o) - (Z_\theta + U_o Z_w) M_z] = 0$$

The roots of this equation were found using the program STAB which took as input data values of the stability derivatives plus the crafts mass, velocity and inertia, I_y . From these input values, the coefficients of the polynomial were calculated and the roots found using a call to the NAg library routine CO2AEF which solves for the zero's of a polynomial with real coefficients (139) This routine uses the method of Grant and Hitchins.

Solution of the Equations of Motion

The solution of the equations of motion which is described in detail earlier in this chapter was implemented in the routine SEA1 (fig. 6.6). This program required as

Fig. 6.6 Block Diagram for Program SEA1 - solution of the Equations of Motion

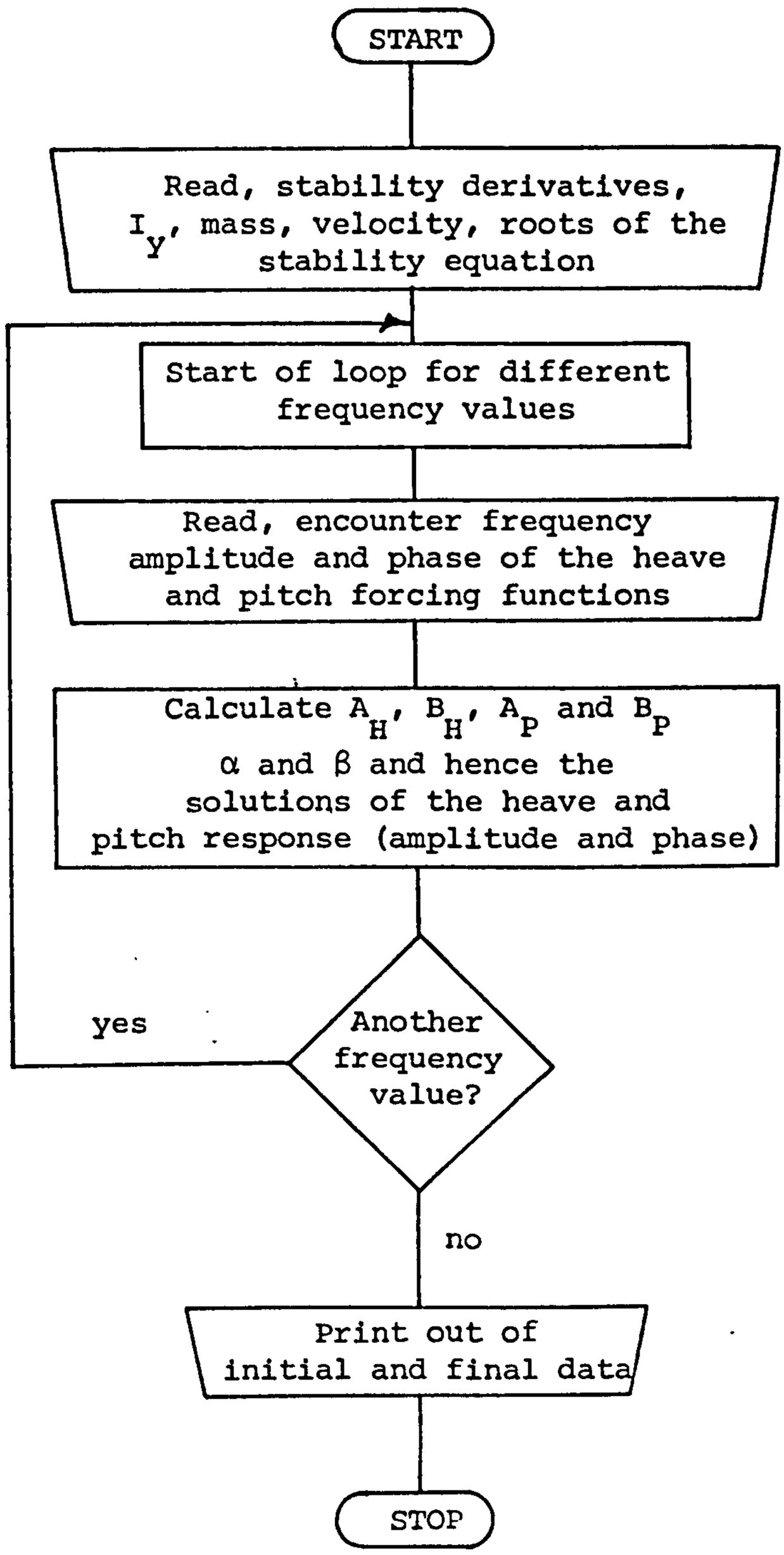

input, the stability derivatives, craft mass, velocity and inertia, the roots of the stability equation plus the exciting forces (amplitudes and phase lags) for each encounter frequency of interest. The amplitudes of the resulting motions and their phase lags are output.

The results in head and following seas for the model described in Chapter 4 are presented in Chapter 8 alongside a series of model tests in these wave conditions.

CHAPTER 7

Seakeeping Studies - Non-linear Solutions in the Time Domain

In chapter 8 it is shown how the linearised methods of chapter 6 do not give good agreement with the experimental results of the motion response over the whole of the frequency range. Even in the following sea tests where the agreement was good, considering the frequency of hull/wave impacts, it was felt that these good results were obtained for the wrong reasons because no account had been taken of the wave impact forces. Also the assumption that the craft did not move when the forcing functions were calculated meant that the values of the amplitudes of these functions would be larger than those actually encountered. However this result was offset by the fact that the craft had to oscillate further from the equilibrium position to the real solution than would be the case if the craft had already been allowed to move along its expected path. In reality the problem is even more complicated than this because of phase differences and the coupling between heave, pitch and surge motions. The major factor contributing to the amplitude of the forcing functions are the relative differences in position between the water surface and the orientation of the foil system as the waves pass the craft.

Seakeeping Studies - Non-linear Solutions in the Time Domain

A more realistic method of finding the motion response which is formulated in this chapter, involved a step-by-step time calculation where the forces on the hydrofoil system were calculated at each time step. In these force calculations account was taken of the variations in immersed foil areas and the effects of velocities and accelerations which arose both from the water particle motions in the waves and from motions of the boat itself. The initial studies assumed a quasi-steady approach where the full instantaneous values of velocity, acceleration and displacement were allowed to apply with no time delay (this point will be expanded upon later).

The equations of motion were set up by equating the forces incident on the craft to the acceleration terms for a three-dimensional rigid body (Equations 6.1,6.2 and 6.3 of Chapter 6, neglecting X_G and Z_G terms because the origin was assumed to be at the centre of gravity). For heave this became:

$m(\ddot{z} - v\dot{\theta} - \dot{x}\dot{\theta}\ )$ = - Total Lift (due to craft velocities and displacements and wave accelerations, velocities and displacements) + Total Weight + Forces due to added virtual masses x craft accelerations

$$= -TL + W + Z_{\dot{z}}\ddot{z} + Z_{\dot{x}}\ddot{x} + Z_{\dot{\theta}}\ddot{\theta} \qquad 7.1$$

Similarly for pitch,

$$I_y \ddot{\theta} = TPM - TDR\ z_{ce} + M_{\dot{z}}\ddot{z} + M_{\dot{x}}\ddot{x} + M_{\dot{\theta}}\ddot{\theta} \qquad 7.2$$

The term $(-TDR\ z_{ce})$ can be broken down further to incorporate the effects of the drag and the thrust separately if required. The term would become $(-TDRz_{cLR} - T_h z_T)$ where z_{cLR} is the lever from the centre of gravity to the hydrodynamic centre and z_T is the lever from the line of thrust to the centre of gravity.

Also for surge,

$$m(\ddot{x} + \dot{\theta}\ \dot{z}) = -\ TDR + T_h + X_{\dot{x}}\ddot{x} + X_{\dot{z}}\ddot{z} + X_{\dot{\theta}}\ddot{\theta} \qquad 7.3$$

where TL,TPM and TDR are the total instantaneous values of the lift, pitching moment and drag respectively,

T_h is the total thrust force and the values $Z_{\dot{z}}$,$Z_{\dot{x}}$,$Z_{\dot{\theta}}$ etc. are the added mass and cross coupled added mass terms which were formulated in Chapter 6 (these are -ve in the sign convention used here).

Seakeeping Studies - Non-linear Solutions in the Time Domain

Solution of the Equations of Motion

As for the linear work, most of the following work was undertaken considering only pitch and heave coupling because of the uncertainties involved in predicting the variation of the thrust force with time. The thrust force (from the sails in this case) will vary in some kind of oscillatory manner, which will probably be of small amplitude compared to the variation in the drag force. If the thrust was assumed to match the drag exactly, the surge equation would be meaningless in any case, but it is probably more realistic to assume a constant value for thrust. This was done when the surge equation was incorporated in the later studies.

These two second order differential equations, in pitch and in heave were solved using a numerical technique. The NAg library routines (139) cover the solution of n coupled single order ordinary differential equations in some depth, utilising various different methods for the various types of problem. The equations faced here formed an initial value problem where the solution was obtained starting from initial values of the dependent variables ($\dot{z}$, z, $\dot{\theta}$ and θ) and integrating with respect to time in a step-by-step manner. Various methods for solving this type of problem were studied (44,85,110,113,133), but in order to classify the problem, the initial calculations were carried out using a Runge-Kutta Merson routine as suggested by the NAg library manual, routine D02BDF, from which it

could be ascertained whether the problem was stiff (i.e. had rapidly decaying transient solutions) and of what order the errors were in the calculation.

It was first necessary to convert the two second order equations (equations 7.1 and 7.2) into a four coupled first order equations (133). Writing $y_1=z, y_2=\dot{z}$, $y_3=\theta$ and $y_4=\dot{\theta}$, and solving the two simultaneous equations in $\ddot{z}$ and $\ddot{\theta}$, these became:

$$\dot{y}_1 = y_2 \ (= \dot{z}) \qquad \dot{y}_3 = y_4 \ (= \dot{\theta})$$

$$\dot{y}_2 = \left\{ \frac{1}{\frac{m - Z_{\ddot{z}}}{Z_{\ddot{\theta}}} - \frac{M_{\ddot{z}}}{I_y - M_{\ddot{\theta}}}} \right\} \left\{ \frac{- TL + W + mV\dot{\theta}}{Z_{\ddot{\theta}}} + \frac{TPM - TDR\ z_{ce}}{I_y - M_{\ddot{\theta}}} \right\} (= \ddot{z})$$

$$\dot{y}_4 = \left\{ \frac{1}{\frac{I_y - M_{\ddot{\theta}}}{M_{\ddot{z}}} - \frac{Z_{\ddot{\theta}}}{m - Z_{\ddot{z}}}} \right\} \left\{ \frac{- TL + W + mV\dot{\theta}}{m - Z_{\ddot{z}}} + \frac{TPM - TDR\ z_{ce}}{M_{\ddot{z}}} \right\} (= \ddot{\theta})$$

The calculations for the total lift TL, total drag TDR, total pitching moment TPM, and the added mass terms were made in subroutines which were developed from the program DESIGN7 which has been described in Chapter 6. Additions to the calculation of DESIGN7 included an adjustment to the immersed portion of the hydrofoil system due to the displacements of the craft (z and θ), a direct change to the angle of attack of the hydrofoils due to the pitch angle θ and changes to the angle of attack and local

velocity of the foil elements due to the velocities, $\dot{x}$, $\dot{z}$ and $\dot{\theta}$. These latter were incorporated in the subroutine WAVEX, a development of WAVE1 (see Chapter 6), which calculates local velocity changes and variations in the angle of attack of the foil elements in waves. The corrections made were :

Corrected forward velocity, $V_{corr} = V + z_i\dot{\theta} + \dot{x}$

Change in the angle of attack = $\frac{\dot{z}}{V_{corr}} - \frac{x_i\,\dot{\theta}}{V_{corr}}$

where x_i and z_i are the coordinates of the foil element from the centre of gravity, and the surge velocity, $\dot{x}$, is taken to be zero in the case when pitch and heave motions only are considered.

DIFF4 - Runge-Kutta Merson Method

The NAg routine D02BDF was implemented from the program DIFF4. The subroutine FCN4 (which called subroutines FOIL5, WAVEX, WAVEY and COORD) returned the values of $\dot{y}_1, \dot{y}_2, \dot{y}_3$ and $\dot{y}_4$ from calculations on the hydrofoil system and input values of y_1, y_2, y_3, y_4 and time. The routine D02BDF computes a global error estimate and makes a stiffness check.

From a series of runs of this routine over the range of frequencies of interest, it was found that the system of equations describing the surface piercing hydrofoil system

here did in fact constitute a stiff problem. A detailed description of the characteristics that constitute a stiff problem are discussed in Hall and Watt (85), but in engineering terms a stiff problem is one in which the solutions contain rapidly decaying transient terms. These rapidly decaying transients can be seen in all of the computed motions, examples of which are given in fig. 7.1. An alternative way of describing a stiff problem, is to say that certain eigenvalues of the matrix $\partial f_i/\partial y_i$ have large negative real parts compared to others, where the system of differential equations is written in the form:

$$\dot{y}_1 = f(t, y_1, y_2, y_3, y_4)$$
$$\vdots \quad \vdots \quad \vdots \quad \vdots \quad \vdots \quad \vdots$$
$$\dot{y}_4 = f(t, y_1, y_2, y_3, y_4)$$

This effectively means that the solution of the characteristic equation of the matrix $\partial f_i/\partial y_i$ (for example, for the linearised system, equation 6.14 of chapter 6) has certain roots with large negative real parts compared to others. This can be seen to be the case for the linearised system for the model considered here which had two sets of complex conjugate roots with real parts -16.68 and -2.08. The former indicates a transient which decays very rapidly indeed. The ratio of the maximum to the minimum eigenvalue (-ve real parts) is in this case 8 which by the criterion due to Lambert (85,page 125) indicates a marginally stiff problem. Comparing runs of DIFF4 for the linearised system (chapter 6) and for the non-linearised system it was found

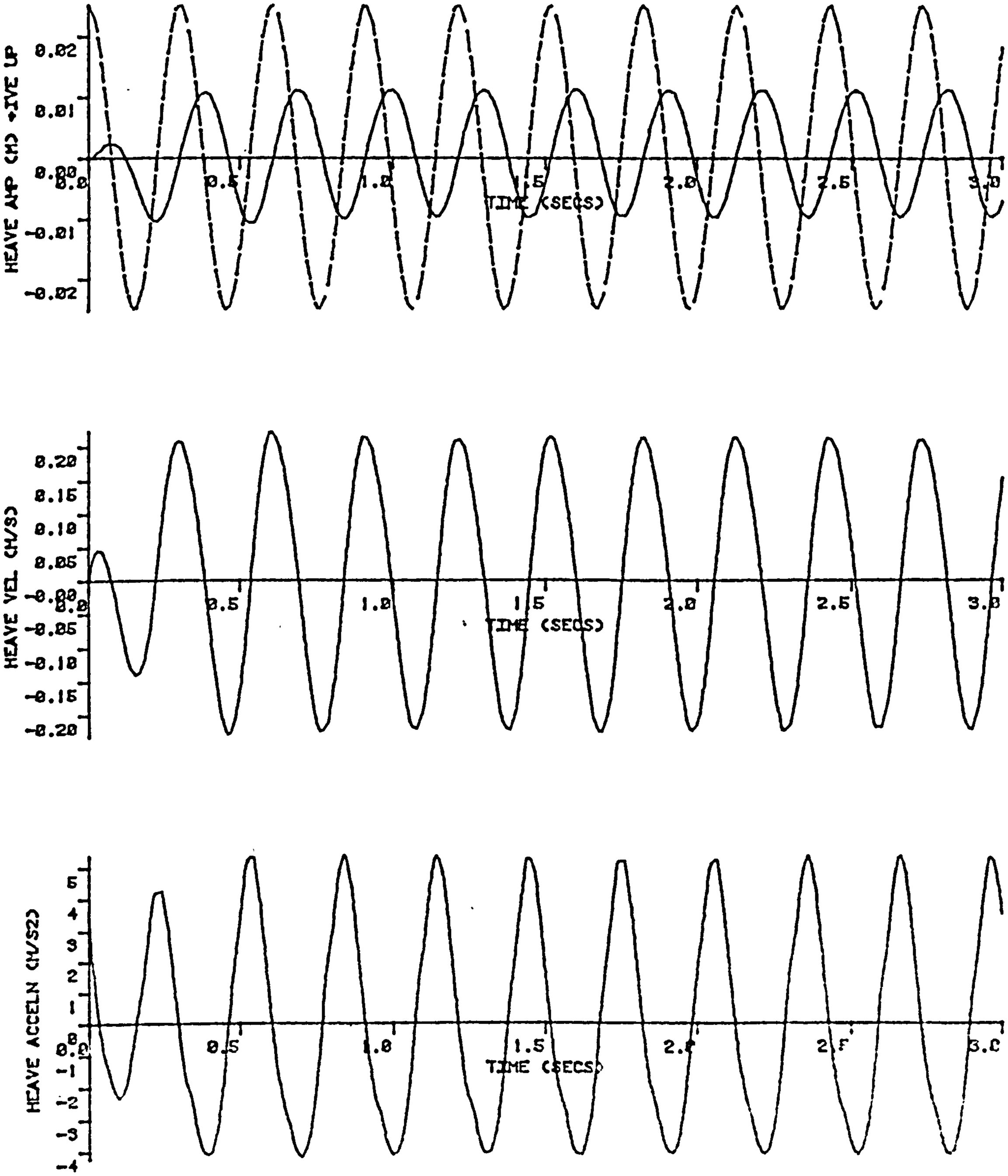

Fig. 7.1 Output of the Non-linear Time Domain Solutions for Seakeeping of the Hydrofoil Model

---------- Wave Profile (amplitude 0.025m)

Fig. 7.1a Head Sea (frequency 6 rad/sec) Heave Motions

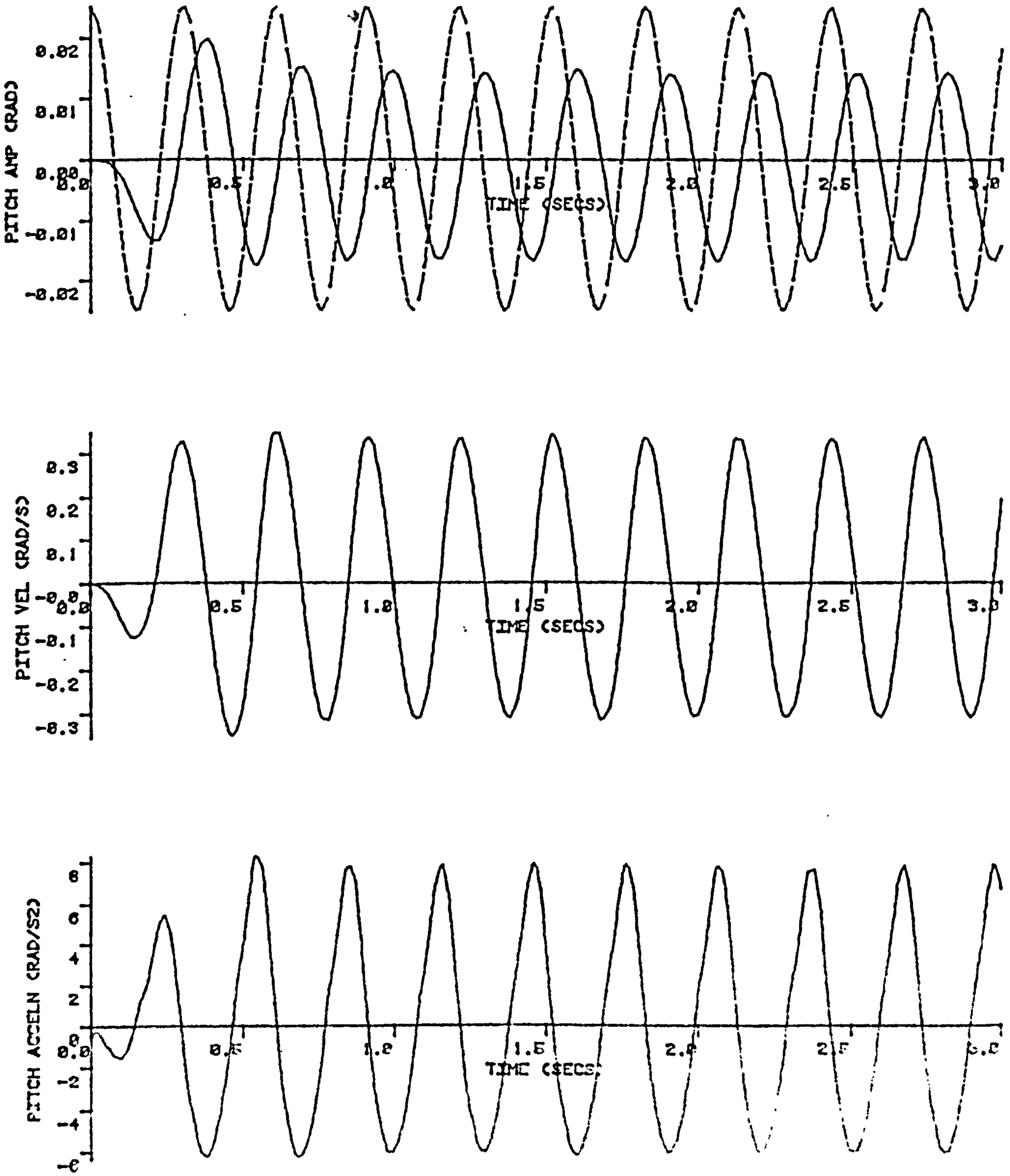

Fig. 7.1b Head Sea (frequency 6 rad/sec) Pitch Motions

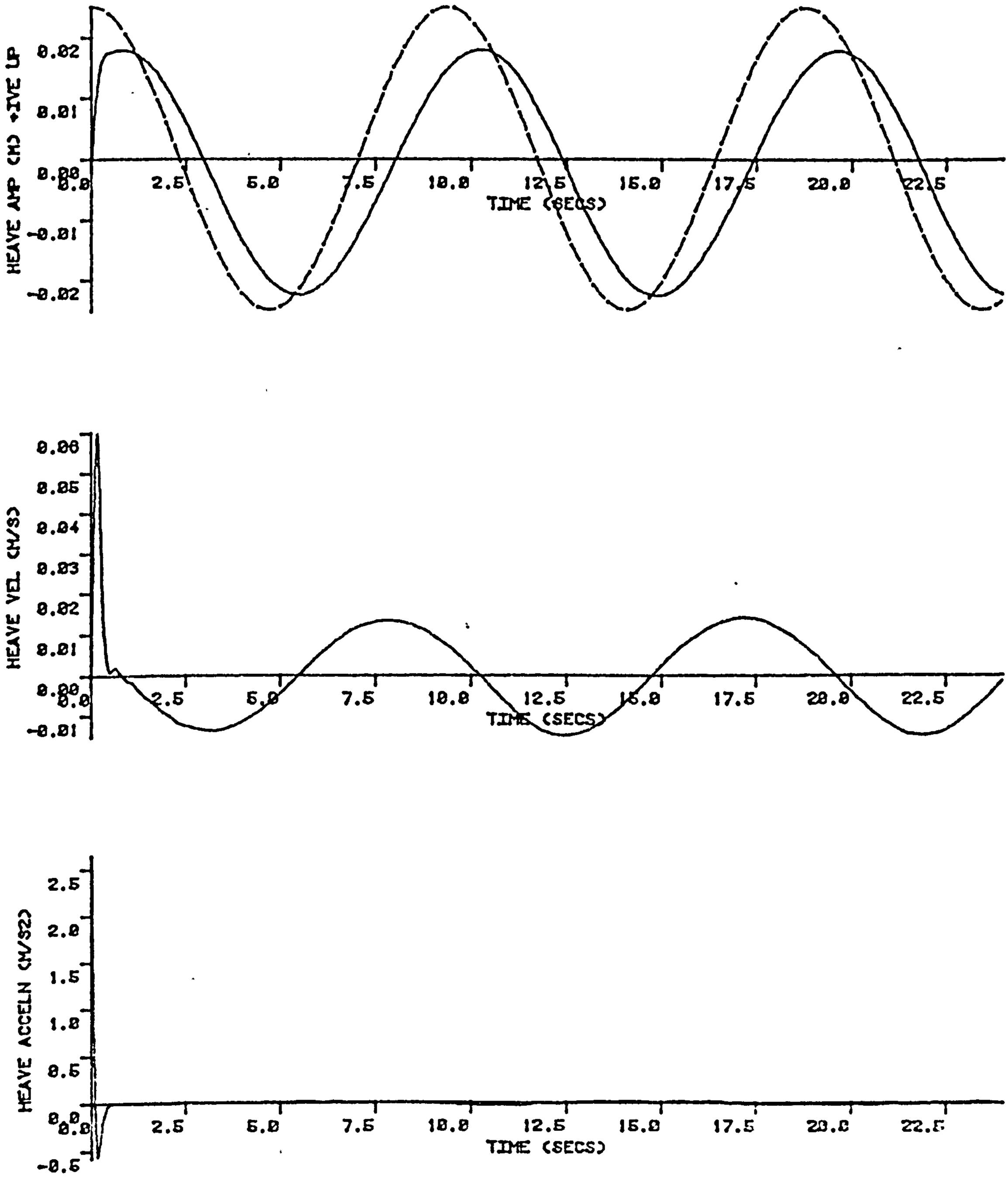

Fig. 7.1c Following Sea (frequency 3 rad/sec) Heave Motions

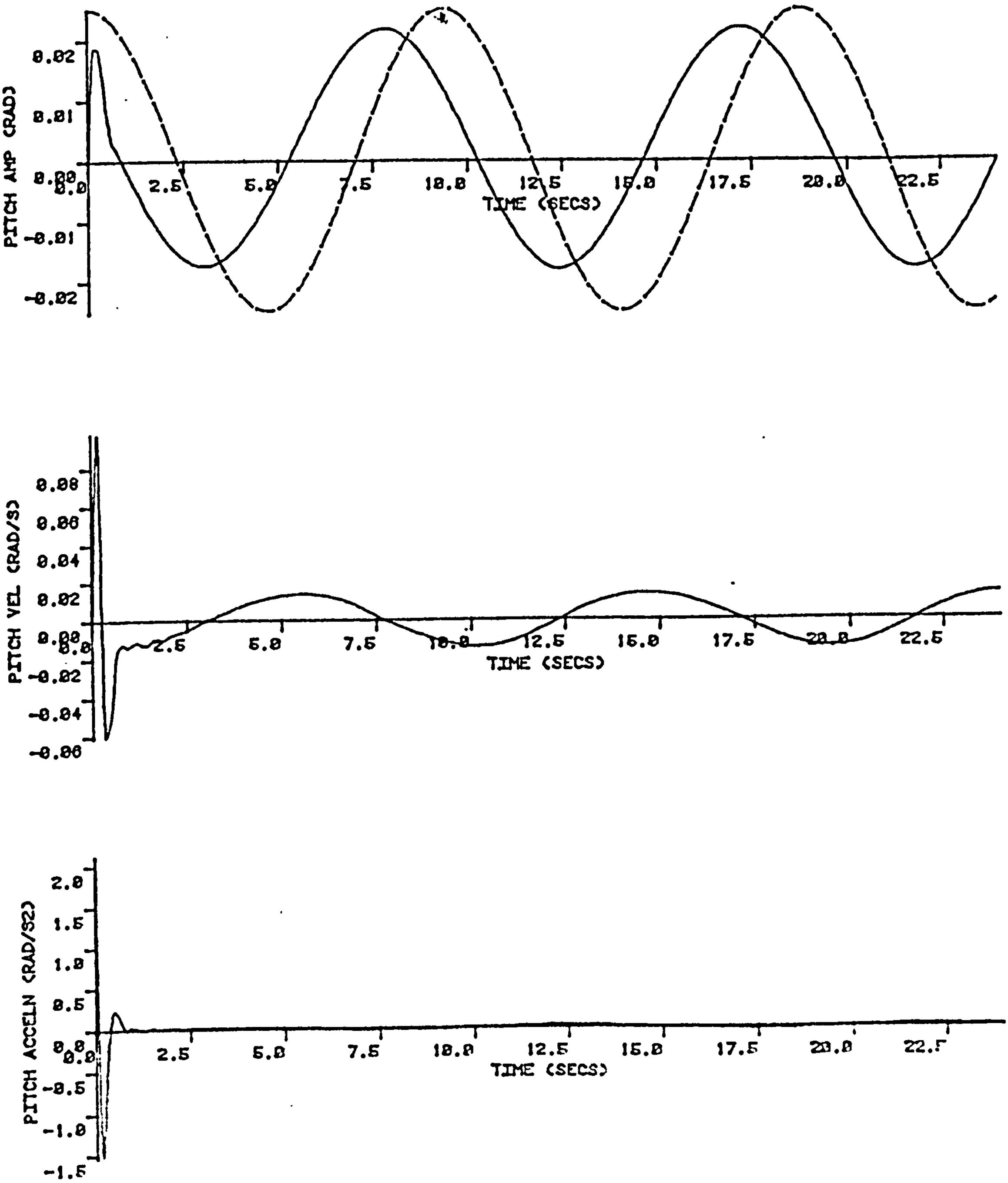

Fig. 7.1d Following Sea (frequency 3 rad/sec) Pitch Motions

that the latter returned higher values of the stiffness parameter which would in turn indicate an even higher value than 8 of Lambert's ratio here.

GEAR4/GEARS - Gear Variable-Order,Variable-Step Method

For stiff problems it is more efficient to use the NAg routine D02EBF, which is a variable order, variable step, implementation of the stiffly stable backwards differentiation methods due to Gear (85,chapter 11). A computing problem was encountered with the implementation of this method on the PDP 11/40 mini computer which was unable to cope with the combined size of the NAg routines and the hydrofoil force calculation routines. This was overcome (see Appendix A) by building two interactive programs GEAR4 and GEARS (fig 7.4a and b). GEAR4 called the NAg routines and produced output in the form of a data file in FILE and as a hard copy in GOUT. GEARS is the same calculation as that carried out in FCN4 above and it calls the same subroutines FOIL5,WAVEX,WAVEY and COORD.

To make a run of this program, it is necessary to provide the information shown in fig. 7.2. GEAR4 requires values of the initial time value, which is usually zero, the final time value, which has to be a multiple of 3 second periods (this is a restriction imposed for the format of the output), initial values of the dependent variables (y_1,y_2,y_3 and y_4), an accuracy parameter and a

```
>RUN GEARS
>RUN GEAR4
READ X - INITIAL TIME VALUE :
>0.
READ XEND - FINAL TIME VALUE (DOUBLE PRECISION):3.
READ Y(1), Y(2), Y(3), Y(4) - INITIAL VALUES :0.,0.,0.,0.
READ TOL - ACCURACY PARAMETER :1.D-3
READ IRELAB    0 - NO CHOICE OF ERROR CONTROL
               1 - ERROR BASED ON NO OF DECIMAL PLACES
                2 -  ERROR BASED ON NO OF SIGNIFICANT FIGS. (INTEGER):
1

                TIME                    Y(1)                    Y(2)                    Y(3)                    Y(4)
    0.0000000000D+00     0.0000000000D+00     0.0000000000D+00     0.0000000000D+00     0.0000000000D+00
ENTER  DATA  FILE  NAME :MOD3.DAT
READ  VEL, HEIGHT, TRIM, YAW, AHEEL, ZCG, YI :4.,.11,1.3,0.,0.,-.09,.626
READ  DENSITY, KINEMATIC VISCOSITY :1000.,.00000113902
READ L (1-HEAD SEAS, 2-FOL SEAS), WA (WAVE FREQ) WAMP (WAVE AMP) :1,5.,\,.5\3.,.025
1,3.,.025

                TIME                    Y(1)                    Y(2)                    Y(3)                    Y(4)
 0.1999999955D-01     -0.6579328959D-03     -0.6182214721D-01     0.1642536782D-03     0.2377756491D-01

                TIME                    Y(1)                    Y(2)                    Y(3)                    Y(4)
 0.3999999911D-01     -0.2308844431D-02     -0.9872162425D-01     0.1001313013D-02     0.6866266558D-01

                TIME                    Y(1)                    Y(2)                    Y(3)                    Y(4)
 0.5999999866D-01     -0.4474240444D-02     -0.1135918122D+00     0.2735497015D-02     0.1091581835D+00

                TIME                    Y(1)                    Y(2)                    Y(3)                    Y(4)
 0.[illegible]21D-01     -0.6752892565D-02     -0.1108376470D+00     0.5165005704D-02     0.1331239131D+00
```

Fig. 7.2 Information Required to Run GEAR4 and GEARS

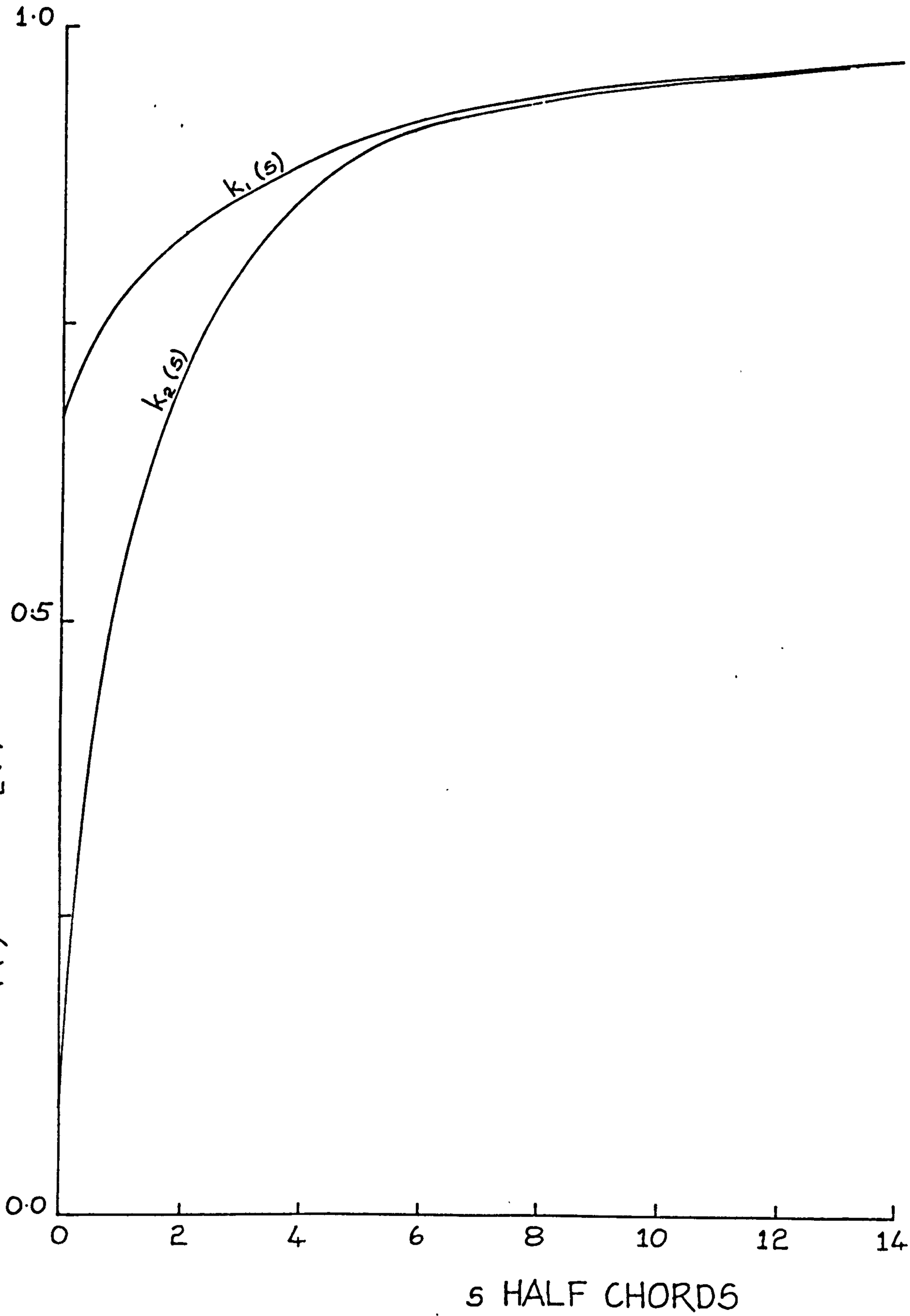

Fig. 7.3 Indicial Lift Functions $k_1(S)$ and $k_2(S)$

Fig. 7.4a Block Diagram for Program GEAR4 - solution of the non-linear equations of motion

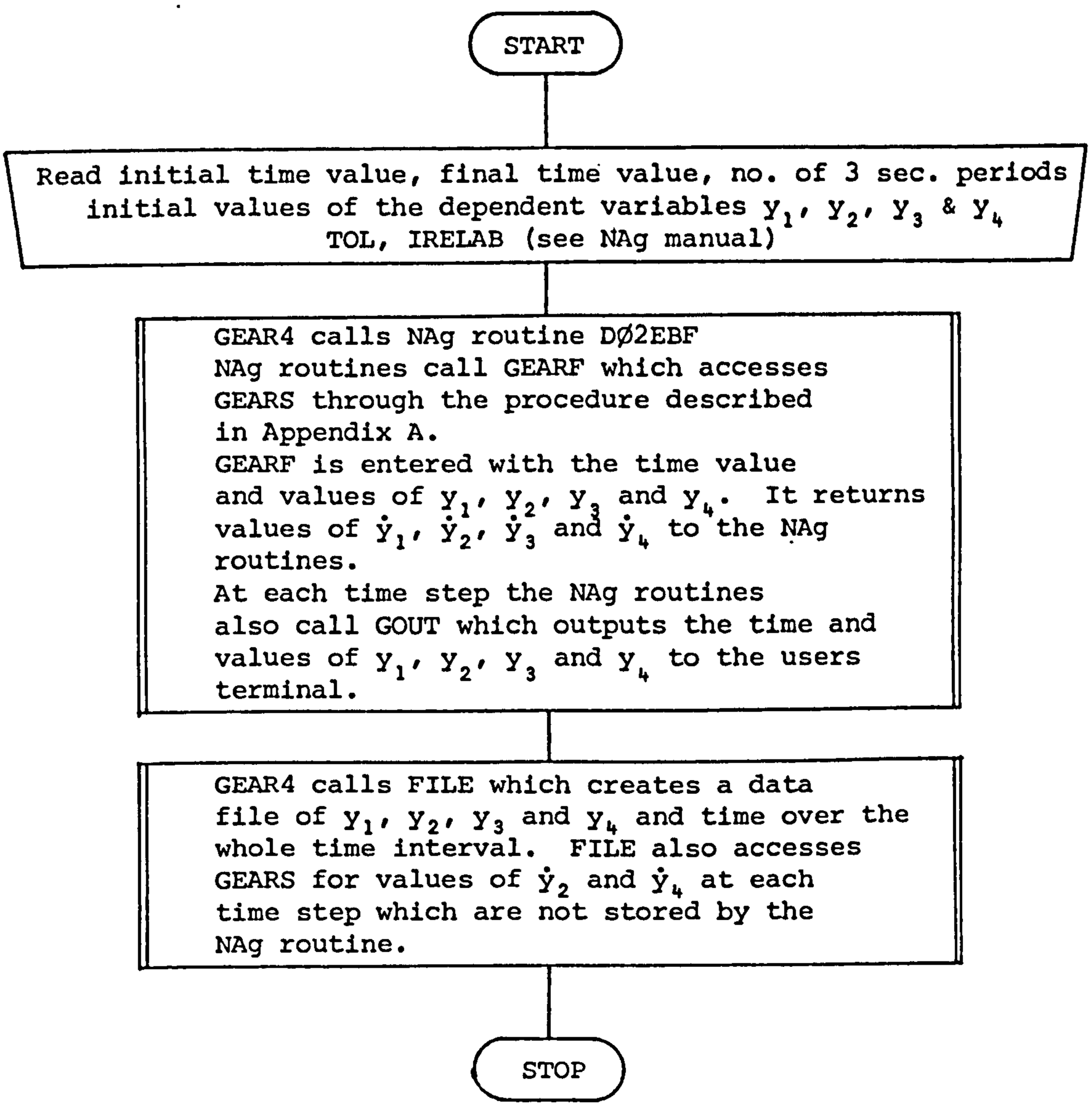

Fig. 7.4b Block Diagram for Program GEARS - solution of the non-linear equations of motion

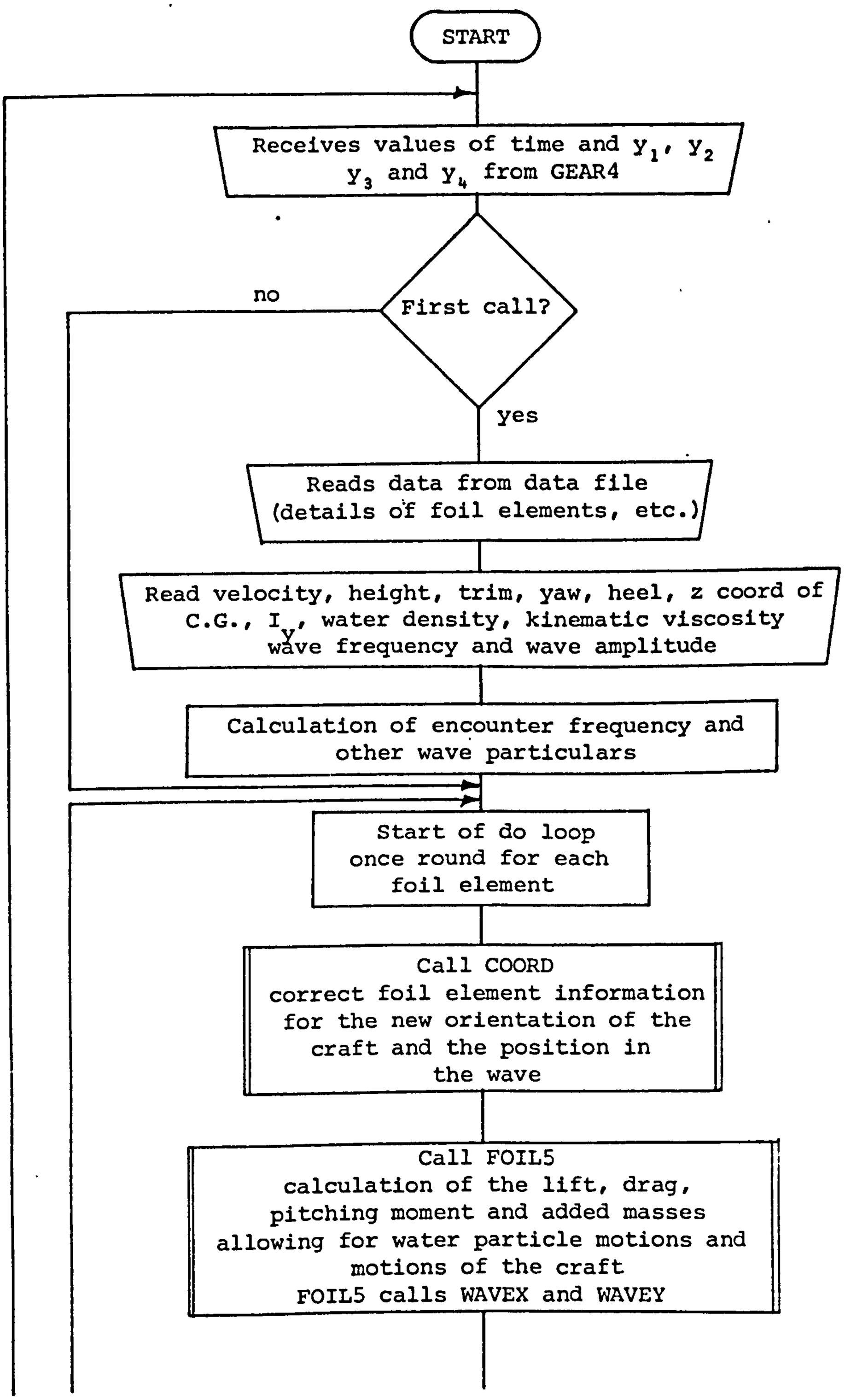

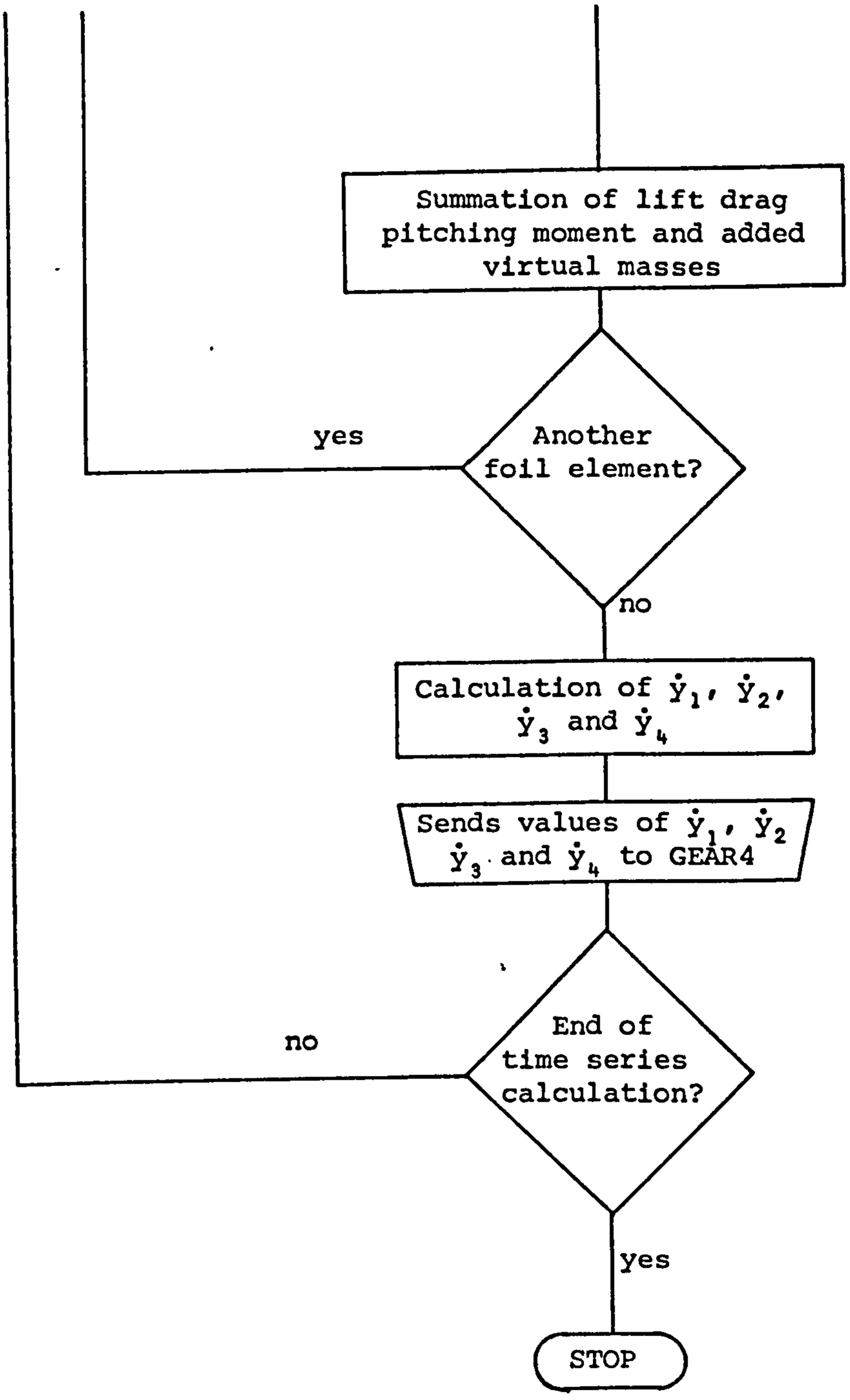
Summation of lift drag pitching moment and added virtual masses
Another foil element?
yes
no
Calculation of $\dot{y}_1$, $\dot{y}_2$, $\dot{y}_3$ and $\dot{y}_4$
Sends values of $\dot{y}_1$, $\dot{y}_2$ $\dot{y}_3$ and $\dot{y}_4$ to GEAR4
End of time series calculation?
no
yes
STOP

flag for the choice of error control. The accuracy value and the error control flag are discussed in detail in the NAg library manual (139). Output is presented in three different forms. A copy of the time and dependent variables , (y_1,y_2 ,y_3 and y_4) appears on the users terminal in order that a monitor can be kept on the progress of the run which takes thirty or more minutes to complete on this computer. A hard copy of the same information is also presented. An optional output can be made and stored as a data file; this form includes the pitch and heave acceleration terms as well as the dependent variables and time values.

PLOT - Plotting Routine

PLOT is a program which utilises the SIMPLEPLOT library plotting routines and it plots the information from the output data which is stored in a data file. Typical output is shown in fig. 7.1.

GEAR4U/GEARSU - Inclusion of Unsteadiness or Time Delay Effects

The above studies were all carried out by assuming that the full instantaneous values of the velocities, accelerations and displacements applied with no time delay. In practice this is not the case and there is a definite time lag for these motions to be realised. For example when the angle of attack of a foil is suddenly changed, the

corresponding change in the pressure distribution is not instantaneous, nor is the build up in circulation when a foil element is suddenly immersed. It was felt that such effects may account for some of the discrepancies which occurred at certain frequencies between the model test results and the theoretical estimates especially where these were large which was the case for some of the following seas results. Various approaches have been used to obtain the correction of the forces arising from sudden changes in angle of attack (53,108 and 148), but the correction for forces arising from sudden changes in the immersion depths of the foils has not been quantified. It was expected, and this was corroborated by some initial trial calculations that this latter effect would have the larger influence on the forces on a foil element. Inclusion of the term for correction to changes in the angle of attack on its own made relatively small differences to the motion response and this is borne out by the results given in references (53 and 148).

There has been very little work carried out on the problem of unsteady flow around a hydrofoil operating near the free water surface and all the correction methods that have been used to date have been based on calculations applied to the unsteady forces on aircraft wings in an infinite fluid, and even these studies are deficient in any significant experimental corroboration (57,103,114 and 128). However, as a first approximation and in the absence of more detailed data, these methods were also applied

here, but in the form of the indicial lift functions described by Jones (103) and Drischler (57).

Corrections Due to a Sudden Change in Sinking Speed or Angle of Attack

The normalised indicial lift functions $k_1(s)$ for a sudden change of normal velocity, or what amounts to the same thing, a sudden change in angle of attack are given by Drischler (57) for a variety of three dimensional wings of different aspect ratios and for a variety of different calculation methods. For simplicity and because of the other uncertainties inherent in this approach, the curve for a wing of aspect ratio 6 was used as the correction for all the foil elements. This was a conservative assumption as the lower the aspect ratio the smaller the response time to reach the steady state lift and the smaller the discrepancy between the initial and final values of lift. The aspect ratio of 6 was typical of the most highly loaded elements of the foil system. A curve fit was made to this curve giving $k_1(s)$ as a function of s, the distance travelled in half chords (fig. 7.3):

$$k_1(s) = 1.0 - 6.2748\ (s + 5.0)^{-1.8413}$$

for $$s = 2Vt/c_r$$

where c_r is the root chord or maximum chord length of the element and t is the 'time delay'.

The value of the indicial lift is given by:

Seakeeping Studies - Non-linear Solutions in the Time Domain

Indicial Lift arising from

a change in angle of attack $= \frac{1}{2} \rho V^2 S \frac{dC_L}{d\alpha_i} \Delta\alpha_i \, k_1(S)$

where $dC_L/d\alpha_i$ is the three dimensional lift curve slope and $\Delta\alpha_i$ is the sudden change in the angle of attack.

This correction was applied to the changes in angles of attack resulting from the vertical velocities of the water particles in the waves and the vertical motions of the boat in response. They were also made to the changes in angles of attack due to displacements in pitch. The choice of the time delay in the calculation is quite important, and not easily calculated. Ideally, the indicial lift should be calculated as a summation of the indicial lifts calculated using the values of the changes in the angle of attack between each time step and its appropriate time delay to the present time step. This would be unduly complex however when the accuracy of the method in general is considered and it would be difficult to implement on the variable step methods employed here. The approach used here was to multiply the total value of the change in angle of attack at each time step by the indicial lift function for a time delay, t, which could be set before a run of the program by the operator. Depending on the value of t decided upon this method would normally be somewhat pessimistic, but it was possible to obtain an indication of the effect of the time delay between the predictions with and without a correction.

Seakeeping Studies - Non-linear Solutions in the Time Domain

Corrections for a Change in Immersion Depth

The corrections for a sudden change in immersion depth of a hydrofoil which result when sections of the foil elements pass from air to water and vice versa are even less adequately treated in the literature. The approach formulated here was to assume that when a portion of a hydrofoil element was suddenly immersed, the build up of lift was similar to that experienced when an aerofoil encounters a gust. This can only be regarded as a first approximation because the flow characteristics are not the same, but in both cases the lift changes from zero and gradually reaches a steady state value. The exponential curves which model the lift coefficient in a gust would be expected to be of a similar form to the build up of lift as a foil element becomes immersed but this similarity must be used with some caution until further reseach and model tests have been carried out. In this case the indicial lift function $k_2(s)$ is given by Jones (103) for an aspect ratio 6 aerofoil as (fig. 7.3);

$$k_2(s) = 1.0 - 0.448e^{-0.29s} - 0.272e^{-0.725s} - 0.193e^{-3.0s}$$

where s is the distance travelled in half chords as above.

This correction was applied to the changes in immersion depths of the foil elements which arose from the changes in displacement of the hydrofoil system and the passage of the wave:

Indicial Lift due to changes

in immersion depth $= \frac{1}{2} \rho V^2 C_L \Delta S \, k_2(S)$

where ΔS is the change in immersed area of the foil (which is directly proportional to the change in depth for hydrofoil elements of constant chord length).

The effects of the time delay were treated in a similar manner to the approach used for the corrections due to changes in the angle of attack. Again depending on the value of the time delay,t, this approach would normally be pessimistic but an indication of the effects of a time delay could be studied.

The effect of these corrections would be greater at higher encounter frequencies and it is suggested that they should vary in such a manner that there are no time delay effects at encounter frequencies below about 8 rad/sec. (i.e. $t=\infty$). The calculations using these methods which are described for the model system in chapter 8 were carried out with a value of t=0.005 secs. A suggested variation in the time delay over the frequency range is made for the case of the model boat and the results using this variation are also presented.

These effects were incorporated in the routines GEARSU and GEAR4U which are essentially the same calculations as GEARS and GEAR4 with the above unsteadiness effects added.

Seakeeping Studies - Non-linear Solutions in the Time Domain

It was felt that a program of model experiments was required in this area of hydrofoil research in order to formulate a more accurate set of correction values for these unsteady effects. This might utilise some form of high speed water channel or tunnel and vertical planar motion mechanism apparatus where measurements of the forces on an oscillating hydrofoil element could be made.

Solution of the Three Degree of Freedom Problem (Incorporating Freedom in Surge)

The three coupled equations of motion have already been given at the beginning of this chapter in equations 7.1, 7.2 and 7.3. These equations were split up into six first order differential equations and they were solved using the same Gear techniques described above. The routines used were GEARSS and GEAR4S. The solution was calculated by assuming a constant value of thrust which had to be arrived at by trial and error in order to avoid the craft speeding up or slowing down. Only a few calculations were undertaken using this method and they were used mainly as a comparison against the other solutions already described. The results are given in chapter 8.

CHAPTER 8

Seakeeping Studies - Model Tests

Model tests in both head and following seas were carried out on the same quarter scale model of the wind propelled hydrofoil trimaran which is described in Chapter 4. Unlike the calm water tests, the tests in waves could not be made using the dynamometer described in Chapter 4 because the method of connection between the top of the model mast and the strain gauged tow bar effectively coupled the mass of the moving parts of the dynamometer to the mass of the model. This would have led to an incorrect modelling of the mass inertia of the system in heave and pitch even though the model would have been free to move in the vertical plane.

The method used was to restrain the model in sway and to arrange the tow again from the top of the mast to the strain bar previously used, but in this case the connection was made by means of an interconnecting tow wire. The length of the tow wire was made as long as possible in order to minimise the effects of vertical forces which would occur from the tow wire as the model moved in the waves. The restriction in sway was achieved by means of two parallel tubes which just fitted either side of the

model mast. Only one guide was required at this position as the model was inherently stable in yaw because of the influence of the stern foil strut, which is the equivalent of the rudder foil on the full scale craft.

Measurements of speed, resistance from the strain gauged bar and heave acceleration from an accelerometer mounted at the centre of gravity were taken. The motions were recorded from the output of fine piano wires attached to two linear displacement transducers (LVDT's), one of which was connected at the longitudinal position of the centre of gravity and the other at a position on the stern deck. The forward transducer measured pure heave displacement and the pitching motions could be measured from the difference between the signals of the two transducers.

The waves were monitored by means of two capacitance wave probes. One of these was fastened to the tank wall and measured the wave amplitude and the actual wave frequency. The other probe was designed specially for use at high carriage speeds and consisted of a streamlined strut and pod which provided the support for the wires (fig.8.1). This latter was mounted alongside the model and measured the wave encounter frequency. Its output of wave amplitude, however, was in error because air cavities formed behind the wires at the test speed of 4 m/sec, but this did not matter because an accurate record of wave amplitude was made from the static wave probe.

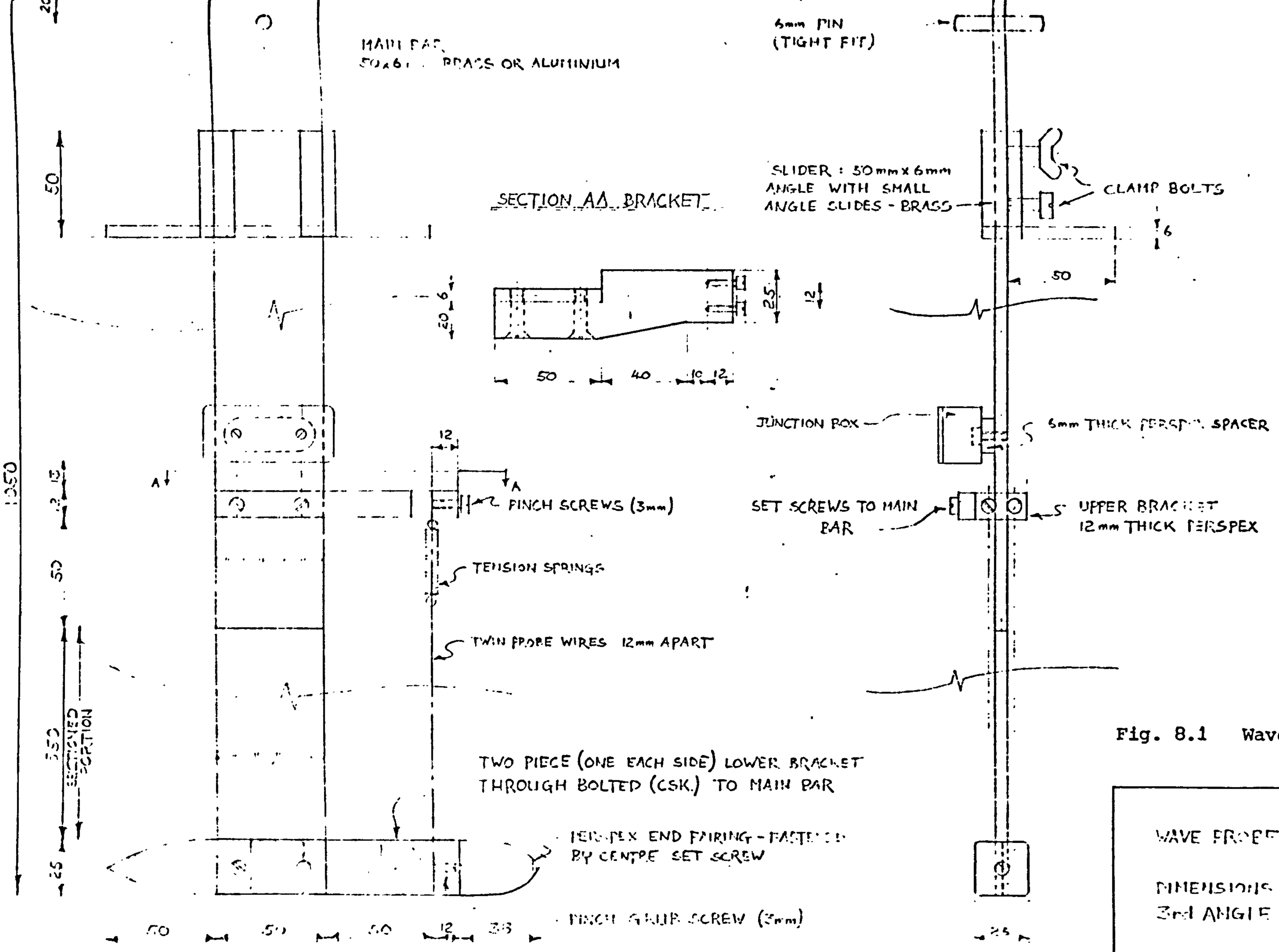

Fig. 8.1 Wave Probe

WAVE PROBE

DIMENSIONS IN mm
3rd ANGLE PROJ.

All these measurements were recorded on a pen recorder. An example of a recording is given in fig.8.2 for a run at a fairly high encounter wave frequency. All the runs were made at, or as near as possible to, 4m/sec. This was a speed which was high enough for stable flight to be attained while sufficient run time in the limited length of the tank was allowed for a reasonable analysis to be made. Runs were made in regular head and following seas of a frequency of just over 1 rad/sec to a frequency of 8 rad/sec. The following sea tests were achieved by running the model in the reverse direction along the tank, that is by starting at the wave maker and proceeding to the beach. In addition a few runs were made in each direction in irregular waves.

Each run was categorised by a run number and the analysis was made from the pen recorder tracings. From the recordings taken on the carriage, values of encounter wave frequency and amplitude, the heave amplitude, phase lag and mean offset, the heave acceleration, the pitch amplitude phase lag and mean offset and the mean drag and the amplitude of the oscillation of the drag values were noted. Another pen recording which did not move with the carriage and model provided values of the actual wave amplitude and frequency. A note was made of the steady state velocity of the carriage.

Response amplitudes and phase difference values were analysed as if the oscillations were sinusoidal. This was

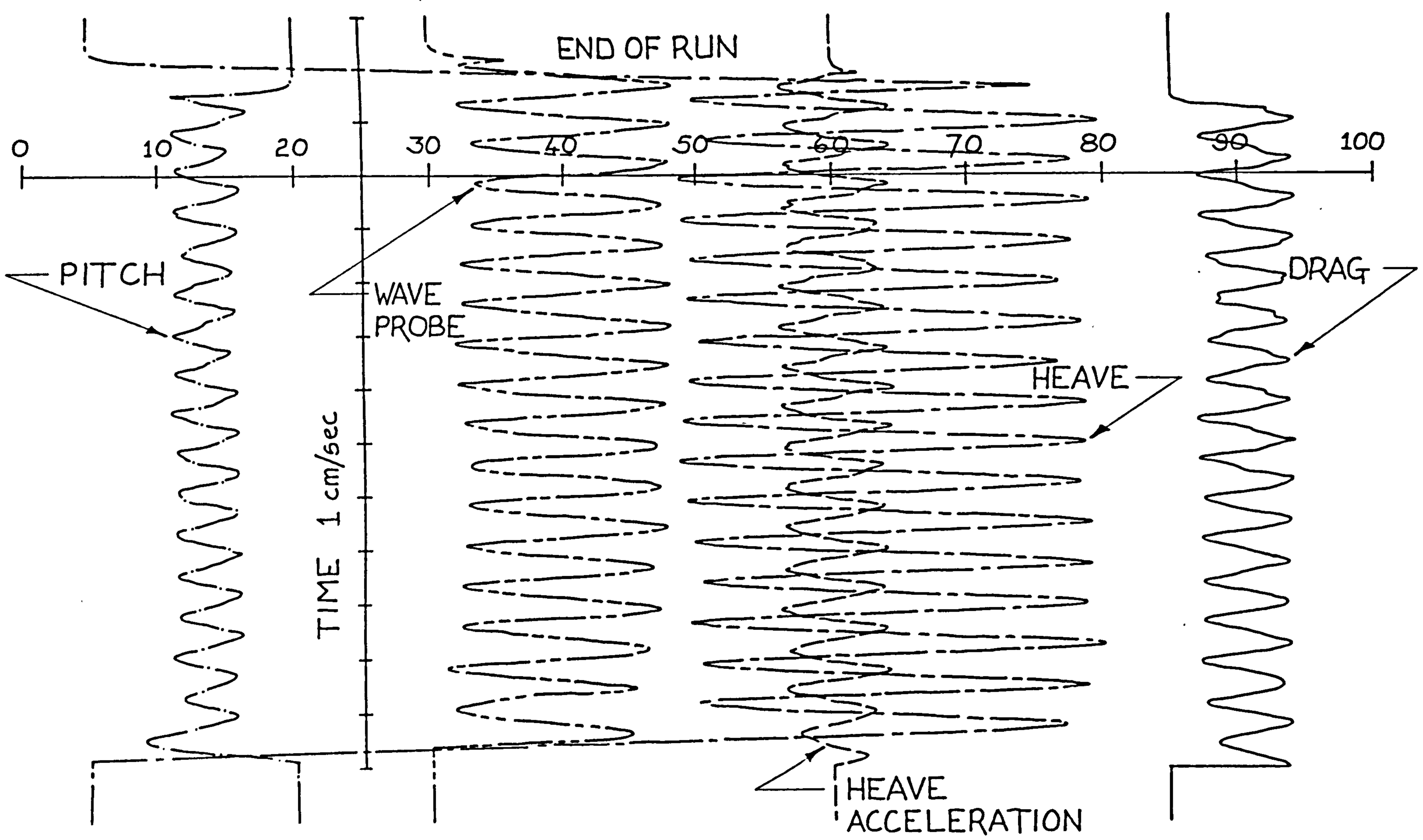

Fig. 8.2 Head Sea Wave Frequency 3.46 rad/sec - Model Speed 4 m/sec

the approach used also when comparing the theoretical time-domain calculation results with the experiments. In practice neither of these responses were true sinusoids, but it can be seen from figure 7.1 (theory) and figures 8.2 and 8.3 (experiment) that any errors associated with this approach would be small. In regular waves direct comparisons between response records and theoretical output would therefore have been unnecessary and would have clouded the discussion of the results over the whole frequency range. In irregular seas direct comparisons between records would have been the only method of analysis for the very short experimental runs possible at these speeds in a tank of restricted length. Although the theoretical calculations were not extended to include irregular seas this would have been a logical and straightforward addition to the existing calculations in the time-domain.

For convenience each run was also allocated a quality categorisation. This was necessary because not all of the input waves and heave and pitch responses were well behaved. To a certain extent this was expected, because the strongly non-linear nature of the hydrofoil problem would be expected to produce non-linear output responses even from sinusoidal input waves. In some cases, in particular at the low wave frequencies below about 2.5 rad/sec, the input waves were not truly sinusoidal. In other cases the lifting foils would suffer from sudden ventilation (partial or otherwise) and a crash would occur

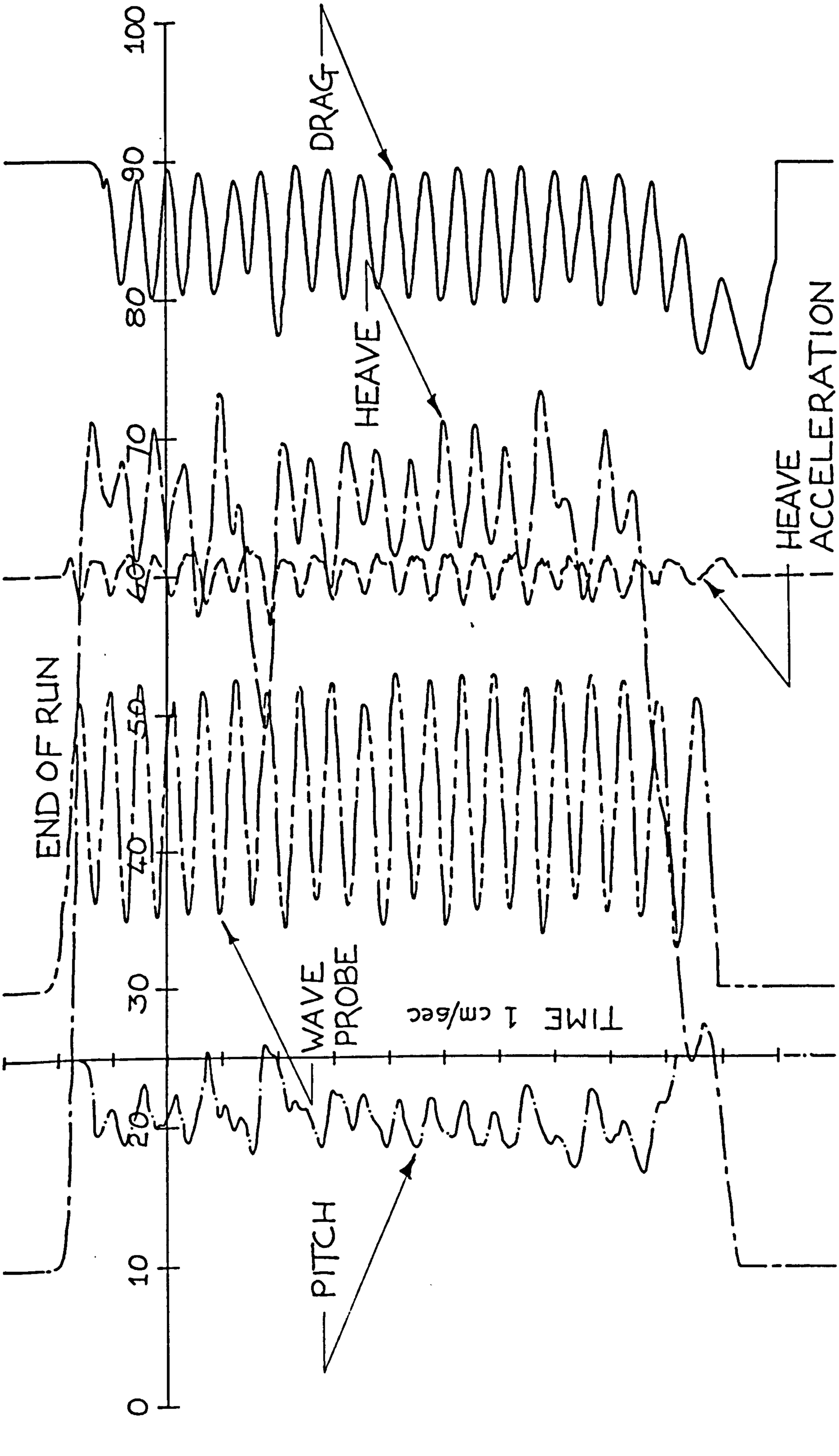

Fig. 8.3 Following Sea Wave Frequency 6.6 rad/sec - Model Speed 4 m/sec (Classified G2)

although the model never crashed to the extent that the hulls were fully re-immersed. Each run was given a mark from G for good, through G1,G2 to G3 for bad. Fig. 8.2 is an example of a good run, G, and fig. 8.3 is an example of a run which was classified as G2. These categories were not marked on the graphs of the results, but they were used for the discussion of trends in the results.

Runs were made mainly for a wave amplitude around 0.025m, although a series of runs at higher wave amplitudes (0.035 - 0.045m) were also made in each of the two series of tests (head and following seas). It was not possible to guarantee the exact wave amplitude before a run and the actual wave amplitudes experienced varied over a small range. Values of heave, pitch and oscillatory drag amplitudes were normalised because of this by dividing the actual results by the wave amplitudes in which they were made. By applying this procedure to the results from runs at a larger wave amplitude also, it was possible to plot these values alongside the values for a wave amplitude of 0.025m. An indication could be obtained from these plots of the degree of linearity of the response with wave amplitude.

Results

The plot shown in fig. 8.4 is of the encounter wave frequency against the actual wave frequency and it serves as a check on the operation of the two wave probes. Apart

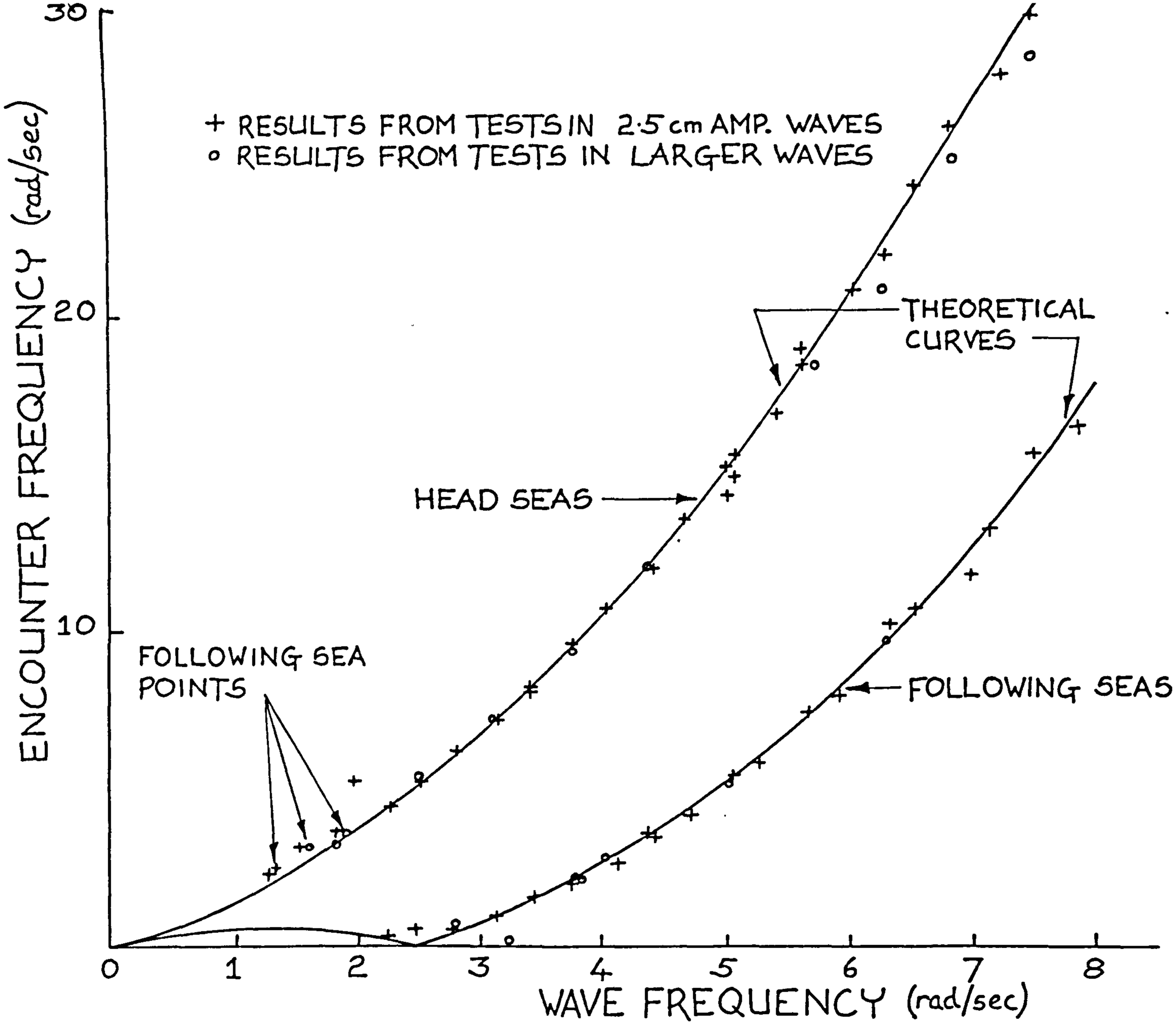

Fig. 8.4 Variation of Encounter Frequency with Wave Frequency for the Test Speed of 4 m/sec

from a few points at very low encounter frequencies in following seas the agreement between these points and the theoretical curves is very good. This indicated that the wave probe on the carriage could be relied upon for measurements of frequency even though it was known that at high encounter frequencies it would under-read values of wave amplitude.

Graphs of heave response, heave phase difference, pitch response and pitch phase difference are given in figs 8.5 a,b,c,d and figs 8.6 a,b,c,d for head and following seas respectively. In these graphs the experimental points are plotted alongside the various theoretical methods. Table 8.I shows the breakdown of the total number of runs made into their respective quality categories for the head and following seas test series. A quick glance at this table shows how in general the head sea test results are of a better quality and hence more reliable than the following sea test results. In the head sea tests over 66% of the runs are above the middle G1-G2 quality division whereas for the following sea tests 76% of the runs are below this division. This must be borne in mind when considering the standard of the agreement between the experiments and the theoretical predictions. The poorer quality of the following sea test results are a characteristic of the more erratic behaviour of the model in following seas.

TABLE 8.I

Run Category	Head Seas Test Series No. of Runs	% of Total	Following Seas Test Series No. of Runs	% of Total
G	13	$33\frac{1}{3}$	3	8
G1	13	$33\frac{1}{3}$	6	16
G2	6	$15\frac{1}{3}$	15	41
G3	7	18	13	35
Total No. of Runs	39		37	

Head Sea Response

Figure 8.5a is a plot of the heave response/wave amplitude against the actual frequency of the regular waves. It can be seen that all of the results, including some from an earlier trial series of tests, fall within a fairly well behaved band which can be taken as an indication of the scatter in the experimental data. The results at higher wave amplitudes exhibit a slightly greater scatter than that for the results at the wave amplitude of 0.025m.

The theoretical curves can be broken down into six different approaches;

1. The linearised approach which was described in detail in chapter 6. This is a solution of the linear coupled heave and pitch equations with constant coefficients.

2. The non-linear quasi-steady approach which was described in the first part of chapter 7. This is a solution of the non-linear coupled heave and pitch equations with time dependent coefficients.

3. The non-linear approach, as in Approach 2, but incorporating the effects of unsteadiness or 'time delay' components (chapter 7).
   The effects were considered to act on the changes

in immersion depths and the changes in trim, as well as on changes in the sinking speed or the angle of attack of the foil elements.

4. A non-linear approach as in Approach 2, but with the inclusion of the surge equation (chapter 7). This is a solution of the coupled heave, pitch and surge equations.

5. A single degree of freedom approach, applying a linearised equation with constant coefficients.

6. A non-linear approach incorporating unsteadiness effects as in Approach 3, but where the time delay varied over the frequency range and where an allowance was made for hull/wave slamming in following seas.

For the heave response curve (fig. 8.5a) it can be seen that the linear approach, Approach 1, has a resonant peak at a wave frequency of just over 3 rad/sec which indicates a response of double that observed from the experimental results. At higher wave frequencies above 4.5 rad/sec, the agreement between this linear method and the experiments is good. The non-linear method of approach 2, is in general a better prediction over the whole frequency range, but in this case, the response is under predicted in the range of wave frequencies from 2 to 4 rad/sec and over predicted in the range 4.5 to 7 rad/sec.

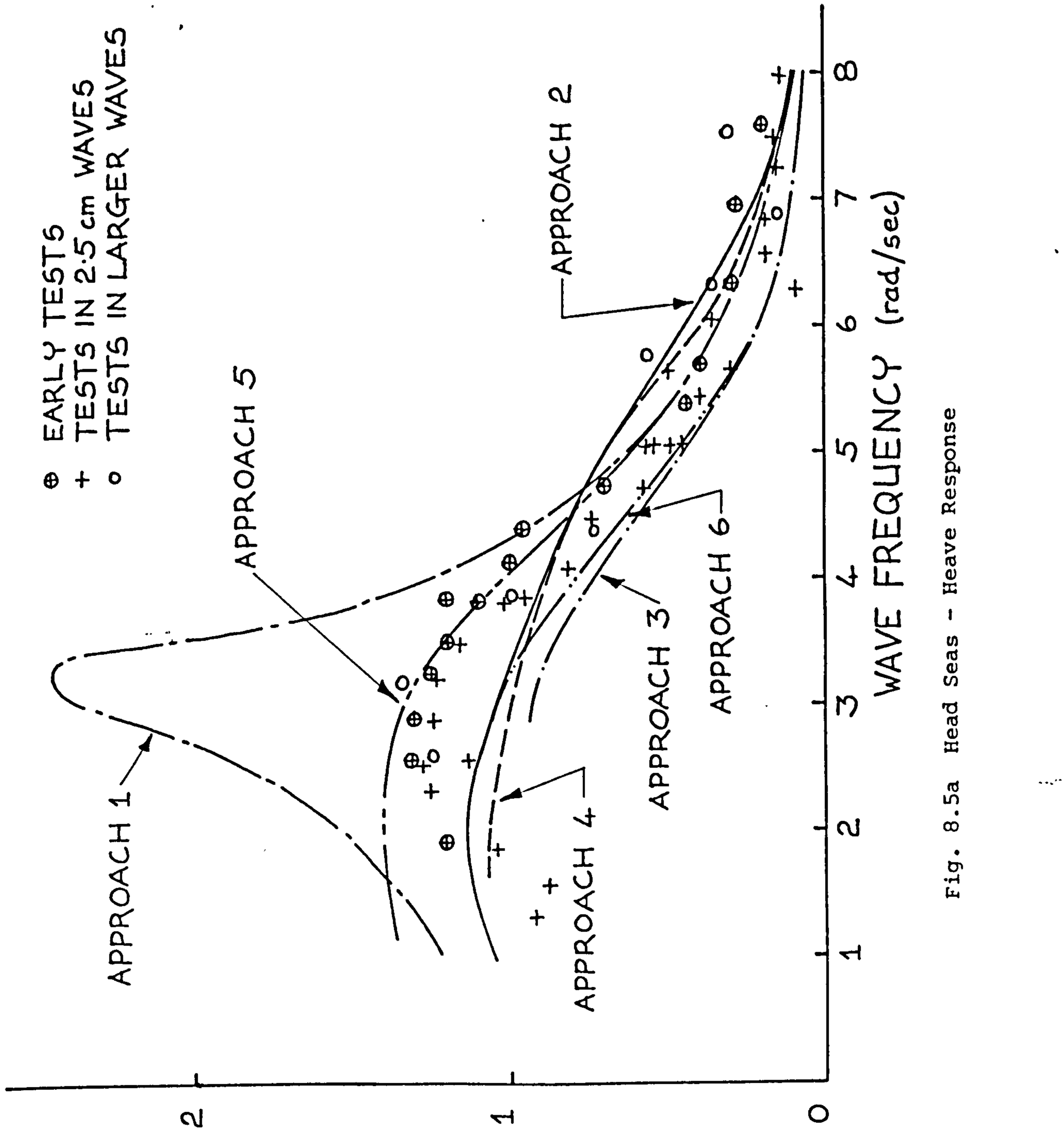

Fig. 8.5a Head Seas - Heave Response

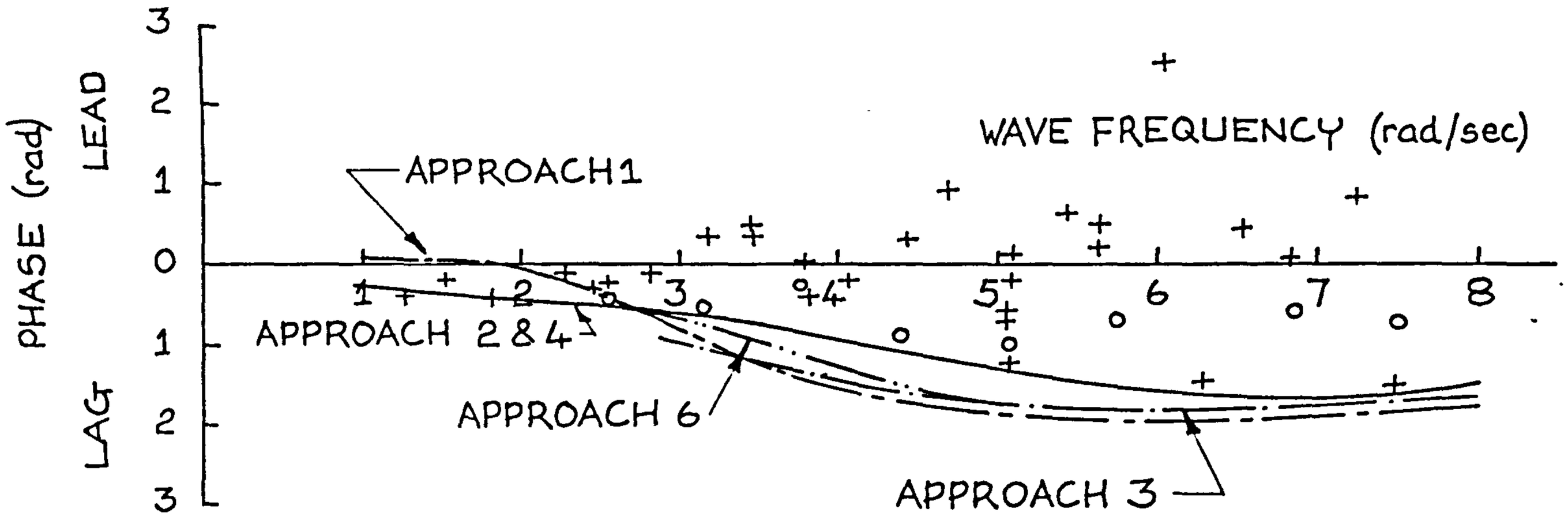

Fig. 8.5b Head Seas - Heave Response (Phase)

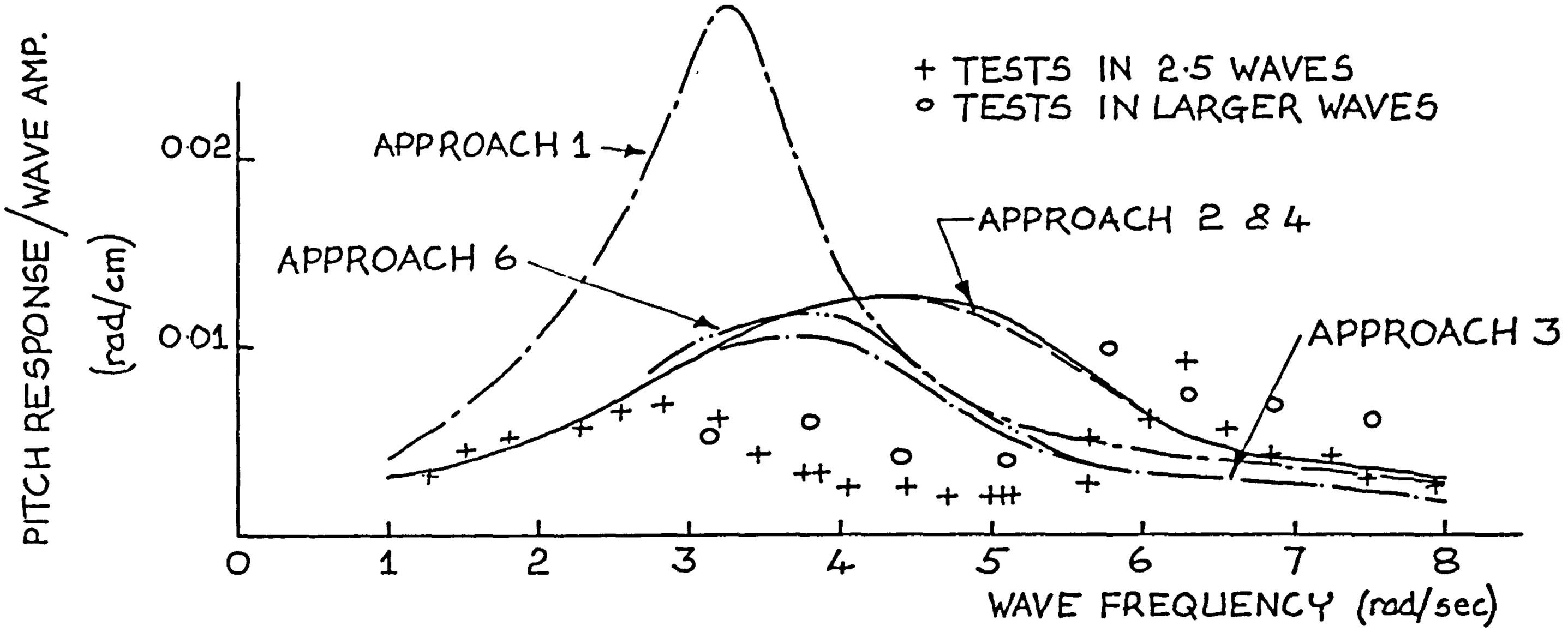

Fig. 8.5c Head Seas - Pitch Response

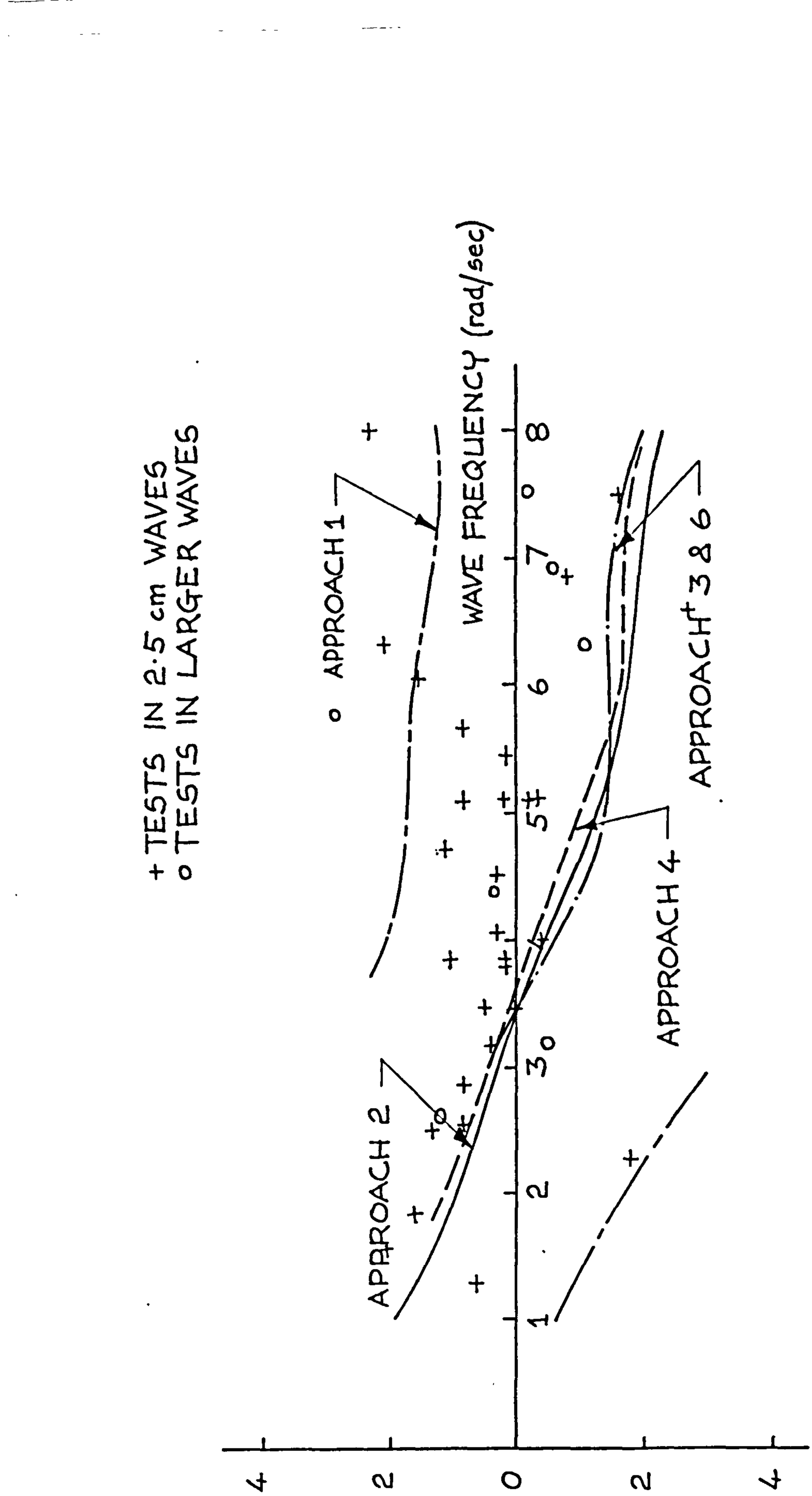

Fig. 8.5d Head Seas - Pitch Response (Phase)

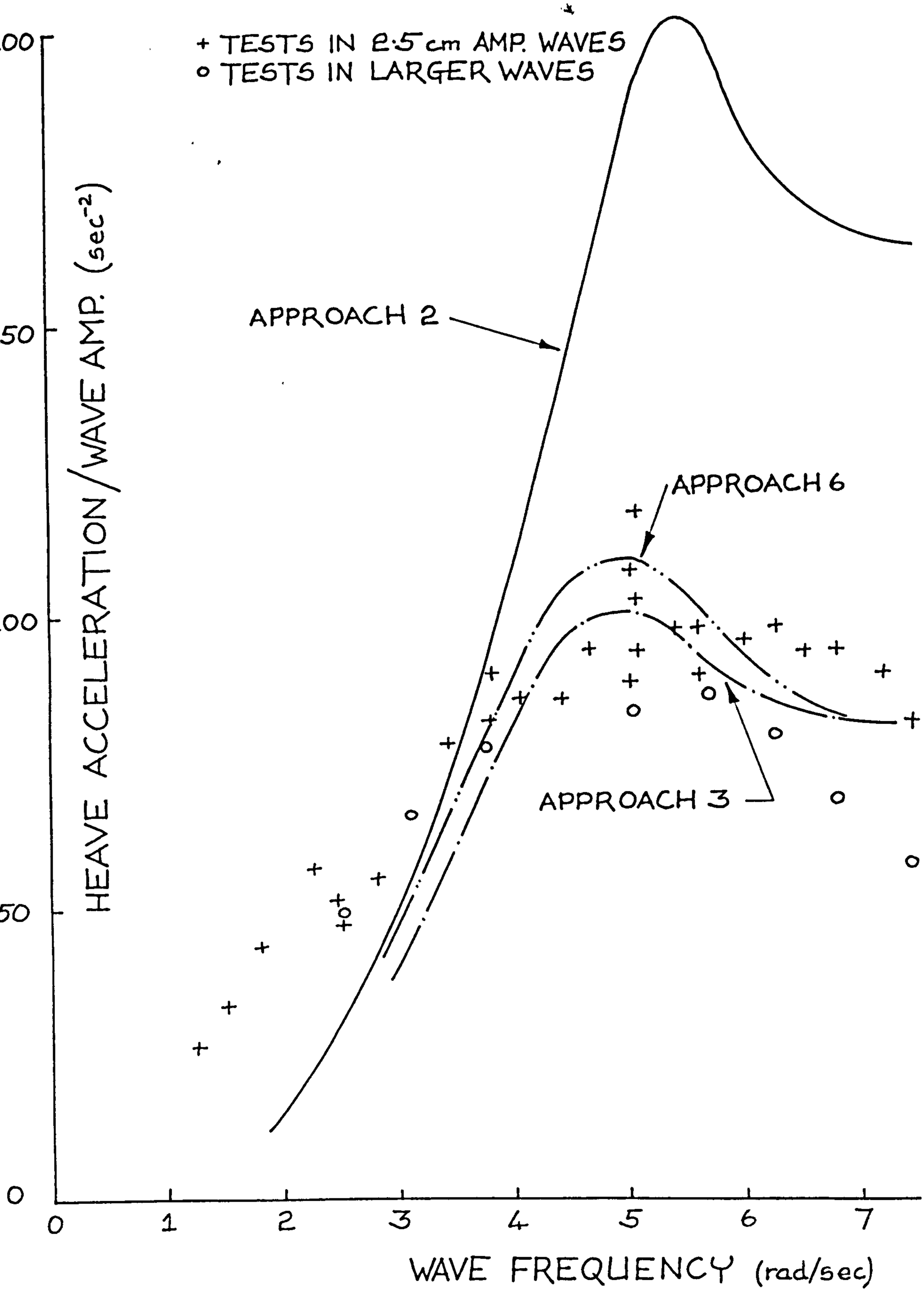

Fig. 8.5e Head Seas - Heave Acceleration

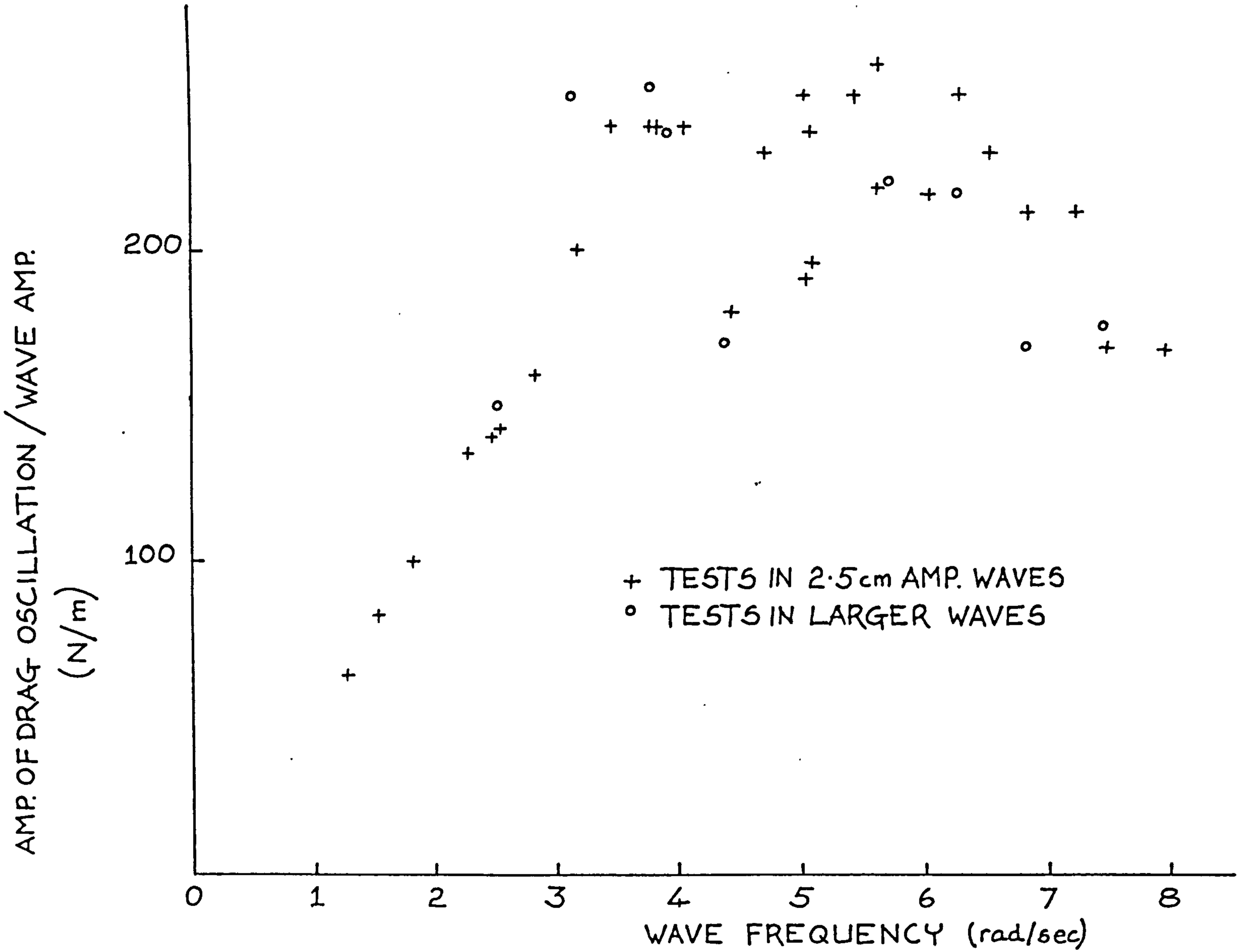

Fig. 8.5f Head Seas - Drag Response

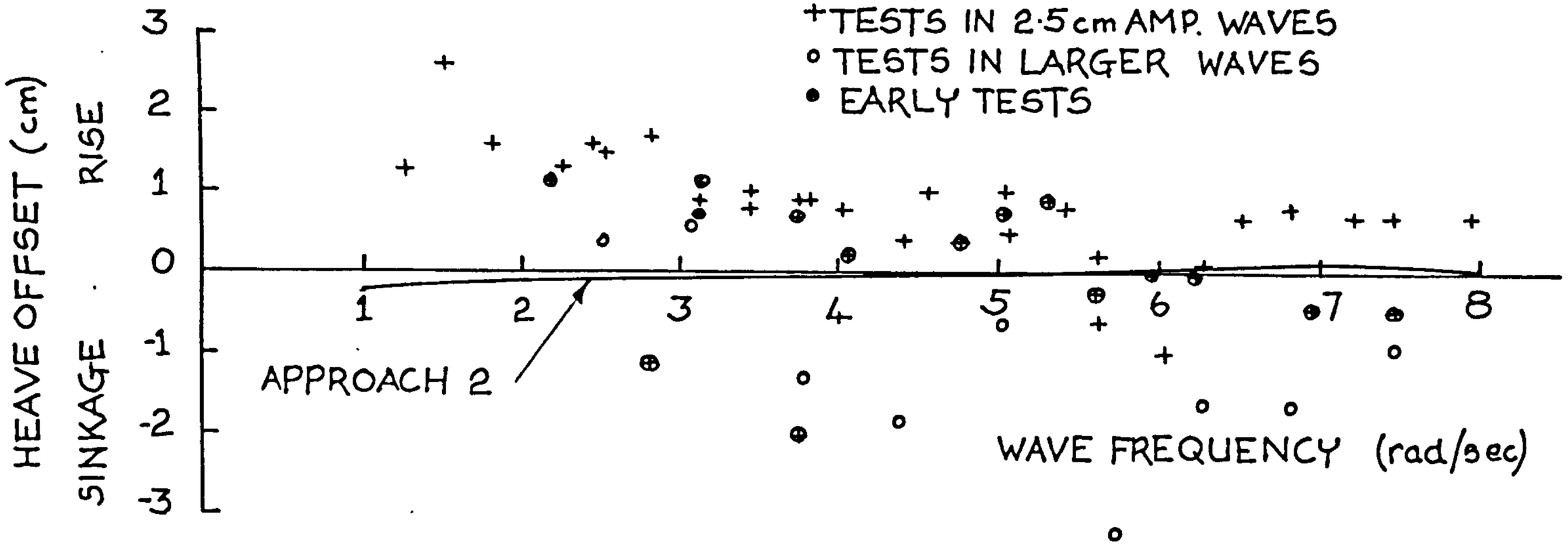

Fig. 8.5g Head Seas - Heave Offset

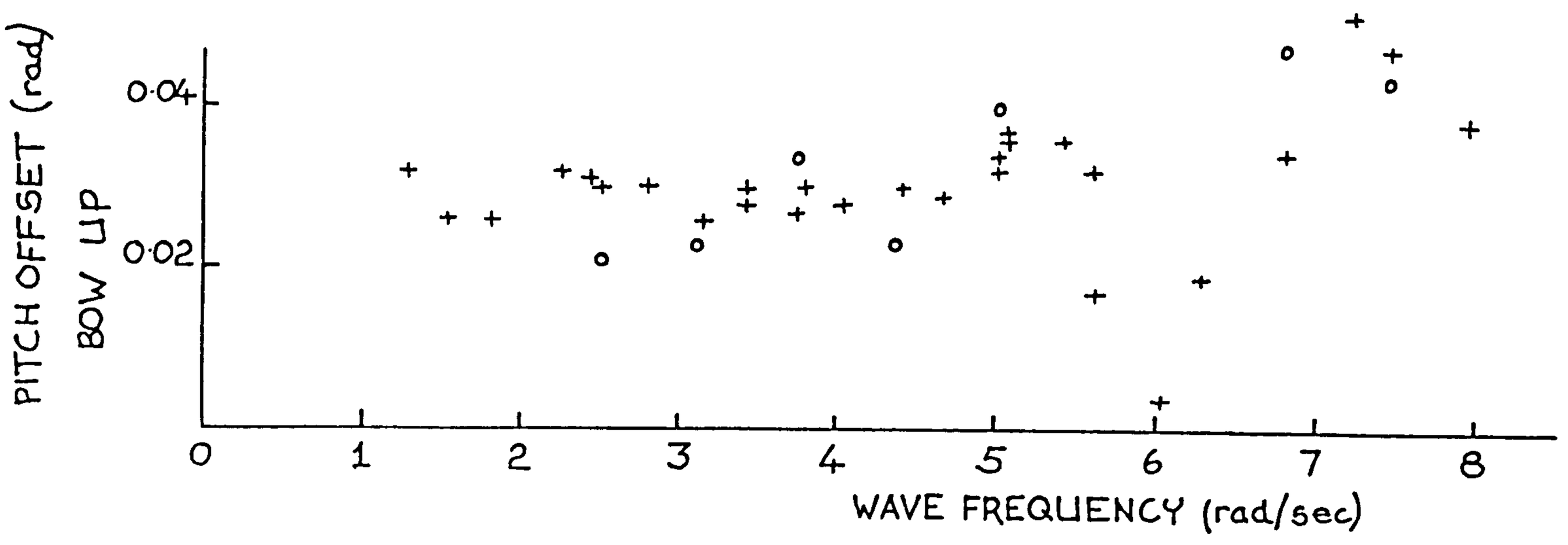

Fig. 8.5h Head Seas - Pitch Offset

The effects of unsteady flow were calculated at a constant 'time delay' value of 0.005 secs (Approach 3, chapter 7). The value of these effects would in reality vary from having almost no influence at low wave frequencies to having a large influence at high frequencies. To take account of this , the 'time delay' value should strictly vary in some way from a high value at low frequencies to a low value at high frequencies. Since the way in which this should occur was not known, a constant value was chosen, and the two curves with and without unsteadiness effects can be considered as an envelope, the response tending towards the corrected curve at high frequencies and the uncorrected curve at lower frequencies.

Approach 6 is an attempt to quantify this variation in the unsteadiness correction over the frequency range. In this approach the time delay factor was assumed to be a function of the encounter frequency, and an empirical expression for this function which fitted the experimental data of these tests was formulated as (figure 8.7):

$$\text{Time delay, } t, = \frac{1}{100\ (\omega_e - 7.9)} + 0.0045 \quad \text{for } \omega_e > 8 \text{ rad/sec}$$

$$\text{Time delay, } t, = 0.1 \quad \text{for } \omega_e < 8 \text{ rad/sec}$$

A time delay of 0.1, because of the the exponential decay nature of the indicial lift functions, meant that there was effectively no unsteadiness correction. As the time delay factor reduced with increasing encounter frequency, the correction became more and more important. The results found from the calculations of this approach are also plotted in the graphs of the response.

Approach 4, which incorporated the surge equation into the analysis shows how the addition of this extra degree of freedom has a very small effect on the computation of the response in all cases, both in head and following seas. This result justifies the neglect of the surge equation in the majority of calculations.

Approach 5, the single degree of freedom solution, assumed an equation of motion in heave of:

(Mass+Added Virtual Mass)$\ddot{z}$ + (Damping Coeff.)$\dot{z}$ + (Spring Constant)$z = Z_1 \sin \omega_e t$

where Z_1 is the amplitude of the forcing function in heave. The damping coefficient and the spring constant were taken as the derivatives $Z_{\dot{z}}$ and Z_z which were calculated from the methods described in chapter 6 (Table 6.I of chapter 6). The Z_1 values, the amplitudes of the forcing functions were the same as those used in heave for the solution of the linear coupled equations of motion. (chapter 6). The equation became:

$$(-5.2 - 0.4329)\ddot{z} - 82.59\dot{z} - 532.9z = Z_1 \sin \omega_e t \qquad (8.1)$$

where the mass of the model is 5.2kg and the added virtual mass is 0.4329kg. The sign convention is the same as that of equation 6.10 of chapter 6. This equation was solved in the normal way and gave the curve shown in fig. 8.5a. This curve agreed suprisingly well with the experimental results at all wave frequencies above 3 rad/sec. This indicates that this approach is a good method for preliminary response studies, but any results obtained in this fashion must be treated with caution. Note that the agreement is not so good for the following sea test series.

Figure 8.5b shows the values of the phase differences of the heave response. All the methods used here agree with each other, but the experimental points above a wave frequency of 4 rad/sec could not be relied upon because at these high encounter frequencies small errors in lifting off data from the pen recordings made large differences to the phase results. The phase results agree with the predictions up to a wave frequency of 3 rad/sec , but above this frequency there is a large amount of scatter in the results. (The phase results for the following sea test series are more consistant because of the lower encounter frequencies experienced (figs 8.6b,d).)

Figure 8.5c shows the results of the pitch response. These results were normalised by dividing by the wave amplitude and again the plot is against the actual wave frequency. The method of non-dimensionalising the pitch

results by dividing through by the maximum wave slope was rejected because of the distortion this produced by introducing an ω^2 term. The agreement between the experiments and the theoretical methods 2,3,4 and 6 is shown to be good at wave frequencies from 1.0 to 3.0 rad/sec and from 6.5 to 8.0 rad/sec. In the wave frequency range from 3.0 to 6.5 rad/sec the response actually obtained was very much lower than that predicted. Again the methods of approaches 3 and 6 are seen to give the best predictions. The linearised methods of approach 1, predict a much higher response than that obtained except at the higher wave frequencies above 6.5 rad/sec where the agreement is good. The experimental results from a higher wave amplitude show in general a larger pitch response which indicates that the pitch response is not linear with wave amplitude.

The pitch phase difference results are shown in fig. 8.5d. As for the heave results, the predictions are seen to be reasonable up to 3.5 rad/sec, at least for approaches 2,3,4 and 6. Above this wave frequency a large amount of scatter is again apparent in the results. The prediction from the linearised solution of approach 1 shows a difference with respect to the non-linear approaches of approximately π and this could account for the poor prediction of the pitch response obtained using this method (fig. 8.5c).

Normalised heave acceleration values

(acceleration/wave amplitude) were plotted against wave frequency in fig. 8.5e. These results corroborate the results of the heave response curve, and they emphasise how bringing in the effects of unsteady flow into the solution corrects the prediction. The curves are for the non-linear approaches 2,3 and 6. The agreement between the corrected curves and the experimental results are good above 4.0 rad/sec. Below this wave frequency, the acceleration values are under predicted which explains in part the under-prediction of the heave response in this region.

The drag response in head seas, again normalised by dividing the results by the wave amplitude, are shown in fig. 8.5f. Only experimental points are shown. The mean value of the drag is 9.0-9.5 Newtons. For the tests in waves of amplitude 0.025m, this shows the large value of the oscillation in the drag values, which reach in some cases almost 7.5 Newtons. To a certain extent these results must be dependent on the characteristics of the towing system, that is the tow wire and strain bar. The oscillation is shown to be greater in following seas where the model behaviour is more erratic (fig.8.6f), and during some experiments the tow wire went slack over a part of the cycle. (i.e. the oscillation exceeds the mean drag of 9.0-9.5N).

The heave offset, the offset of the mean value of the heave oscillation from the position of the height of flight of the model in calm water is shown in fig. 8.5g. The

results are inconclusive because the scatter in the experimental results hides any obvious trends. The theoretical curve from the non-linear calculations of approach 2 show much lower offset values than those found in practice. In general there appears to be a lower mean height of flight in higher wave amplitudes. The experimental values of the pitch offset (the mean trim value) are shown in figure 8.5h. No theoretical curve is shown because the calculated values of the pitch offset vary depending on the value of the thrust force supplied to the calculation. This value of thrust force does not affect the prediction of the response. Its effect is merely to alter the trim position about which the motion is made. The variation in the calculated value of the pitch offset is small over the frequency range.

Following Sea Response

The heave response curves in following seas are shown in fig. 8.6a. It can be seen that the scatter of the experimental data is far greater than was the case for the head sea tests especially at wave frequencies below 5.5 rad/sec. The agreement between the predictions and the experiments is in general rather poor. The best predictions in this case are the linearised solution of approach 1 and the non-linearised approach which includes hull/wave slamming (approach 6). The non-linear approaches 2,3 and 4 under-predict the experimental 'peak' from 3.0 to 6.0 rad/sec and over-predict the response from 6.0 to 8.0

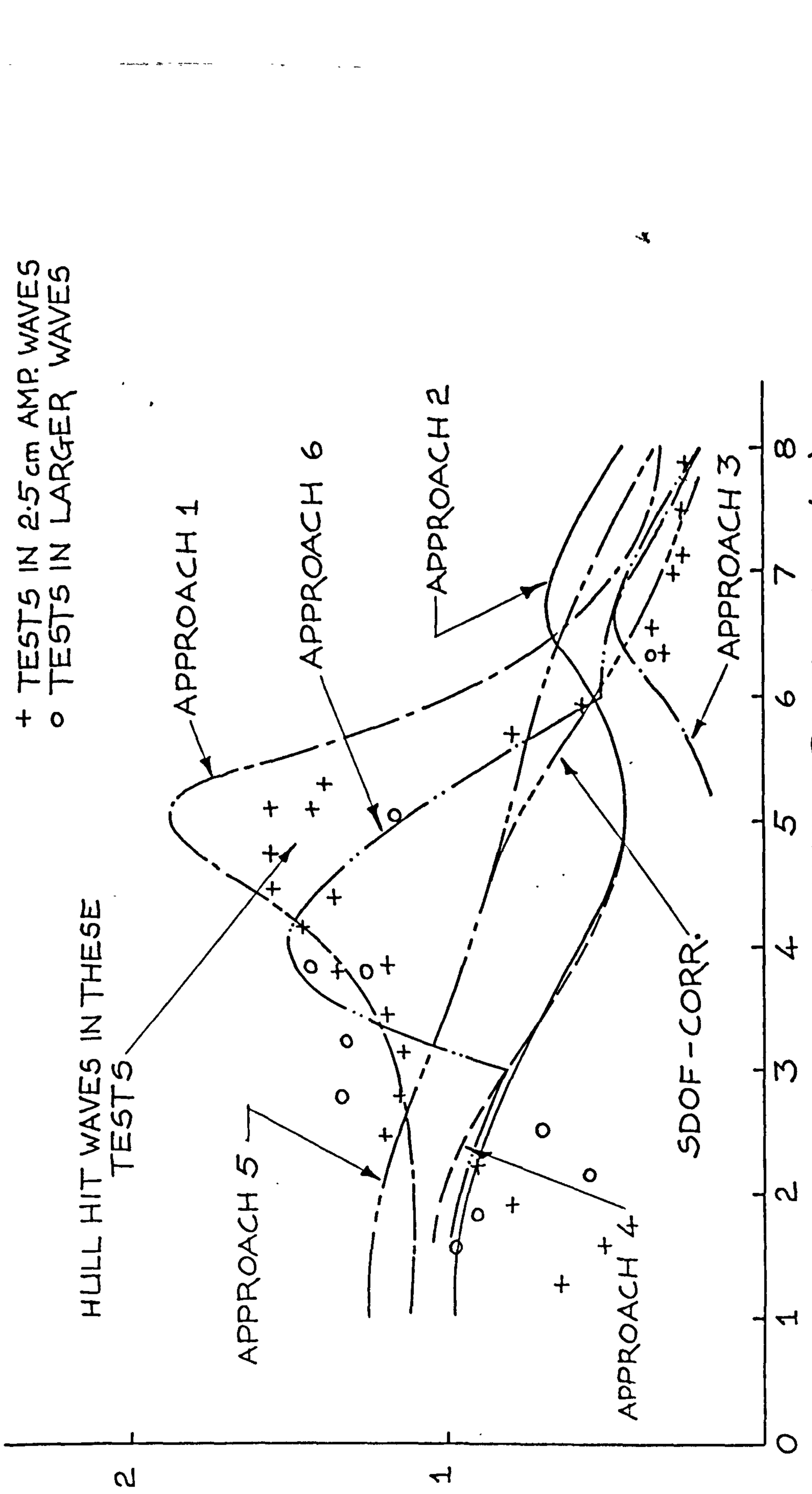

Fig. 8.6a Following Seas - Heave Response

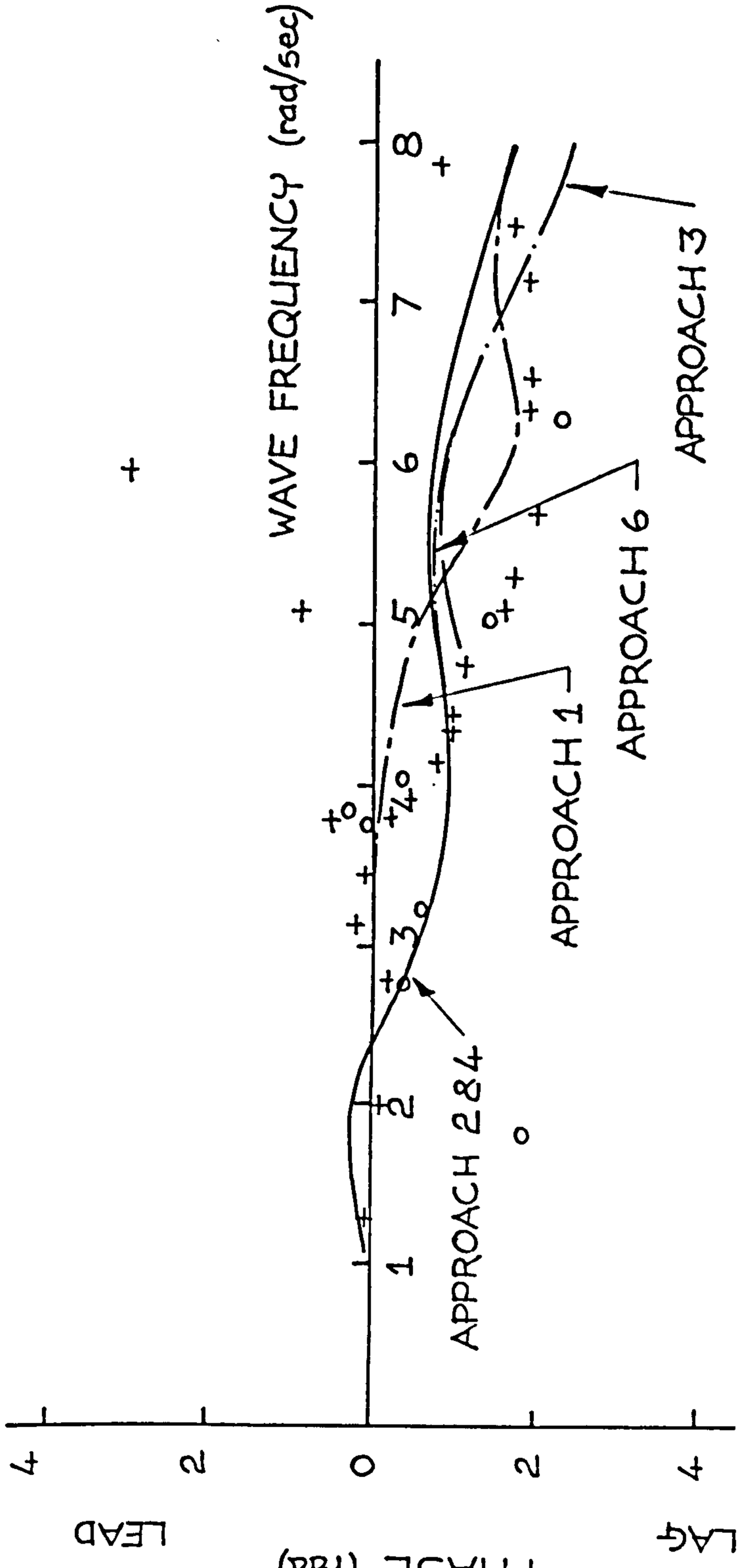

Fig. 8.6b Following Seas - Heave Response (Phase)

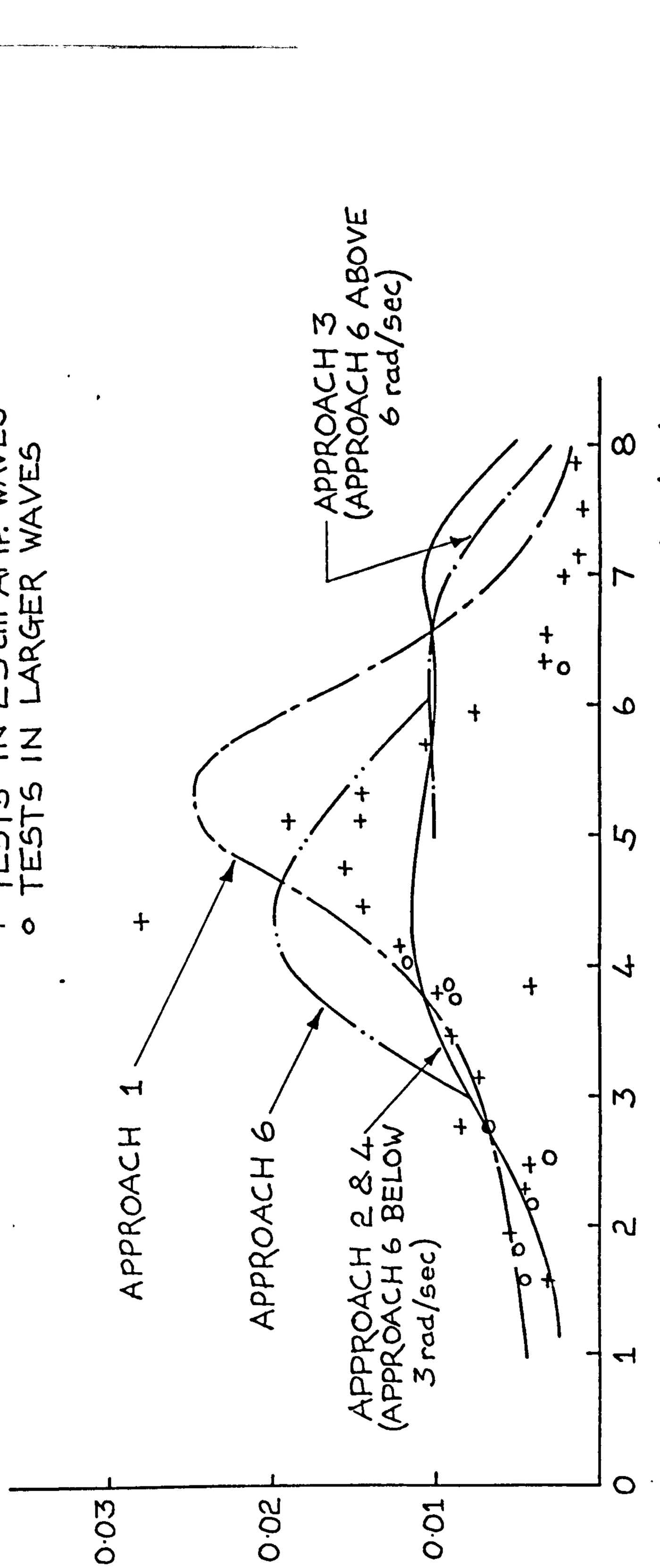

Fig. 8.6c Following Seas - Pitch Response

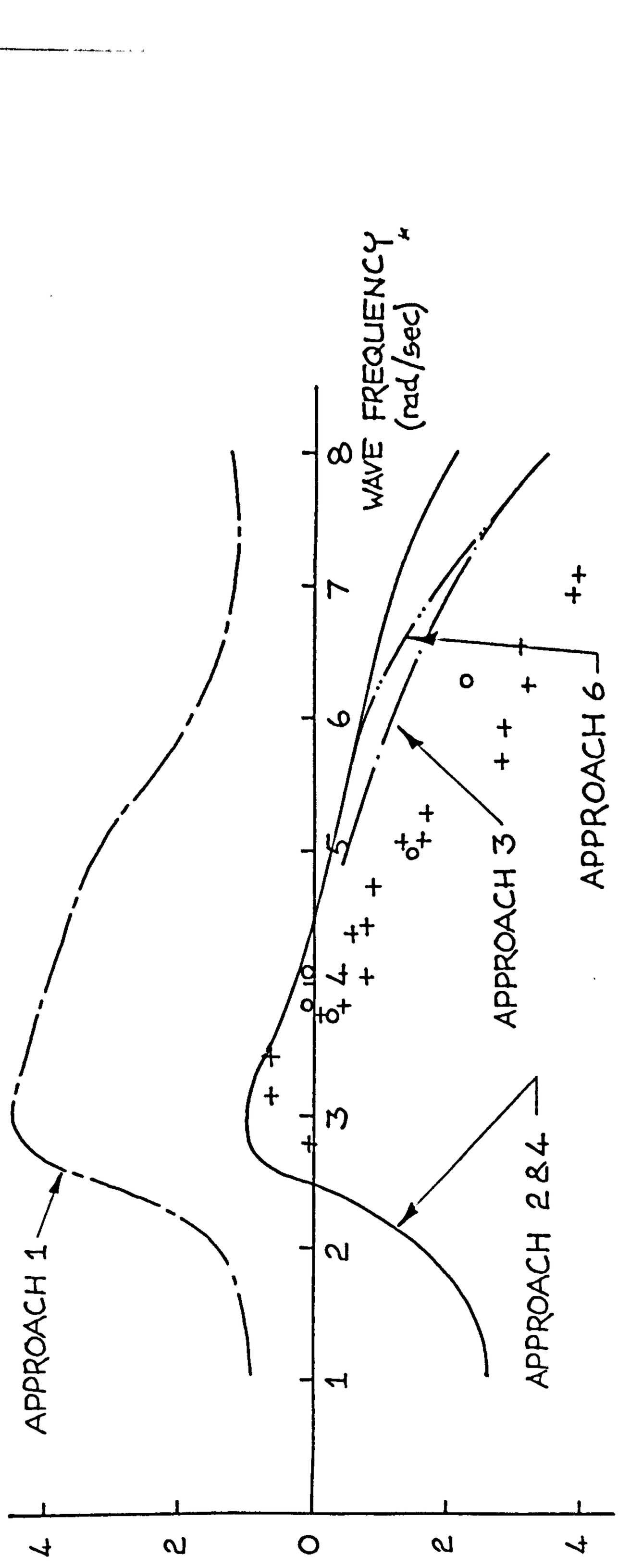

Fig. 8.6d Following Seas - Pitch Response (Phase)

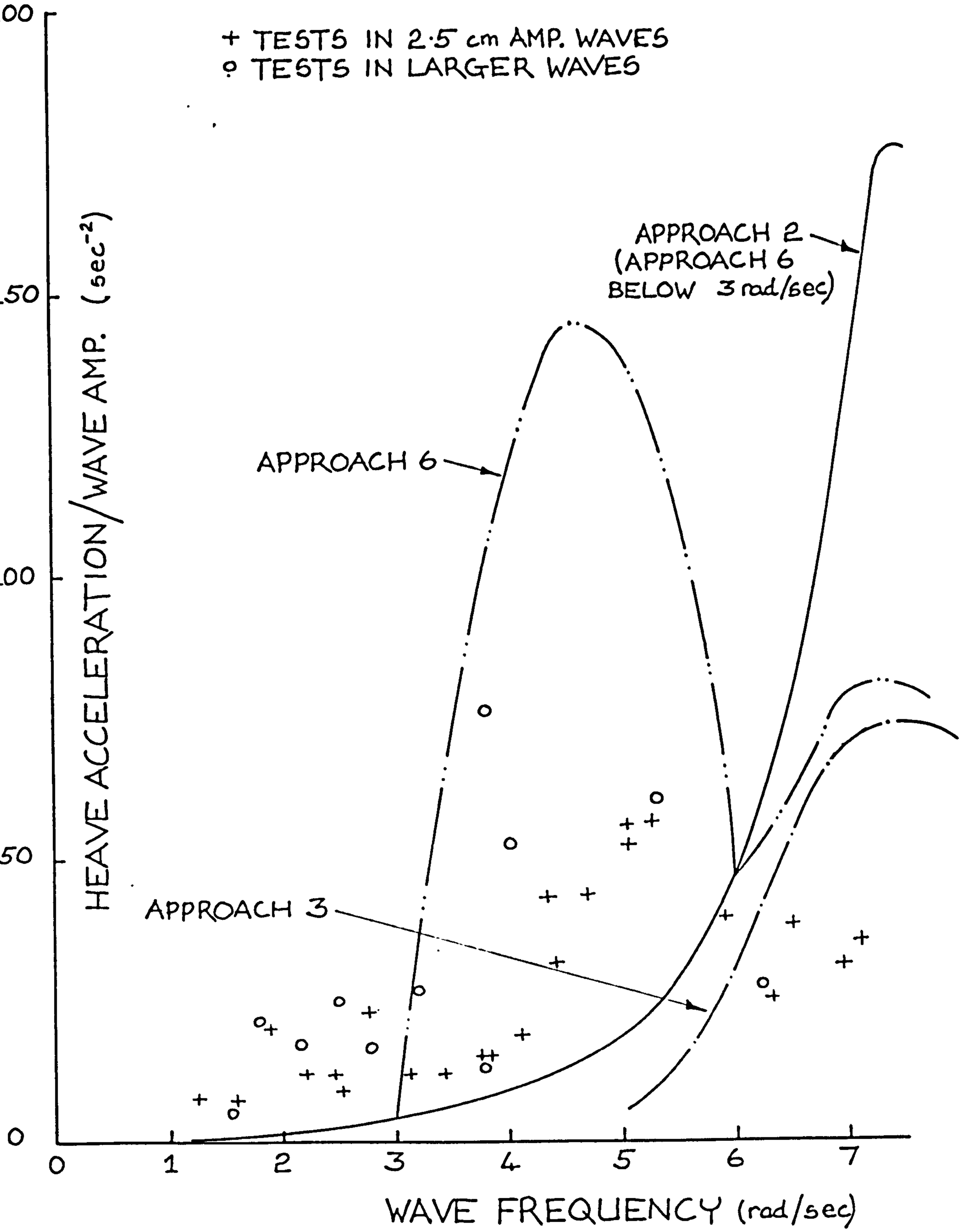

Fig. 8.6e Following Seas - Heave Acceleration

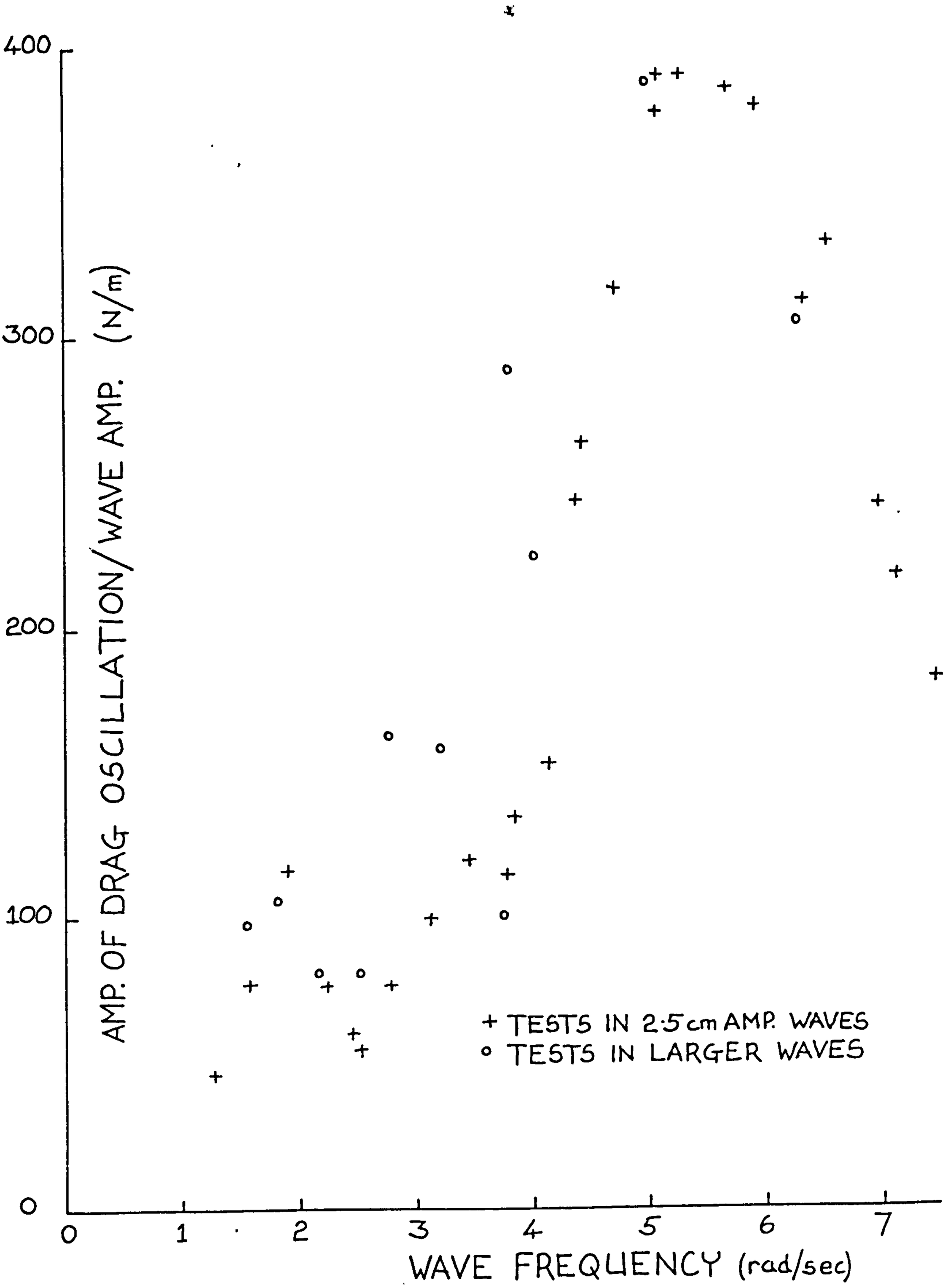

Fig. 8.6f Following Seas - Drag Response

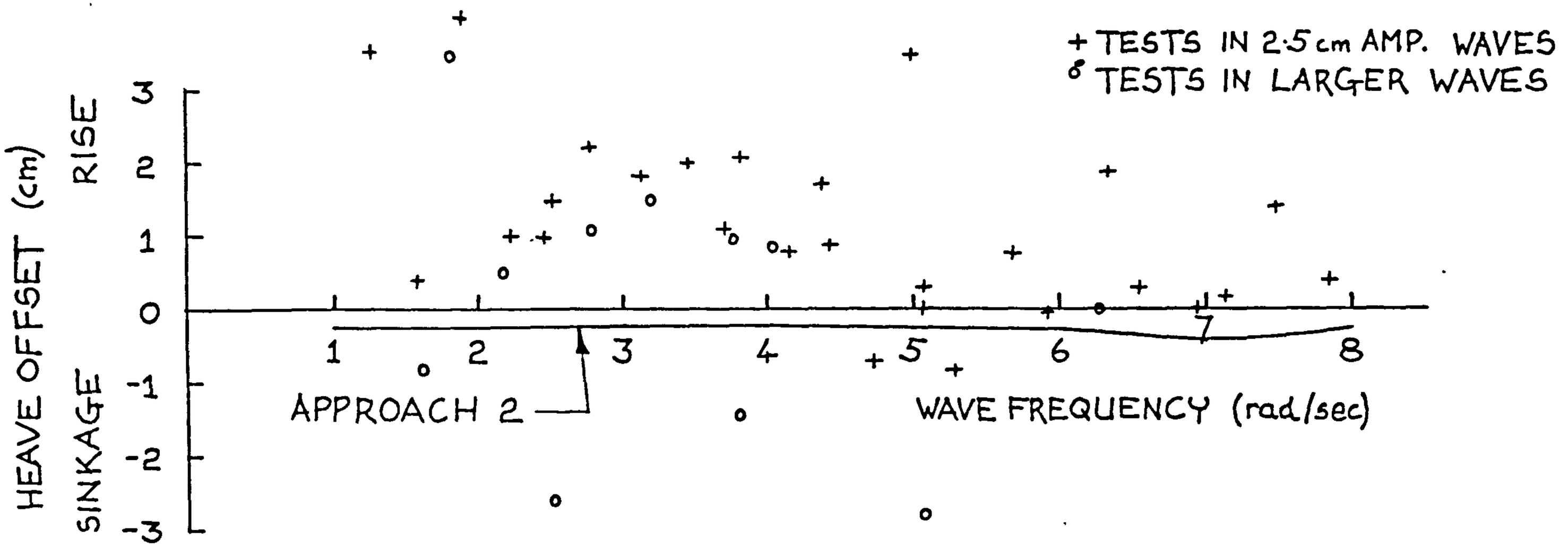

Fig. 8.6g Following Seas - Heave Offset

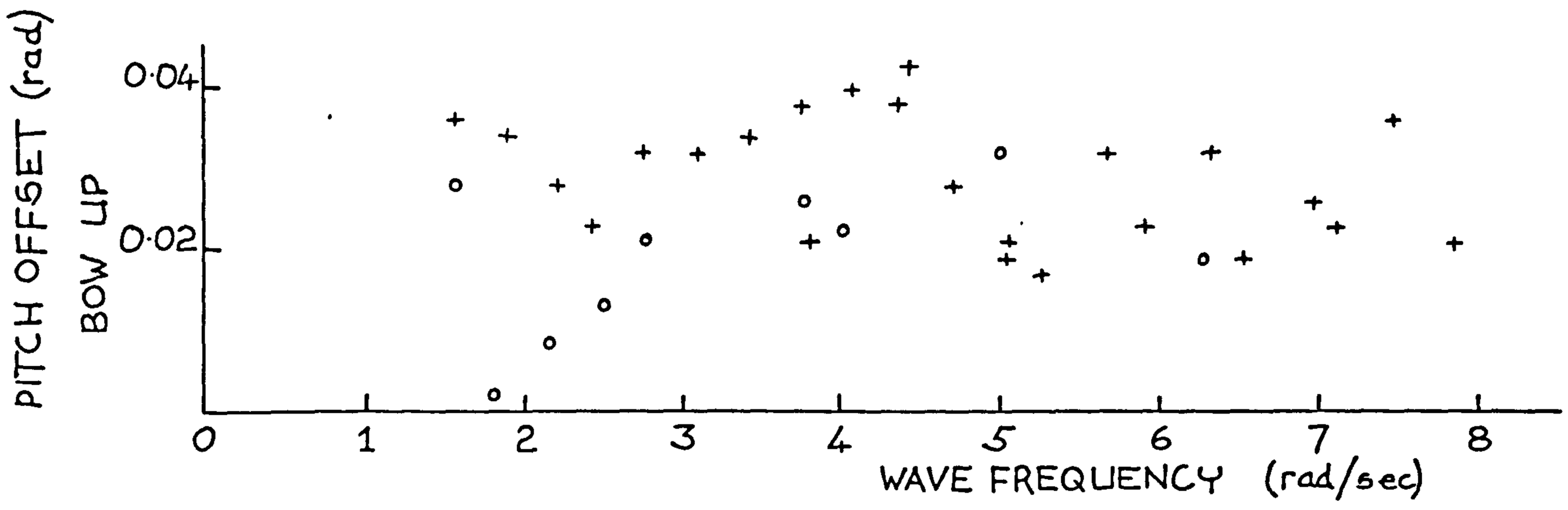

Fig. 8.6h Following Seas - Pitch Offset

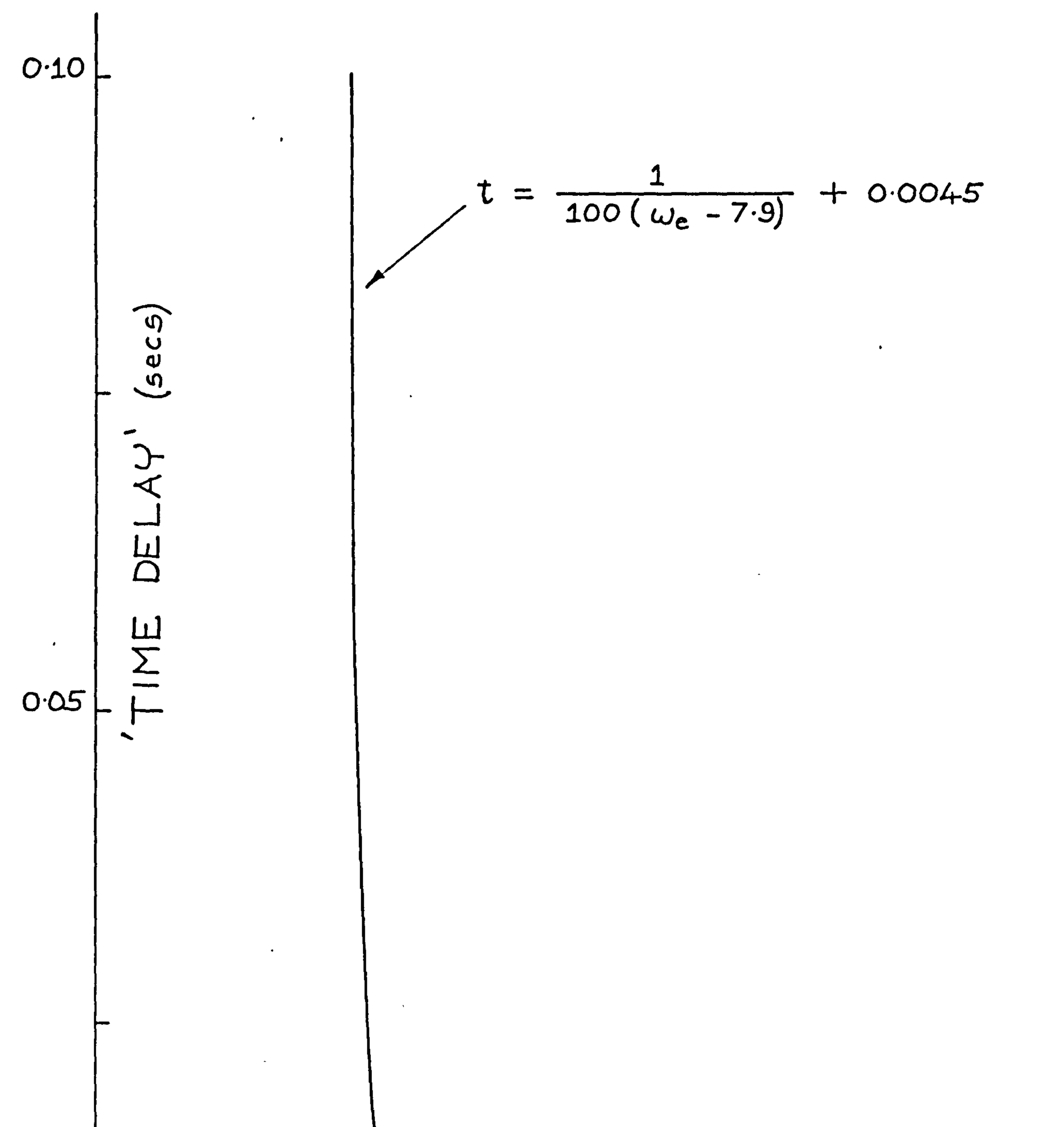

Fig. 8.7 Variation of 'time delay' factor with encounter frequency

rad/sec. The best prediction of these three is given by approach 3 which includes the corrections for unsteady flow , but this is only true at wave frequencies above 6.0 rad/sec. The single degree of freedom method (approach 5) does not in this case give a good prediction, the curve following a middle course between the linear and non-linear solutions.

This rather poor agreement can be explained as the combination of two factors:-

1. Discrepancies in the prediction of the values of the natural frequencies.

2. Neglecting the effects of slamming on the hulls.

The difference in the predicted and apparent values of the natural frequencies of the system explain the peaks in the non-linear prediction curves around a wave frequency of 6.5 rad/sec. From the study of the system as a single degree of freedom problem, the natural frequency in heave was found to be 9.7 rad/sec and from a study of the non-linear heave response curves both in head and following seas it appeared that a natural frequency in heave was predicted somewhat higher than this value, between 10 and 12 rad/sec encounter frequency. A natural frequency value in heave from the experimental results seemed to be lower than the above values, nearer to a value predicted from the linear coupled solutions, about 3-4 rad/sec. The exact

values are difficult to ascertain because of the heavily damped nature of the response.

An explanation for these differences in the natural frequency values can be found by going back to the equation which describes the single degree of freedom system (equation 8.1). The inclusion of the effects of unsteady flow on increases in the depths of immerson of the hydrofoils means an effective reduction in the spring stiffness constant. These effects have been assumed to be mainly dependent on the delay associated with the build up of the circulation around the hydrofoils (chapter 7), but an equally important influence may come from the intermittent ventilation which was observed on parts of the hydrofoils at certain wave frequencies. Taking an extreme case where the correction factor is 0.5(i.e. the spring stiffness is halved), this would reduce the predicted natural frequency in heave from 9.7 rad/sec to 6.9 rad/sec. The forcing functions (Z_1) would also be halved by the same argument and the static displacements (Z_1/spring stiffness) would remain the same. If unsteady forces were incorporated for changes in the angle of attack also, the damping coefficient would be reduced. A correction factor of 0.67 on the damping coefficient would be a reasonable value to correspond with the value of 0.5 chosen for the correction to the stiffness. The magnification factors would alter and the corrected curve is shown in fig. 8.6a also (denoted SDOF-CORR). The curve for approaches 3 and 6 which include corrections for the unsteady flow show a

similar though not such a pronounced trend.

In the wave frequency range from 3.0-6.0 rad/sec the centre hull of the model was seen to collide with the wave crests to a variable degree which was dependent on the wave frequency. The largest amount of this slamming occurred at a wave frequency between 4.0 and 5.0 rad/sec where the largest amplitude of the heave motion was observed. This phenomenon was apparent in following seas because of the more erratic nature of the motion and because of the lower heights of flight realised in following seas. A few calculations were made to ascertain the order this effect would have on the heave response. As a rough first approximation, an upwards force was added into the non-linear calculations which had a maximum of half the model weight at a wave frequency of 4.5 rad/sec. This upwards force was assumed to vary in a parabolic manner either side of this maximum, reducing to zero at wave frequencies of 3.0 and 6.0 rad/sec. The empirical expression of this force was assumed to be given by:

$$\text{Upwards Force} = mg\,[0.5 - (\omega - 4.5)^2/4.5]$$

where ω is the wave frequency

This force was assumed to act for one quarter of the wavelength, symmetrically situated about the wave crests. The results from these calculations which were included into approach 6 for following seas are plotted on the heave and pitch response curves (figs 8.6a, 8.6c). It can be

seen that slamming forces influence the model response to a large extent and it might be concluded that the inclusion of a more detailed analysis of these effects would increase the accuracy of the prediction even further.

The pitch response curve shown in figure 8.6c shows how all the approaches 1,2 and 4 agree well with each other and with the experimental results up to a wave frequency of 4.0 rad/sec. At higher values of wave frequency no one curve shows a superiority over another although the linearised solution (Approach 1) and the corrected non-linear solution (Approach 6) follow the trend of the results best while predicting large differences in the actual values of the response.

The phase difference results for the heave and pitch responses are shown in figures 8.6b and 8.6d respectively. The experimental results are more reliable and show less scatter than the head seas results largely due to the lower encounter frequencies involved. This allows greater precision in the lifting off of the data from the recordings. In most cases the ageement with the theory is reasonable although as in the head seas case, the linearised solution for pitch shows a discrepancy of approximately π with the other methods and the data.

Figure 8.6e shows the normalised heave acceleration results. There is a large amount of scatter in this data which emphasises the erratic behaviour of the model in

following seas. In general the normalised acceleration values are higher in the higher amplitude waves mainly because of the increased frequency of slamming in these waves. As would be expected from the heave response results the non-linear theory under-predicts the acceleration values up to a wave frequency of 6.0 rad/sec. The effects of slamming as built into approach 6 produce a peak in the proper place, but greatly overestimate the accelerations.

The oscillatory drag amplitudes are shown in figure 8.6f. The drag values vary more in following seas than in head seas especially around the region of wave frequencies where slamming is known to occur.

The heave and pitch offset data are given in figures 8.6g and 8.6h. The same arguments apply as were discussed under the head seas response.

Conclusions

The preceding results show how no one method is completely reliable in all cases. In head seas, the best predictions are given by a non-linear approach with correction for the unsteady forces (Approaches 3 and 6). The best predictions in following seas are due to the linearised approach (Approach 1) and the corrected non-linear method (Approach 6). However, since the forcing functions of the linear approach are calculated by assuming

that the craft does not respond to the waves, it was felt that while this method gave good results it was for the wrong reasons. Note that the differences in the predictions between the linear and non-linear approaches are similar both in head and following seas. This indicates that the problem is more fundamental and is probably due to the neglect of some aspects of the calculation in both cases (e.g. slamming or ventilation). The non-linear approach which incorporates corrections to the hydrofoil forces for unsteady flow, allowances for intermittent ventilation (which have not been considered here) and allowances for slamming shows the best agreement with the experimental data and the most promise for further development. Much more information especially from model tests is required on the unsteady force problem for hydrofoils, in particular for those foils which intersect the water surface, in order to ascertain the variation of these corrections over the frequency range.

The empirical variations used here can only be regarded as a first step and they are strictly only applicable for the one hydrofoil model. The correction would be expected to be different on the full scale where the wave frequencies are lower.

The inclusion of the extra degree of freedom in surge was not found to alter the results significantly from those calculated assuming only heave and pitch coupling. Difficulties in the prediction of the value of the thrust

force, which for these calculations was assumed to be constant, meant that it was beneficial to neglect the surge coupling and it was felt that this was justified in view of this result.

Calculations where it was assumed that the craft responded as a single degree of freedom model were found to be useful in determining trends in the results. These calculations can also give good results for initial studies in some cases (note the head sea predictions, fig. 8.5a).

CHAPTER 9

Full Scale Trials - The Future

This programme of work had reached a stage where a prototype boat had been built and tested, where experiments had been carried out on a one quarter scale model of this prototype craft both in calm water and in head and following seas, and where theoretical studies had covered topics which included, calm water performance, stability and flight orientation, wind propulsion performance estimates and seakeeping studies both in head and following seas. The theoretical work and the supporting model experiments had in most cases yielded satisfactory results and the computer programs, in particular those which calculated lift, drag and flight orientation had served as invaluable design tools for the various hydrofoil combinations.

The full scale trials with the prototype boat on the other hand had not yet reached the stage it had been hoped to reach at the beginning of the project. The situation was that a trimaran had been built and tested and had evolved its way through three sets of hydrofoils. The most recent set of these foils was an aeroplane configuration (chapter 2) with two main lifting foils mounted on the

forward crossbeam and an inverted tee foil at the stern which served as a 'tail plane' for trim control and as a rudder. The main foils were constructed from glass reinforced plastic (uni-directional rovings), but the stern foil was still a wooden construction. This configuration of hydrofoils, which was essentially very similar to that of 'Mayfly' and the most recent version of 'Icarus', had turned out to be the most successful for 'Kaa' also. On her last day of trials with this system, speeds well in excess of 15 knots had been reached before the pintle system of the rudder foil had failed. The boat had manoeuvred well both on and off the foils and had been easily handled under single handed control.

The logical way forward from here would be to rebuild the boat (one of the floats was subsequently holed and some damage was sustained by one of the main foils during a storm) and to reconstruct the hydrofoil system. This would include the replacement of the lower inclined main lifting foil elements of the side foil units with a carbon fibre reinforced equivalent. The method used by Dowty Rotol Ltd., (156) for the construction of air propeller blades although not directly applicable, might be suitable for development here, figure 9.1. The cantilevered tips of these foils could be made with a slightly higher aspect ratio and hence have a higher lift/drag ratio because of the higher strength of carbon fibres and they would be fitted with nose fences for the suppression of ventilation at regularly spaced intervals throughout their span. The

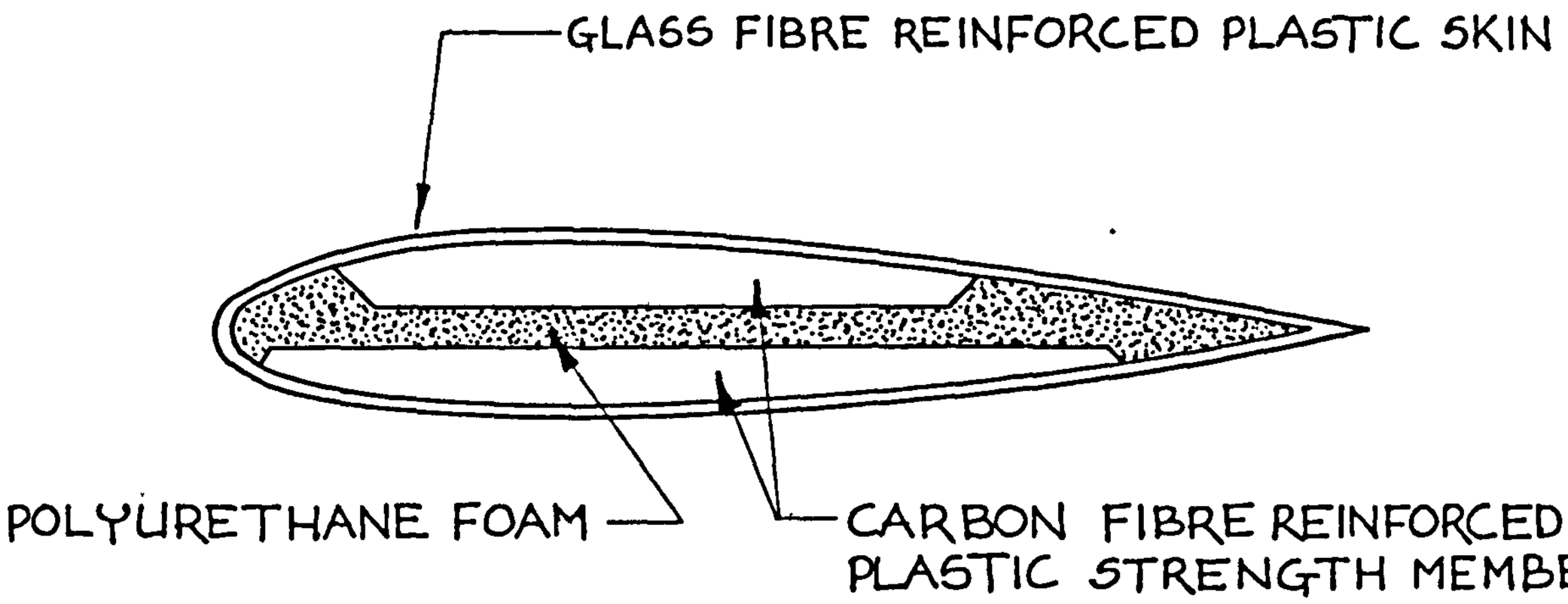

Fig. 9.1 Possible Lay-up for Hydrofoil Laminates

bracing and angle of incidence settings of these foils would be made in such a manner that fine adjustments could be made to the angle of incidence during the trials.

The stern foil would be reconstructed from glass reinforced plastic and would also incorporate carbon fibres in the strut to withstand the large bending forces in this element during foilborne course changes. Nose fences would be fitted on the strut. The pintle fittings to the hull would be re-designed in such a manner that this foil could be easily retracted. An alternative rudder would be fitted for hullborne operation when the foil system was raised. (Further research into the casting of high strength aluminium alloy hydrofoils might be worthwhile as an alternative to the fibre reinforced plastic described here).

When this system had been tested and tuned, (the latter would include the fitting of a more efficient mainsheet track system and a replacement boom as well as other additions such as replacement jib cleats etc...) it is expected that the boat would have the potential for speeds in excess of the record speed achieved by 'Icarus' of 24.5 knots.

Once this configuration had been 'debugged' and was working well, steps could be taken to fill in the other deficiency in this work, the lack of full scale recordings of speed, flight orientation, windspeed, apparent wind

speed, course to the true wind direction, etc... This had not been attempted with the previous versions of the boat for several reasons. All the initial effort had gone into finishing the actual boat and hydrofoil system because it was felt that it was first important to get the prototype working well before it was worthwhile to fit data measuring and recording equipment. Generally by the time each foil system had been set up and the boat was flying consistently, a breakage would occur rendering the fitting of recording equipment redundant. The fitting of transducers and recording equipment was not a task to be taken lightly. There were problems of power supply, extra weight, water inundation of valuable electronic equipment, operation of equipment while trying to sail the boat (itself a full time task) and of the design of transducers which would undoubtedly have affected the overall performance of the boat to a greater or lesser degree.

Even so, it would have been useful to have had on board a display of speed which could have been referred to in order to keep the boat flying fast and which would have been useful as a rough tally of the instantaneous speed. This is a good example of the sort of problems encountered when designing and fitting transducers to a sailing hydrofoil vehicle because none of the standard equipment on the market would have been suitable for fitting to the foil system without serious disruption to the flow. The two most promising arrangements were either a pitot tube or an electronic doppler type speed counter and in both cases the

transducers and wires would have had to have been built into the foils at the construction stage, the wire connections running through the fibre reinforcement of the laminate. The advantage of the Weymouth trials is that very accurate averaged speeds over 500 metres are recorded and the elaborate course system used enables courses to be sailed at any direction relative to the wind.

The Future

Apart from the rebuilding of 'Kaa' which can be considered as a natural progression from the stage that this project has already reached, there are the considerations of an ocean going sailing hydrofoil which was mentioned in chapter 2 and of a more futuristic type of vessel which could be sailed in a manner more like an aeroplane is flown. It was felt that this latter in particular will be the way ahead for the development of this type of craft, especially for larger vessels where the effect of movements in the crew mass become small, and there is already one sailing hydrofoil in existence, 'Force 8' (90), which uses this sort of principle.

One can imagine a boat of say 10 metres overall length, a trimaran, but with interconnecting wing decks between the hulls and of a generally streamlined appearance in order to reduce the aerodynamic drag. The 'cockpit' could be positioned in the centre hull with all controls leading to this positon. The hydrofoil system would be an

aeroplane configuration with the main foils positioned on the outer floats and the rudder at the rear of the centre hull. The outer floats would be shorter than the centre hull and they would be positioned towards the bow in order to provide the maximum stability against adverse pitching moments during hullborne operation. The power source would be either a solid aerofoil wing sail rig or a windmill, the former having the potential for the highest speeds and the latter having the potential for sailing at all angles to the wind.

The interconnecting wing decks could be constructed as an aerofoil section. Trial calculations have suggested that the lift from these wings on a boat the size of 'Kaa', taking into account the wing in ground effect, (22, 41, 149) could be as high as 5% of the total weight of the boat at a speed of 20 knots. By incorporating some measure of incidence control to the cantilevered tips of the forward foils which could be arranged as the equivalent of both aileron and flap control on an aircraft, the restoring moments against heeling forces could be improved and some control could be maintained over the trim of the whole boat.

It will be interesting to see whether the future will bring the construction of such a vessel.

CHAPTER 10

Conclusions

The Calm Water Design Programs and Model Tests

A series of computer programs were written which were able to predict the lift, drag and height of flight and trim of a hydrofoil vessel fitted with a complex arrangement of surface piercing hydrofoils and travelling at a given speed in calm water. This series consisted of programs which calulated the height of flight and trim for given values of the speed and heel and yaw angles by an iterative process, and programs which calculated the lift, drag and lift/drag ratios for given values of the height of flight, and trim, heel and yaw angles. This latter series could be used for calculations on fully submerged hydrofoil systems at fixed angles of incidence. In this manner it was possible to compare a large number of different hydrofoil systems as well as to judge the effects of small changes to a particular system in order to achieve an efficient design.

The accuracy of the predictions found from these programs was judged by comparing the results with the experimental results obtained from a programme of experiments carried out on a hydrofoil model in calm water

in the towing tank. A large amount of data was obtained, both for tests where there was no heel or yaw and for tests where these angles were incorporated. The results show how the design programs are an efficient and generally accurate method for the calculation of the forces incident on complex surface piercing hydrofoil systems. The predictions of the drag and flight orientation of the model agree well with the experiments for tests where there was no heel or yaw although there were small variations of the order of one degree in the results of the trim predictions. For tests where angles of heel and yaw were included, the scatter in the results was higher and as a consequence their agreement with the theoretical predictions is not as accurate. However, trends in the results are predicted correctly and in most cases the experimental results fall within a well defined scatter band.

Ventilation on parts of the hydrofoil system was found to affect the results significantly and was in all cases detrimental to performance. Ventilation increased the scatter in the experimental results.

Wind Propulsion

Performance prediction analyses were formulated for two types of wind propulsion systems, a soft sail rig (this type of system was used on the prototype boat) and a wind turbine system. Polar diagrams were plotted of the driving force available from these systems in all directions of

travel relative to the true wind direction. Predictions for the wind turbine were made in the windmill mode at different operating points of the rotor and also for operation in the autogyro mode.

It was found that a soft sail rig, and by analogy a solid aerofoil rig, was capable of providing large values of propulsive force, but that these values were restricted in head wind and following wind conditions. The wind turbine offered the possibility of propulsion directly to windward, but the propulsive forces available in beam and following wind conditions were less than those provided by a sail rig. This situation could be improved by operating the wind turbine in the autogyro mode in beam wind conditions. It was concluded that for high boat speeds in low wind conditions over a limited range of courses relative to the true wind direction, the soft sail or solid aerofoil rig was superior to the wind turbine. The wind turbine system on the other hand was a more versatile rig because it provided propulsion over a greater range of headings to the wind direction. The wind turbine is an attractive contender for the exploitation of wind propulsion in the commercial shipping industry because it is a system which offers efficient energy conversion with the expectation of low manning requirements.

Seakeeping

Several approaches were made in order to solve the problem of the prediction of the motion response of a surface piercing hydrofoil vessel in wave motions. These were based on two main methods, an approach which used a linearised theory and an approach which solved the non-linear equations of motion using a digital computer. Model tests were carried out both in head and following sea conditions and the results from these were compared with the results from the various calculation methods.

It was found that no one approach gave completely reliable results in all cases over the whole of the frequency range for which tests had been made. In head seas it was found that the best predictions were obtained from the non-linear theory where corrections had been incorporated for the unsteady nature of the forces incident on the foil system as a result of the oscillatory flow. In following seas the predictions which gave the best agreement with the experimental results were those which were based on a linearised theory and those which were calculated from a non-linear approach where corrections were made for the unsteady forces and for slamming. In view of the fact that the hulls of the model were seen to slam into the wave crests during these following sea tests and that allowances for these impulse forces were not made in the linear theory it was felt that the non-linear approach was the most reliable overall solution.

It was found that the inclusion of the degree of freedom in surge did not affect the prediction of the heave and pitch response to any great extent.

The non-linear theoretical approach showed the most promise for further development into the treatment of oblique and irregular seas although some further ground work was felt to be necessary, both experimental and theoretical, on the nature of the forces acting on hydrofoils operating near the free water surface in oscillatory flow.

Linearised, single degree of freedom solutions for the heave response were found to give predictions which could be useful for preliminary response studies especially in head seas. The reliability of this approach in following seas is not so good.

The Prototype

A 5m length prototype sailing hydrofoil trimaran with a soft, fully battened sail system was constructed and tested on the open water. The most successful and latest hydrofoil system consisted of an aeroplane configuration of foils with the majority of the weight of the vessel supported on forward hydrofoils which were mounted on the outer floats. Speeds in excess of 15 knots had been reached and the boat was found to manoeuvre well both foil-borne and hull-borne and to be easily handled under

single handed control. Structural problems had been encountered in constructing hydrofoils with a high strength/weight ratio and these had prevented the boat from flying at even higher speeds. Many of the constructional problems and structural failures of the hydrofoils in particular came about because of the limited budget available for the building of this boat. Reconstruction of this prototype boat was planned.

APPENDIX A

Interactive Computer Programs

Problems were encountered with the overall size of the computer programs on the PDP 11/40 mini computer when the hydrofoil routines were combined with the NAg routines for the solution of the differential equations using Gear's methods (chapter 7). The structure of these routines meant that this size restriction could not be circumvented using the more usual techniques for reducing the size of a program (e.g.- virtual array space, etc.) neither could overlay techniques be used because of the chain nature of the subroutines (i.e. the main program called the NAg subroutine which called the hydrofoil routines). This problem could have been solved by transferring the particular routines over to a main frame computer, but because of the convenience of using the mini-computer it was decided to try and avoid this transfer if possible.

The routines were run by splitting the program into two main parts. One part dealt only with the solution of the differential equations while the other part consisted of the hydrofoil routines which calculated the forces on the hydrofoil system at each time step. The information passed between these programs was minimal and consisted of

five real numbers outgoing (the time value and the values y_1,y_2,y_3 and y_4) and four real numbers on the return ($\dot{y}_1$,$\dot{y}_2$,$\dot{y}_3$ and $\dot{y}_4$). These two parts incorporated the system directives CALL SEND and CALL RECEIV which can transfer a limited amount of data between programs and they were compiled and task built separately, forming two interactive programs (RSX-11M Manual - Executive). It was necessary to install these programs in the system using the install command (INS Program name/SLV=YES) before a run could be made. The programs worked as shown in TABLE A.I.

TABLE A.I

Main Program (incorporating NAg routines)	Main Program (Hydrofoil Routines)
Start (GEAR4)	Start (GEARS)
1 CONTINUE	2 CONTINUE
	CALL WAITFR (35) - waits for event flag 35
	CALL RECEIV (GEAR4....) - Receive Data
Program text	CALL CLREF (35..) - Clears event flag 35
CALL SEND (GEARS.,35.) - Sends Data Sets event flag 35	Program text
CALL SUSPND (...) - Halts Program	
CALL RECEIV (GEARS....) - Receives Data	
Program text	CALL SEND (GEAR4...) - Sends Data
	CALL RESUME (GEAR4..) - Resumes Operation of GEAR4
GO TO 1 (or STOP)	GO TO 2 (or STOP)

APPENDIX B

Experiment for I_y (Moment of Inertia about the y-axis)

The moment of inertia about the y-axis, that is for pitching motions, was found for the model by an experiment which consisted of oscillating the model first about the bow and then about the stern and timing the period of these oscillations. From the theory of the compound pendulum:

$$(\text{Natural Frequency, } \omega_n)^2 = \frac{g.l}{(K^2 + l^2)}$$

where l is the distance from the centre of oscillation to the centre of gravity of the pendulum, K is the radius of gyration and g is the gravitational acceleration.

For the model, the period of 10 oscillations (average of five results) was:

About the bow - 17.46 secs (l_{bow} = 525mm)

About the stern - 17.92 secs (l_{stern} = 602mm)

This gave an average radius of gyration of 0.347m and hence, $I_y = mK^2 = 0.626\ kgm^2$, where m was the mass of the model.

APPENDIX C

Cost Breakdown for the Initial Construction of 'Kaa' (1979)

This is an approximate breakdown of the costs which were incurred in the initial construction of the prototype, 'Kaa' previous to October 1979. It does not include the additions and alterations which were made after this date, nor does it include equipment which was purchased or expenses which were incurred during the Weymouth Speed Week in October 1979. A breakdown like this does not show donations in terms of time or in loans of pieces of equipment, some of which may be quite small, but all of which helped in keeping the overall costs to a minimum. Labour is not shown because none of this was paid for, the majority being supplied by the author. The cost to the boatyard does not include the hidden costs which include use of the workshop facilities, heating for the G.R.P. laminating workshop, help with labour, etc. which if included would more than double the value given of £500.

Main Structure (Hulls,etc)*

		£
Resin,Foam,Fibreglass, donated by Scott Bader Ltd., Unitex Marine Ltd., Fibreglass Ltd.,	- approximate value	550
Cape Wrath Boatyard (Durness) fittings,fastenings,glue,laminating ancillaries, moulds, etc.	- paint,wood	500

Rigging

Sails - Saturn Sails, second hand	160	
Mast - second hand	250	
Sail Battens - Aquabatten	40	
Rigging - trapeze wires,shrouds,bracing wires	50	
	500	
Donation from Mrs. N.M. Bose		500
Transport to and from London from Durness to collect mast,battens,sails,rigging and fittings (July '79) plus purchase of additional fittings and crossbeams etc.	- The Author	250
		1800

A further £200 was donated to the project by Mr. S. Penoyre of Windlesham in Surrey and this was used for the supply of extra fittings and equipment for the refitting in 1980. Terylene decking was supplied by the University at this time also. All further expenses during 1980 and 1981 were supplied by the author.

REFERENCES

1. Abbott, I.H., von Doenhoff, A.E.:"Theory of Wing Sections". McGraw Hill, 1959.

2. Abkowitz, M.A.:"Stability and Motion Control of Ocean Vehicles". M.I.T. Press, Massachusetts, 1969.

3. Abramson, H.N.:"Structural Dynamics of Advanced Marine Vehicles". The Dynamics of Marine Vehicles and Structures in Waves, RINA, ONR Symposium, April 1974.

4. Alexander, A., Grogono, J., Nigg, D.: "Hydrofoil Sailing", Kalerghi Publications, 1972.

5. Allan, J.F., Doust, D.J., Ware, B.E.: "Yacht Testing". Transactions RINA, 1957. p.136.

6. Allday, W.J.:"Aluminium for Small Craft". Symposium on Small Craft, RINA, Paper No.4, Part 1.

7. Ashley, H., Windall, S., Landahl, M.T.:"New directions in Lifting Surface Theory". AIAA Journal, Vol.3, January 1965.

8. A.Y.R.S. (Amateur Yacht Research Society). Pamphlets and Publications, Newbury, Berkshire.

9. Baker, R.M.L., Douglas, J.S.:"Four-Dimensional Simulation of a Hydrofoil Craft". 8th AIAA Symposium on the Aer/Hydronautics of Sailing, March 1977.

10. Baker, R.M.L., Douglas, J.S.:"Preliminary Mathematical Analysis of a Rigid-Airfoil Hydrofoil Water Conveyance". 2nd AIAA Symposium on the Aero/Hydronautics of Sailing, April, 1970.

11. Barkla, H.M.:"High Speed Sailing".Transactions RINA 1952

12. Batchelor, C.:"Winds of Change in the Dutch Power Industry". Financial Times, November 26, 1980 .

13. Bates, J., Letter to the Editor, The Naval Architect, March 1980.

14. Bauer, A.B.:"Sailing all points of the Compass". 3rd AIAA Symposium on the Aero/Hydronautics of Sailing, November 1971 .

15. Bernicker, R.P.:"Heaving and Pitching Motions of Super-Ventilated Hydrofoil Craft in Irregular Seas". Davidson Lab. Report 958, June 1963 .

16. Bernicker, R.P.:"Hydrofoil Motions in Irregular Seas". Davidson Lab. Report 909, November 1962 .

17. Bernicker, R.P., Brown, P.W.:"The Force Moment and Hinge Moment Characteristics of Surface Piercing Dihedral

Hydrofoils". Davidson Lab. Report 964, May 1964 .

18. Berry, L.W.:"Lift Coefficients for NACA 16-series foils at low Incidences". NPL Ship Div. Tech. Mem. No2, 1959 .

19. Betz, A.:"Windmills in the Light of Modern Research". NACA TM 474, 1927 .

20. Bishop, R.E.D., Neves, M. de A.S., Price, W.G.:"On the Dynamics of Ship Stability". RINA Spring Meetings, 1981 .

21. Blount, D.:"Resistance Characteristics of a 70-foot Hydrofoil Missile Range Patrol Boat". David Taylor Model Basin Report 1607, April 1962 .

22. Borst, H.V.:"Analysis of Vehicles With Wings Operating in Ground Effect". AIAA/SNAME Advanced Marine Vehicle Conference, October 1979.

23. Bose, N.:"The Design and Development of a Sailing Hydrofoil Vessel" University of Glasgow - Final Year Project, NAOE-FYP-78-01, 1978.

24. Bose, N.:"Initial Sailing Trials of a Hydrofoil-Supported, Wind-Propelled, Trimaran". University of Glasgow Hydrodynamics Laboratory Report NAOE-HL-80-03.

25. Bose, N., McGregor, R.C.:"A Record of Progress made on a Purpose Built Hydrofoil Supported Sailing Trimaran". High Speed Surface Craft Conference, June 1980.

26. Bose, N.:"Windmills-Propulsion for a Hydrofoil Trimaran". RINA Symposium on Wind Propulsion of Commercial Ships, November 1980.

27. Bose, N.:"Model Tests for a Wind-Propelled Hydrofoil Trimaran". High Speed Surface Craft Magazine, October/November 1981.

28. Bradfield, W.S., Griswold, L.M.:"An Evaluation of Sailing Vehicle Rig Polars from Two-Dimensional Wind Tunnel Data". 8th AIAA Symposium on the Aero/Hydronautics of Sailing, 1977 .

29. Bradfield, W.S.:"Comparative Performance of the Flying Fish Hydrofoil and the Tornado Catamaran". 3rd AIAA Symposium Aero/Hydronautics of Sailing, November, 1971 .

30. Bradfield, W.S.:"On the Design and Performance of Radical High-Speed Sailing Vehicles". Marine Technology Vol.17 No1, January 1980 .

31. Bradfield, W.S.:"Predicted and Measured Performance of a Daysailing Catamaran". Marine Technology - SNAME, January 1970 .

32. Bradfield, W.S.:"Some Observed Effects of Foil Control on Hydrofoil Sailing Vehicle Performance". SNAME Chesapeake Sailing Yacht Symposium, 1974 .

33. Bradfield, W.S.: "The Development of a Hydrofoil Daysailer". 2nd AIAA Symposium on Aero/Hydronautics of Sailing, 1970 .

34. Bradfield, W.S., Madhavan, S.:"Wing Sail Versus Soft Rig: An Analysis of the Successful Little America's Cup Challenge of 1976". SNAME Chesapeake Sailing Yacht Symposium 3rd, 1977 .

35. Bradley, C., Incecik, A.:"Two Dimensional Frame Analysis Program - FRAN2". Glasgow University, Hydrodynamics Lab. Report NAOE-HL-79-05 1979.

36. Breslin, J.P.:"Application of Ship Wave Theory to the Hydrofoil of Finite Span". Journal of Ship Research, 1957.

37. Breslin, J.P.:"The Wave and Induced Drag of a Hydrofoil of Finite Span in Water of Limited Depth". Journal of Ship Research, September 1961 .

38. Brown, D.K.:"Hydrofoils, a Review of their History, Capability and Potential". IESS Glasgow, February 12th, 1980.

39. "Calculator and Computer Aided Design for Small Craft - The Way Ahead". RINA - Small Craft Group Conference, 31st March, 81 - 1st April,81.

40. Cannon, R.H.:"Performance of Hydrofoil Systems". MIT Ph.D. Thesis, 1950.

41. Carter, A.W.:"Effect of Ground Proximity on the Aerodynamic Characteristics of Aspect-Ratio-1 Airfoils with and without End Plates". NASA TN D-970, October 1961.

42. Chapman, R.B.:"Spray Drag of Surface-Piercing Struts". AIAA/SNAME/USN Advanced Marine Vehicles Meeting, No72-605 AIAA Paper, July 17-19 1972.

43. Clauser, M.U.:"The Tow Testing of Full Scale Yachts". 6th AIAA Symposium on the Aero/Hydronautics of Sailing, 1975.

44. Clough, R.W.:"Dynamics of Structures". McGraw Hill Kogakusha Ltd., 1975.

45. Colquhoun, L.R.:"Jetfoiling Over the Channel". Presented at A.G.M. of IHS, November 15th, 1979.

46. Comstock, J.P.:"Principles of Naval Architecture". SNAME, 1967.

47. Conolly, A.C.:"Designing for Cavitation Free Operation on Hydrofoils with NACA 16-Series Sections". J. Aircraft Vol.3 No6, 1966.

48. Crago, W.A.:"The Prediction of Yacht Performance from Tank Tests". Transactions RINA Vol.105, 1963.

49. Crewe, P.R.:"The Hydrofoil Boat; Its History and Future

Prospects". Transactions Vol.110, 1958.

50. 'Crystic Monograph No.2, Polyester Handbook', Crystic Research Centre, Scott Bader Co. Ltd., Wellingborough, 1977.

51. Cummins, W.E.:"The Impulse Response Function and Ship Motions". DTMB Report 1661, October 1962.

52. Davidson, Ken. S.M.:"Some Experimental Studies of the Sailing Yacht". Transactions SNAME Vol.44, 1936.

53. Davis, B.V., Oates, G.L.:"Hydrofoil Motions in a Random Seaway". 5th Symposium on Naval Hydrodynamics, September 1964.

54. De La Cierva:"The Development of the Autogyro". Journal of the Royal Aeronautical Society, 1926.

55. Dodd, R.E.:"A Design Analyses of 1974 World's Multihull Cup Competitors". 6th AIAA Symposium on the Aero/Hydronautics of Sailing, 1975.

56. Dodd, R.E.:"A Variable Geometry Flying Hydrofoil". 8th AIAA Symposium on Sailing Hydronautics, 1977.

57. Drischler, J.A.:"Approximate Indicial Lift Functions for Several Wings of Finite Span in Incompressible Flow as Obtained from Oscillatory Lift Coefficients". NACA TN 3639, May 1956.

58. Drummond, T.G., Mackay, M., Schmitke, R.J.:"Wave Impacts on Hydrofoil Ships and Structural Implications". 11th Symposium on Naval Hydrodynamics, 1977.

59. Du Cane, P. (Editor), Eames, M.C.:"High Speed Small Craft". David and Charles, 1974.

60. Durand, W.F.:"Aerodynamic Theory Vol IV". Julius Springer, 1935.

61. Eames, M.C.:"Advances in Naval Architecture for Future Surface Warships". RINA, Paper 1, 1980 Spring Meetings.

62. Eames, M.C., Jones, E.A.:"H.M.C.S. Bras D'Or - An Open Hydrofoil Ship". Transactions RINA Vol.113, 1971.

63. Eames, M.C., Drummond, T.G.:"H.M.C.S. Bras D'Or - Sea Trials and Future Prospects". Transactions RINA Vol.113, 1973.

64. Eames, M.C.:"Hydrofoil Drag and Cavitation". Ass. of Northern Universities Sailing Clubs ANUSC Tech. Paper No5, 1954.

65. Eames, M.C.:"Problems and Requirements of Directional Stability, Control and Manoeuvrability; High Speed Craft". Journal Mechanical Engineering Science, Vol.14 No7, 1972.

66. Eames, M.C.:"The Influence of Cavitation on Hydrofoil Craft Design". Canadian Aeronautical Journal Vol.6 Nol, January 1960.

67. Eames, M.C., Jones, E.A.:"Treatment of Aspect Ratio - Private Correspondence". D.R.E.A., 1979.

68. Eames, M.C.:"The Canadian Hydrofoil Project Intermediate Hydrofoil System for the R-100". Defence Research Board Canada PHx-106, 1957.

69. Ebbutt, P.W.:"Aerodynamics in the 1977 America's Cup". The Naval Architect, March 1978.

70. Eppler, R., Shen, Young, T.:"Wing Sections for Hydrofoils - Part 1: Symmetrical Profiles". Journal of Ship Research Vol.23 No3, September 1979.

71. Farrar, A.:"Commercial Sail- has it a future?" Yachting Monthly, March 1981.

72. Feifel, W.M.:"Advanced Numerical Methods Hydrofoil System Design and Experimental Verification". Third International Conference on Numerical Ship Hydrodynamics, June 1981.

73. Fishlock, D.:"CEGB Plans to Farm the Wind". Financial Times, July 7th, 1981.

74. Flatt, R.:"Speed Polar of a Wind Turbine Powered Cargo Boat". Wind Engineering Vol.1 No.3, 1977.

75. Furuya, O., Acosta, A.J.:"An Experimental Study of a Super-Ventilated Finite Aspect Ratio Hydrofoil Near a Force Surface". 11th Symposium on Naval Hydrodynamics, 1977.

76. Furuya, O.:"(a) Non-Linear Calculation of Arbitrarily Shaped Supercavitating Hydrofoils near a Free Surface ". J. of Fluid Mech. 68 part 1 p.21-40, 1975.

77. Furuya, O.:"(b) Three-Dimensional Theory of Supercavitating Hydrofoils near a Free Surface". J. of Fluid Mech. Vol.71 part 2 p.339-359, 1975.

78. Glauert, H.:"The Elements of Aerofoil and Airscrew Theory". Cambridge, 1948.

79. Golding, E.W.:"The Generation of Electricity by Wind Power". E. and F.N. Spon. Ltd., 1955.

80. Goman, W.J.:"Sailing Yacht Construction in Fibreglass". SNAME Chesapeake Sailing Yacht Symposium, 1977.

81. Grogono, J., Wynne, B.:"Mayfly: A Sailing Hydrofoil Development". AIAA Symposium on Sailing, 1977.

82. Grogono, J.:"The Sculling Hydrofoil". Yachts and Yachting, 1979.

83. Haarstick, S.:"Principles of Sail Design". SNAME

Chesapeake Sailing Yacht Symposium, 1977.

84. Hafner, R.:"A Novel Method to Achieve Optimum Sailing Performance". RINA Paper for Written Discussion W1(1979).

85. Hall, G., Watt, J.M.:"Modern Numerical Methods for Ordinary Differential Equations". Clarendon Press, Oxford, 1976.

86. Hammitt, A.G.:"Technical Yacht Design". Adlard Coles, 1975.

87. Harris, R.I.:"Requirements for the Provision of Offshore Wind Data Relating to Wind Energy Conversion Systems". NMI R75, Feltham Middlesex, February 1980.

88. Henry, C.J.:"Application of Lifting-Surface Theory to the Prediction of Hydroelastic Response of Hydrofoil Boats". Journal of Ship Research, December 1968.

89. Henry, C.J., Ali, M. Raiham:"Hydrofoil Lift in Head Seas". Davidson Lab. Report 982, October 1963.

90. High-Speed Surface Craft. Exhibition and Conference Proceedings. Kalerghi Publications, June 24-27 1980.

91. Hirsch, I.A.:"Prediction of the Seakeeping Characteristics of Hydrofoil Ships". Journal of Hydrodynamics Vol.2 No.1, January 1968.

92. Hoerner, S.F.:"Fluid Dynamic Drag". Hoerner Fluid Dynamics, 1958.

93. Hoerner, S.F., Borst, H.V.:"Fluid Dynamic Lift". Hoerner Fluid Dynamics, 1975.

94. Hook, C.:"A Self Tending Rig with Feed Back and Compass Course". AIAA Symposium on Sailing Hydronautics, 1977.

95. Hook, C., Kermode, A.C.:"Hydrofoils". Pitmans, London.

96. Hughes, G., Allan, J.F.:"Turbulence Stimulation on Ship Models". Transactions SNAME 1952.

97. Hyman, M.C.:"The Effects of Pitching Rate on the Hydrodynamic Properties of Hydrofoils". AIAA/SNAME Advanced Marine Vehicles Conference, October 1979.

98. International Symposium on Wind Energy Systems, 1st and 2nd. BHRA Fluid Engineering, 1976 and 1978.

99. Jeffrey, T.:"Tabarly's Sea Bird". Yachting World, June 1979.

100. Johnston, R.J., O'Neill, W.C.:"A Ship Whose Time has come and gone Plainview (AGEH-1)". AIAA/SNAME Advanced Marine Vehicles Conference, October 1979.

101. Johnston, R.J., Virgil, E.:"Theoretical and Experimental Investigation of Supercavitating Hydrofoils Operating Near

the Free water Surface". NASA TR R-93, 1961.

102. Johnson, W.J.:"Fullscale Performance Testing of Wind Driven Vehicles". 8th AIAA Symposium on Aero/Hydronautics of Sailing, 1977.

103. Jones, R.T.:"The Unsteady Lift of a Wing of Finite Aspect Ratio". NACA Report 681, 1940.

104. Kaplan, P.:"Longitudinal Stability and Motions of a Tandem Hydrofoil System in a Regular Seaway". Stevens Institute of Technology Report 517, December 1959.

105. Kaplan, P., Jacobs, W.R.:"Dynamic Performance of Scaled Surface-Piercing Hydrofoil Craft in Waves". Stevens Inst. of Technology Report 704, June 1959.

106. Keiper, D.A.:"Hydrofoil Ocean Voyager"Williwaw"". Proceedings of the 3rd AIAA Symposium on the Aero/Hydronautics of Sailing , November 1971.

107. Keiper, D.A., Fifield, J.E.:"Progress with Hydrofoil Sailing". 6th AIAA Symposium on Aero/Hydronautics of Sailing, 1975.

108. Keuning, J.A.:"A Calculation Method for the Heave and Pitch Motions of a Hydrofoil Boat in Waves". International Shipbuilding Progress, 1979.

109. Kirkman, K.L.:"Scale Experiments with the 5.5 metre Yacht "Antiope"". SNAME Chesapeake Sailing Yacht Symposium, 1974.

110. Kreyszig, Erwin:"Advanced Engineering Mathematics (Third edition)". John Wiley and Sons, 1972.

111. Krezelewski, M.:"The Longitudinal Behaviour of a Hydrofoil Craft in Rough Seas". Hovering Craft and Hydrofoil.

112. Laugan, T.J., Wong, H.T.:"Evaluation of Lifting Surface Programs for Computing the Pressure Distributions on Planar Foils in Steady Motion". NSRDC Report 4021, May 1973.

113. Lapidus, L., Seinfeld, J.H.:"Numerical Solution of Ordinary Differential Equations". Academic Press, 1971.

114. Lawrence, H.R., Gerber, E.H.:"The Aerodynamic Forces on Low Aspect Ratio Wings Oscillating in an Incompressible Flow". Journal of the Aeronautical Sciences, Vol.19, 1952.

115. Lunde, J.K., Walderborg, H.A.A.:"300 tons, 50 knots Hydrofoil Craft Reports I and II". Office of Naval Research Contract N62558-2596.

116. McCarthy, J.H., Power, J.L., Huang, T.T.:"The Roles of Flow Transistion, laminar Separation and Turbulence stimulation in the an alysis of Axisymmetric body Drag". 11th Symposium on Naval Hydrodynamics, 1977.

117. McGregor, R.C., Foster, J.L., Rothblum, R.S., Swales, P.D.:"The Influence of Fences on Surface Piercing Struts and Foils". 10th Symposium of Naval Hydrodynamics, 1974.

118. McGregor, R.C.:"Recent Hydrofoil Studies at the University of Glasgow". Presented at the A.G.M. of I.H.S., University of Glasgow Hydrodynamics Laboratory Report NAOE-HL-79-19, November 1979.

119. McGregor, R.C., Wright, A.J., Swales, P.D., Crapper, G.D.:"An Examination of the Influence of Waves on the Ventilation of Surface-Piercing Struts". J. Fluid Mech. Vol.61, part 1, pp85-96, 1973.

120. McGuigan, D.:"Small Scale Wind Power". Prism Press, Dorchester, 1978.

121. McMullen, M.:"Multihull Seamanship". Nautical Publishing Co., 1976.

122. Marchaj, C.A.:"A Critical Review of Methods of Establishing Sail Coefficients and their Practical Implications in Sailing and in Performance Prediction". 5th HISWA Symposium, 1977.

123. Marchaj, C.A.:"Sailing Theory and Practice". Adlard Coles, 1964.

124. Marchaj, C.A., Tanner, T.:"Wind Tunnel Tests of a 1/4 Scale Dragon Rig". University of Southampton SUYR, Paper 14, June 1964.

125. Marine Engineering/Log:"Shin Aitoku Maru". Marine Engineering/Log, December 1980.

126. Mason, Piper A. Jr.:"Full Scale Tow and Heel Resistance and Test Procedures". 6th AIAA Symposium on Aer/Hydronautics of Sailing, 1975.

127. Masuyama, Yutaka:"Performances of a Hydrofoil Sailing Boat" (in japanese), Japan.

128. Mazelsky, B.:"Numerical Determination of Indicial Lift of a Two Dimensional Sinking Airfoil at Subsonic Mach Numbers from Oscillating Lift Coefficients with Calculations for Mach No.0.7". NACA TN 2562, December 1951.

129. Meyers, W.G., Sheridon, D.J., Salvesen, N.:"Manual NSRDC Ship Motion and Sea-Load Computer Program". NSRDC Report 3376, February 1975.

130. Milgram, J.H.:"Sail Force Coefficients for Systematic Rig Variations". SNAME Technical and Research Report R-10, September 1971.

131. Milgram, J.H.:"Section Data for Thin Highly Cambered Airfoils in incompressible Flow". NASA CR-1767, 1971.

132. Miller, B.L.:"Hydrodynamic Drag of Roughened Circular Cylinders". The Naval Architect, March 1977.

133. Milne, W.E.:"Numerical Solution of Differential Equations". Chapman and Hall Ltd., London, 1953.

134. Mossum,L.T., Nicholson, NSON:"Some Aspects of Hydrofoil Motions and their Implications for Crew Performance". 11th Symposium on Naval Hydrodynamics, 1977.

135. Morwood, J.:"Sailing Hydrofoils". AYRS, 1970.

136. Murray Smith, D.:"An Introduction to Continuous System Simulation Using the EAI 2000 Computer". Course Notes Glasgow University, September 1980.

137. Musgrove, P.J., Mays, I.D.:"Development of the Variable Geometry Vertical Axis Windmill". 2nd International Symposium on Wind Energy Systems - Royal Tropical Inst. Amsterdam, BHRA Fluid Eng. Cranfield, 1978.

138. Musgrove, P.J.:"The Variable Geometry Vertical Axis Windmill". Int. Symposium on Wind Energy Systems, BHRA Fluid Engineering, September 7-9, 1976.

139. NAg: Fortran Library Manuals: Mark 7. Numerical Algorithms Group, 1978.

140. New Civil Engineer:"Windmill - South Ronaldsay". New Civil Engineer, January 1-8, 1981.

141. Newick, D., Private Correspondence. April 1979 and July 1980.

142. Nigg, D.J.:"A Sailing Hydrofoil Development". Marine Technology, April 1968.

143. Nikolsky, A.A.:"Helicopter Analysis". Wiley, 1951.

144. Noreen, A.E., Gill, P.R., Feife, W.M.:"Foilborne Hydrodynamic Performance of Jetfoil". AIAA/SNAME Advanced Marine Vehicles Conference, October 1979.

145. Ocean Industry:"Are Sail-assisted Tankers Feasible?" Ocean Industry, February 1980.

146. Ocean Industry:"North Sea Wind Power - a New Source of Energy". Ocean Industry, March 1977.

147. Ocean Industry:"Tug with Sails is Forerunner of New Class". Ocean Industry, August 1979.

148. Ogilvie, T.F.:"The Theoretical Prediction of the Longitudinal Motions of Hydrofoil Craft". David Taylor Model Basin Report 1138, November 1958.

149. Ollila, R.G.:"An Historical Review of WIG Vehicles". AIAA/SNAME Advanced Marine Vehicles Conference, October

1979.

150. Page, F.:"Articles on 'Paul Ricard'". Observer, 18th March, 1979, 13th May, 1979, 10th August, 1980.

151. Palmer, D.:"The Atlantic Challenge". Hollis and Carter, 1977.

152. Parham, H.J., Farrar, A., Macalpine-Downie, J.R.:"Class "C" Racing Catamarans". Transactions RINA, Vol. 110, 1968.

153. Parkyn, B.:"Glass Reinforced Plastics". Iliffe books, 1970.

154. Pelly, D.: 1975,1976,1977 (November Issue) "Speed Week". Yachting World, IPC Business Press.

155. "Plywood for Marine Craft". British Standard 1088, 1966.

156. "Propeller Development". Aircraft Engineering, Vol.53, No.8, August 1981.

157. Raybould, K.B. Martech Marine Consultants Private Correspondence, March 1979.

158. Riegels, F.W.:"Aerofoil Sections". Butterworths, 1961.

159. Ripken, J.F., Straub, L.G.:"Interference Effects of a Strut on the Lift and Drag of a Hydrofoil". St. Anthony Falls Hydraulic Lab. Report 65, 1961.

160. Rothblum, R.S.:"Scale Effects in Models with Forced or Natural Ventilation Near the Free Water Surface". Proceedings of the 18th General Meeting of the American Towing Tank Conference, Vol. II, August 23-25, 1977.

161. Royal Yachting Association - World Sailing Speed Week. Portland Harbour, 1979, 1980, 1981. Manuals published by the Royal Yachting Association.

162. Rypinski, D.F.:"The Dynamics of Sailing on Land". 3rd AIAA Symposium on the Aero/Hydronautics of Sailing, November 1971.

163. Salisbury, V.H.:"Jetfoil in Operation". AIAA/SNAME Advanced Marine Vehicles Conference, October 1979.

164. Schmitke, R.T., Jones, E.A.:"Hydrodynamics and Simulation in the Canadian Hydrofoil Program". 9th Symposium on Naval Hydrodynamics, August 1972.

165. Schmitke, R.T., "A Computer Simulation of the Performance and Dynamics of HMCS Bras D'Or (FHE-400)". Canadian Aeronautics and Space Journal, Vol.17, No3, 1971.

166. Schmitke, R.T., "Longitudinal Simulation and Trials

of the Rx Hydrofoil Craft". Canadian Aeronautics and Space Journal, Vol.16, No3, 1970.

167. Schmitke, R.T., "Prediction of Wave-Induced Motions for Hullborne Hydrofoils". AIAA/SNAME Advanced Marine Vehicles Conference, September 20-22, 1976.

168. Scott Bader, Fibreglass Ltd., Unitex Marine Ltd.:"Resin, Fibreglass and Foam Information". 1978.

169. Sharphouse, R.P.:"The Use of Timber in Small Craft Construction". RINA Symposium on Small Craft, Paper No.4, Part 4.

170. Silverleaf, A., Cook, F.G.R.:"A Comparison of Some Features of High Speed Marine Craft". Transactions RINA, Vol.112, March 26, 1969.

171. Smith, C.S.:"Calculation of Elastic Properties of GRP Laminates for Use in Ship Design". Symposium on GRP Ship Construction, RINA, October 1972.

172. Spens, P.G., De Saix, P., Brown, P.W.:"Some Further Experimental Studies of the Sailing Yacht". Transactions SNAME, November 15-18, 1968.

173. Stretensky, L.N.,:"Motion of a Cylinder under the Surface of a Heavy Fluid". NACA TM 1335, 1953.

174. Swales, P.D., Cole, B.W., Smith, G.L.:"Some Aspects of the Ventilation of Surface Piercing Struts and Foils". Transactions RINA, 1973.

175. Swales, P.D., Rothblum, R.S.:"Ventilation and Separation on Surface Piercing Struts and Foils". Department of Mechanical Engineering, University of Leeds, 1977.

176. "Symposium on Wind Propulsion of Commercial Ships". RINA, November 4-7, 1980.

177. The Motor Ship:"Wind Power - just something in the air?". The Motor Ship, December, 1980.

178. The Naval Architect:"Sail Equipped Motor Ships (Shin Aitoku Maru)". The Naval Architect, March 1981.

179. The Sunday Times - Colour Supplement:"Now What are the Japanese up to? Launching Sail Ships". October, 1980.

180. Thomas, R.L.:"Large Experimental Wind Turbines : Where we are now". NASA TM-X-71890, 1976.

181. Tilgner, C.:"Design, Development and Initial Tests of ONR Supercavitating Hydrofoil Boat XCH-6". Report 133 Grumman, 1962.

182. Tulin, M.P., Hsu, C.C.:"Leading Edge Cavitation on Lifting Surfaces with Thickness". Proceedings of the 18th

General Meeting of the American Towing Tank Conference, Vol. II, August 23-25, 1977.

183. Uhlman, J.S. Jnr.:"A Partially Cavitating Hydrofoil of Finite Span". Journal of Fluids Engineering, September 1978, Vol.100, p.353., August 1, 1977.

184. Van Holten, Th.:"Concentrator Systems for Wind Energy, with Emphasis on Tip Vanes". Wind Engineering Vol.15, No.1, 1981.

185. Varney, J. (Capt.):"Comsail `80". Seaways, February 1981.

186. Vladimirov, A.N.:"Approximate Hydrodynamic Design of a Finite Span Hydrofoil". CAHI translated as NACA TM 1341, 1955.

187. Wadlin, K.L., Christopher, K.W.:"A Method of Calculation of Hydrodynamic Lift for Submerged and Planing Rectangular Lifting Surfaces". NASA TRR-14 or NACA TN 4168, 1959.

188. Wadlin, K.L., Shuford, C.L., McGehee, J.R.:"A Theoretical and Experimental Investigation of the Lift and Drag Characteristics of Hydrofoils at Subcritical and Supercritical Speeds". NACA Report 1232, 1955.

189. Wellicome, J.:"A Broad Appraisal of the Economic and Technical Requisites for a Wind Driven Merchant Vessel". The Future of Commercial Sail. Occasional Publication, No.2, RINA, 1975.

190. Wetzel, J.M., Schiebe, F.R.:"Lift and Drag on Surface-Piercing Dihedral Hydrofoils in Regular Waves". St. Anthony Falls Hydraulic Lab. Project Report 64, September, 1960.

191. Wharram, J.:"The History and Problems of Design of Modern Yacht Multihulls". 5th HISWA Symposium, 1977.

192. Willoughby, R.M., Capt.:"Why Square Rig?" The Motor Ship, p.134, September 1979.

193. Wilson, R.E.:"Aerodynamics of Wind Turbines". Proceedings of Conference on Energy Conversion and Fluid Mechanics. Published by SIAM Institute, June 1979.

194. Wyland, G.:"Aluminium Construction". SNAME Chesapeake Sailing Yacht Symposium, 1977.

195. Wynne, J.B.:"Possibilities for Higher Speeds Under Sail". Transactions NECIES 1979.

196. Yeoh, Ken.H.G.:"The Comparison between Theory and Experiment of the Forces on a Bowfoil of a Sailing Hydrofoil Trimaran". University of Glasgow - Final Year Project, April 1979.

197. Young, T.Sheh, Wermter, Raymond:"Recent Studies of Struts and Foils for High Speed Hydrofoils". Marine Technology Vol.16 No.1 pp.71-82, January 1979.